工業技術研究院
能源與資源研究所
Industrial Technology Research Institute
Energy & Resources Laboratories

一些能資所的熱流研究與應用

王啟川

工研院能資所熱流技術組

E-mail: ccwang@itri.org.tw

Acknowledgements

- Financial supports provided by the **Energy Bureau & Department of Industrial Technology from the Ministry of Economic Affairs, Taiwan, R.O.C.**
- Technical Supports from Mr. **Y. J. Chang**, Mr. **M.S. Liu**, Mr. **M.T. Lu**, Mr. **C.Z. Wei**, Dr. **K. H. Chien**, Dr. **K.S. Yang**, and Miss **CoCo Hsu**.
- Advisory support from Dr. **R.J. Shyu** , Dr. **B.C. Yang**, Dr. **R. Hu**, and Dr. **H.S. Chu**.
- Major Collaborating Professors: **Chen I.Y.** (Yulin Tech. Univ.), **Lin Y.T.** (YZU), **Shyu W.T.** (NTHU), Yeh R.H. (NTOU).
- Also, significant thanks go to about ***60*** (from 1994~) graduate students for their devoted efforts.

Outline

- Conventional Thermofluids system – Focused upon heat exchangers, two-phase, and related stuff.
- Electronic cooling – System as well as Component Level – Fundamental Understanding and performance characterization.
- Micro and Nano thermofluids application – micro pumps, micro/nano energy conversion, and nanofluids.
- Summary

工業技術研究院
能源與資源研究所
Industrial Technology Research Institute
Energy & Resources Laboratories

典型空調機應用

IN THE SUMMER

Cooled Air
60°F
2
Supply Duct
Indoor Fan
1
45°F
Indoor Coil (Evaporator)
Expansion Device
5
Return Duct
80°F
125°F
Reversing Valve
95°F Air Flow
Outdoor Fan
60°F
4
210°F
3
Bypass Valve
Outdoor Coil
Compressor

工業技術研究院
能源與資源研究所
Industrial Technology Research Institute
Energy & Resources Laboratories

Technology needed in an Air-conditioner

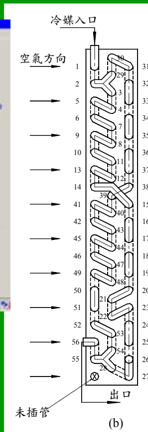

CAD Design of Complex Circuitry and System

Enhanced Compact Heat Exchanger Design

Micro-fin tube, louver fin

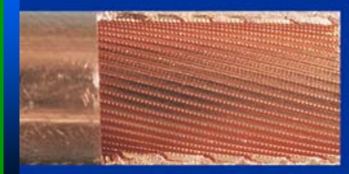

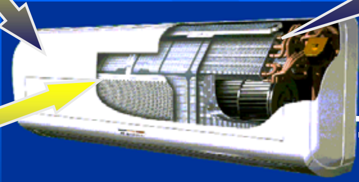

Indoor Unit

Low Noise Cross-flow Fan

Alternative Refrigerants Information

High Efficiency Mixed Flow Fan

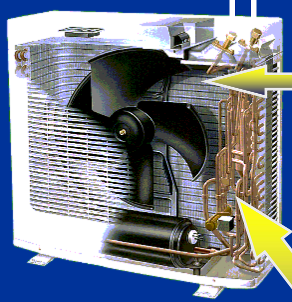

Outdoor Unit

Rotary, Scroll Compressor

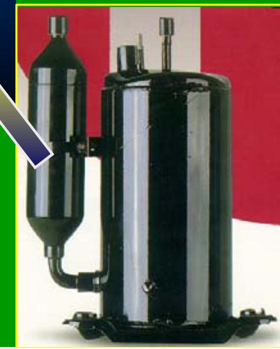

Reliability Test and Mass Production Technology

Analysis of Air-cooled Heat Exchanger

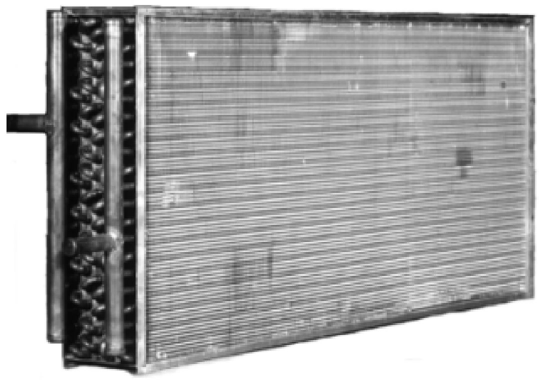

Heat Transfer

- Tube Side
  - Tubing: Smooth / Microfin / Enhanced
  - Flow Phenomenon
    - Condensation
    - Evaporation
    - Single-phase
    - Flow Pattern
    - Friction
    - New Refrigerant

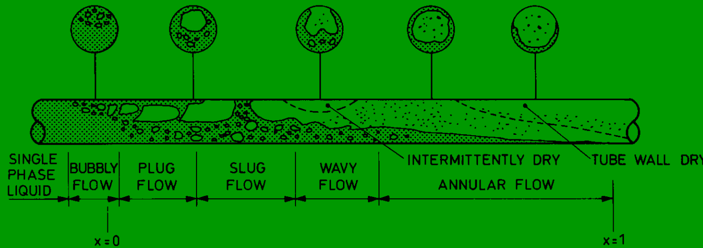

Complicated Two-phase Flow Pattern

- Air Side
  - Mode: Dry Coil (Outdoor) / Wet Coil (Indoor)
  - Fin Type
    - Plain
    - Louver
    - Wavy
    - Convex-Louver
    - Slit/Lanced
    - Hydrophilic Coating

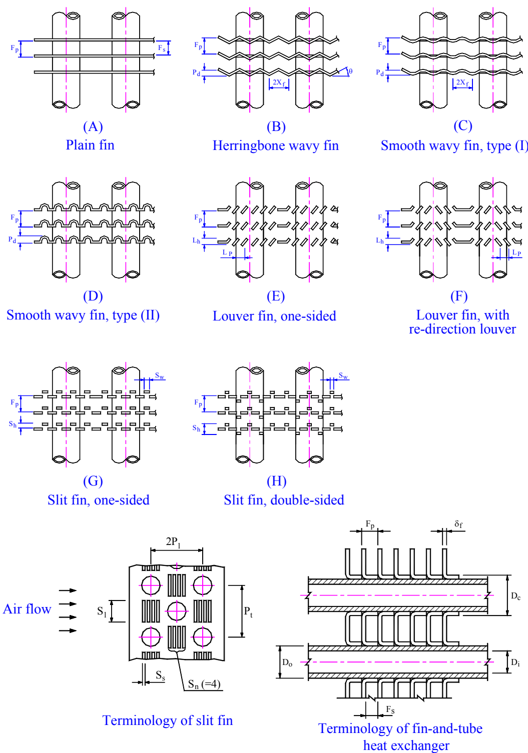

What are the problems in this "Simple" Heat Exchanger?

- Lack of systematic data – especially in airside
- Enough (in fact, too many!) heat transfer data/correlations in the tube side.
- Frictional correlation needed (two-phase small diameter tube - straight tube,)
- Influence of return bend must be justified.
- Influence of Mal-distribution (Tube side not Airside).
- Influence of lubricant oils.

In 1994~2000

- In 1994~2000, intensive data for fin-and-tube HX are collected. Systematic influence of parameters are investigated (row number, fin pitch, longitudinal/transverse tube pitch, fin types, surface coatings, dry and dehumidifying conditions, inlet humidity, tube size, …). More than 40 papers were published.
- Data are presented in correlations form. Many software implement our correlations, including the most influential OAK Heat Pump Model and the NIST Heat Pump program.
- Raw data are curve-fitted and implemented in a very complex computer model which is the mostly used by Taiwan companies.

Air side Performance subject to Fin Pattern

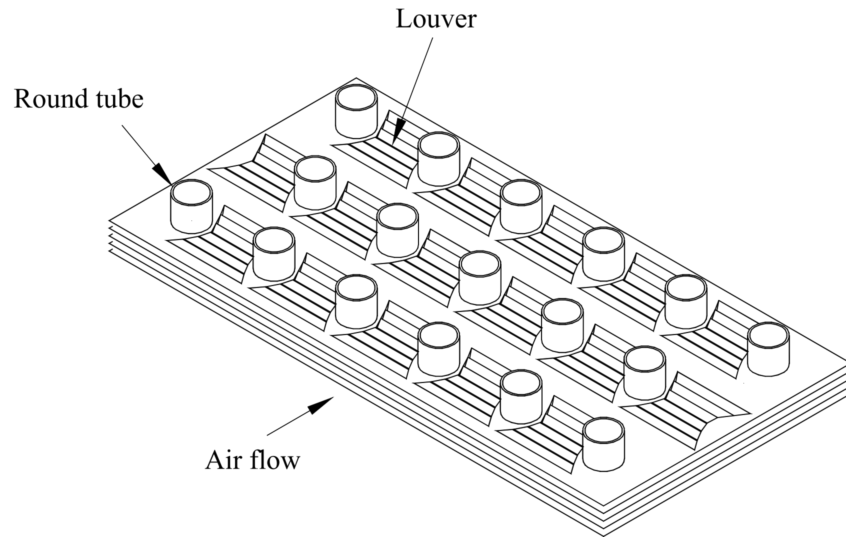

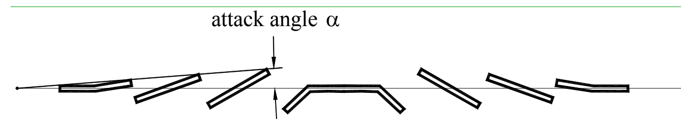

(a) Successively increased louver angle

(Pattern I)

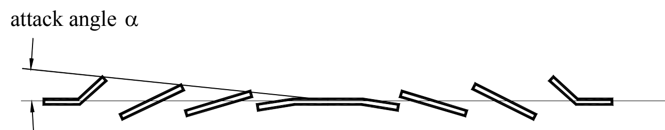

(b) Successively decreased louver angle

(Pattern II)

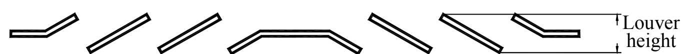

(c) Uniform louver angle

(Pattern III)

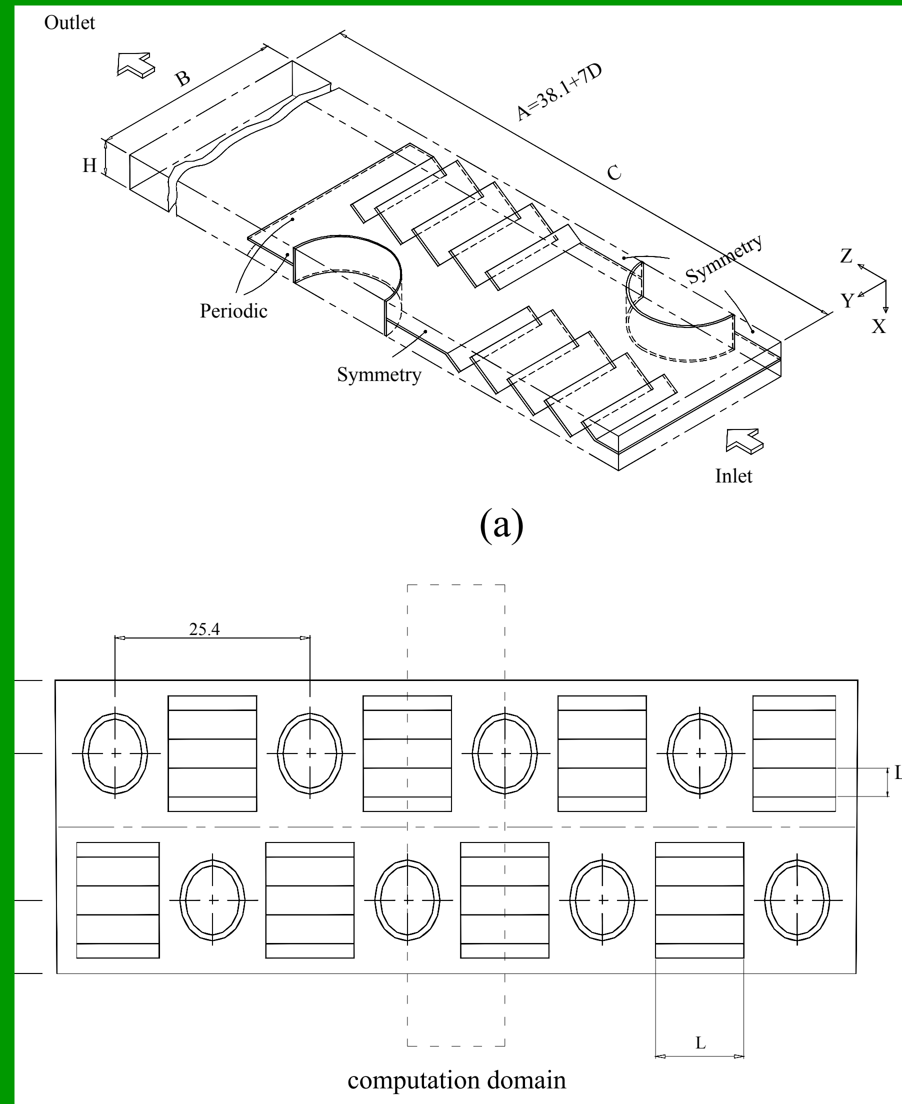

Int. J. Heat Mass Transfer, Vol. 44, pp. 4235-4243, 2001

ASHRAE Transactions, Vol. 107, part 2, pp. 510-516, 2001

Software: Phonics

Other relevant CFD software for Design/Analysis

- FLUENT
  - 熱流相關領域
  - 風扇性能研究
    - 滑動格點
    - 參數設計
  - 室內氣流模擬
    - 流場分佈
    - 污染控制
- STAR-CD
  - 室內機流場改善
  - 空氣清淨機元件設計
- FLOVENT
  - 節能示範屋
    - 速度與溫度分佈
    - 二氧化碳濃度分佈
    - 太陽輻射影響
  - 電梯氣流模擬
    - 流場最佳化設計
    - 污染控制
- ICEPAK
  - LED溫度場模擬
  - Heat sink最佳化設計

Solar Altithde Angle
Azimuth Angle

Passive method to improve airside performances - Technology Evolution

- Thermal Boundary Layer Restart
- Instability
- Thermal Wake Management
- Swirl

Air Flow

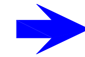

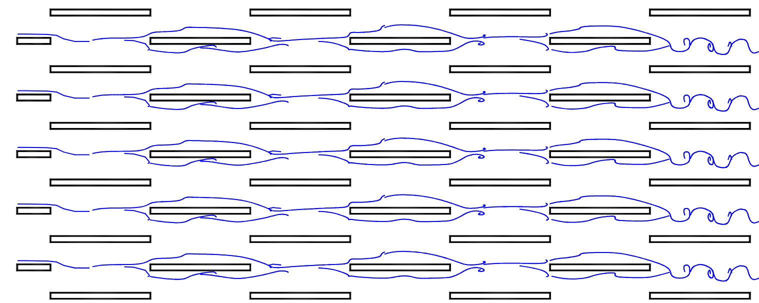

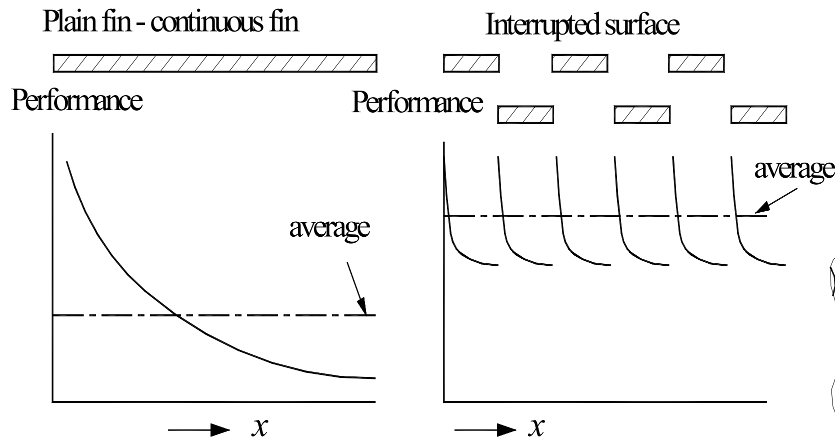

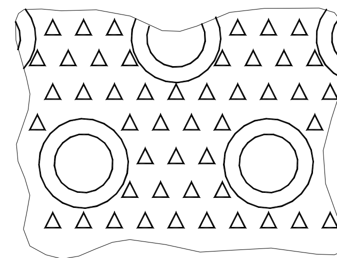

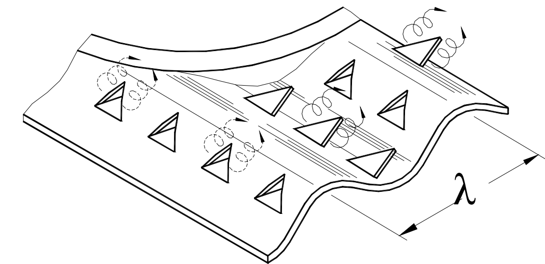

US patent 4817709

Type of vortex generators

Longitudinal vortex outperforms the transverse vortex

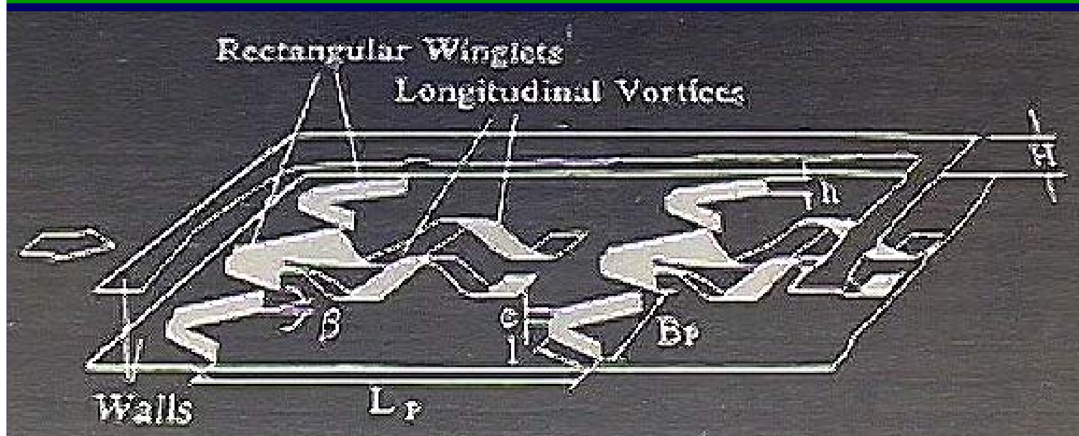

Longitudinal vortex

Transverse vortex

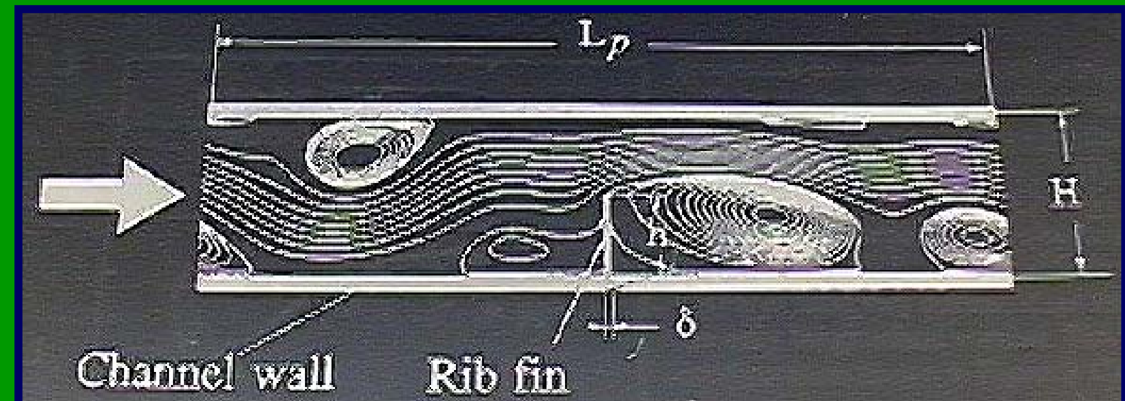

Benefits of vortex generator

- Prevent Boundary Layer separation
- Improve heat transfer performance with acceptable pressure drop

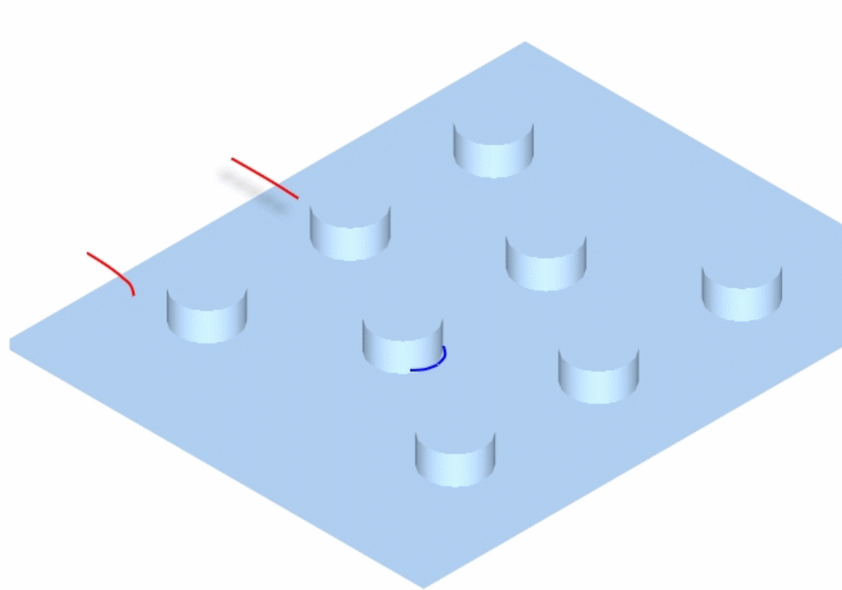

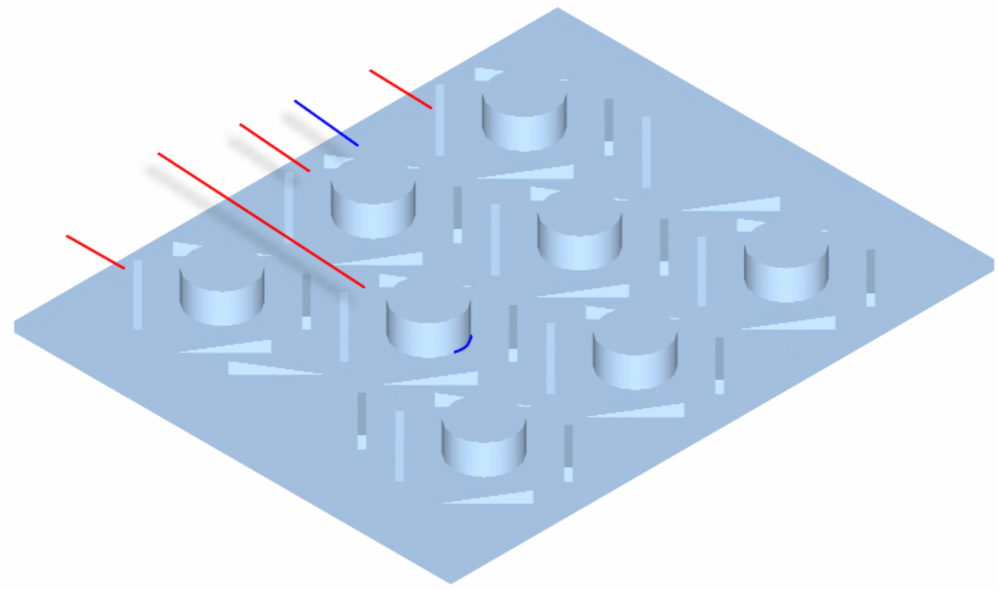

Int. J. of Heat and Mass Transfer, Vol. 45, pp. 1933-1944.
Int. J. of Heat and Mass Transfer, Vol. 45, pp. 3803-3815.

Influence of vortex generator on flowfield

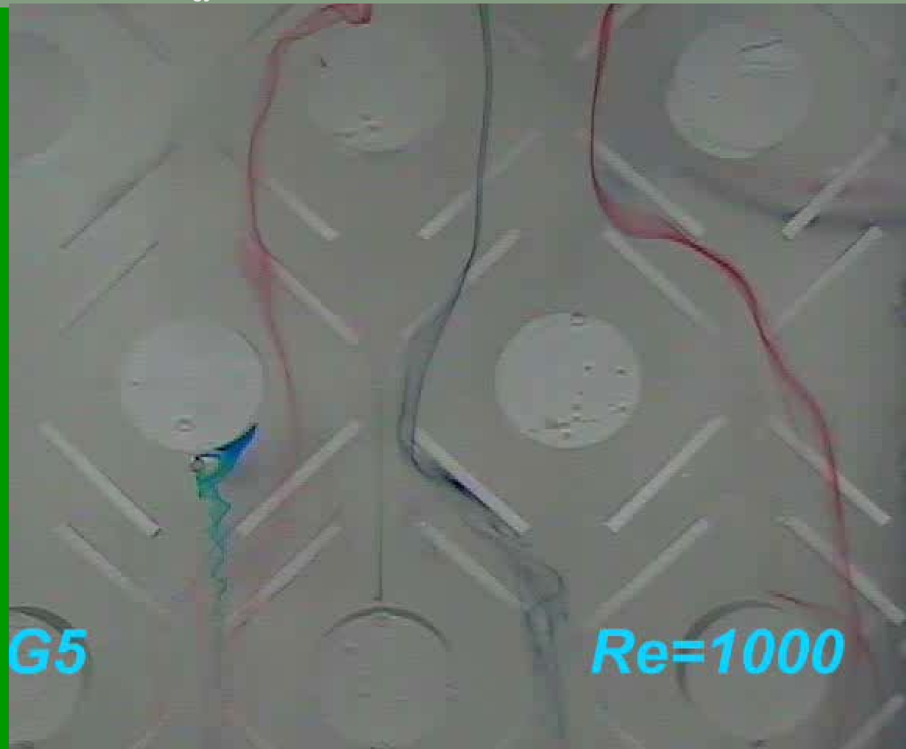

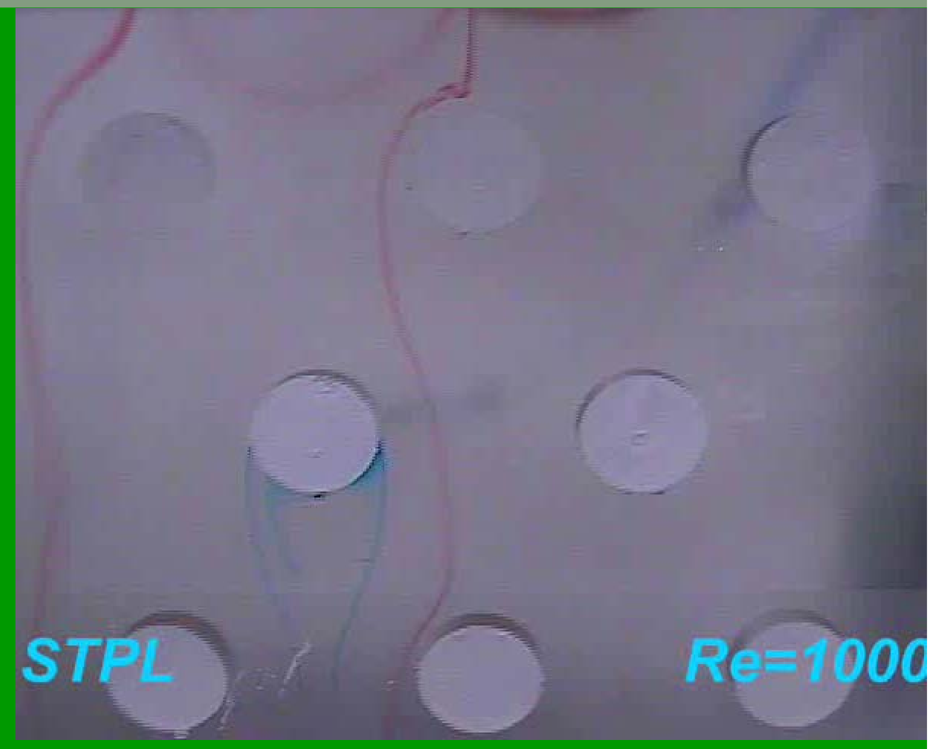

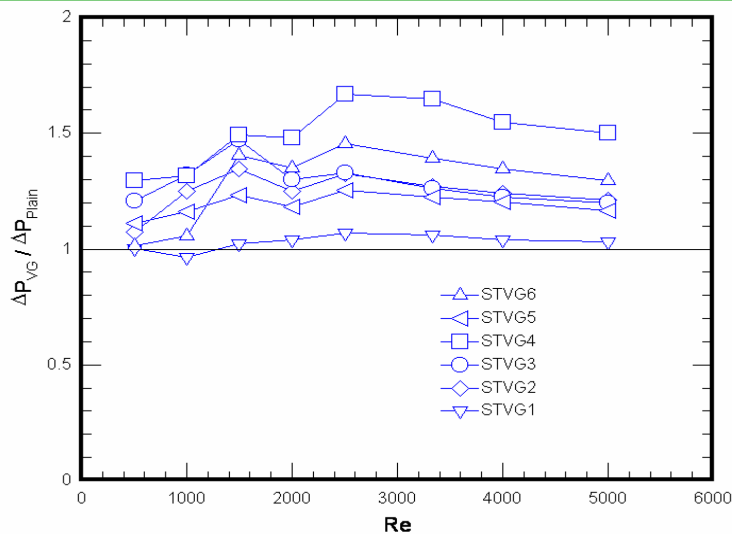

Int. J. of Heat and Mass Transfer, Vol. 45, pp. 1933-1944.
Int. J. of Heat and Mass Transfer, Vol. 45, pp. 3803-3815.

Condensate Flow Patterns

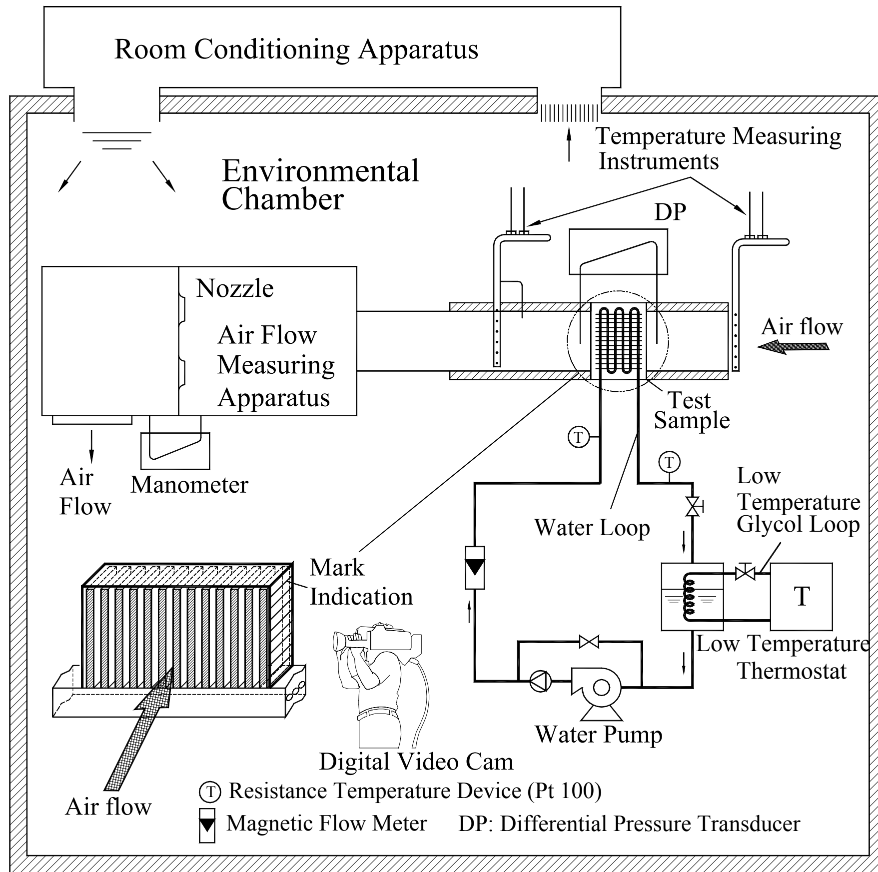

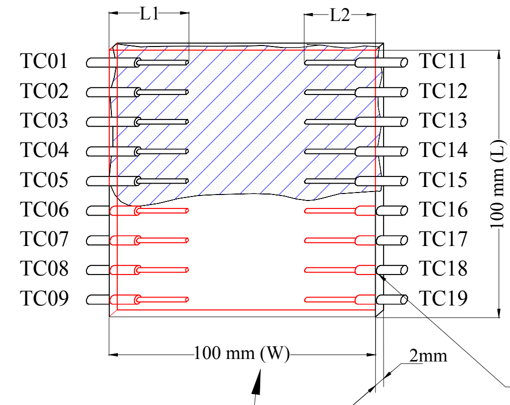

No.	L1 (mm)
TC01	22
TC02	25
TC03	30
TC04	26
TC05	36
TC06	26
TC07	35
TC08	26
TC09	24

No.	L2 (mm)
TC11	24
TC12	25
TC13	33
TC14	33
TC15	32
TC16	26
TC17	25
TC18	26
TC19	21

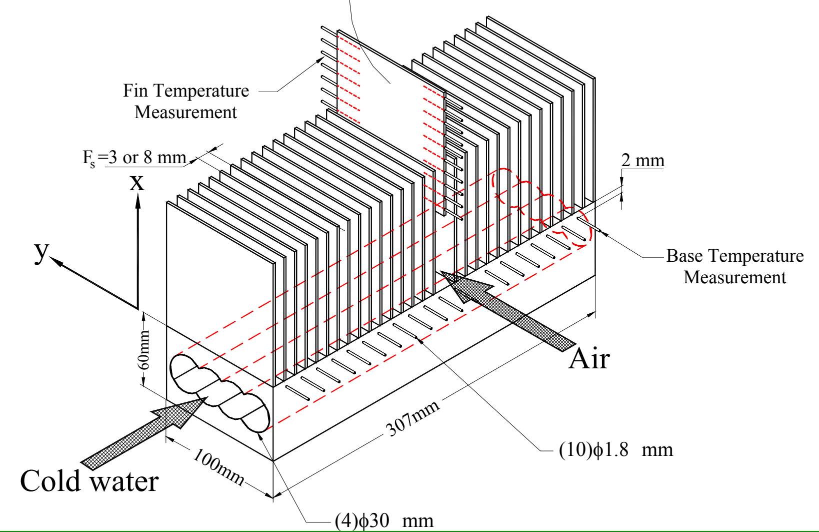

ASME J. of Heat Transfer, Vol. 123, pp. 927-836.

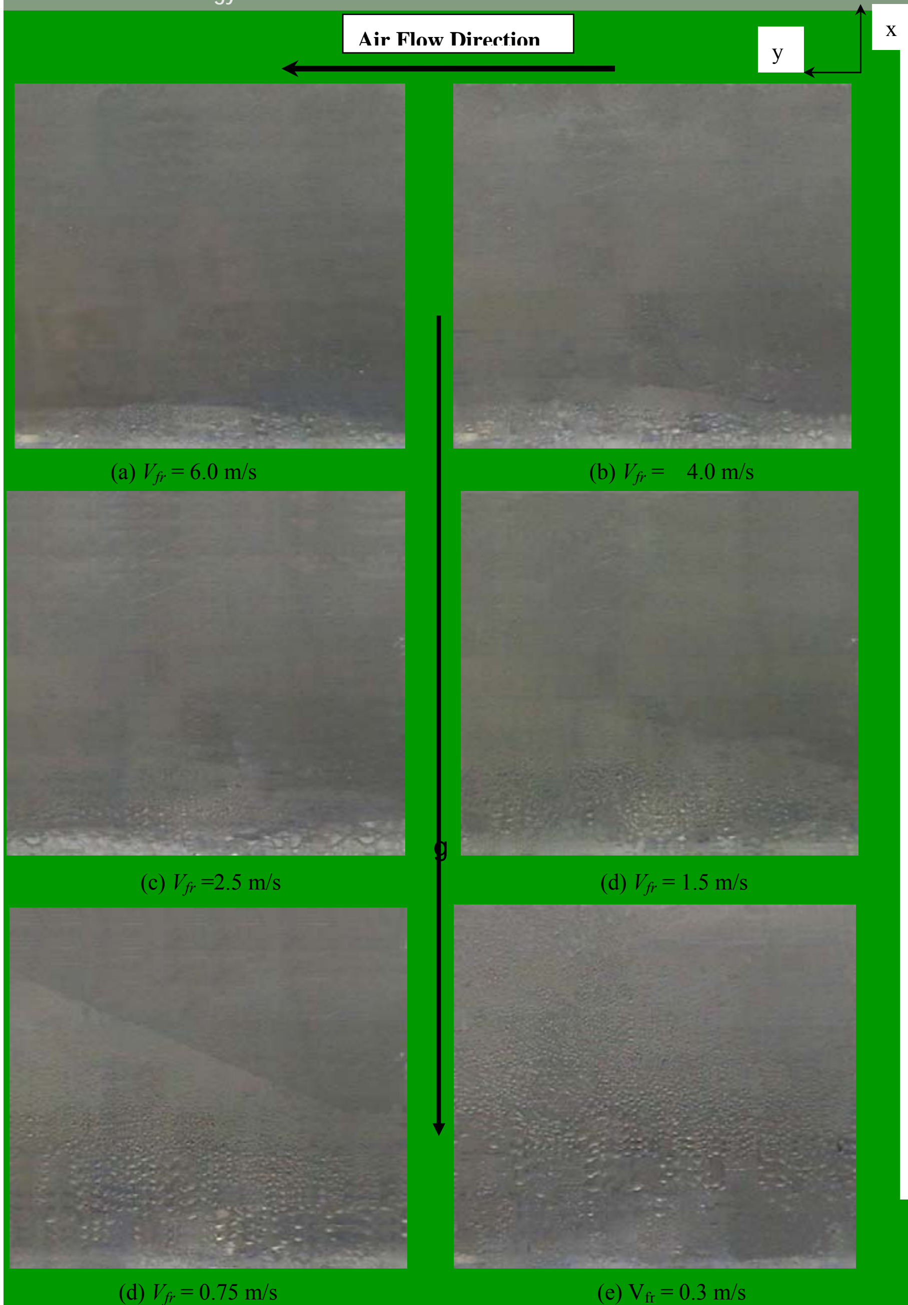

(a) V_{fr} = 6.0 m/s

(b) V_{fr} = 4.0 m/s

(c) V_{fr} =2.5 m/s

(d) V_{fr} = 1.5 m/s

(d) V_{fr} = 0.75 m/s

(e) V_{fr} = 0.3 m/s

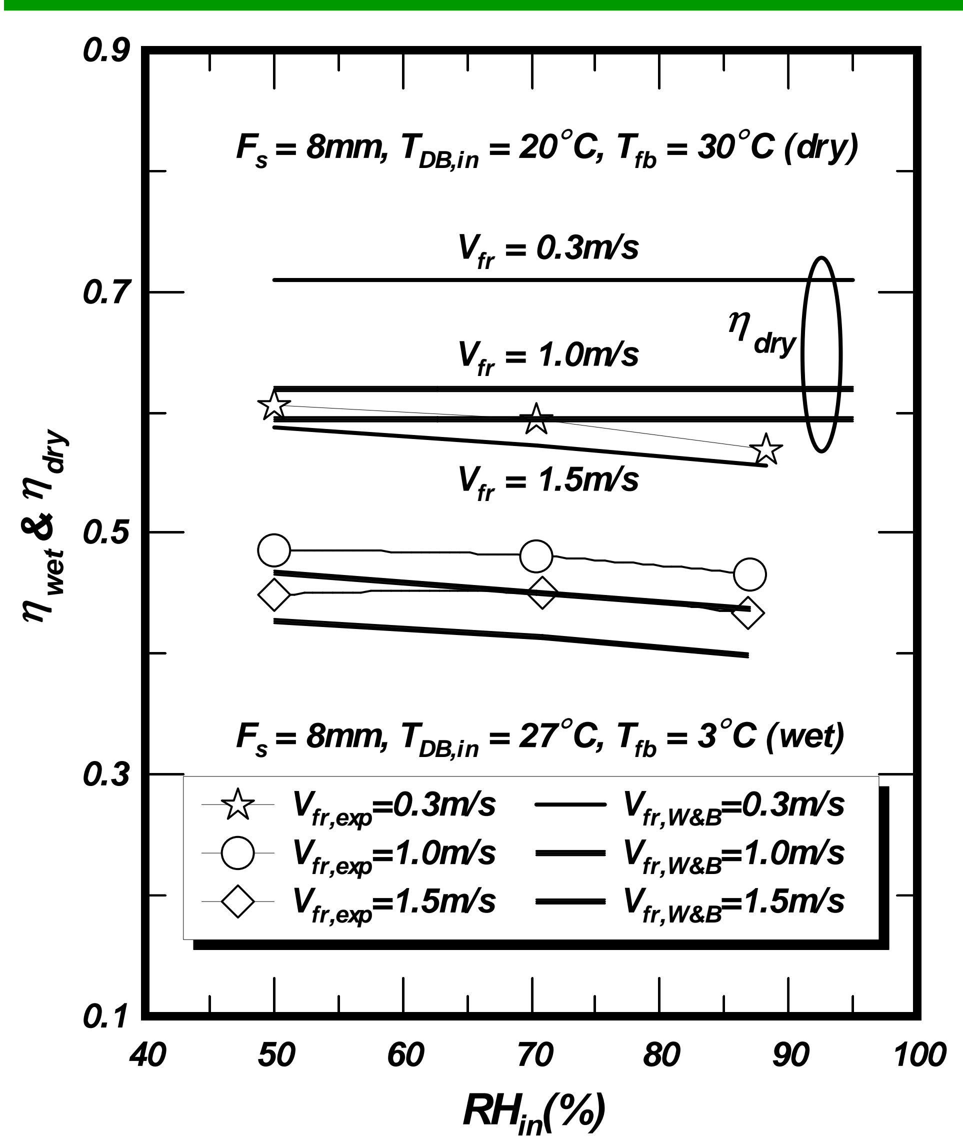

ASME J. of Heat Transfer, 2001, Vol. 123, pp. 927-836.

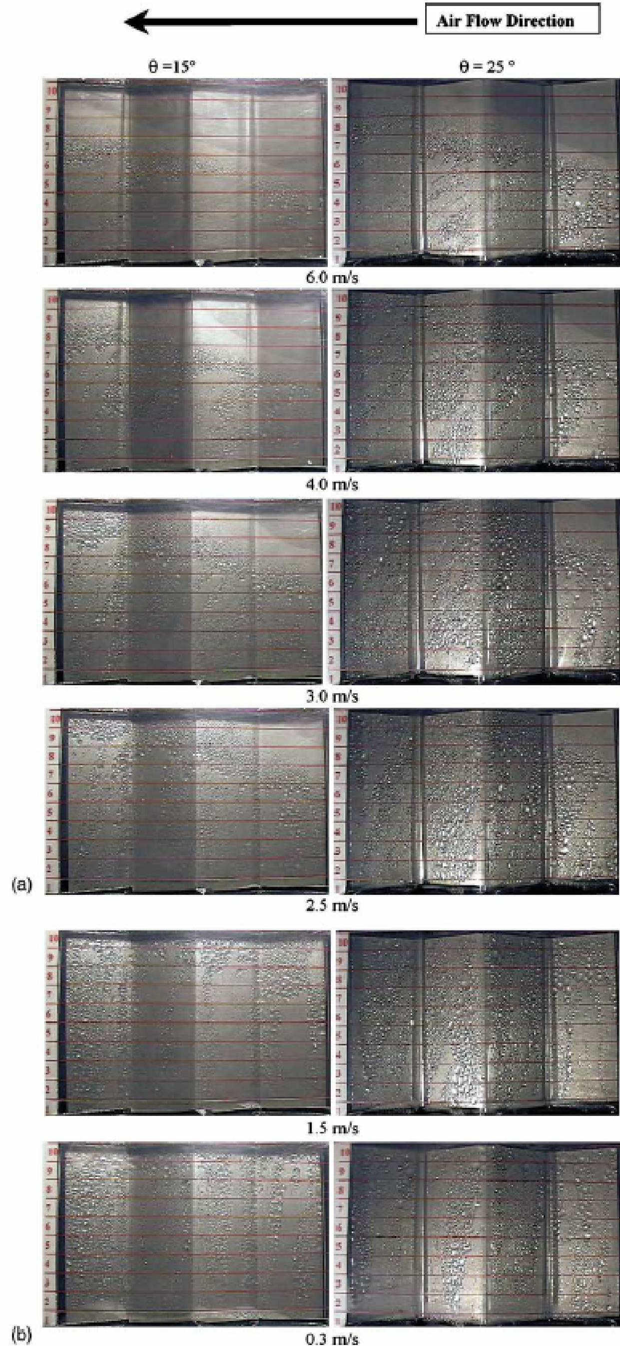

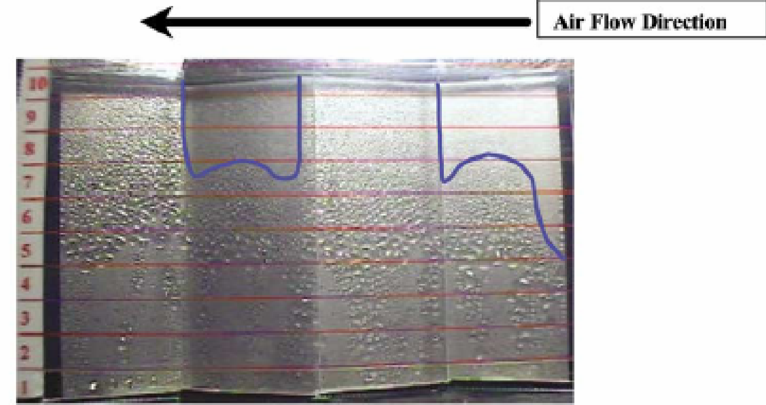

(a) $\theta = 15°$, $T_{dry} = 27$ °C, $T_{wet} = 22$ °C, $F_s = 8.4$ mm, $V_{fr} = 1.0$ m/s.

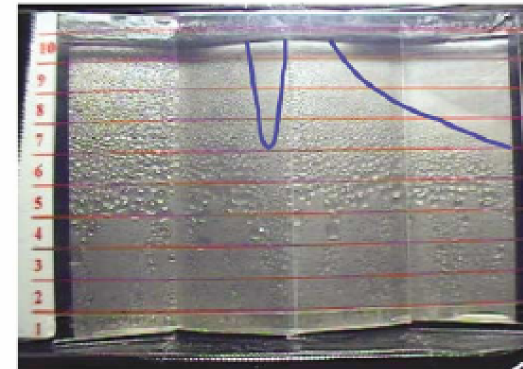

(b) $\theta = 15°$, $T_{dry} = 27$ °C, $T_{wet} = 22$ °C, $F_s = 8.4$ mm, $V_{fr} = 3.0$ m/s.

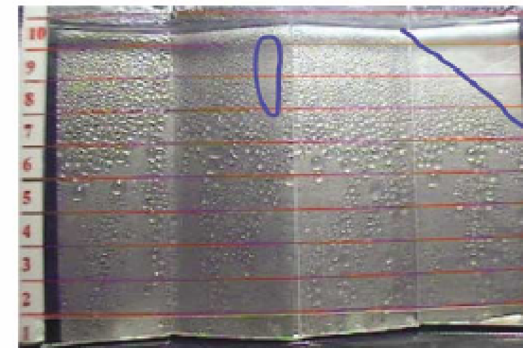

(c) $\theta = 15°$, $T_{dry} = 27$ °C, $T_{wet} = 25$ °C, $F_s = 8.4$ mm, $V_{fr} = 6.0$ m/s.

Int. J. of Heat & Mass Transfer, 2002, Vol. 45, pp. 5035-5044.

Active Heat Transfer Enhancement by EHD (Electrohydrodynamic)

Methods of Heat Transfer Enhancement：

- Active)：Need additional power input, such as vibration, electrical field, magneto field
- Passive：no additional power input such as enhanced surfaces

EHD technology:

- Place high voltage electrode to generate electrical fields, the generated electrical force will disturb the thermal boundary layer for better heat transfer

Frost formation:

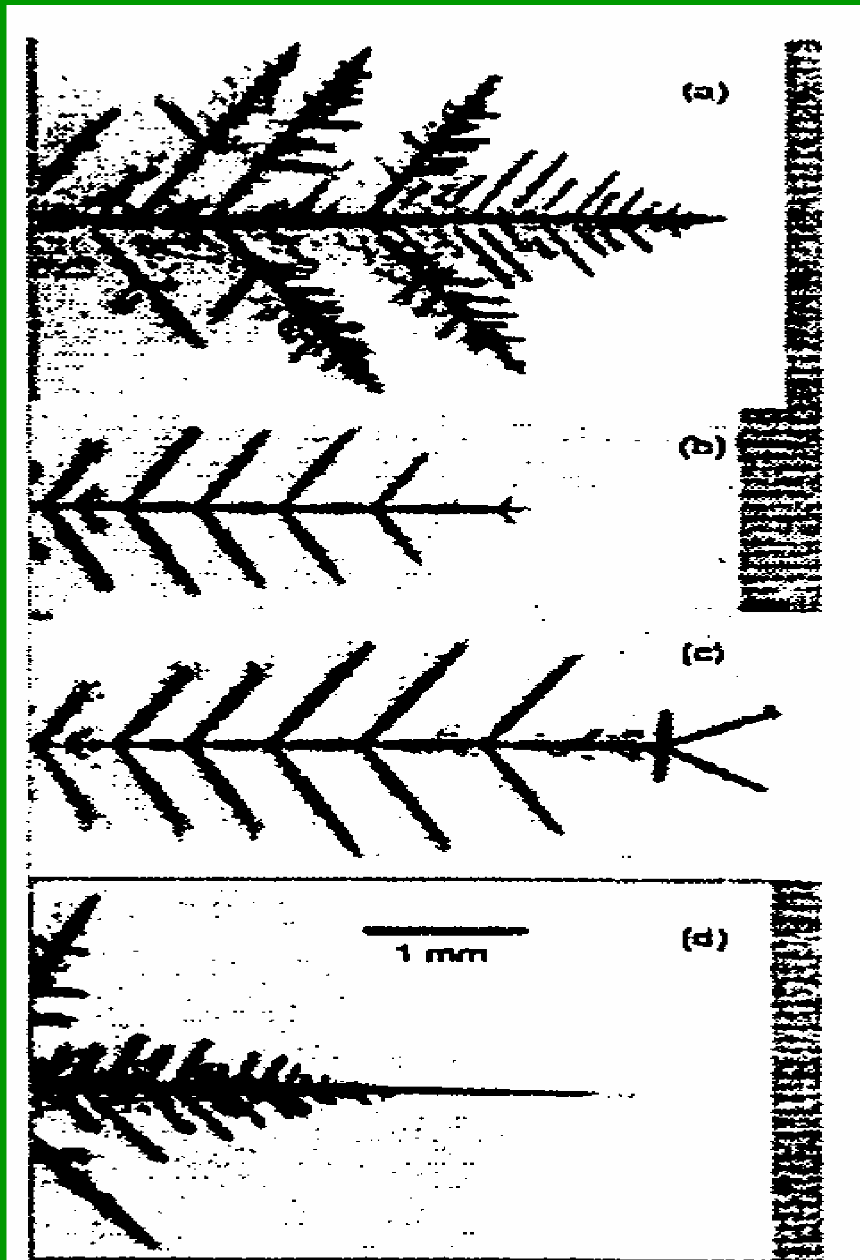

(a) No electrical field

Tree-like crystal structure

(b) E = 2000 V, crystal structure

(c) Continue from (b), crystal structure.

(d) Initially no electrical field and lately with input of electrical field

Fig. 3 Photos of the frost formation at $T_a = \pm 1°C$ and RH = 60% (without EHD).

Time	T_∞ = +1°C , RH = 60 %		T_∞ = -1°C , RH = 60 %	
	Side view	Front view	Side view	Front view
0				
1 min.				
5 min.				
10 min.				
30 min.				
1 hr.				

Fig. 5b Photos of the frost formation at T_a = -1°C and RH = 80% with negative polarity (side view).

Time	T_∞ = -1°C , RH = 80%			
	V = 0 V	V = -5 kV	V = -10 kV	V = -15 kV
0.5 hr.				
1 hr.				
1.5 hr.				
2 hr.				
2.5 hr.				
3 hr.				

***Int. J. of Heat & Mass Transfer*, 2004, Vol. 47, pp. 3491-3505.**

Int. J. of Heat & Mass Transfer, 2004, Vol. 47, pp. 3491-3505..

Tube Side Researches

- Study of Basic Heat Transfer/Friction Characteristics for Two-phase flow/single-phase flow of Alternative Refrigerants (R-134a, R-407C, R-410A, CO_2)
- Two-phase Flow Pattern/Regime Map in Straight Tubes
- Two-phase Flow Distribution in Multi-circuitry system
- Two-phase Flow Across Fittings/Valve/Return Bend/Junction

Two-phase Flow Pattern Map

單相液體 Single phase liquid

氣泡流 Bubbly flow

塊狀流 Plug flow

塊狀流 Slug flow

波浪流 Wavy flow

Intermittently dry

環狀流 Annular flow

Tube wall dry

$x = 0$

間歇流

$x = 1$

Two-phase Flow – Horizontal Tube

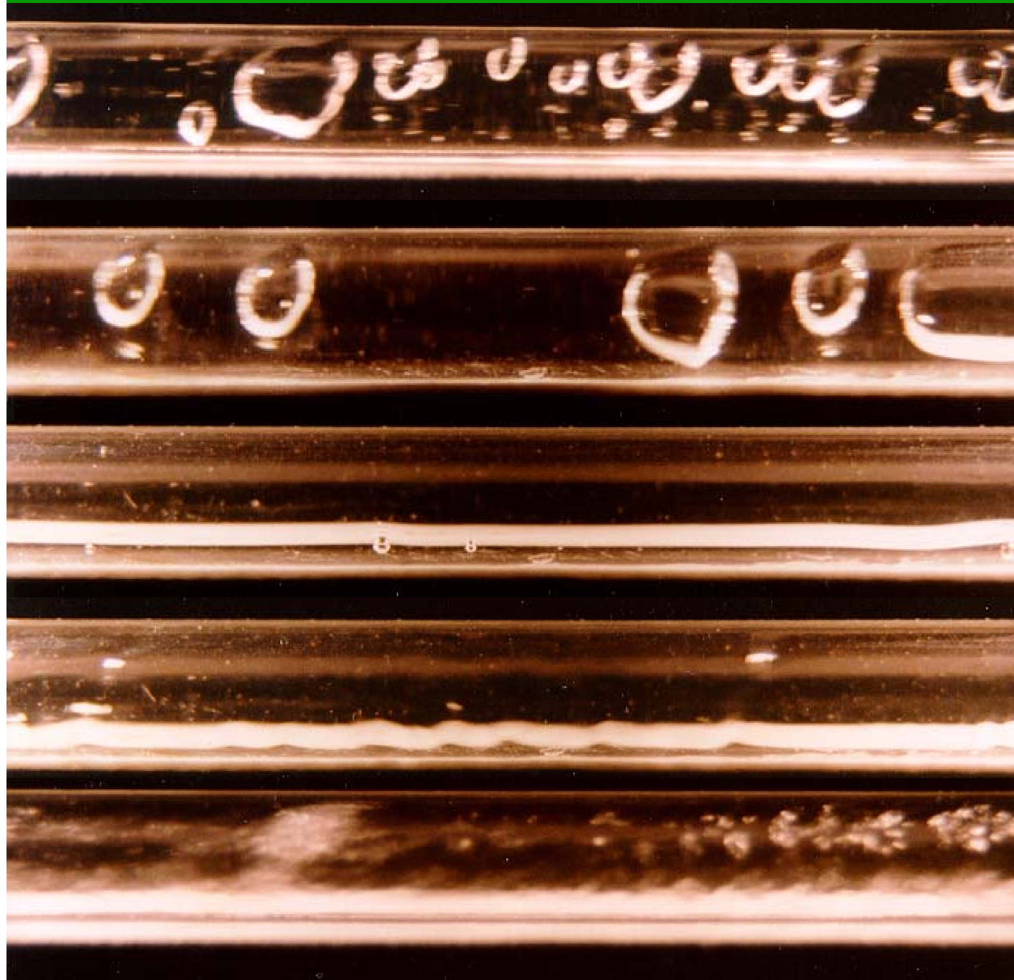

(a) Bubbly flow

(b) Slug flow (Intermittent flow)

(c) Stratified flow

(d) Wavy flow

(e) Annular flow

Single/Two-phase Flow Across Return Bend

Canadian J. of Chemical Engineering, **2001, Vol. 80, pp. 478-484.**

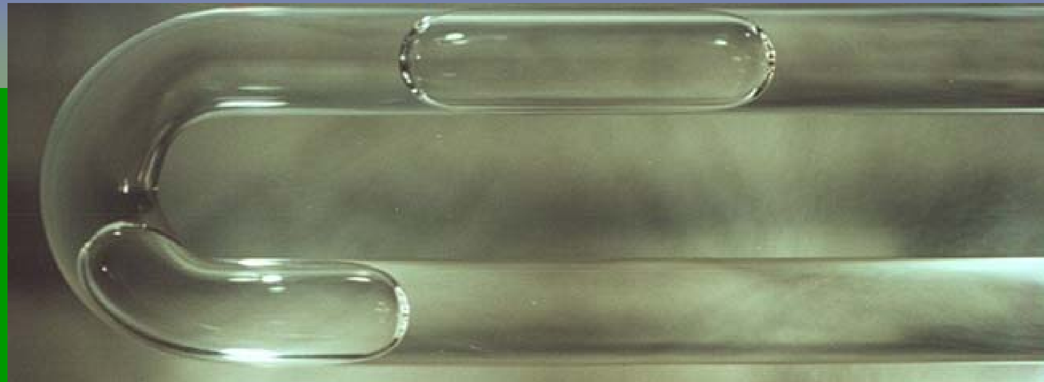

(3a) x = 0.0005, 2R/D =3, top view

(3b) Upstream, x = 0.1, 2R/D =3, side view (3c) Downstream, x =0.1, 2R/D = 3, side view

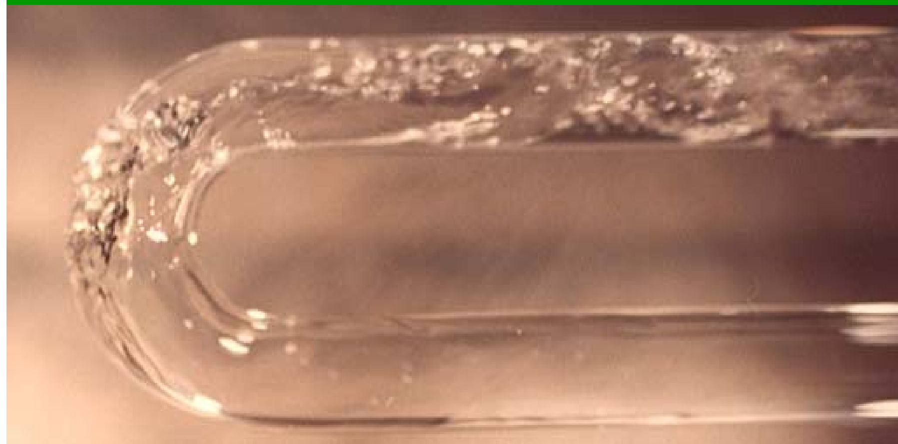

(3d) Bend, x = 0.1, 2R/D = 3, top view

(3e) Bend, x = 0.1, 2R/D = 7, x = 0.1, top view

Int. J. of Heat and Mass Transfer, 2003, Vol. 46, pp. 2975-2981.

Influence of return bend on flow pattern transition – Horizontal

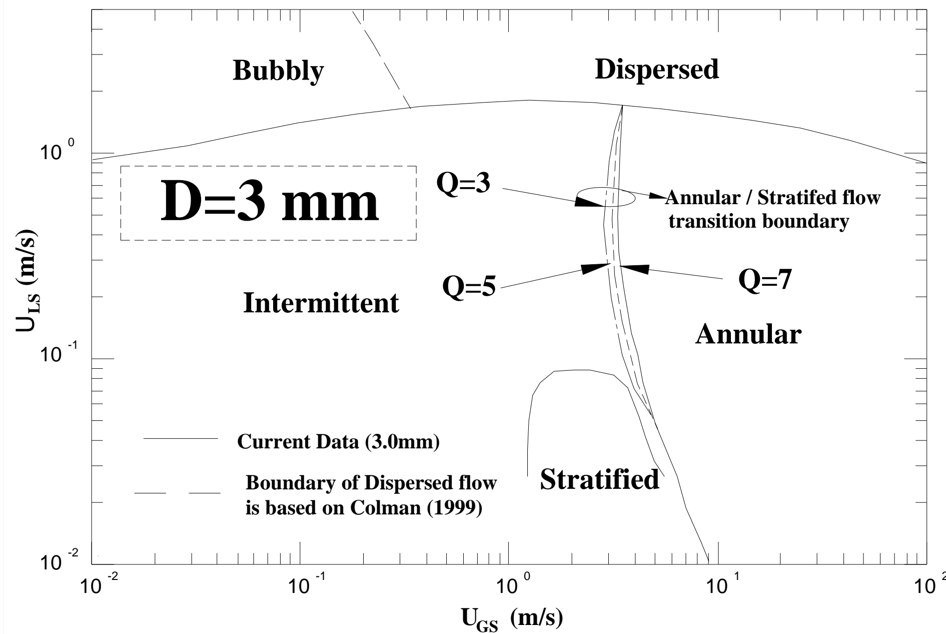

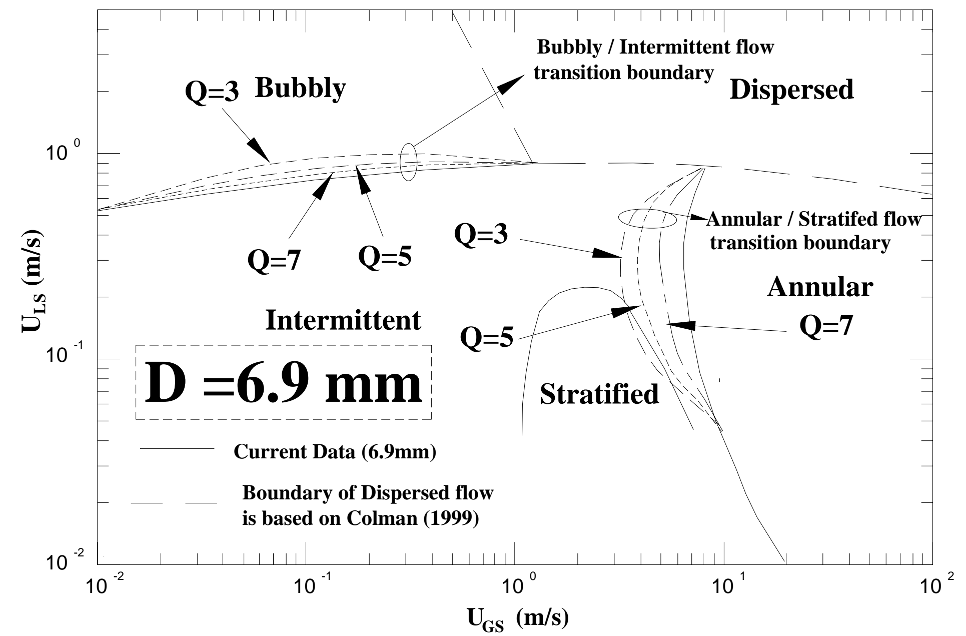

Exp. Thermal & Fluid Science, Vol. 28, pp. 145-152, 2004

Frictional characteristics of small diameter tubes (especially two-phase flow)

Chen et al. (Air-Water)[17]
Zhao and Rezkallah (Air-Water)[16]
Triplett et al. (Air-Water)[5]
Reinarts et al. (Ammonia)[13]
Hasihizume et al. (R-22)[14]
Hasihizume et al. (R-12)[14]
Zhang (R-134a)[15]
Zhang (R-404)[15]
Wang et al. (R-22)[18]
Wang et al. (R-407C)[18]
Wang et al. (R-410A)[18]
Yang et al. (R-125)[7]
Yang et al. (R-407C)[7]

+50%
-50%

Modified Homogenous Pressure Gradient (Pa/m)

Measured Pressure Gradient (Pa/m)

10^1 10^2 10^3 10^4 10^5 10^6 10^7

Int. J. of Heat and Mass Transfer, 2002, Vol. 45, no. 17, pp. 3667-3671.

Frictional Characteristics in Return Bend (single-phase & Two-phase)

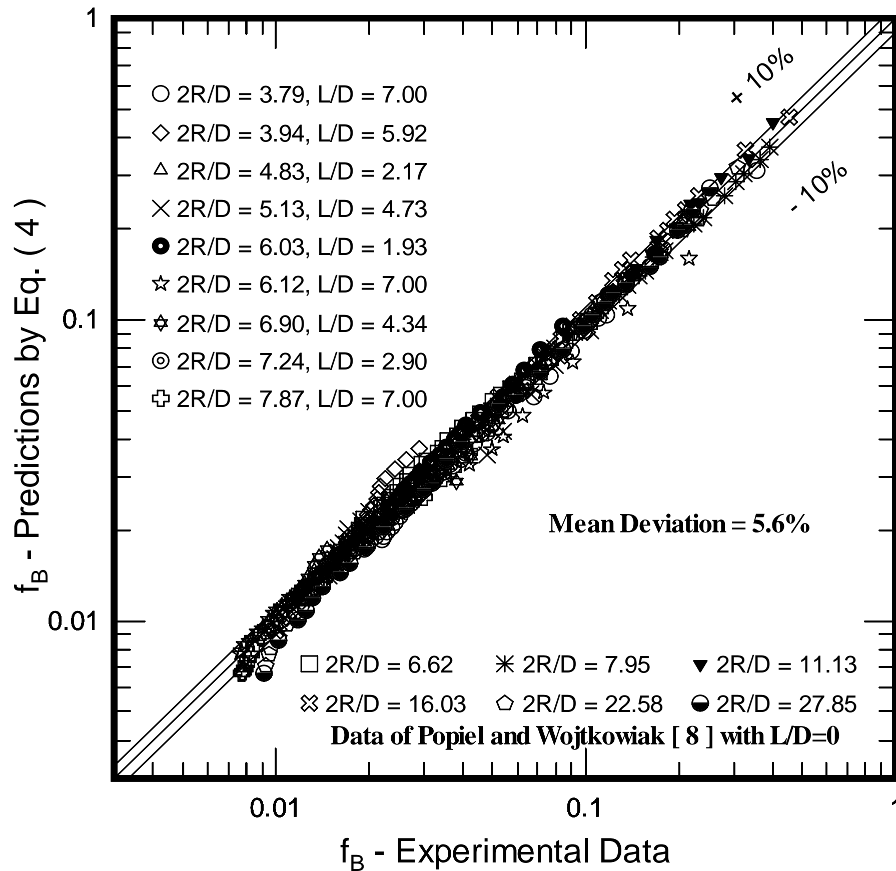

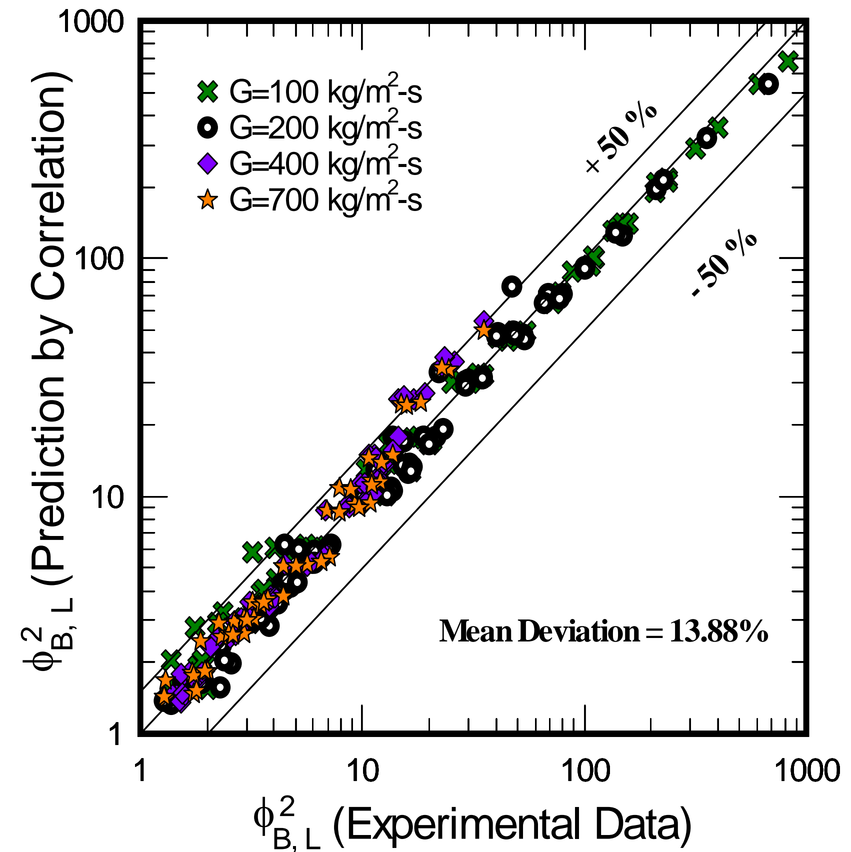

ASME J. of Fluid Engineering, 2003, Vol. 125, pp. 880-886

AIAA J. of Thermophysics & Heat Transfer, 2004, Vol. 18, pp. 364-369.

Two-phase flow across Vertical Return Bend
D = 7 mm, G = 50 kg/m²·s, Entering at Lower tube

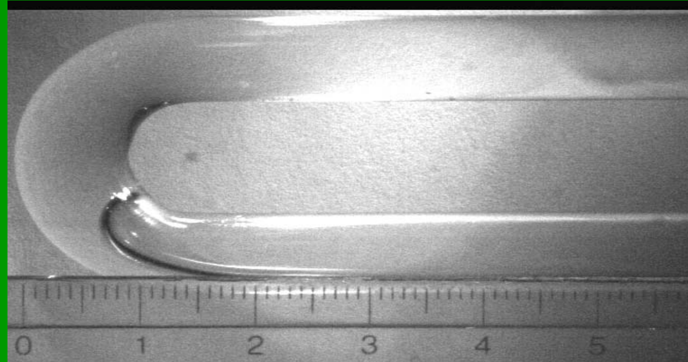

(a) t = 0, $2R/D$ = 3

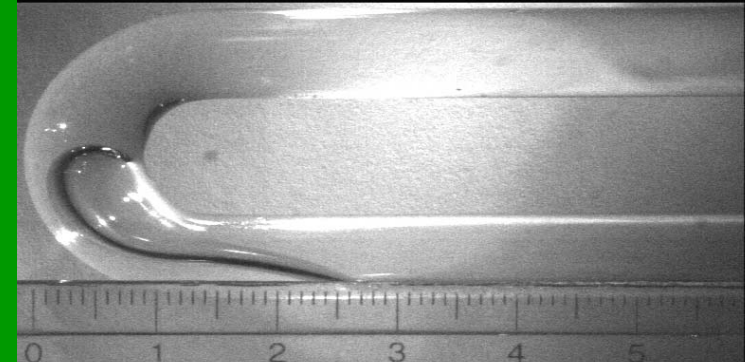

(b) t = 0.385 s, $2R/D$ = 3

(c) t = 0.539 s, $2R/D$ = 3

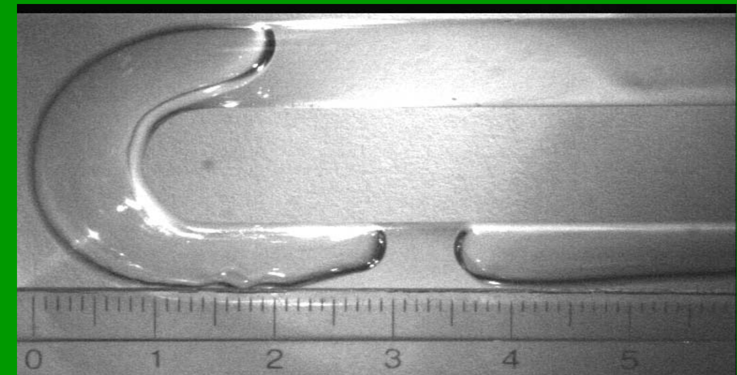

(d) t = 0.616 s, $2R/D$ = 3

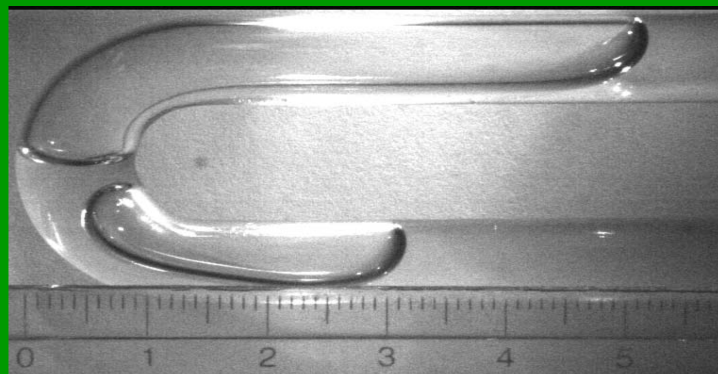

(e) t = 0.77 s, $2R/D$ = 3

(f) t =1.309 s, $2R/D$ = 3

Int. J. of Heat and Mass Transfer, 2005, Vol. 48, pp. 2342-2346.
The Canadian J. of Chemical Engineering, 2005, Vol. 83, pp 548-553

Two-phase flow across Vertical Return Bend

D = 7 mm, G = 50 kg/m^2·s, Entering at Upper tube

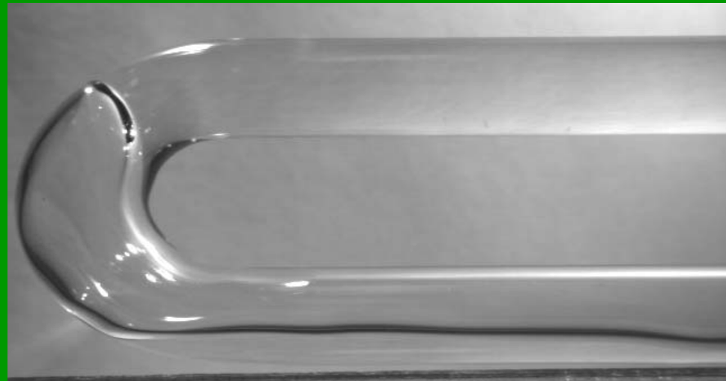

t = 0 s, $2R/D$ = 3

(b) t =0.693 s, $2R/D$ = 3

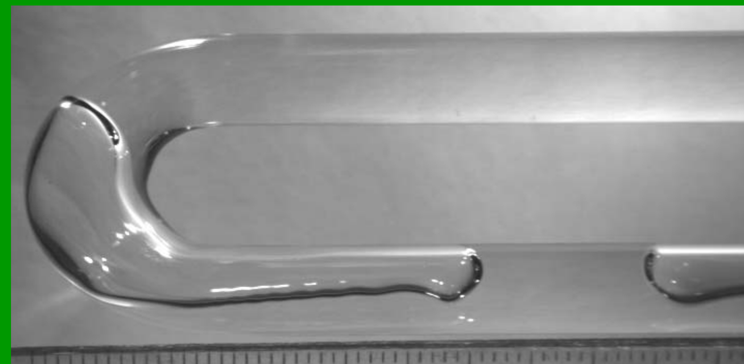

(c) t =0.77 s, $2R/D$ = 3

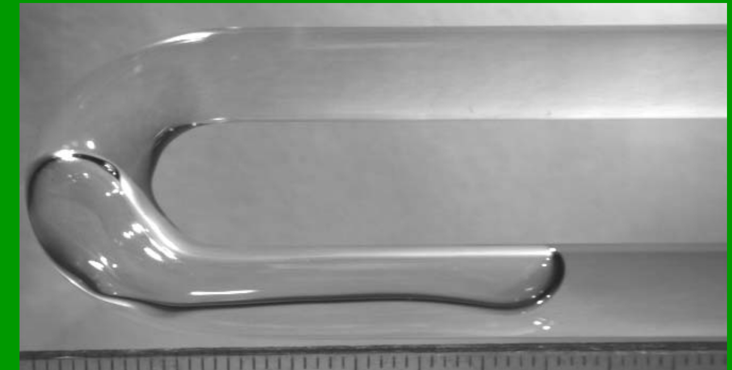

(d) t = 1.309 s, $2R/D$ = 3

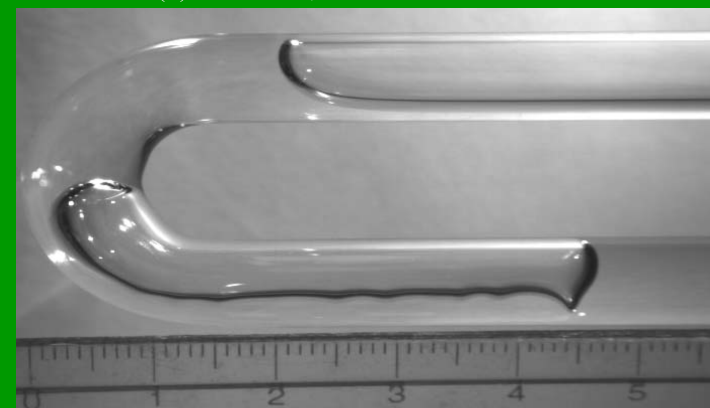

(e) t = 1.771 s, $2R/D$ = 3

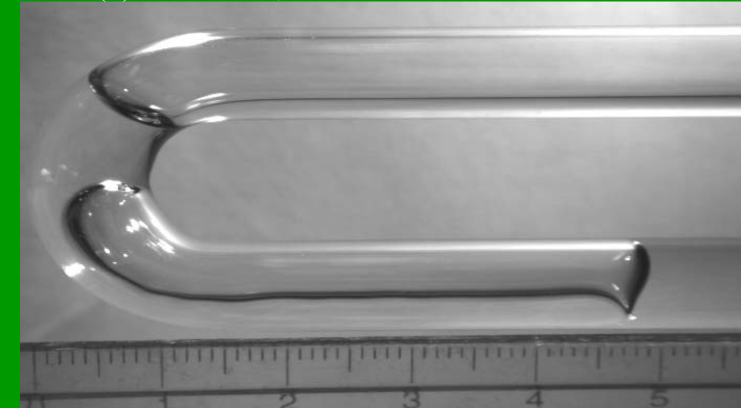

(f) t =1.925 s, $2R/D$ = 3

***Int. J. of Heat and Mass Transfer*, 2005, Vol. 48, pp. 2342-2346.**

***The Canadian J. of Chemical Engineering*, 2005, Vol. 83, pp 548-553**

Two-phase flow across U-tube Junction
D = 3 mm, G = 100 kg/m^2·s, Vertical Arrangement

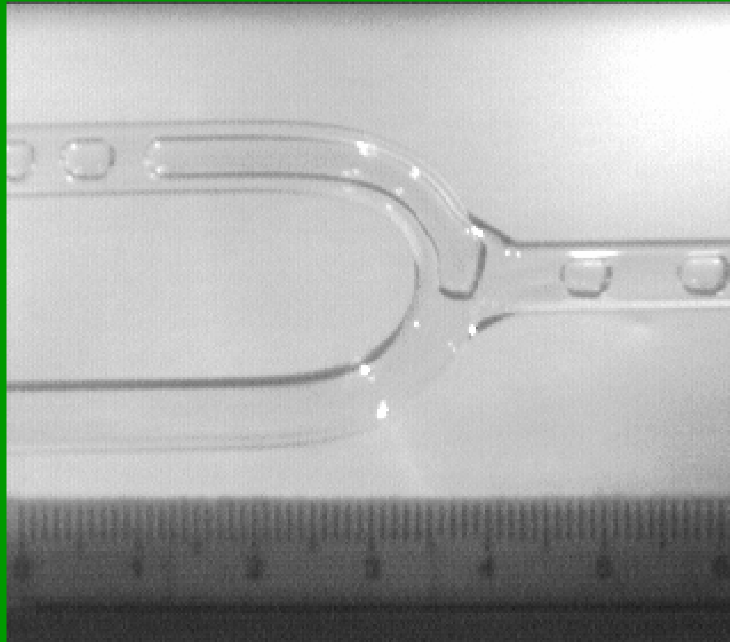

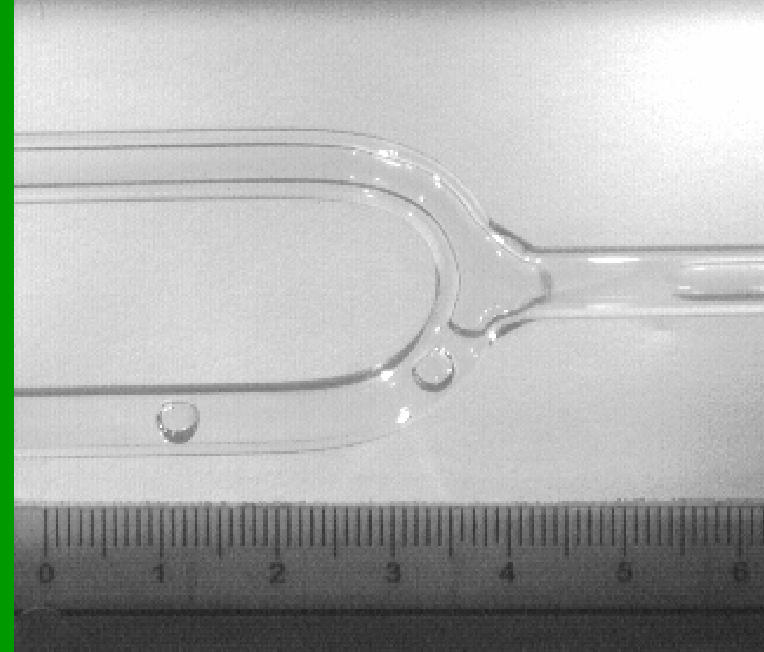

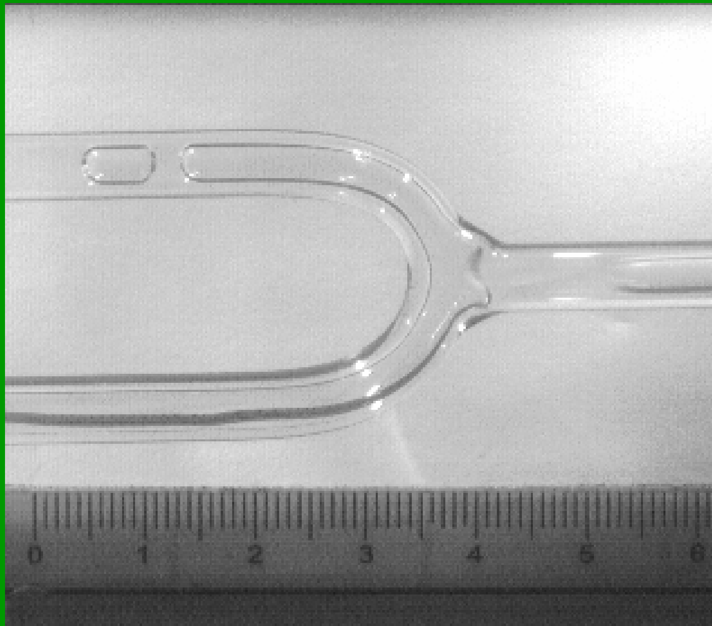

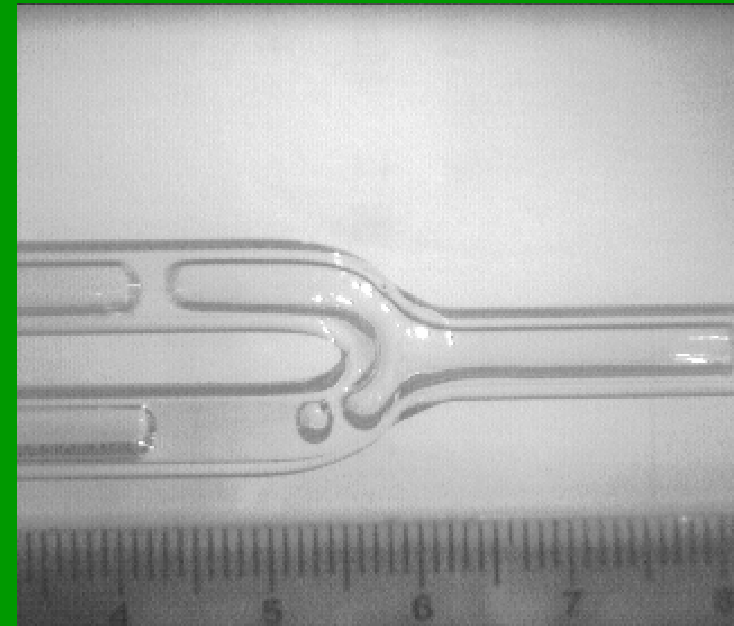

Papers in Review

Influence of Circuitry on the performance of Fin-and-tube HXs

Int. J. of Refrigeration, 1999, Vol. 22, No. 4, pp. 275-282.

ASME J. of Energy Resources Technology, 2003, Vol. 123, pp. 100-103.

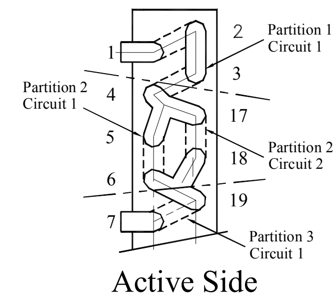

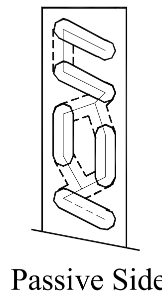

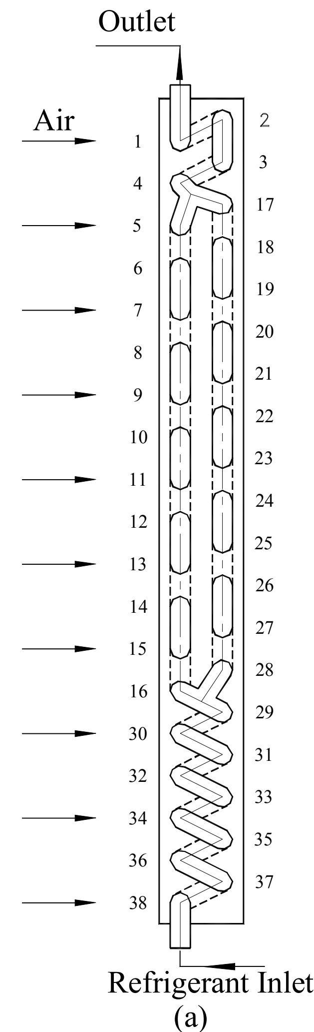

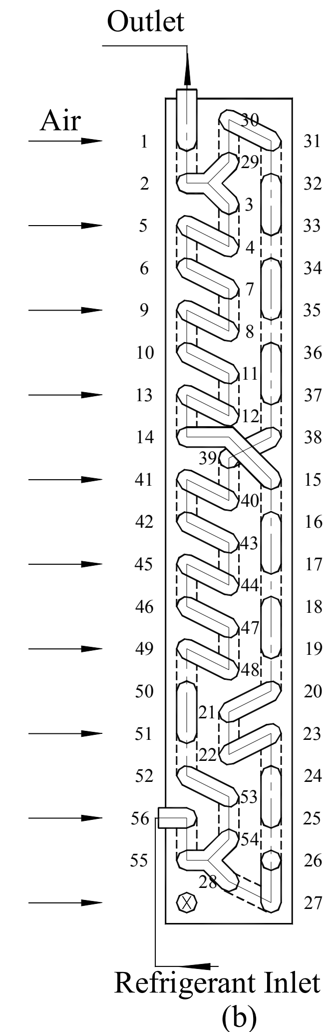

工業技術研究院
能源與資源研究所
Industrial Technology Research Institute
Energy & Resources Laboratories

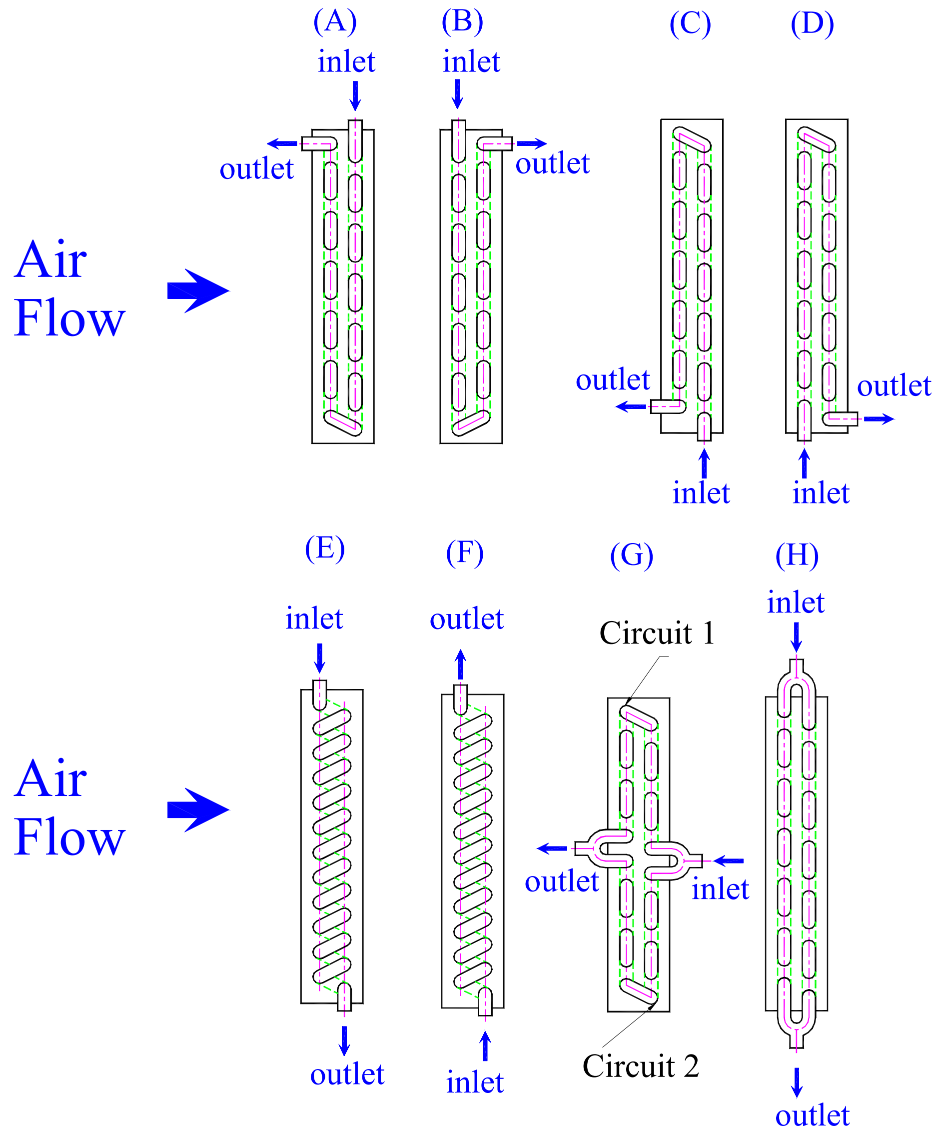

Air Flow
(A)
inlet
outlet
(B)
inlet
outlet
(C)
outlet
inlet
(D)
outlet
inlet
Air Flow
(E)
inlet
outlet
(F)
outlet
inlet
(G)
Circuit 1
outlet
inlet
Circuit 2
(H)
inlet
outlet

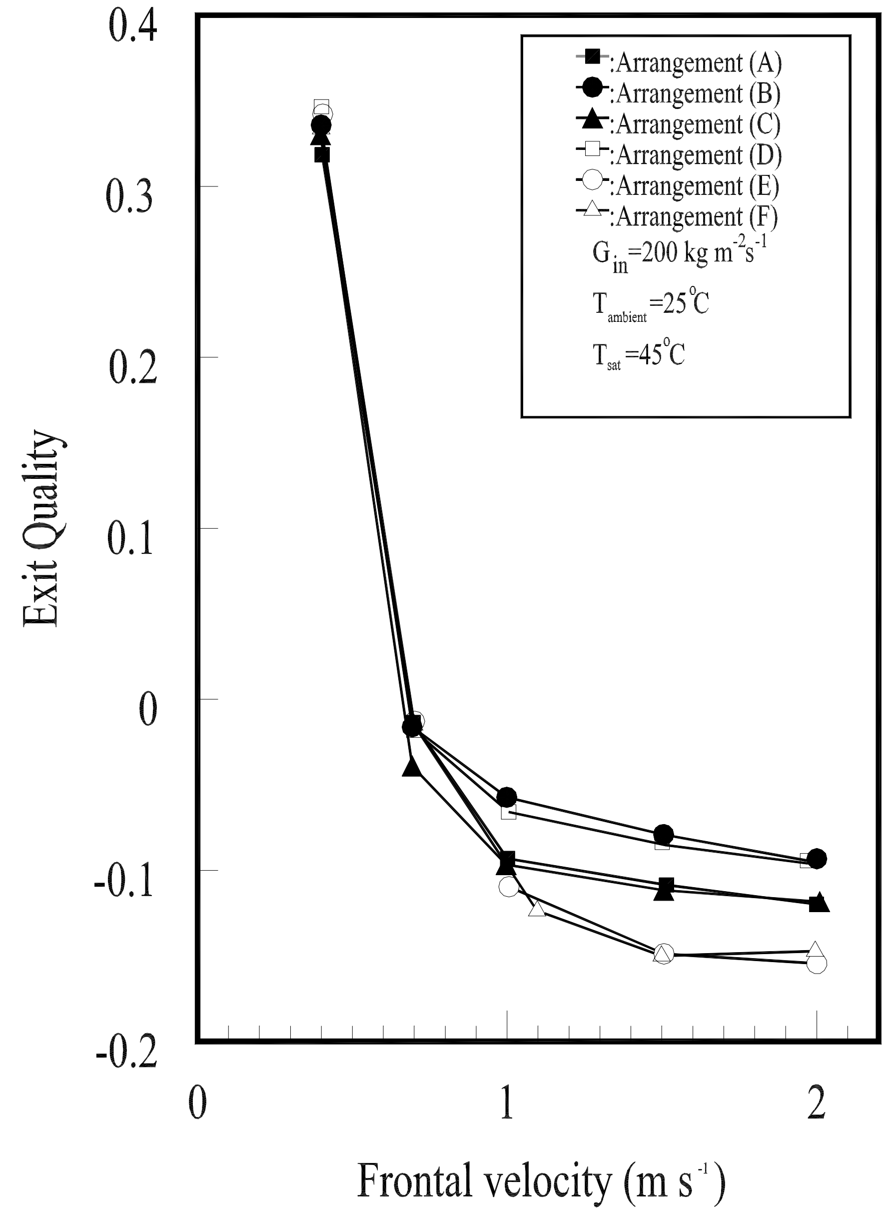

:Arrangement (A)
:Arrangement (B)
:Arrangement (C)
:Arrangement (D)
:Arrangement (E)
:Arrangement (F)
G_{in}=200 kg $m^{-2}s^{-1}$
$T_{ambient}$=25°C
T_{sat}=45°C
Exit Quality
Frontal velocity (m s^{-1})
0.4
0.3
0.2
0.1
0
-0.1
-0.2
0
1
2

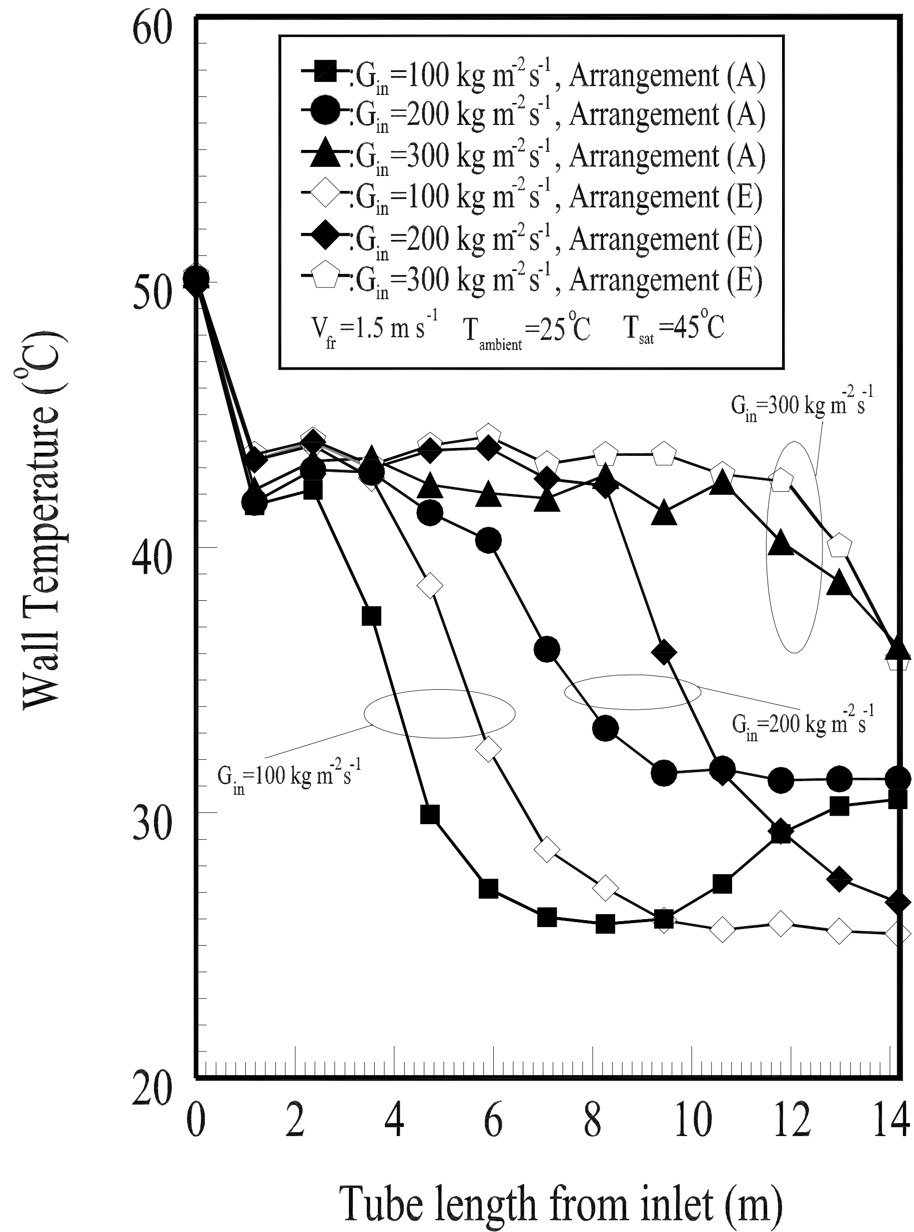

:G_in=100 kg m-2 s-1, Arrangement (A)
:G_in=200 kg m-2 s-1, Arrangement (A)
:G_in=300 kg m-2 s-1, Arrangement (A)
:G_in=100 kg m-2 s-1, Arrangement (E)
:G_in=200 kg m-2 s-1, Arrangement (E)
:G_in=300 kg m-2 s-1, Arrangement (E)
V_fr=1.5 m s-1 T_ambient=25°C T_sat=45°C
G_in=300 kg m-2 s-1
G_in=200 kg m-2 s-1
G_in=100 kg m-2 s-1
Wall Temperature (°C)
Tube length from inlet (m)

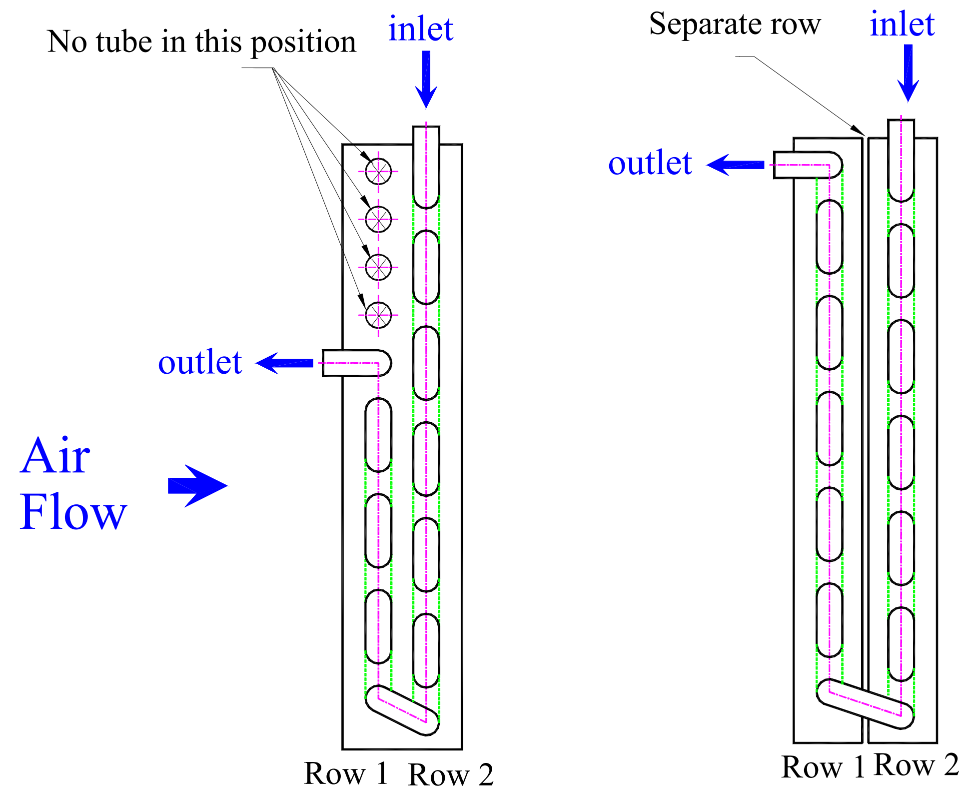

No tube in this position
inlet
outlet
Air
Flow
Row 1
Row 2
Separate row
inlet
outlet
Row 1
Row 2

Applications – Integration of the data/knowledge into design software

- Condenser/Evaporators Design program
- System Performance Design Program
- Capable of simulations of a very complex circuitry integrated with the test data/information
- Detailed program outline can be seen from *ASHRAE Transactions*, 2003, Vol. 108, part 2, pp. 529-534.

On-going Projects associated macro-scale Fluid Flow/Heat Transfer Applications

- Two-phase flow across sharp return bend
- Two-phase flow across sudden contraction/expansion Junctions
- Next generation high performance fin-and-tube heat exchangers – subject to pressure drops concerns – an integration of oval tube & vortex generators
- Performance of fin-and-tube heat exchangers under partially wet conditions

Efforts of Electronic Cooling in our Group …

散熱技術之應用

電子產品在輕薄短小、高性能與多功能之發展趨勢下，除了原有產品散熱能力需求增加外，同時有更多的電子產品需要散熱。

散熱技術已經應用在以下各個產品之中：

- 桌上型電腦、筆記型電腦
- 繪圖加速卡
- 伺服器
- 投影機
- LCDTV
- LED 照明設備
- 電源供應器
- ．．．．．．．．．

Road Map

Estimated Thermal Design Power (W)

80
70
60
50
40
30
20
10

Intel 386
Intel 486 processor
Pentium processor
Pentium Pro processor
P2 processor
P3 processor
P4 processor

Pentium 4-3.0G
Pentium 4-2.8G
Pentium 4-2G
Pentium 4-2.6G
Pentium 4-1.4G
Pentium 4-2.4G
Pentium 4-2.2G
Pentium 3-800
P2 processor-300
Pentium 3-600
Pentium Pro Processor 200
Pentium 3-1G
Pentium Pro Processor 150
Pentium 3-450
P5-66
P2 processor-350
P54C-100
P55C-233
P54CS-200
I486DX2-68
P54CS-133
Io386
I406-25
DX4-100
I486SLE-50

Source : Intel

1988 1989 1990 1991 1992 1993 1994 1995 1996 1997 1998 1999 2000 2001 2002 2003 2004

Needs for Electronic Cooling

RELIABILITY

MECHANICAL

-WIRE BOND FAILURE

-DIE FRACTURE

-CORROSION

ELECTRICAL

-ELECTRICAL OVERSTRESS

-ELECTROMIGRATION

-GATE OXIDE BREAKDOWN

-ION DIFFUSION CAUSING PARAMETER SHIFTS

PERFORMANCE

-OUTPUT LOGIC SWING

-SWITCHING SPEED

-NOISE MARGINS

-SIGNAL DEGRADATION

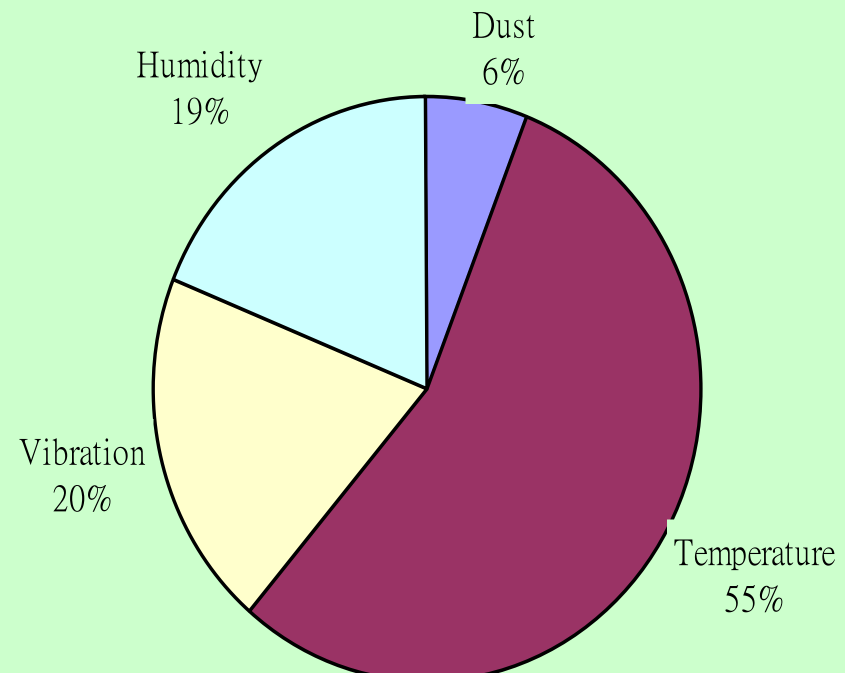

Background

(Intel internal Report for Processor's Thermal Trends)

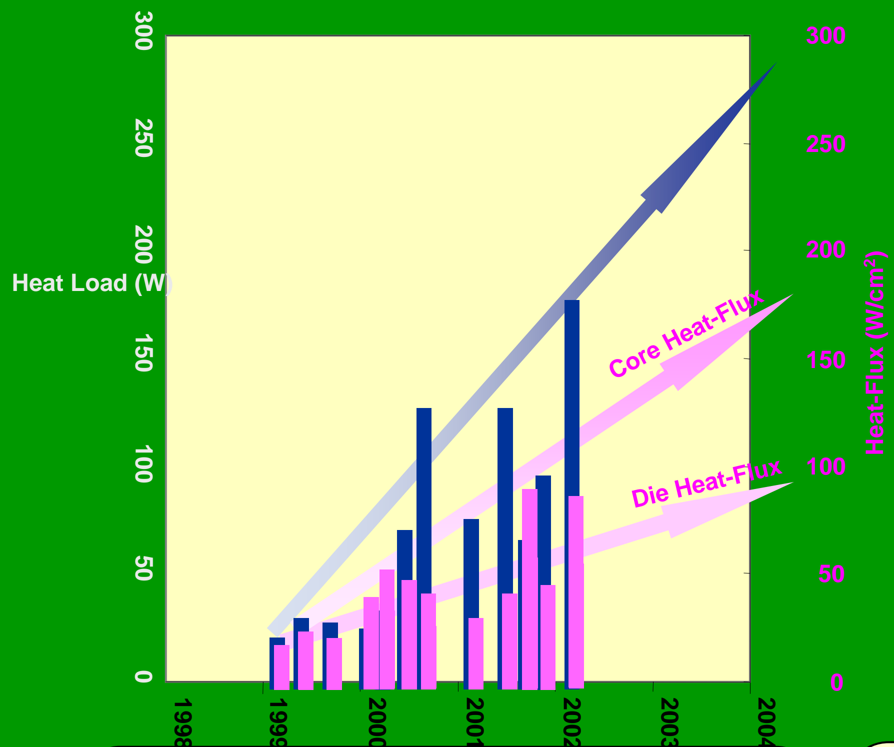

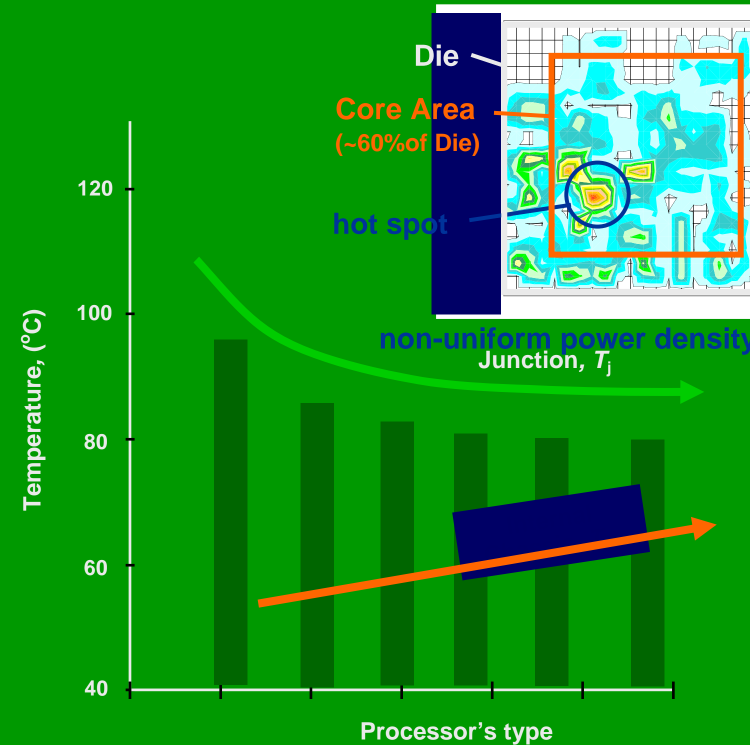

In 5 years:

- Device power reaching 300W
- Average die level heat-flux over 100W/cm²
- Core heat-flux approaching 200W/cm²

- As performance has been increased, a trend toward lower chip temperature requirement and the same time that internal temperatures within the chassis are increasing due to increased thermal loads. The net result is : a lot less thermal Budget to work with.
  - Higher T_{air} due to increased integration and legacy

Heat Dissipation Development

(Based on Intel Internal Report)

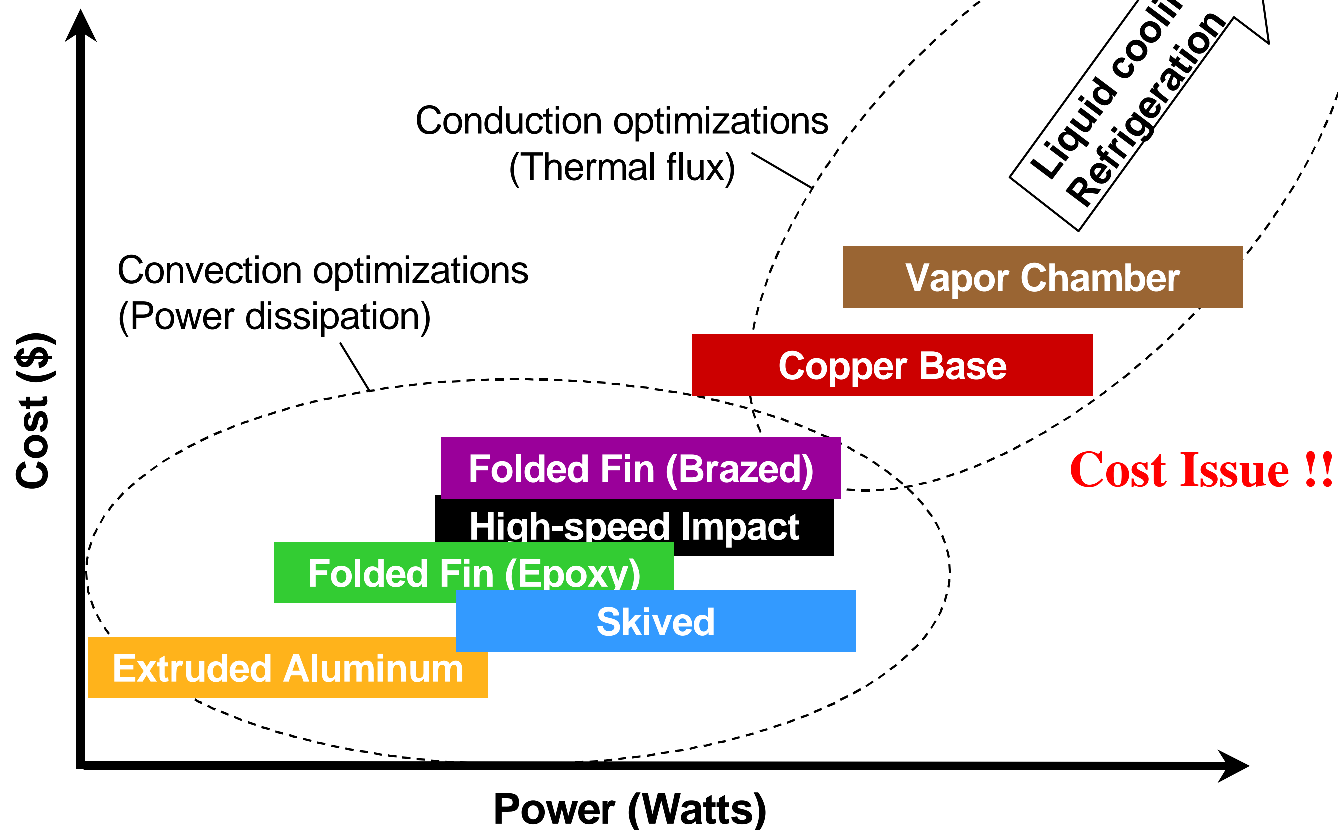

Cost Issue !!

- P4 3.4G with 2mb L3 cache - 102.9 W
  - 空冷
    - 增加風扇轉速
    - 噪音
    - 改善散熱鰭片設計
    - 散熱量已將近極限
  - 水冷
  - 微冷凍系統
  - 市場產值及需求大

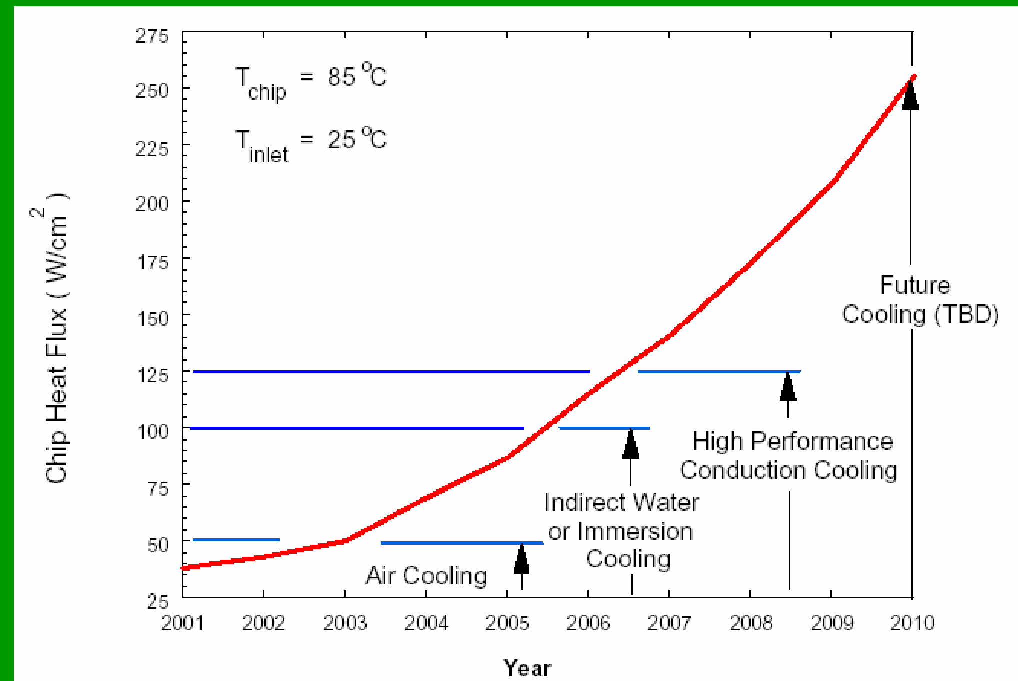

Supply Chain

CPU廠

新規格

New CPU Spec.
要求提供Solution for CPU
(特定廠商)

● 提供Solution
● 若無Solution
CPU可能會延後上市

DT
NB
系統廠

新規格，要求提供Solution for System

Cooler, Module 廠

提供Solution

Thermal Team

Fan
Heat Pipe
Heat Sink
Die-cast
Press
…….

Thermal Solution is a MUST for IT Industry!

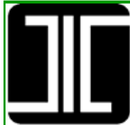

工業技術研究院
能源與資源研究所
Industrial Technology Research Institute
Energy & Resources Laboratories

GLOBAL THERMAL MANAGEMENT HARDWARE REVENUE BY SUBPRODUCTS

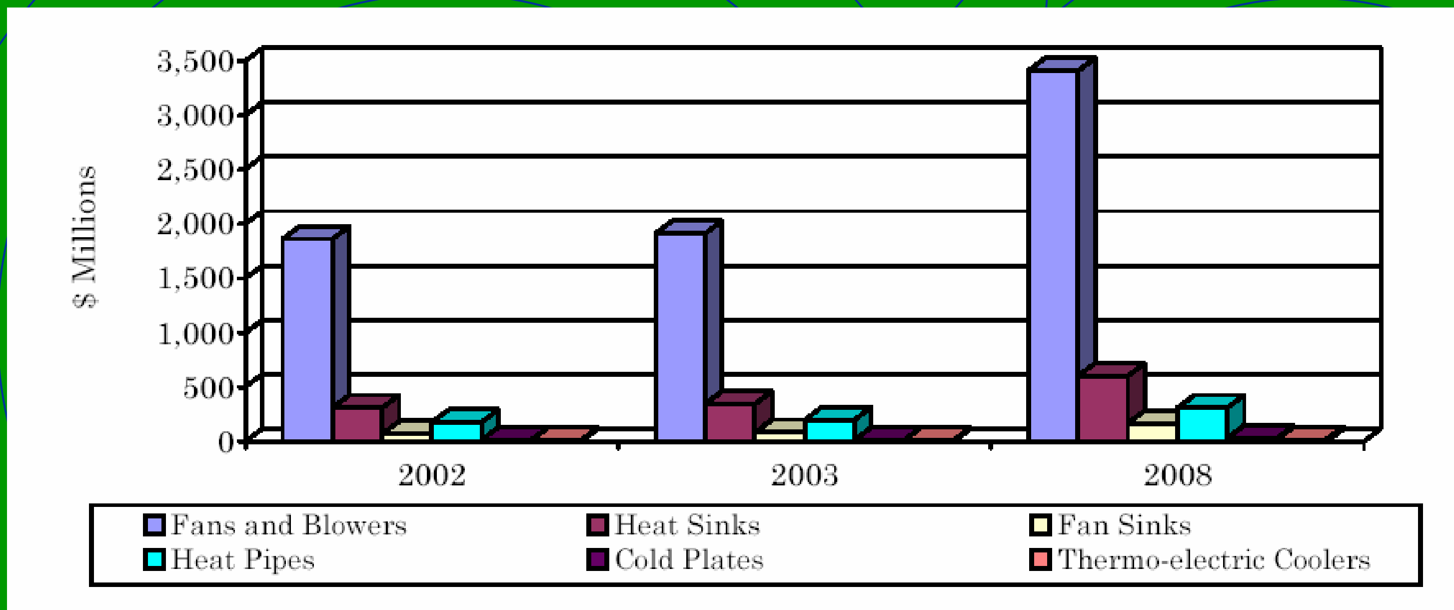

資料來源：BCC

	2002	2003	2008	AAGR% 2003-2008
Fans and Blowers	1,860.0	1,912.0	3,410.0	12.3
Heat Sinks	310.0	344.0	601.0	11.8
Fan Sinks	70.0	82.0	166.0	15.1
Heat Pipes	178.0	197.0	310.0	9.5
Cold Plates	12.9	15.0	31.2	15.8
Thermo-electric Coolers	9.1	10.0	21.8	16.9
Total	2,440.0	2,560.0	4,540.0	12.1

台灣電腦市場規模

全球PC及NB市場規模及台灣出貨量預測

資料來源：資策會

全球市場,仟台	2003	2004	2005(e)	2006(e)	2007(e)	2008(e)	2009(e)
DT PC	110,612	118,572	126,119	131,839	139,265	144,809	150,091
NB PC	37,857	46,138	57,829	67,650	81,190	98,918	115,825
台灣出貨,仟台	**2003**	**2004**	**2005(e)**	**2006(e)**	**2007(e)**	**2008(e)**	**2009(e)**
DT PC (%)	29,673 (26.83)	34,651 (29.22)	39,383 (31.23)	43,151	45,758	48,166 (33.26)	50,758
NB PC (%)	25,238 (66.67)	33,406 (72.40)	47,003 (81.28)	57,389	69,575	84,914 (85.84)	99,756

台灣目前熱管廠商年產量可達1.2億支以上，產能並持續增加中。
(NB已百分百使用熱管，DT年底可能有30%使用熱管)
台灣風扇產量約佔全球總產量的33%，總數達1.65億個。
而散熱片的產量可達5億個以上。

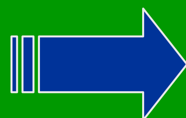

台灣電腦產業總產值達兆元以上

全球散熱處理器於不同應用領域之收益

資料來源：BCC

台灣資訊產業

- 資訊相關產業：2003年產值約為568億美金。
- 全世界第四大規模，僅次於美國、日本及中國大陸。
- 主要產品： 筆記型電腦 (2,425萬台，65%，世界第一)
  LCD顯示器 (3,325萬台，55%，世界第一)
  桌上型電腦 (2,922萬台，26% ，世界第三)
  投影機 (38萬台，17%)
- 電子產品輕薄短小與高性能
- 電子產品散熱需求種類增加
- 散熱產業百家爭鳴

散熱模組至少1.77億套，熱管1.2億支，產值在200億元以上，對國內資訊產業的發展很重要。

Summary of Electronic Cooling

(assumed heat rejection temperature 25℃)

Technology		Maximum Cooling (W)	Minimum Temp- (K)	COP	Reliability	Cost	Size	Comments
Thermoelectric (single -stage)	Present (2000)	125	228 (-45℃)	0.3@0℃	High	High (S43/unit)	Scaleable to micron level	Solid-state device : easily controlled
	Future (2010)	250	163 (-110℃)	0.4@0℃	High	High	Scaleable to micron level	Solid-state device : easily controlled
Thermoelectric (muld – stage)	Present (2000)	60	165 (-108℃)	0.3@0℃	High	High	Scaleable to micron level	Solid-state device : easily controlled
	Future (2010)	120	118 (-155℃)	0.4@0℃	High	High	Scaleable to micron level	Solid-state device : easily controlled
Vapor Compression	Present (2000)							No available small systems
	Future (2010)	350	285 (12℃)	3-6@12℃	Medium	Medium	width : 0(cm) thick : 0(mm)	Utilizes R-134a
Stirling	Present (2000)							Smallest: available system is 7.4kg
	Future (2010)	270 (5 cm long)	30 (-243℃)	~7@0℃	Low	High	0(cm)	Two moving parts (piston & displacer)
Pulse Tube	Present (2000)							Smallest available system is 8.3kg
	Future (2010)	85 (5 cm long)	20 (-253℃)	0.1@0℃	High	Medium	0(cm)	Only 1 moving part. Which is at high temp.
Sorption	Present (2000)							Smallest available system is >100 ks
	Future (2010)	<1	80 (-193℃)	<0.05@80 K	High	Low	0(cm)	Sorption compressor w/JT cooler
Reverse Brayton	Present (2000)							Smallest available system is 14 kg
	Future (2010)		80 (-193℃)	0.2@80K	Medium	High	-7.5cm	Requires miniature turbine & compressor

A very attractive system

Remote temperature control on front shoulder strap

Shoulder harness and waist belt

Battery pack

Battery pack

Supply and return hose (to thermal garment)

Evaporator

Printed circuit boards

Capillary tube

eversing valve

Pump

Reservoir

mpressor

Condenser

fans

Supply and return hose (to thermal garment)

Aspensys Portable cooling system

States of the Art? Air-conditioning in Desktop

(Ref. - Electronics Cooling Aug. 2001)

233K Region
Cold Plate
Insulation
Seals

Thermal Bus
Supply
Return

Condensing Unit
Compressor
Condenser
Fans

Compressor	Size	Weight	Capacity
A	6" x 6" x 8"	16 lbs	30 W @ -40°C
B	8" x 10" x 9"	25 lbs	150 W @ -40°C
Mini-Compressor	1.5" x 4"	2 lbs	200 W @ -40°C

We are here

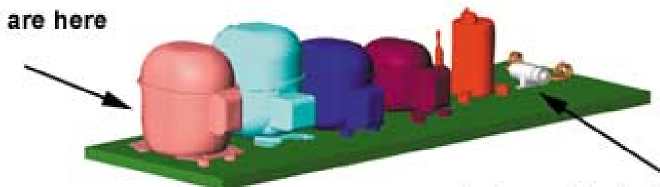

but want to be here

Major Components for Electronic Cooling

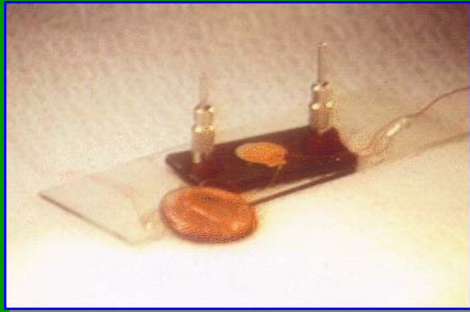

Micro-pump

Micro-compressor

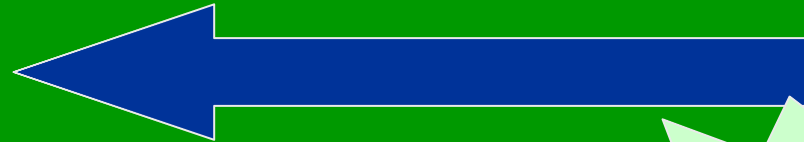

High performance Fan

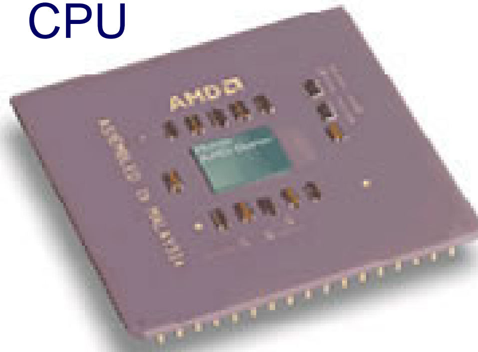

q>150W/cm²

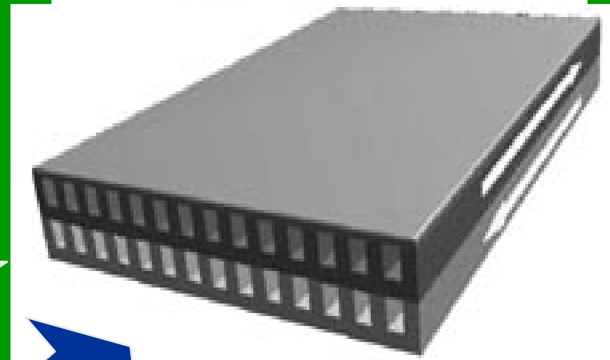

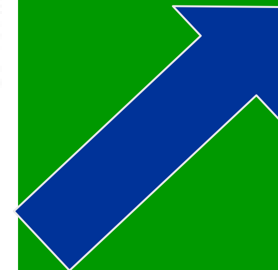

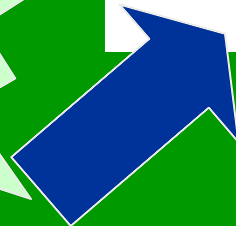

Fluid control

Expansion Device for Two-phase System

Micro-channel

Heat exchanger

High performance

Heat Sink,

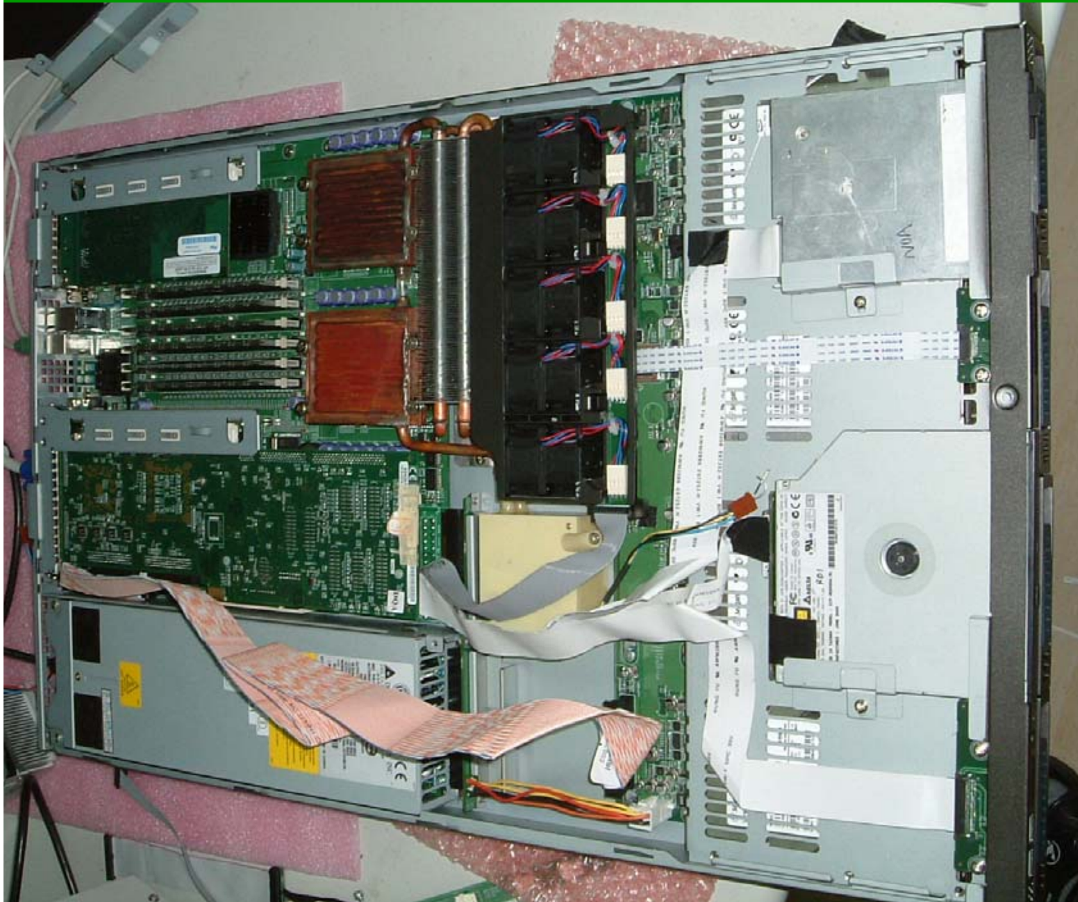

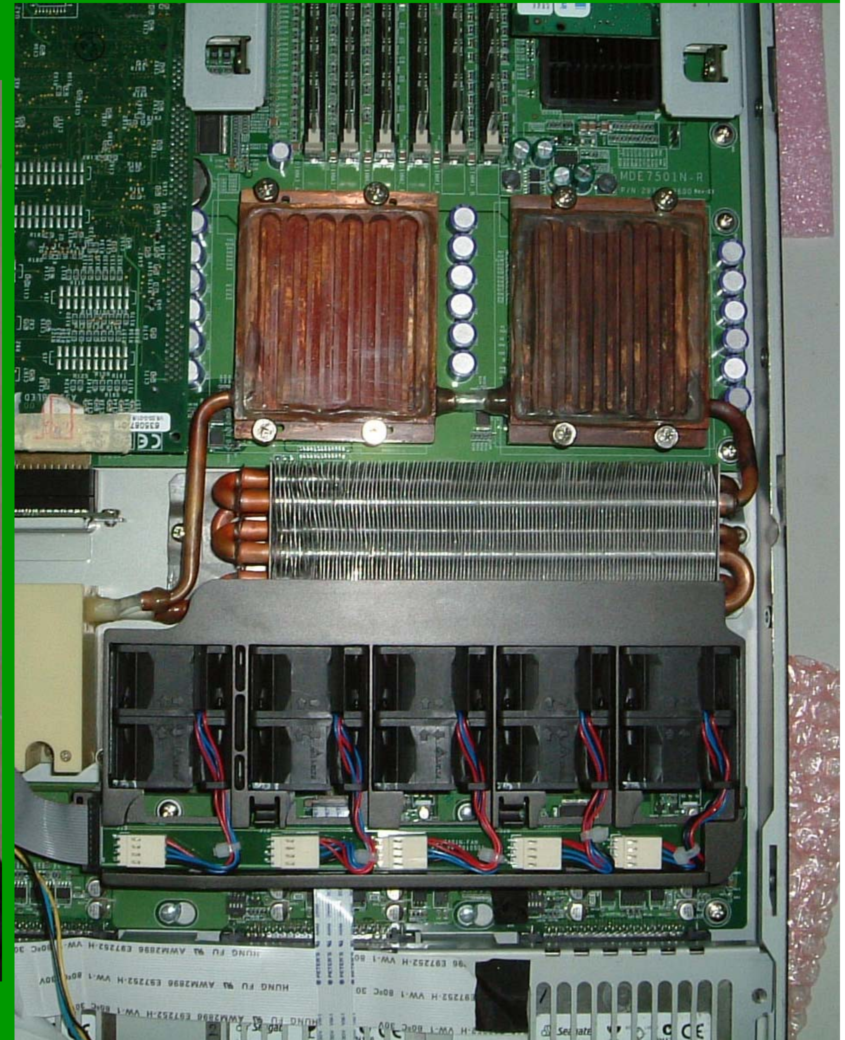
MDE7501N-R

Simple Design of Cold-Plates

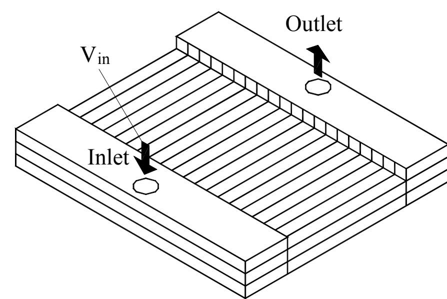

(a) I-arrangement

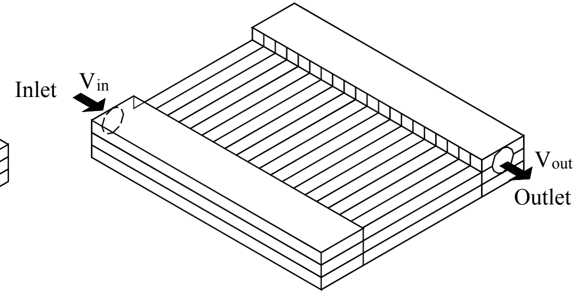

(b) Z-arrangement

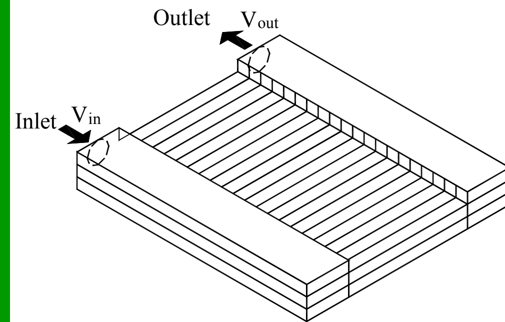

(c)]-arrangement

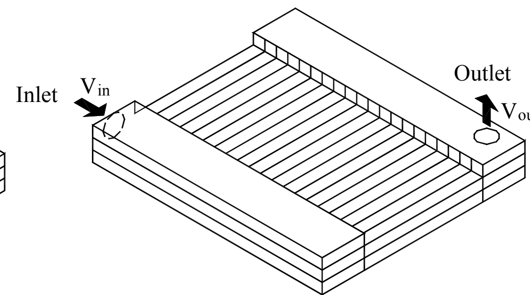

(d) L-arrangement

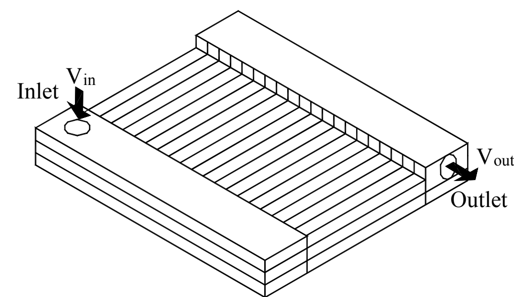

(e) Γ-arrangement

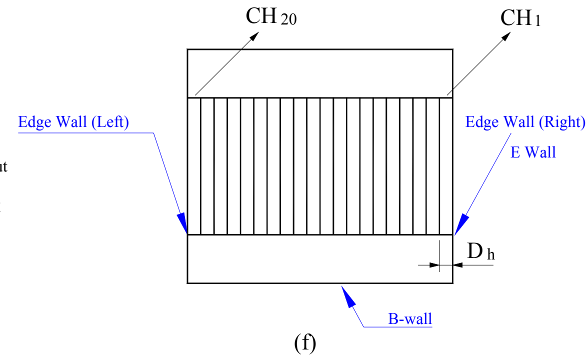

(f)

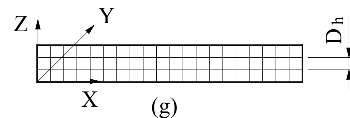

(g)

Current Interests of this Study

- The needs of high-flux cooling in electronic cooling application.
- Water cooling used in cold-plate is one of solutions.
- To avoid excess pressure drops, multi-channels cold plate are often used.
- Objective of this study is to explore the effect of the Inlet Location of Parallel-channel Cold-plate

Simulations of Multi-Channel Cold-Plate

(*IEEE Transactions on Components & Packaging Technologies*, accepted)

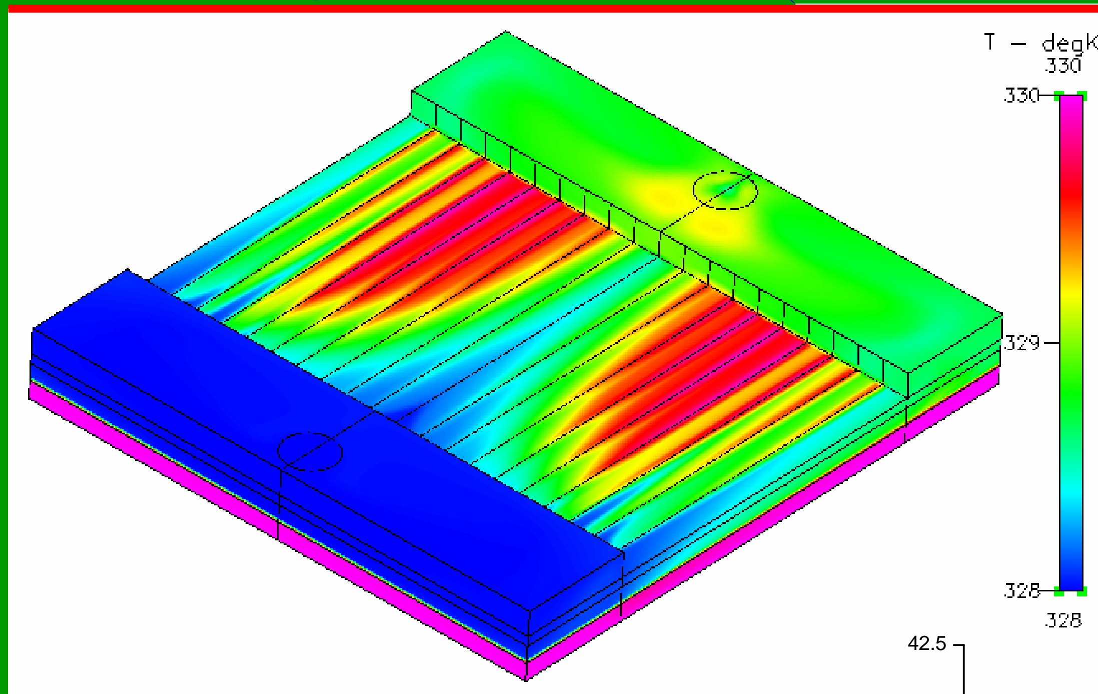

$\Delta P = 2.17$ kPa

$\dot{Q} = 126.91$ J/s

$\dot{Q}$ X 2.7

ΔP X 0.5

(1) $\Delta P = 4.9$ kPa

$\dot{Q} = 47.94$ J/s

$V_{in} = 1.0$ (m/s):

Flow mal-distribution:

$\Delta V_{MAX} = 0.2852$ (m/s)

Non-uniformity of Temperature field:

$\Delta T_{MAX} = 1.345$ (°C)

$\Delta Q_{MAX} = 148$ (W)

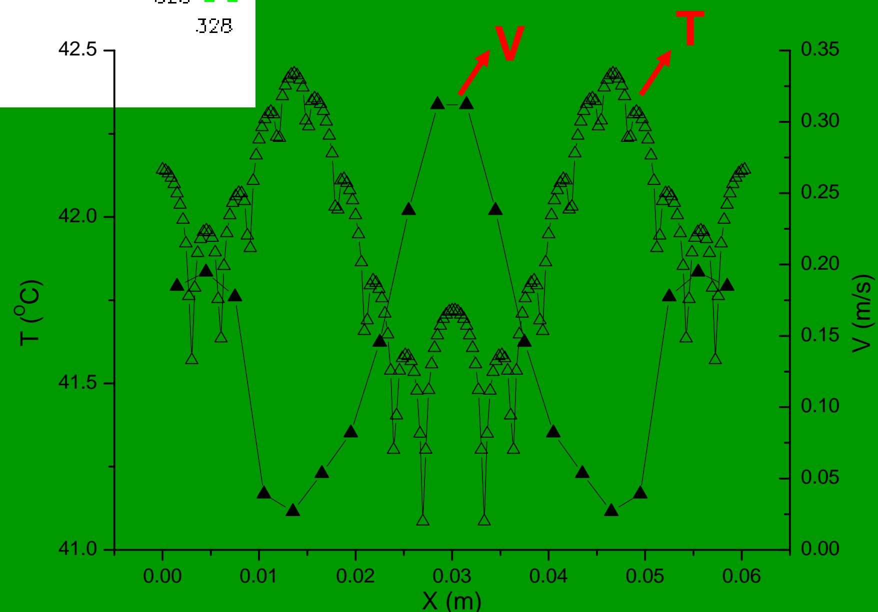

I-Arrangement

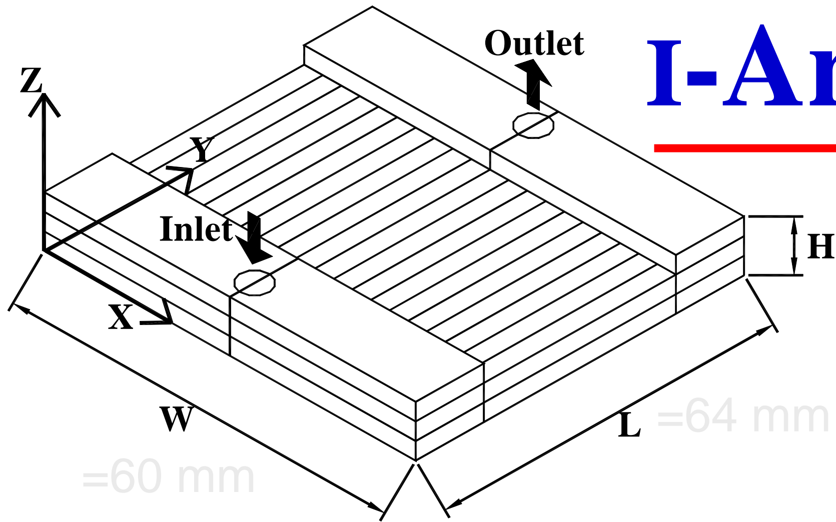

H =7.8 mm

L =64 mm

W =60 mm

D_{in} = 5.8 mm

D_h = 3 mm

Constant Heat Flux: 3.125 W/cm²

T_{in} = 40 ºC

Transverse Velocity Distribution

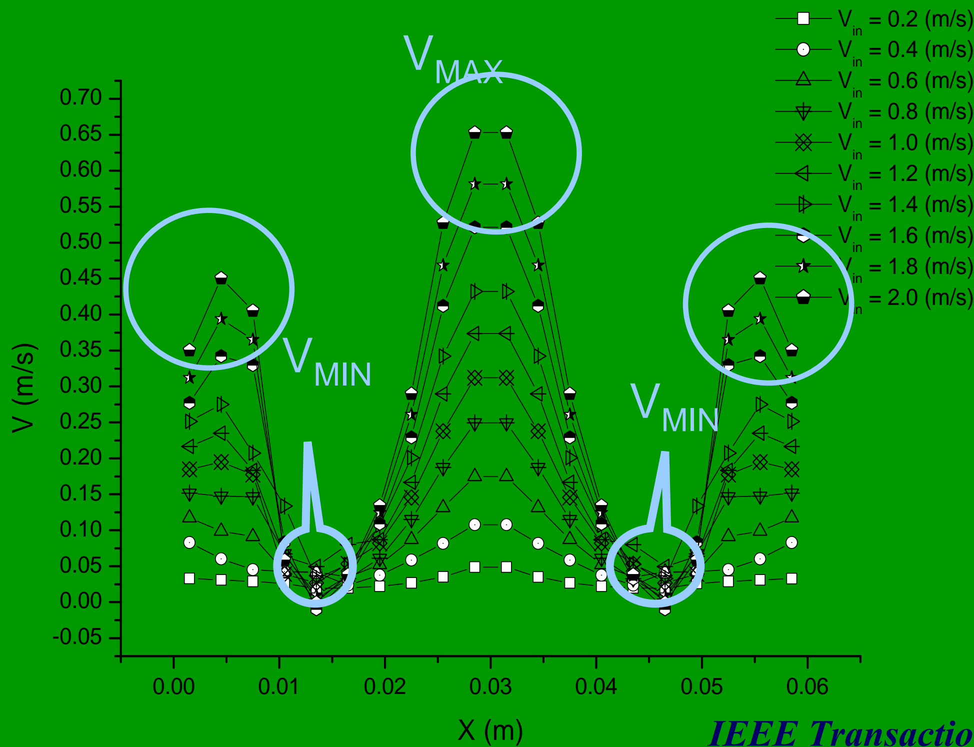

Flow Mal-distribution

V_{STD}/V_{ave}

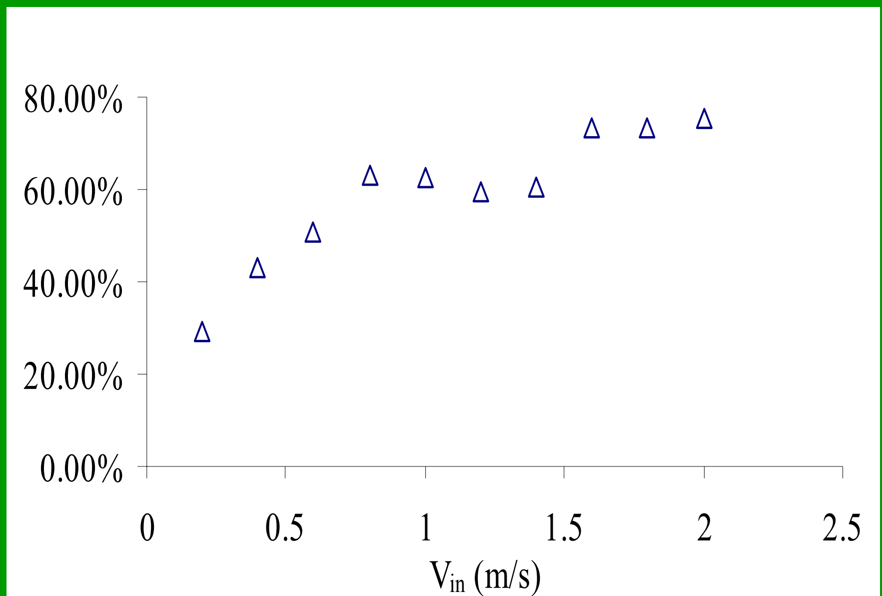

IEEE Transactions on Components & Packaging Technologies, accepted.

Z-Arrangement

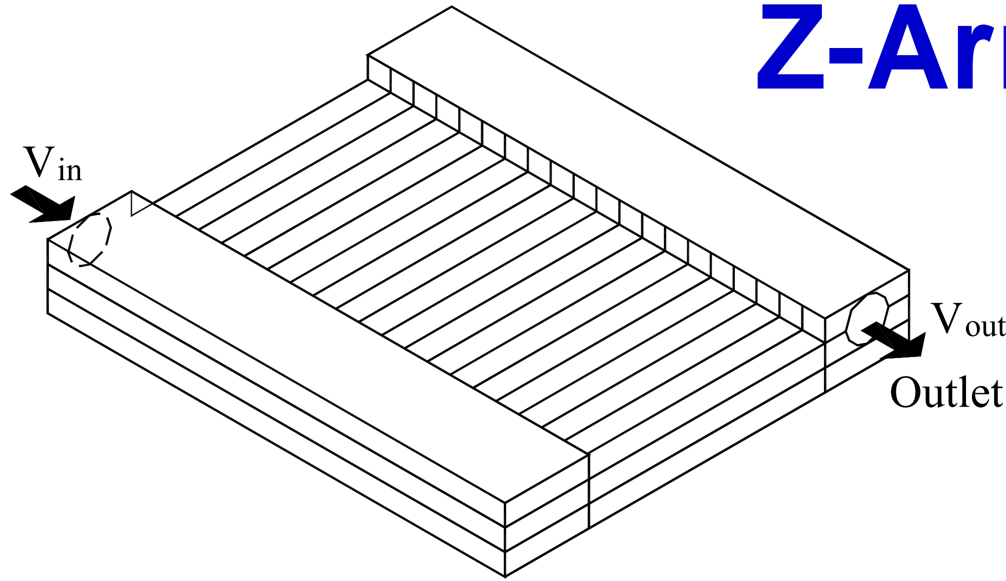

V_{in}=0.2 m/s

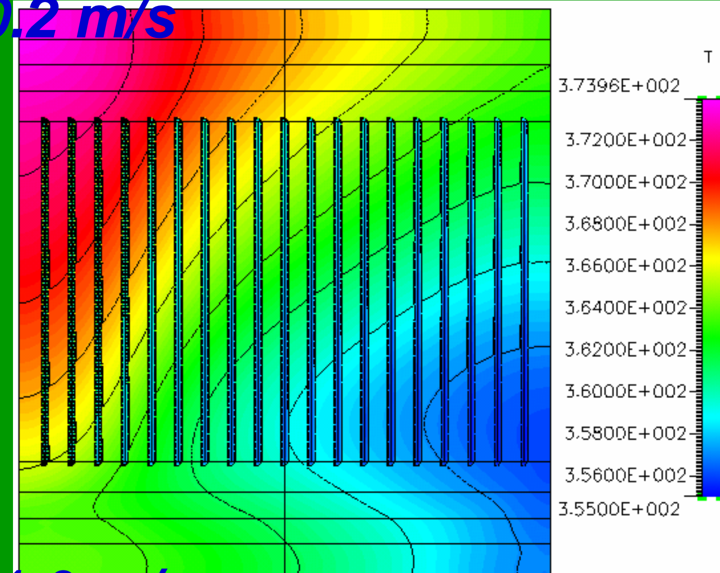

V_{in}=1.0 m/s

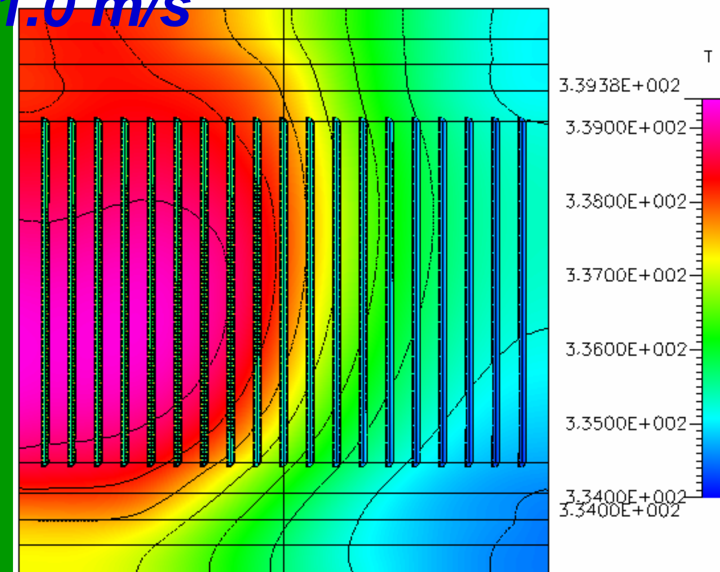

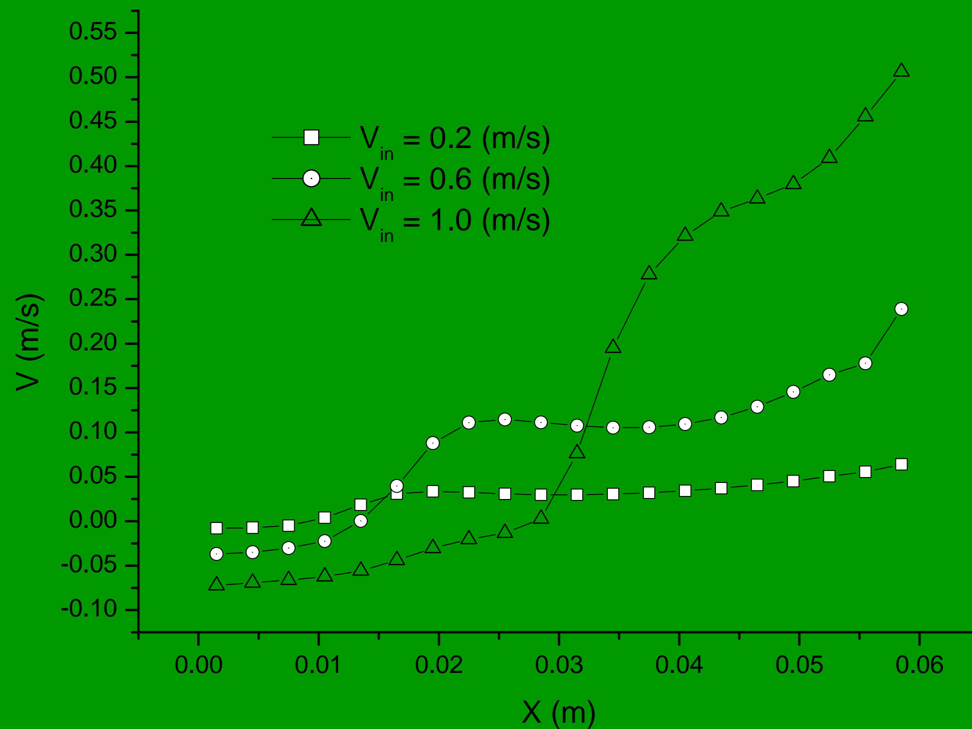

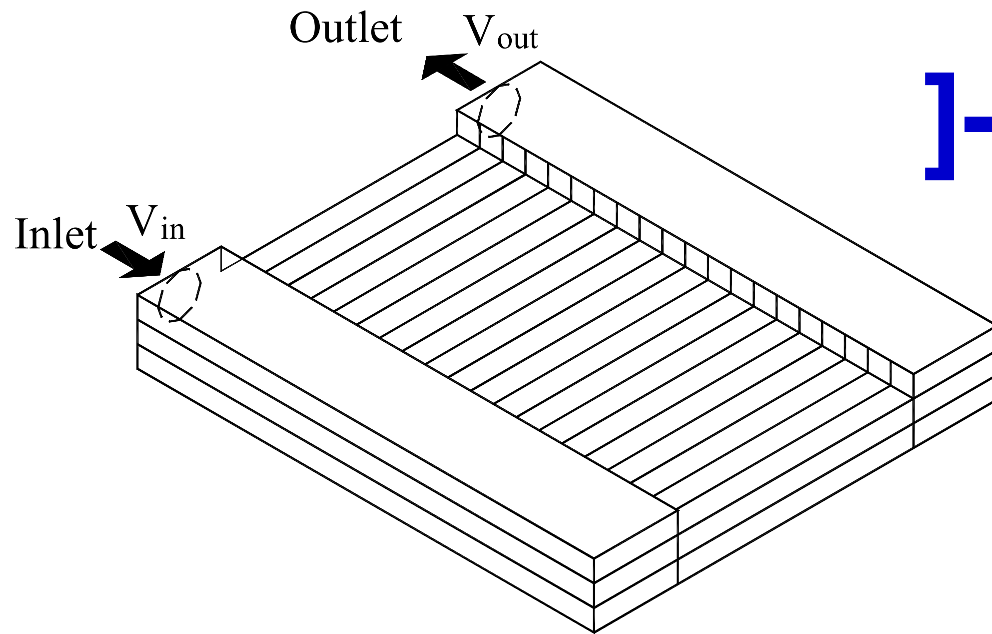
Outlet
V_{out}
Inlet
V_{in}

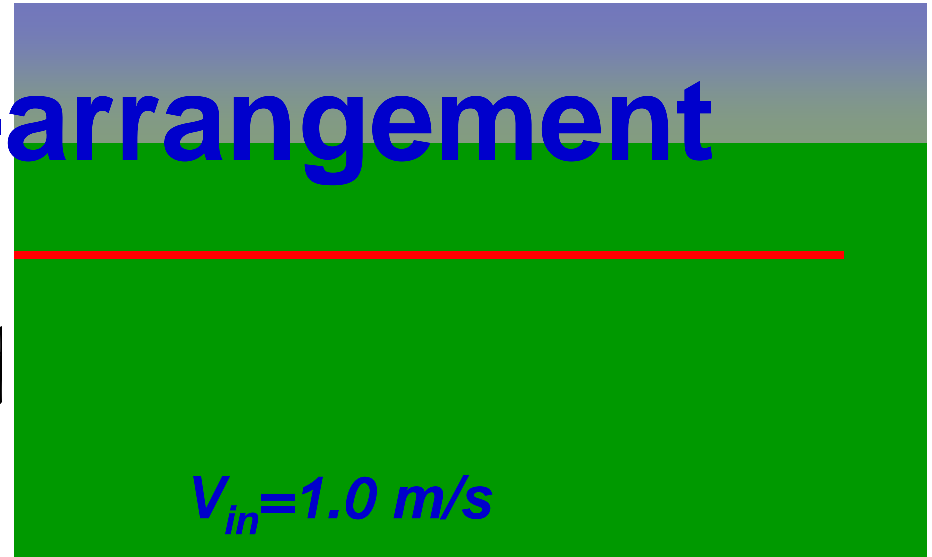
]-arrangement
V_{in}=1.0 m/s

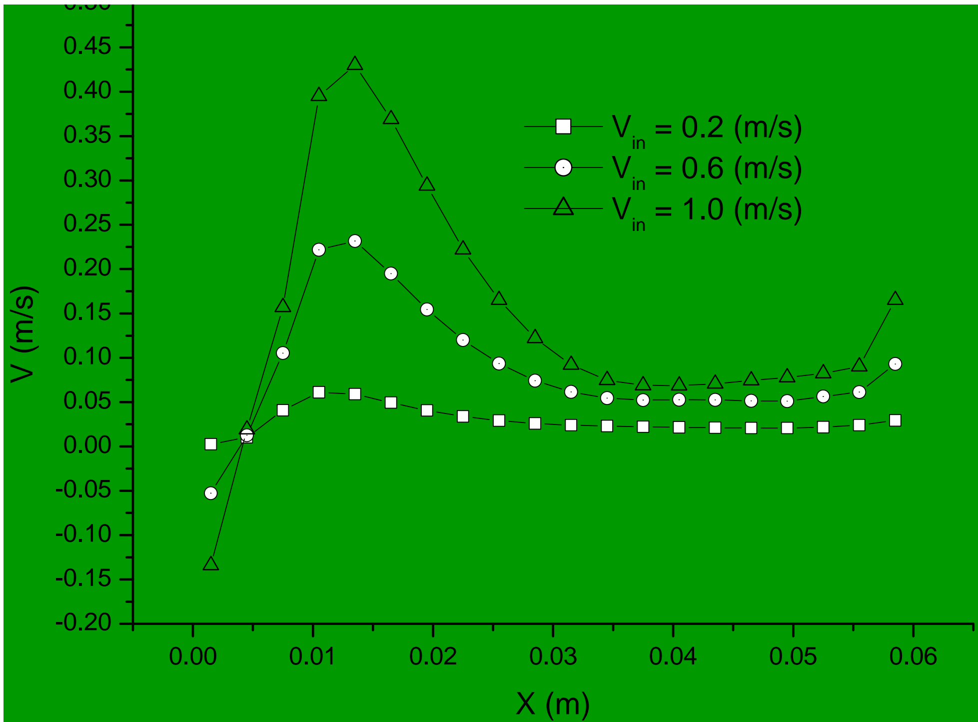
V (m/s)
X (m)
V_{in} = 0.2 (m/s)
V_{in} = 0.6 (m/s)
V_{in} = 1.0 (m/s)

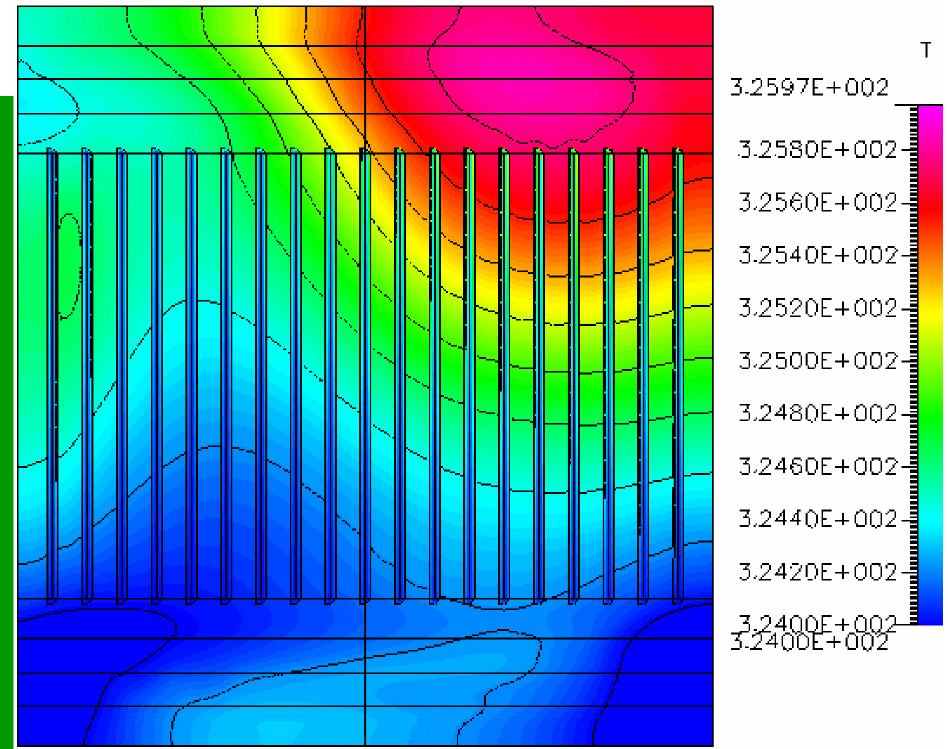
T
3.2597E+002
3.2580E+002
3.2560E+002
3.2540E+002
3.2520E+002
3.2500E+002
3.2480E+002
3.2460E+002
3.2440E+002
3.2420E+002
3.2400E+002

L-arrangement

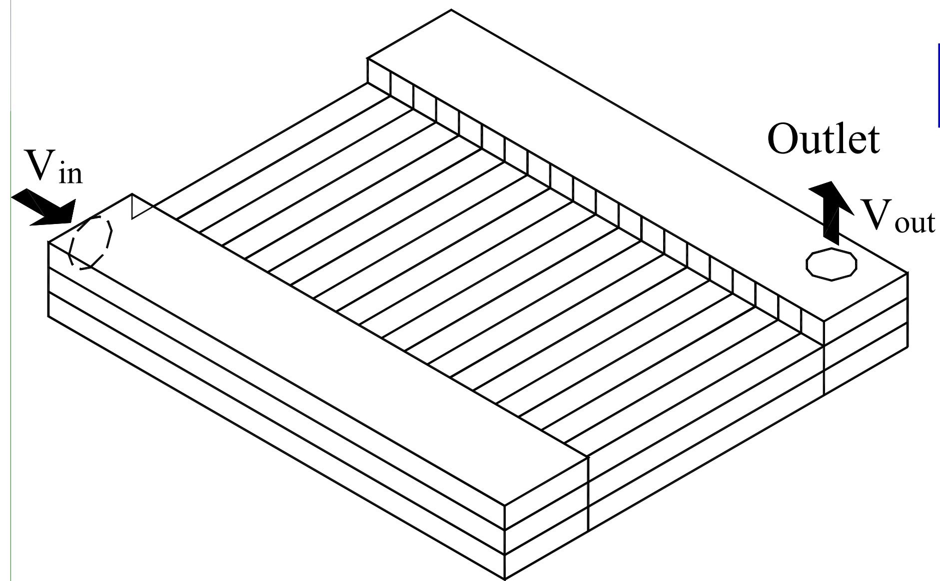

V_{in}=1.0 m/s

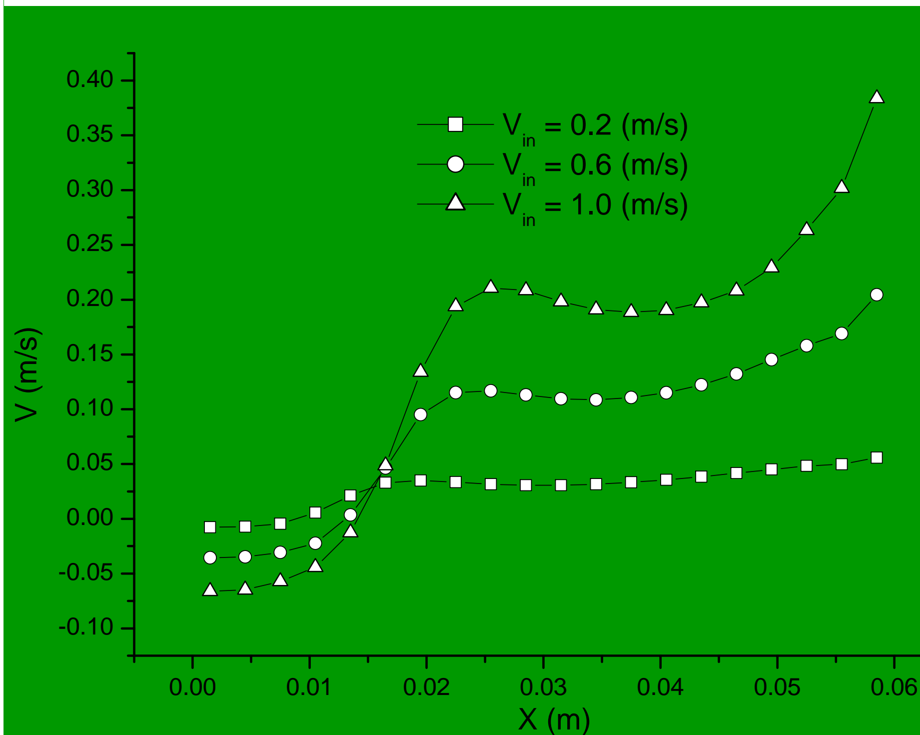

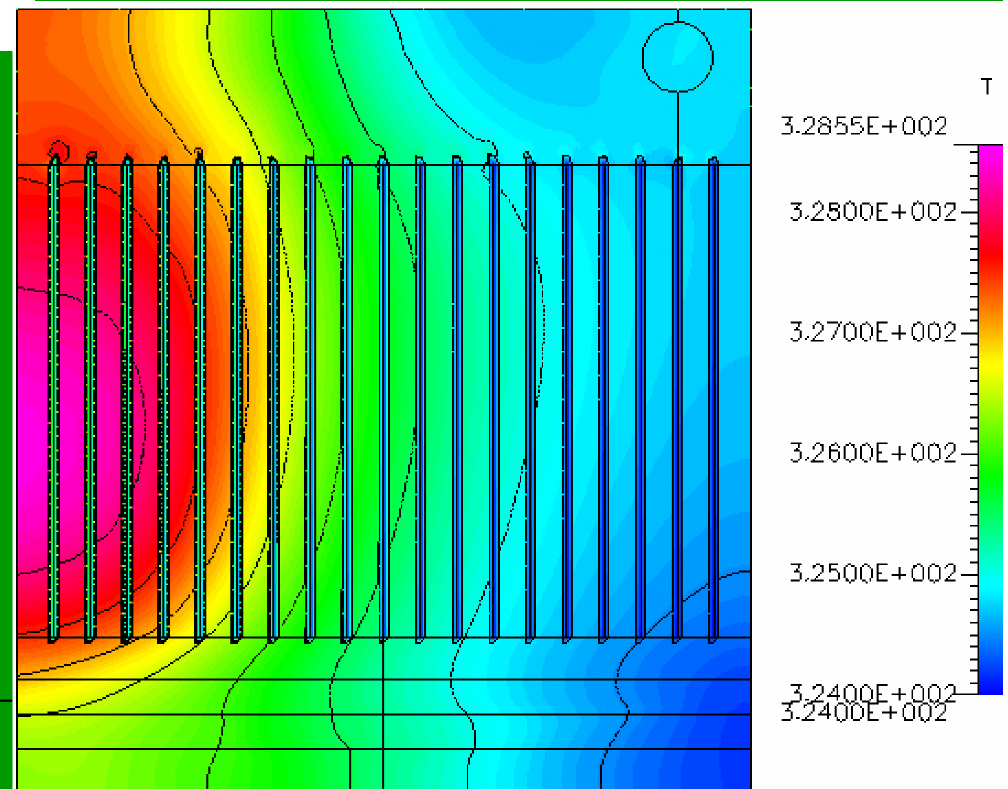

IEEE Transactions on Components & Packaging Technologies, accepted.

Γ-arrangement

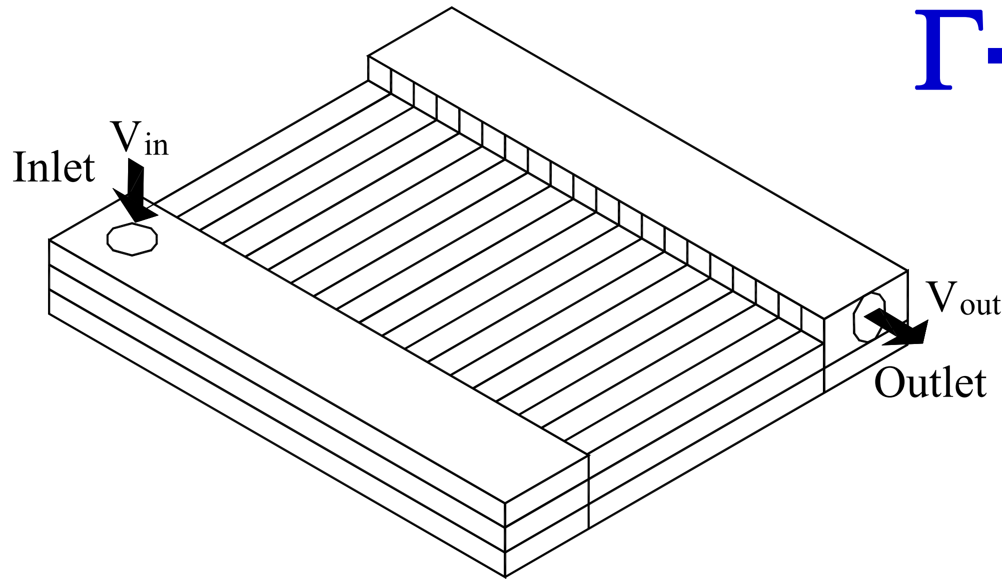

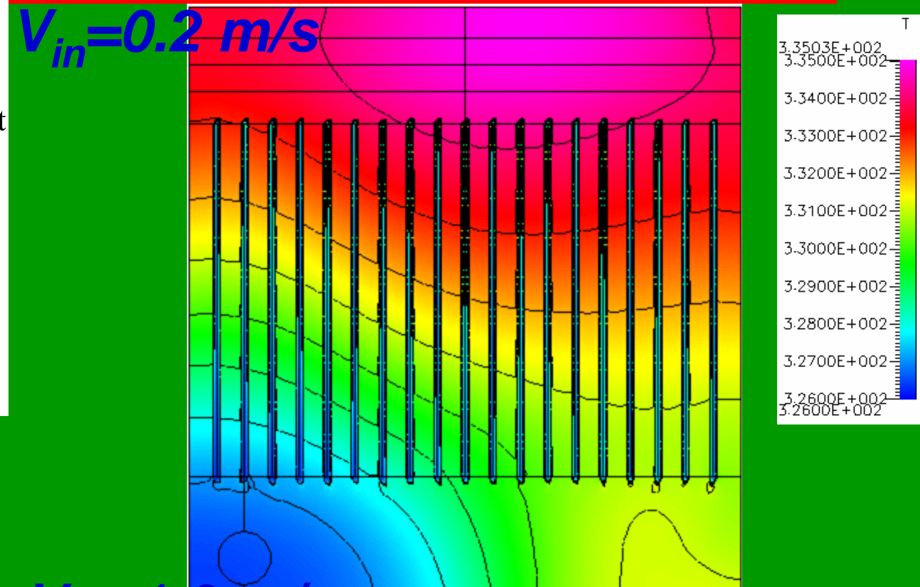

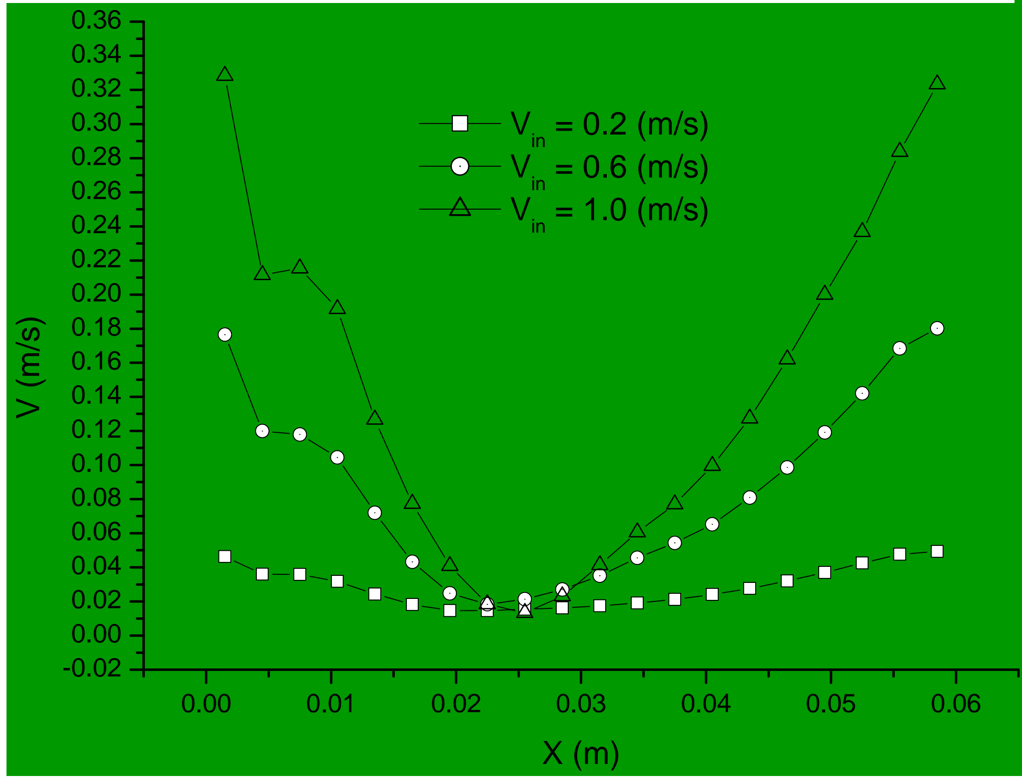

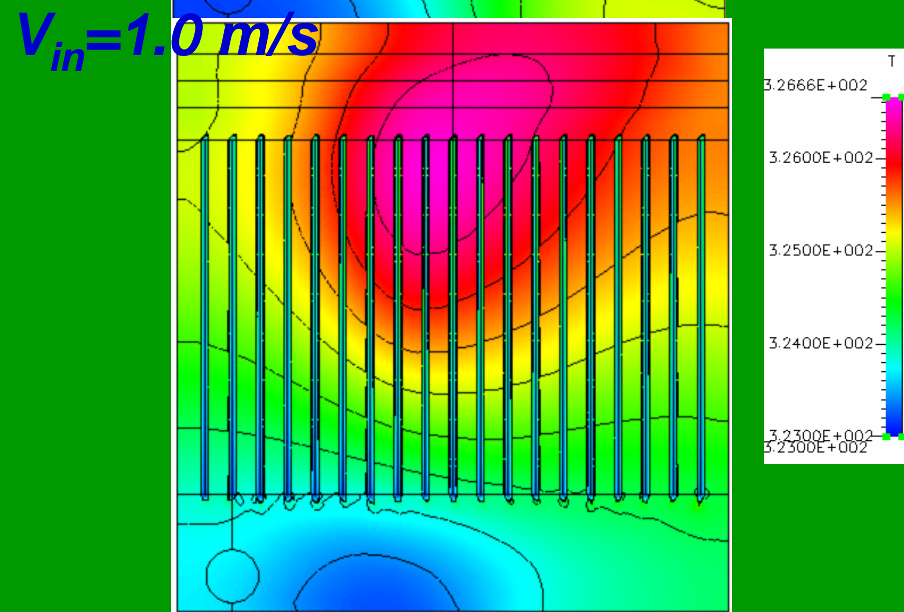

工業技術研究院
能源與資源研究所
Industrial Technology Research Institute
Energy & Resources Laboratories

Thermal Performance

Nu

13
12
11
10
9
8

100 200 300 400 500

Re

I
Z
]
L
Γ

IEEE Transactions on Components & Packaging Technologies, accepted.

PIV Flow Visualization : I Arrangement – Uniform Gap

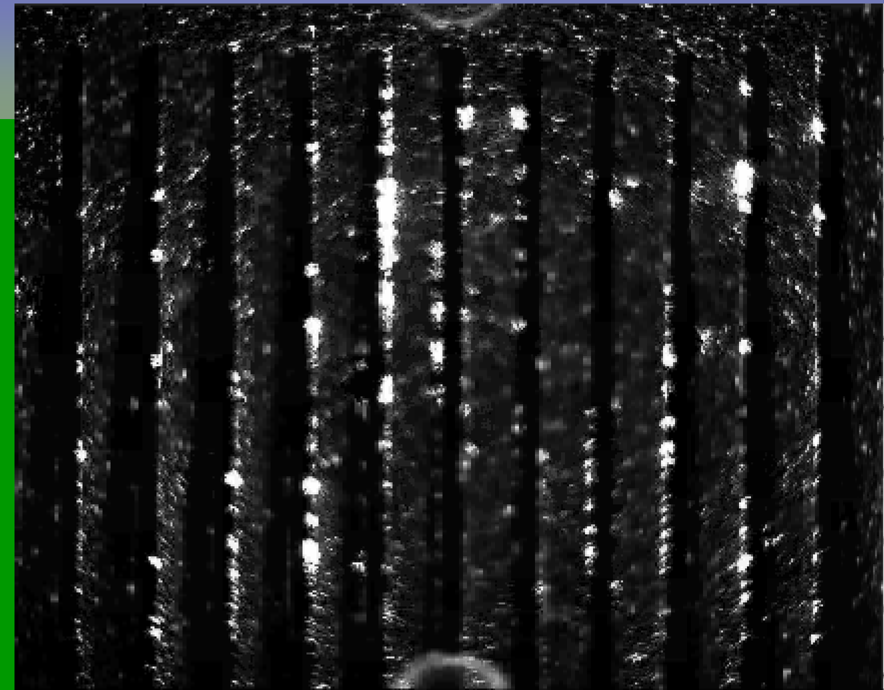

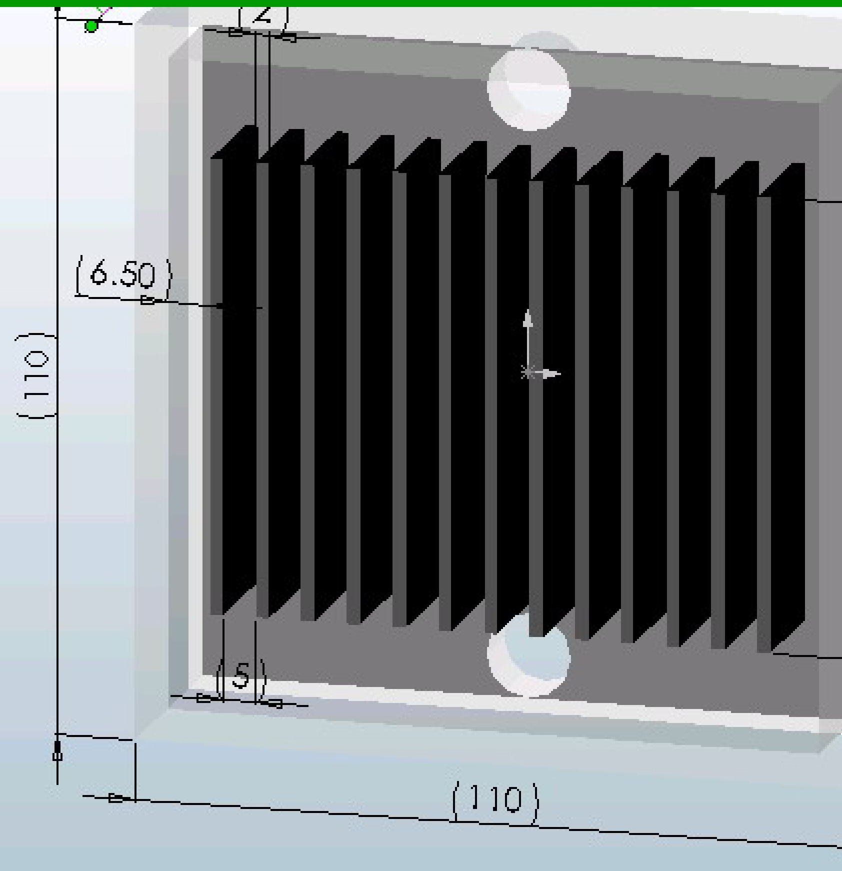

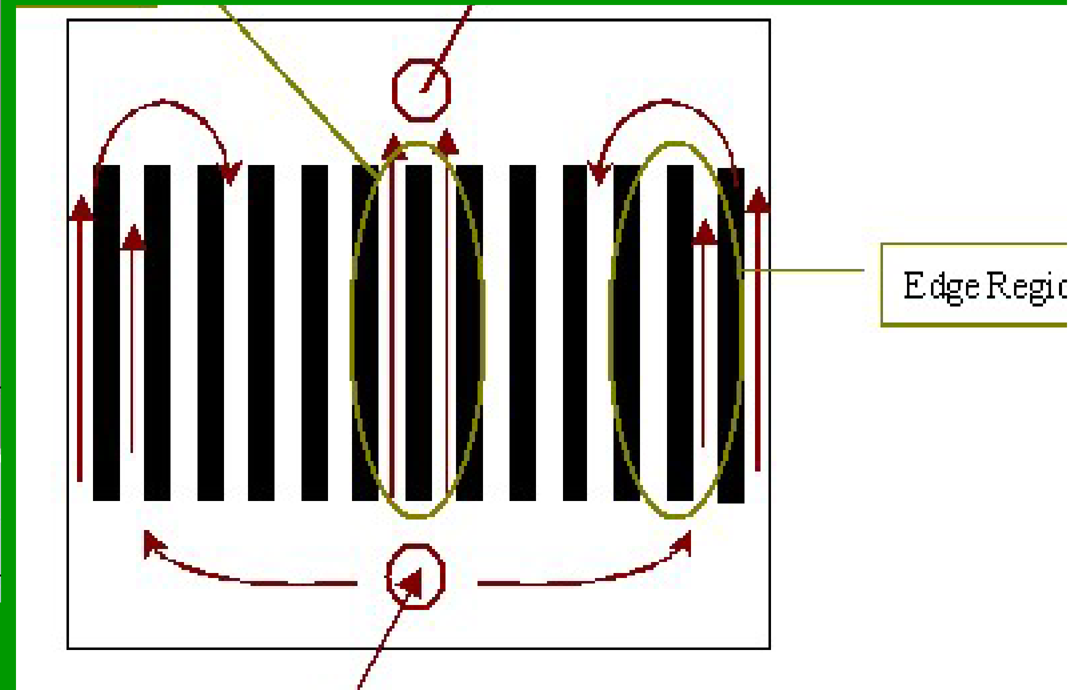

Paper in review

PIV Flow Visualization

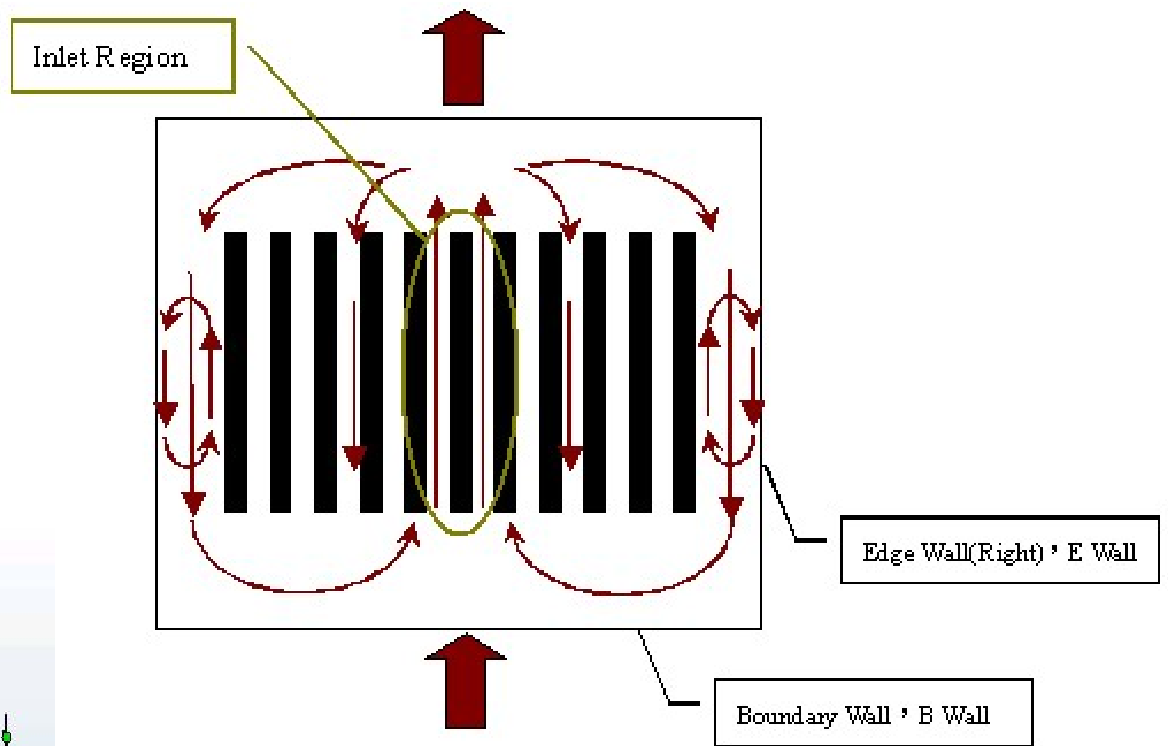

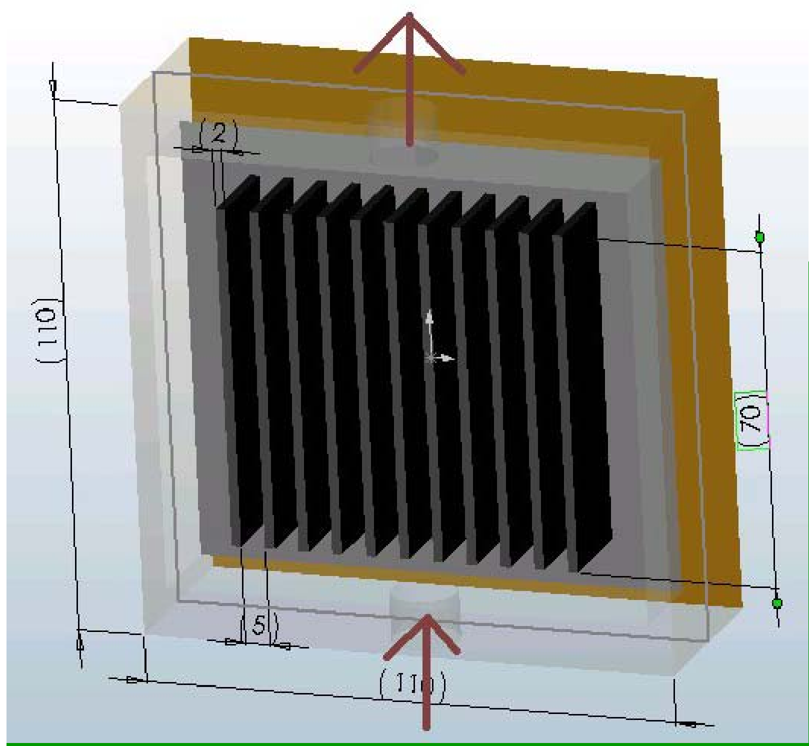

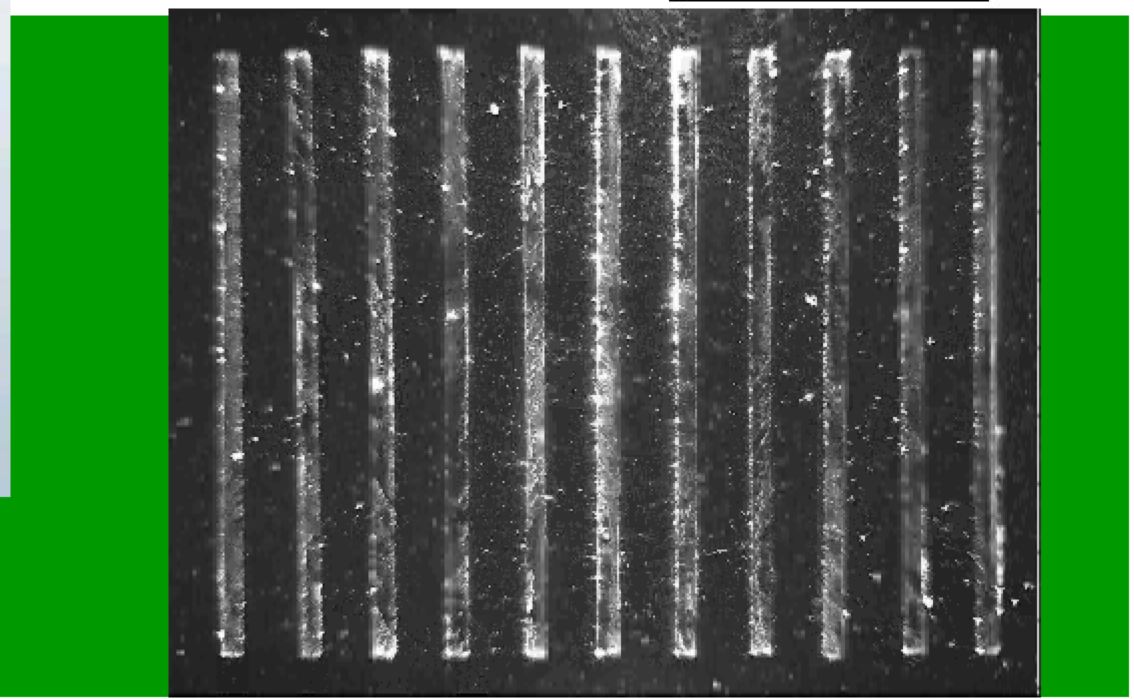

Paper in review

PIV
Flow Visualization

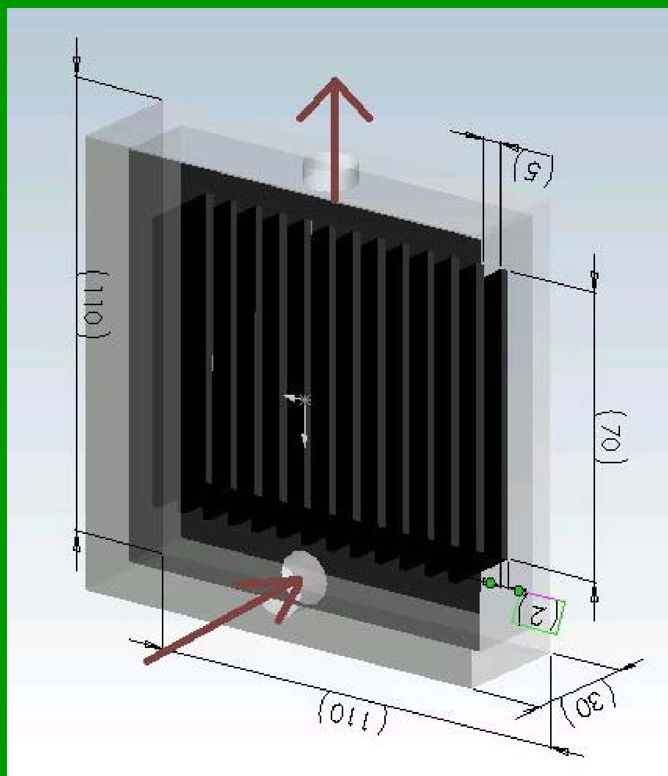

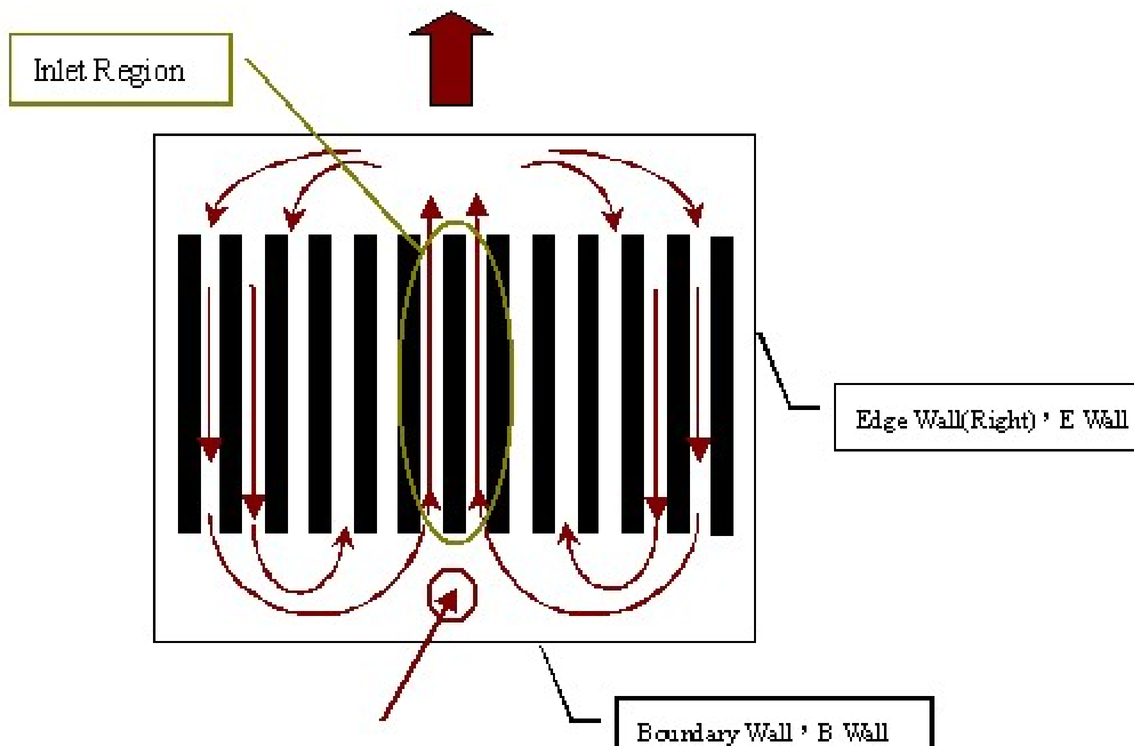

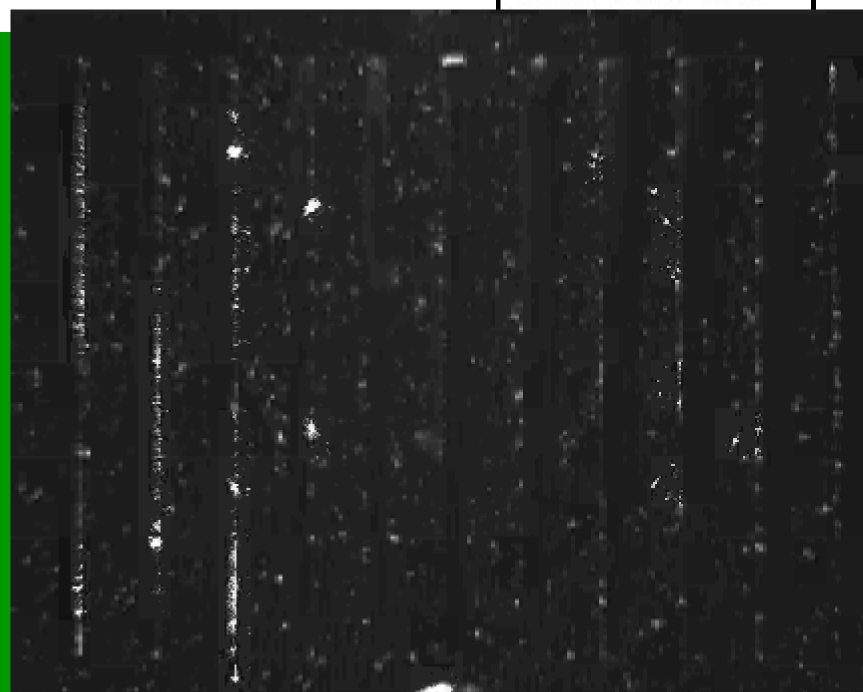

Paper in review

工業技術研究院
能源與資源研究所
Industrial Technology Research Institute
Energy & Resources Laboratories

PIV Flow Visualization

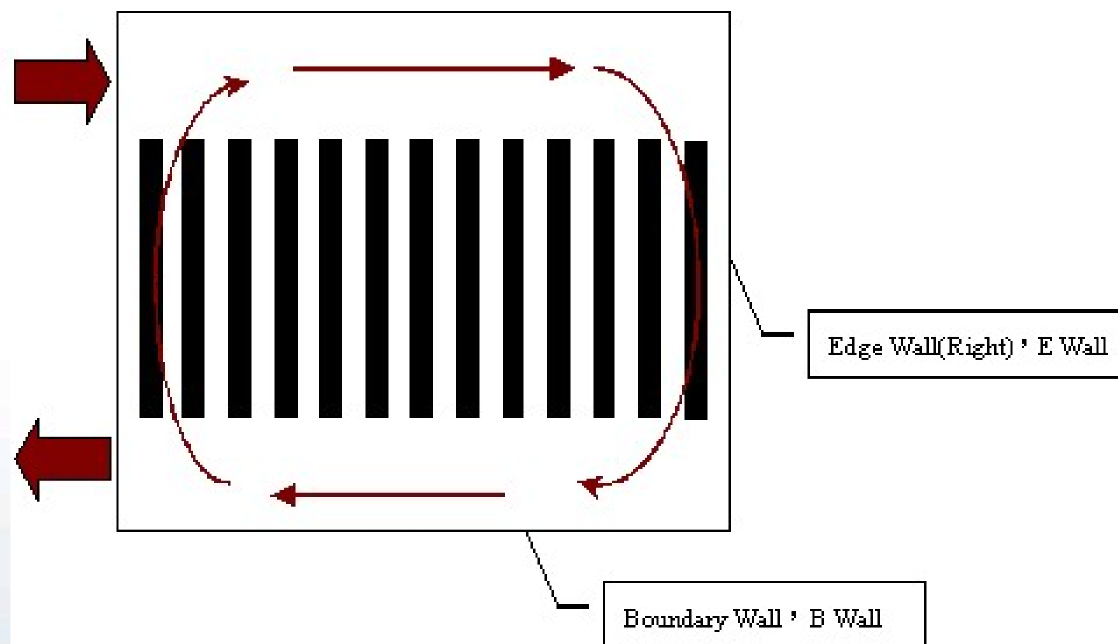

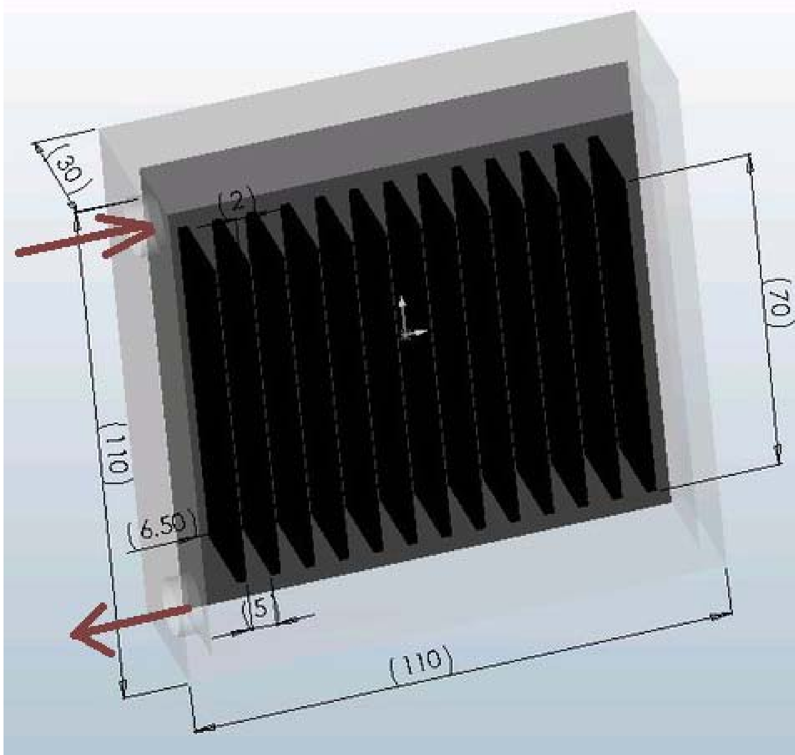

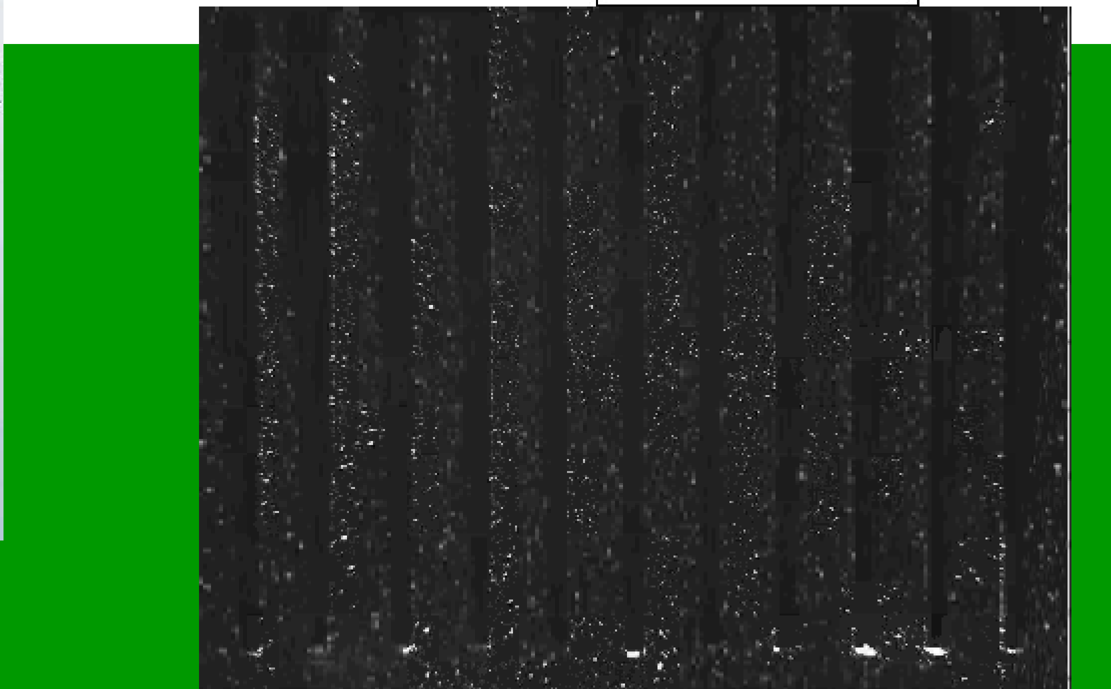

Paper in review

工業技術研究院
能源與資源研究所
Industrial Technology Research Institute
Energy & Resources Laboratories

PIV Flow Visualization

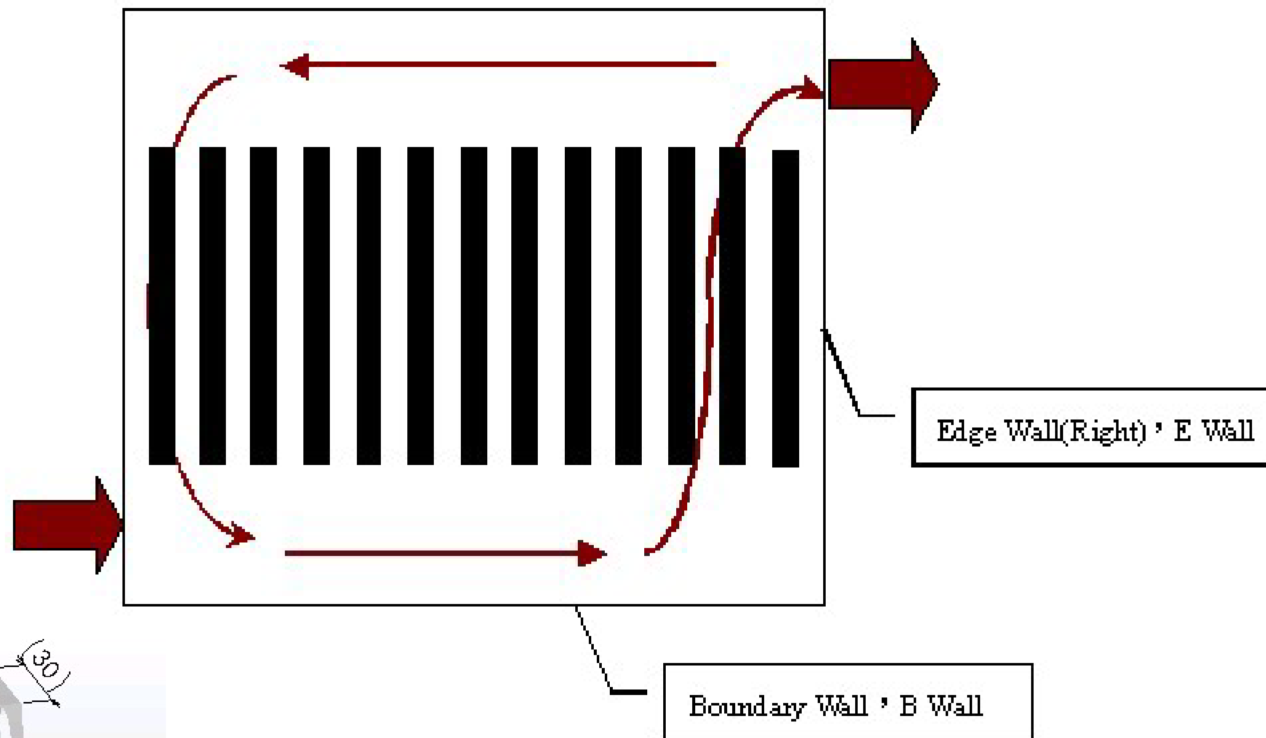

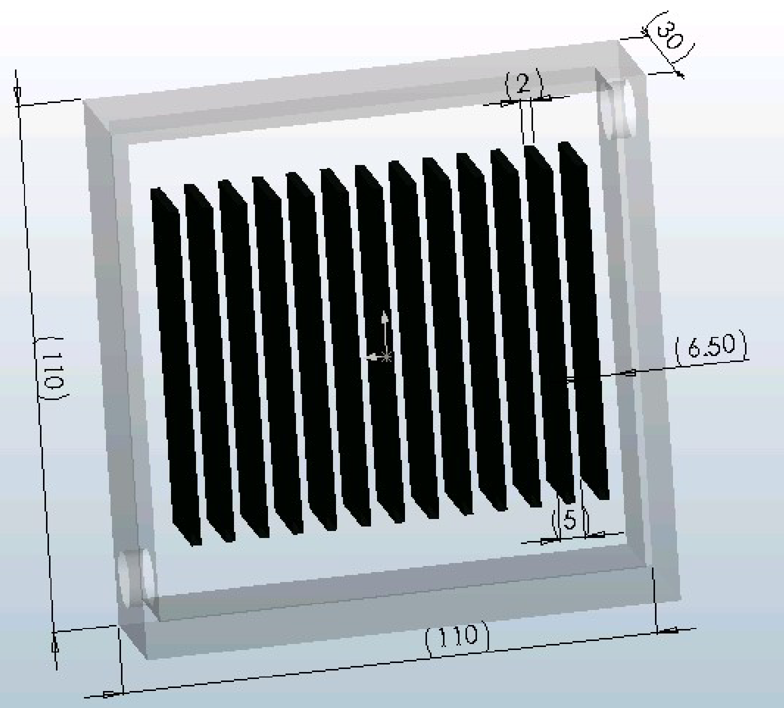

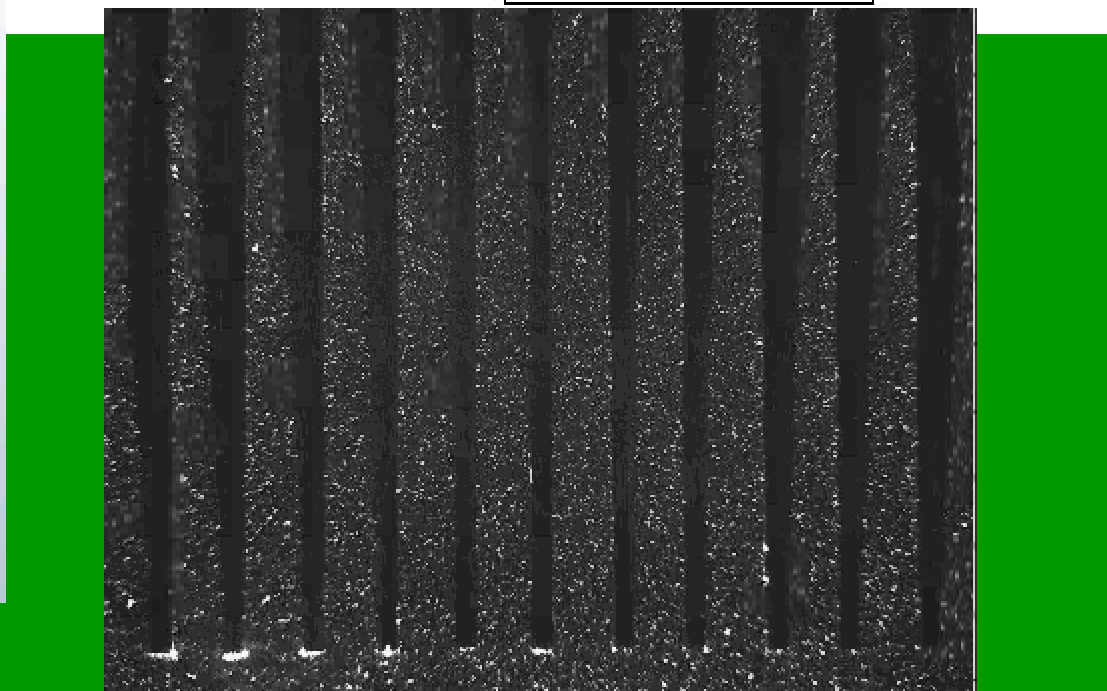

Paper in review

SUMMARY of Cold Plate Simulation

- A total of five inlet configurations (I-, Z-,]-, L- and Γ-arrangement) are examined in this study .
- For I Arrangement, higher inlet flow rate of the cold-plate shows more pronounced flow mal-distribution and it can be decreased by increasing the number of channels of the cold-plate.
- The pressure drops for I-arrangement is the highest whereas the]-arrangement is the lowest.
- The I- and Γ-arrangement give the best heat transfer performance due to their impingement configurations.
- The Z-arrangement shows the lowest heat transfer performance due to its pronounced flow re-circulation and mal-distribution flow .
- PIV Flow Observations confirm the numerical simulations.

Performance of Heat Sinks subject to Free & Forced Convection

& The influence of Impingement Flow

Overview

- Heat sink之定義
- 簡易的Heat sink分析模式
- Fin原理之回顧
- 應用於Heat sink之重要參數介紹
- 常見之Heat sink類型
- 常見之Heat sink流場類型
- 實驗儀器與實驗結果
- 數值模擬結果

Heat sink

- *定義爲可以增加區域熱傳能力的裝置*
- 目前最常使用於解決電子散熱問題的裝置
- 大多以增加熱傳面積的方式達到增加熱傳量
- 散熱鰭片具有容易製作、結構簡單及低成本等優勢
- 常見的的熱沉種類可分爲
  - 被動式熱沉(Passive Heat Sink)
  - 半主動式熱沉(Semi-Active Heat sink)
  - ***主動式熱沉(Active Heat sink)***
  - 液體冷卻系統(Liquid Cooling system)
  - 相變化系統(Phase Change system)

被動式熱沉(Passive Heat Sink)

- *藉由空氣的自然對流來將熱量帶走*

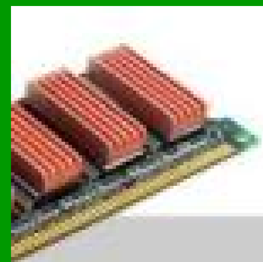

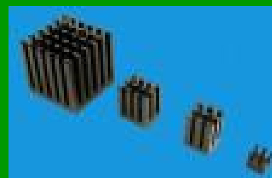
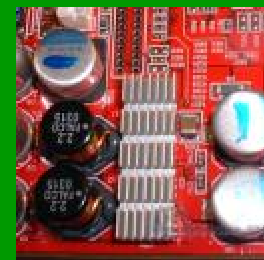

半主動式熱沉(Semi-Active Heat sink)

- 藉由系統風扇來帶走熱量

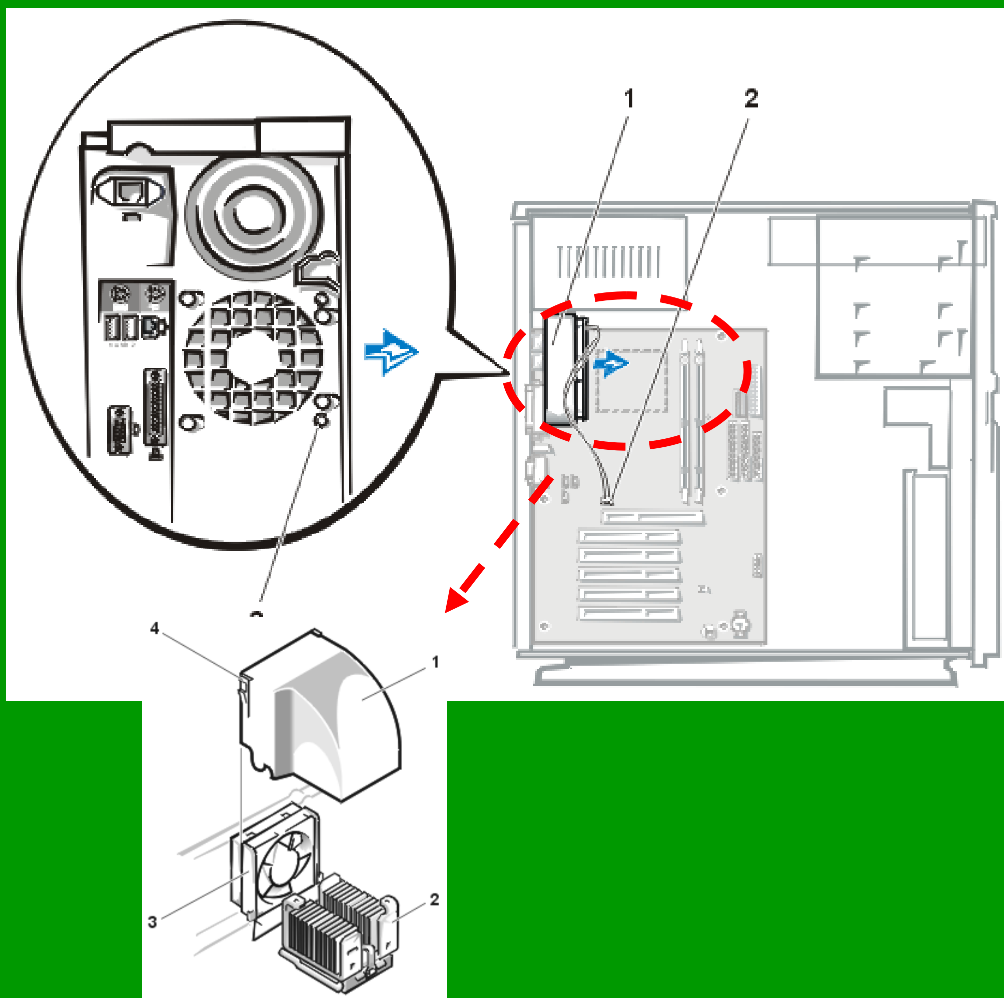

主動式(Active Heat sink)熱沉

- *將風扇直接裝置在熱沉裝置上*

液體冷卻系統(Liquid Cooling system)

- *使用熱容量較高的液體來組成液體冷卻系統*

水 C_p 4.18kJ/kg-K　水 密度 998 kg/m^3
空氣 C_p 1.004kJ/kg-K　空氣 密度 1.17 kg/m^3

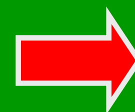

3551 倍

相變化系統(Phase Change system)

水 h_{fg} 2500 kJ/kg

水 C_p 4.18 kJ/kg-K

1 °C → 598 倍

→ 空氣體積的2123498倍

- 具有相變化的熱管裝置

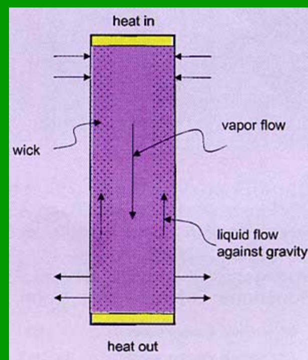

Extended Surfaces

- 在已知的Q、A_s、V及T_a的操作條件下，在表面溫度T_s下對流熱傳率為：

$$Q = hA_s(T_s - T_a) \quad \Longrightarrow \quad T_s = T_a + \frac{Q}{hA_s}$$

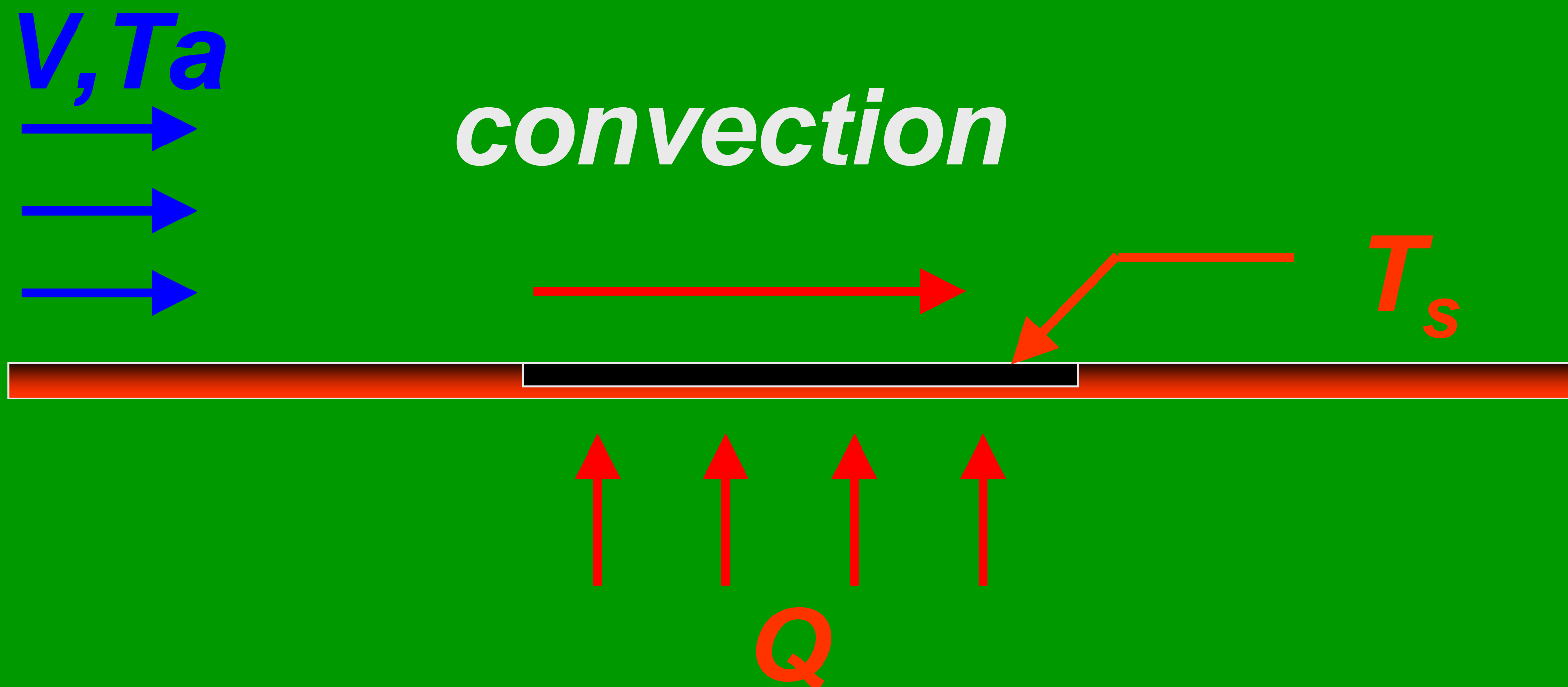

Extended Surfaces

- 增加鰭片使得有效對流面積增加

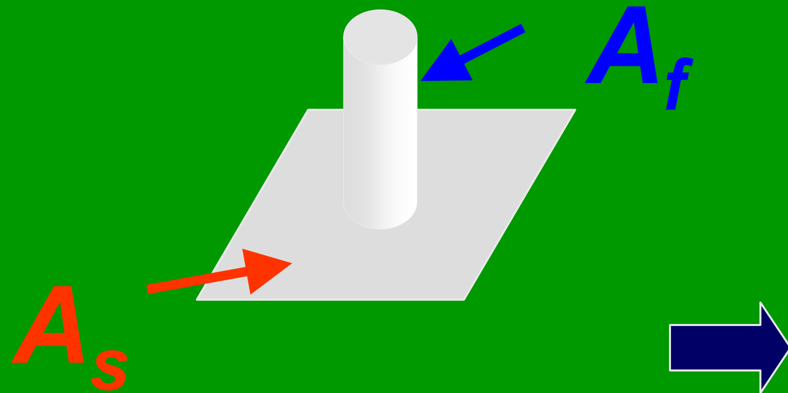

$$Q = h_{eff} A_{eff} (T_s - T_a)$$

$$\Rightarrow \quad T_s = T_a + \frac{Q}{h_{eff} A_{eff}}$$

h_{eff} : effective heat transfer coefficient for the fin and exposed surface.

A_{eff} : effect Area.

Basic Performance Model

- For a given heat input Q we can measure the base temperature resistance.

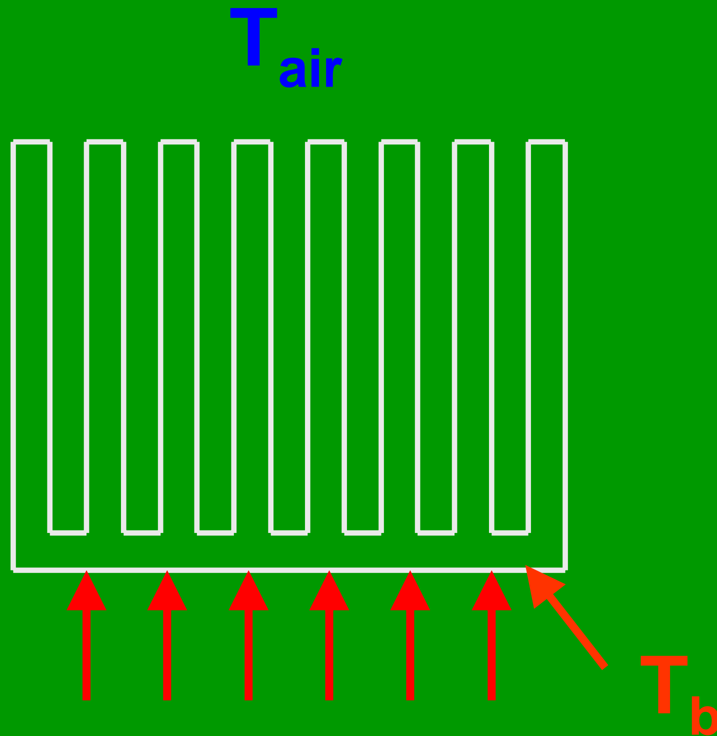

$$R = \frac{T_b - T_{air}}{Q}$$

R is usually available from the manufacturer

Single Fin Theory

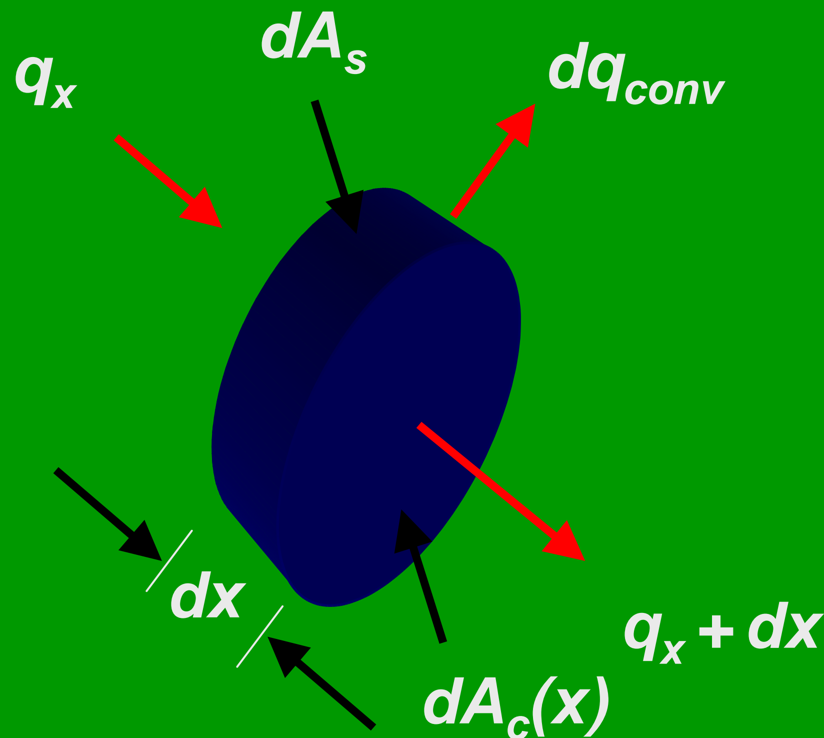

For a fin with constant cross section, Ac,

$$q_x = -kA_c \frac{dT}{dx}$$

$$q_{x+dx} = q_x + \frac{dq_x}{dx} dx$$

$$q_{x+dx} = -kA_c \frac{dT}{dx} + \frac{d}{dx}\left[-kA_c \frac{dT}{dx} \right] dx$$

The convective heat loss a differential slab of width dx is

$$dq_{conv} = hdA_s (T - T_\infty)$$

The differential surface area Is dA_s=Pdx where P is the perimeter of the fin

Single Fin Theory

Energy balance requires:

Net heat flow into the Element by conduction = **Heat lost by convection** ⇒

$$\frac{d}{dx}\left(A_c\frac{dT}{dx}\right)-\frac{h}{k}\frac{dA_s}{dx}\left(T-T_\infty\right)=0$$

Fin of uniform cross-section area.

$$\frac{dA_c}{dx}=0 \qquad \frac{dA_s}{dx}=P \qquad \theta\equiv T(x)-T_\infty \qquad m^2\equiv\frac{hP}{kA_c}$$

For an adiabatic tip.

$$\left.\frac{d\theta}{dx}\right|_{x=L}=0$$

The fin heat transfer rate:

$$q_f=\sqrt{hPkA_c\theta_b}\tanh mL$$

Single Fin Theory

Efficiency:

$$\eta_f = \frac{\text{actual heat transfer}}{\text{maximum possible rate of heat transfer}}$$

$$\eta_f = \frac{\text{actual heat transfer}}{\text{rate of heat transfer if entire surface was at } T_b}$$

For a single fin with an adiabatic tip:

$$\eta_f = \frac{\tanh mL}{mL}$$

Thus, fin efficiency decrease with length.

Heat sink之重要參數

- Reynolds number, ***Re***

$$\mathrm{Re}_{d_h} = \frac{\rho V d_h}{\mu}$$

Ratio of the inertia and viscous force

- Nusselt number, ***Nu***

$$Nu = \frac{\bar{h} D_h}{k}$$

Dimensionless temperature gradient at the surface.

- Friction factor, ***f***

$$\frac{\Delta P}{(L/D)(\rho u_m{}^2/2)}$$

Dimensionless pressure drop

- Colburn ***j*** factor,

$$j \equiv St\,\mathrm{Pr}^{2/3}$$

Dimensionless heat transfer coefficient

Typical air cooled heat sink

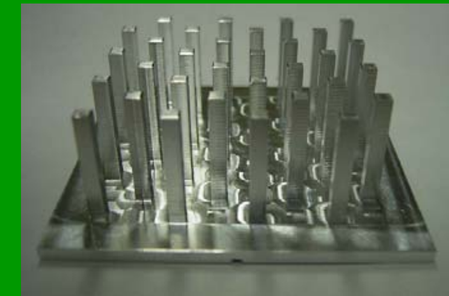

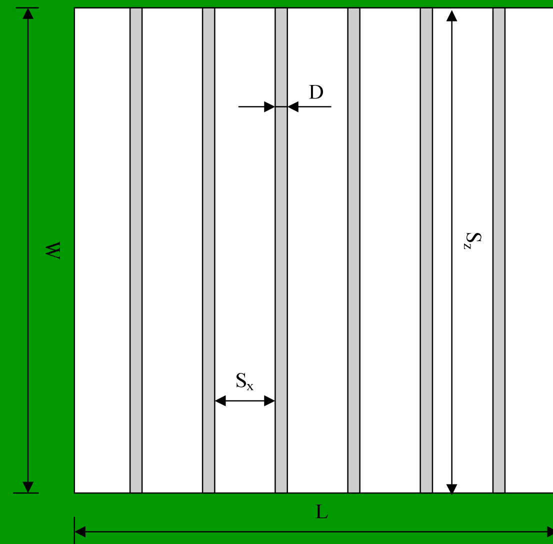

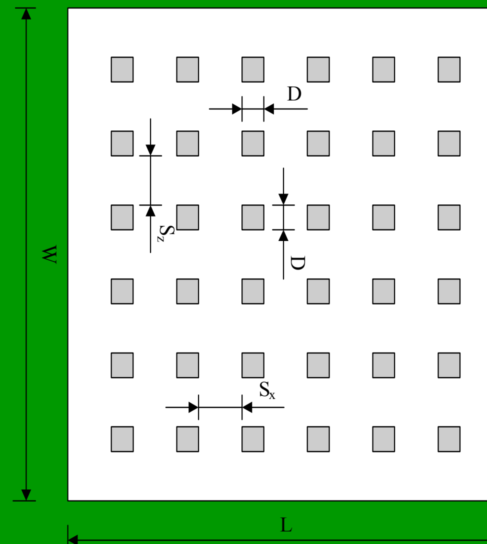

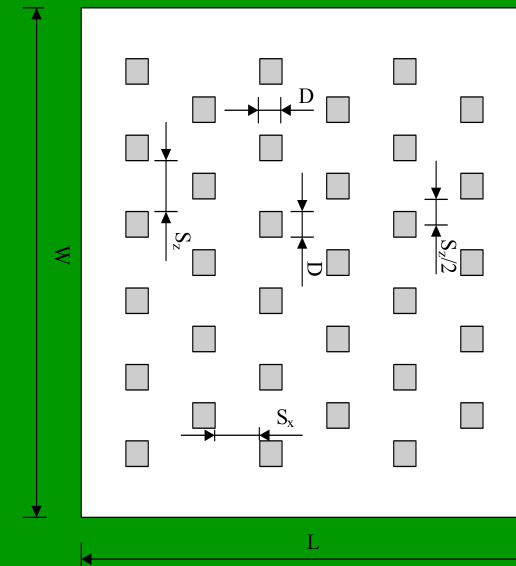

Plate fin ***Pin fin (in-line)*** ***Pin fin (staggered)***

Air flow path through heat sink

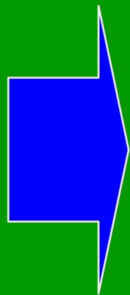

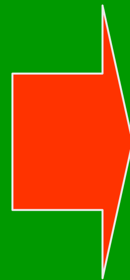

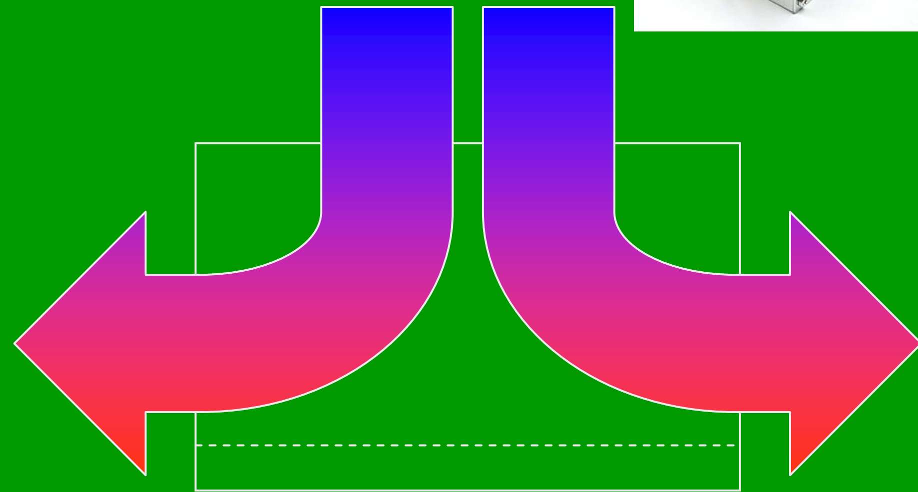

Cross flow

Impingement flow

Confined and bypass flow

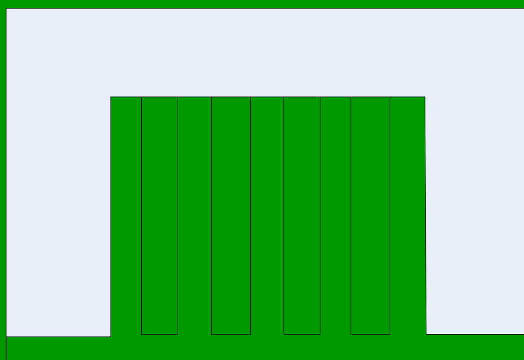

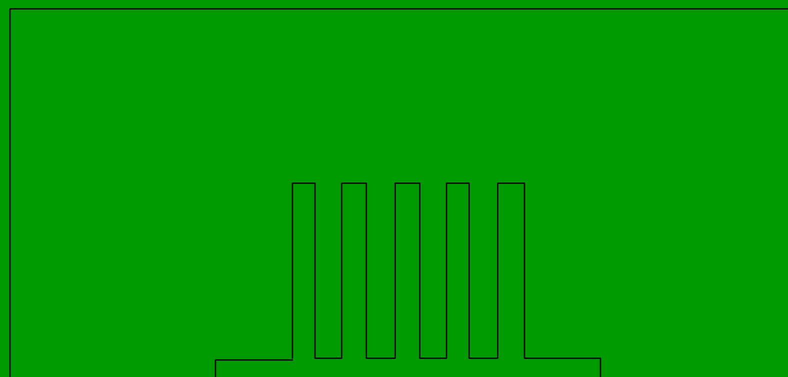

Confined flow

Bypass flow

Pressure drop

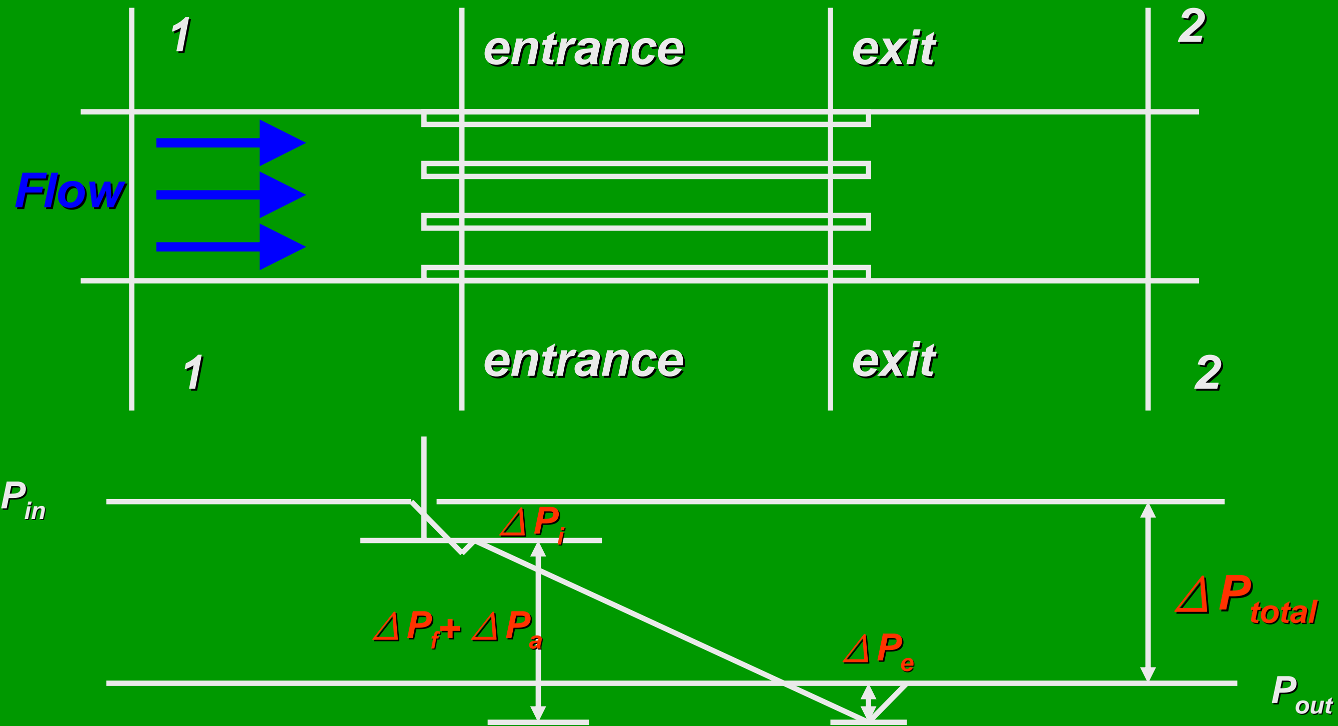

$$\Delta P_{total} = \Delta P_{entrance} + \Delta P_{frictional} + \Delta P_{exit}$$

$$\Delta P_{frictional} = 2f\frac{L}{D_h}\rho V^2 \qquad \Delta P_{entrance,exit} = \xi \times \frac{1}{2}\rho \bar{u}^2$$

$$f = \frac{24\left(1 - 1.3553\alpha + 1.9467\alpha^2 - 1.7012\alpha^3 + 0.9564\alpha^4 - 0.2537\alpha^5\right)}{\mathrm{Re}}$$

Physical Bypass Model

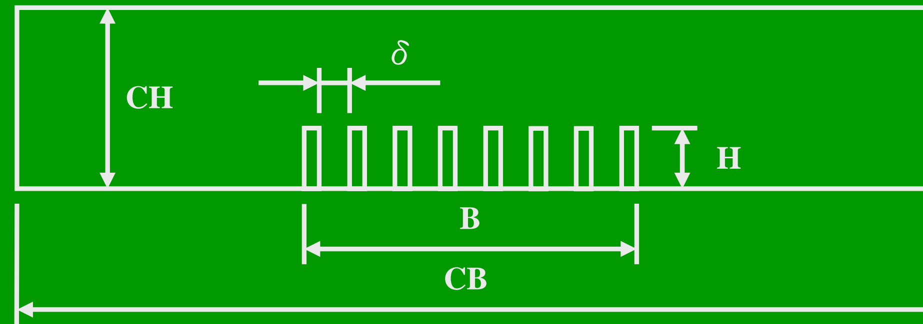

Front view of measurement section.

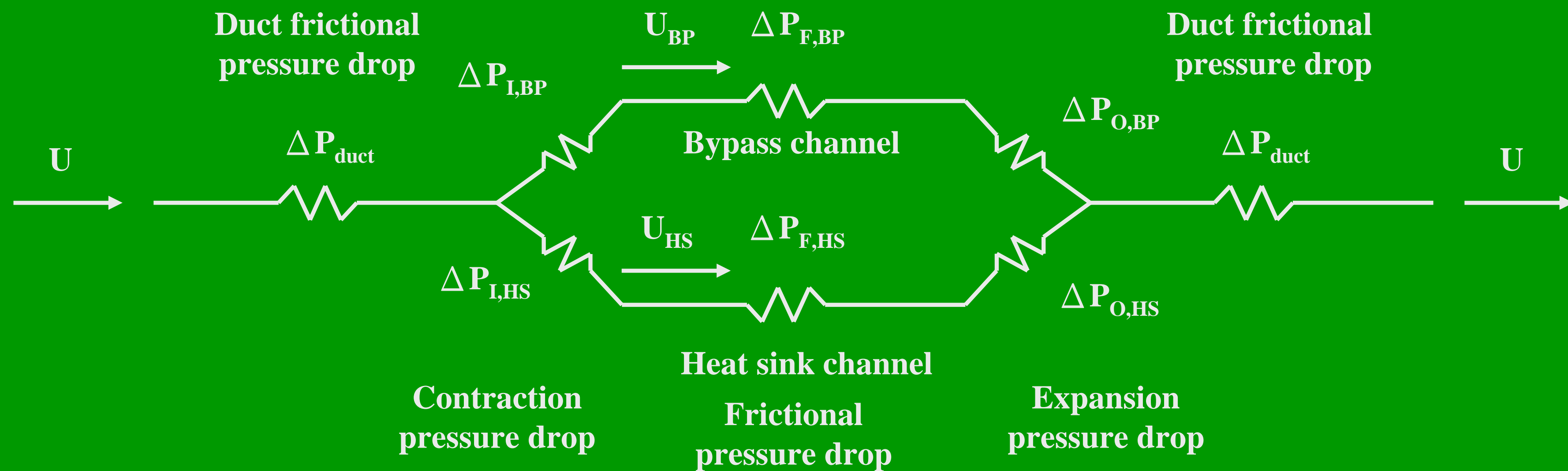

Fluid flow resistance net.

Impingement flow geometric configuration.

$$\Delta P = \left[\left(K_c + K_{90} + 4 f_{app1} \frac{L_{eff1}}{D_{h1}} \right) \frac{4H^2}{s^2} + 4 f_{app2} \frac{L_{eff2}}{D_{h2}} + K_e \right] \frac{1}{2} \rho_{ch2}^{\ 2}$$

Heat Transfer

Contact Resistance

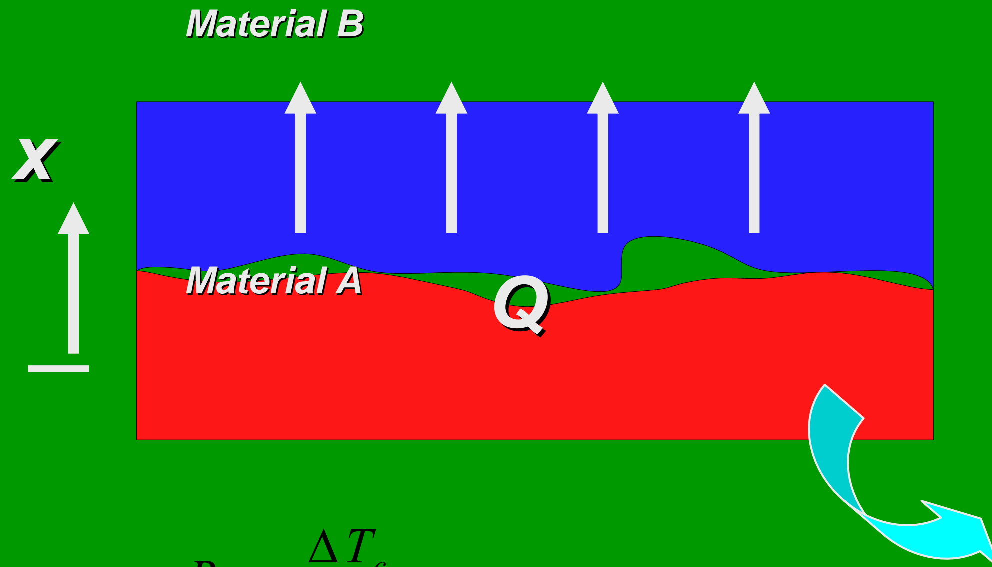

$$R_c = \frac{\Delta T_c}{Q}$$

Depends on:
- *Surface roughness*
- *Hardness of material*
- *Pressure at interface*
- *Fluid in the microscopic gaps*

Reduced by:
- *Thermal grease*
- *Thermal tapes or pad*
- *Secure attachment of heatsink with clip, screws, or other capture /retainment systems.*

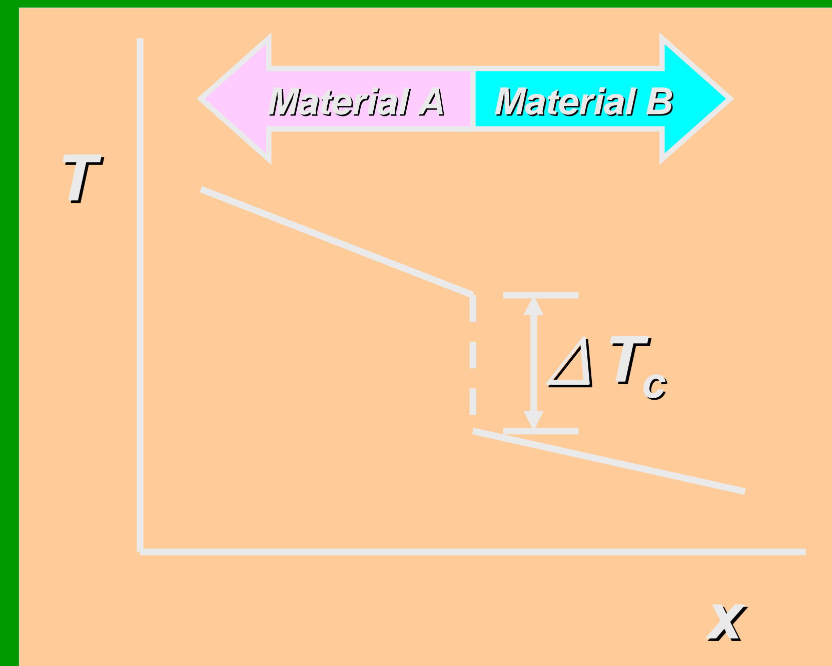

Spreading Resistance

Increasing the size of the heat sink does not always increase the cooling.

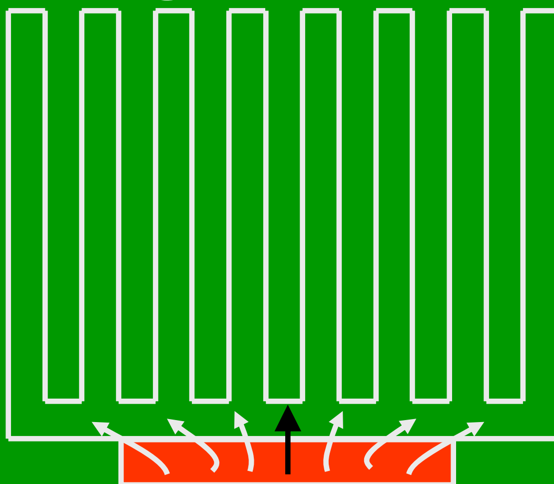

Q

The added temperature drop between the base of the heat sink and the tip of the fins is called a spreading resistance

If the component is smaller than the heat sink,
There may be a large temperature gradient in the base of heat sink.

Thermal resistance network from CPU surface to ambient

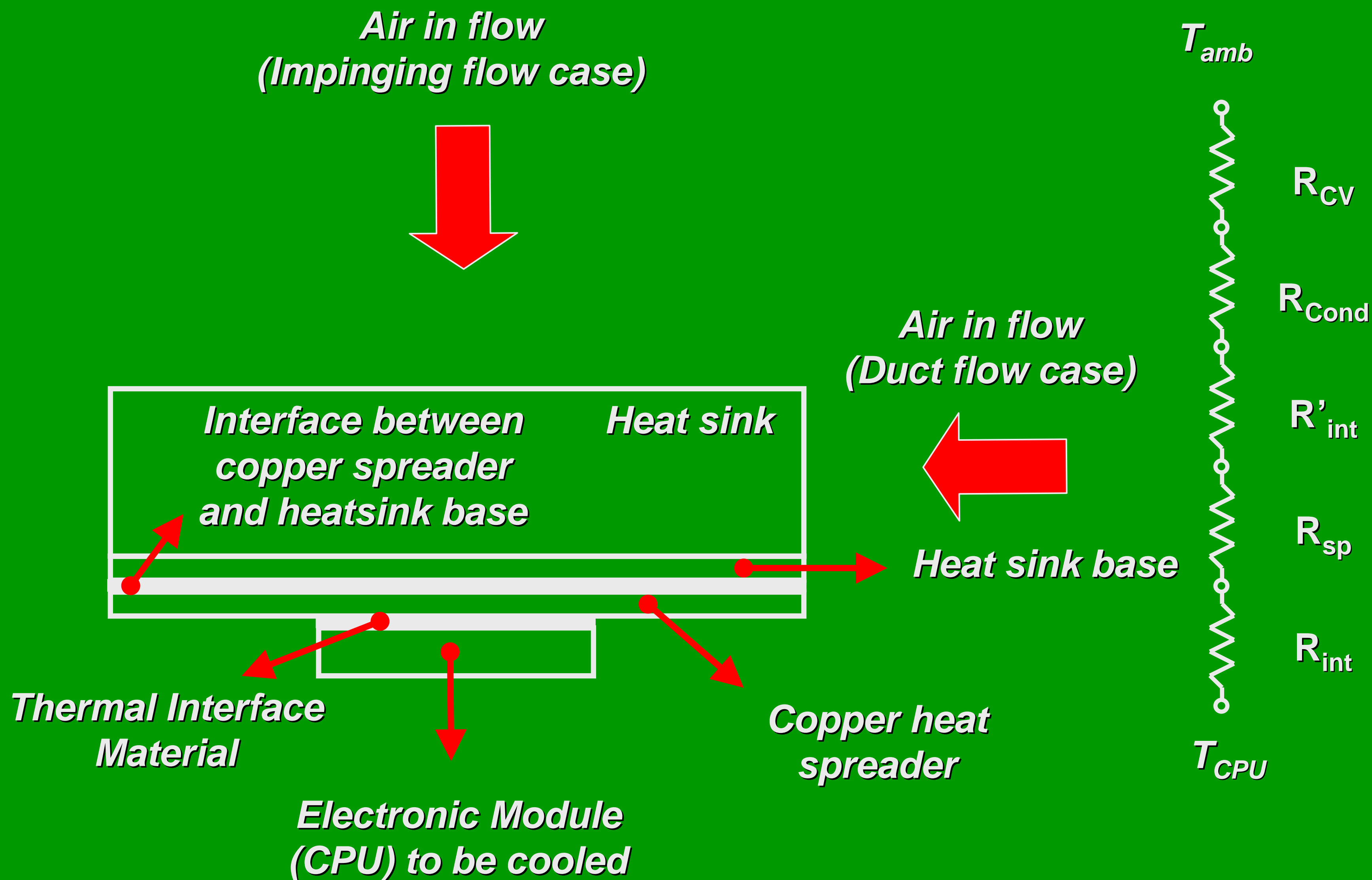

工業技術研究院
能源與資源研究所
Industrial Technology Research Institute
Energy & Resources Laboratories

Experimental set up

D1=9.5mm
D2=12.5mm
D3=17mm

Yokogawa
UNE12

P

Yokogawa
EJA 120A

8Point
T-Type TC

4Point
T-Type TC

P_{out} T_{out}

Test section
Press Load
Location:235mm

T_{in} P_{in}

Blower

470mm

Nozzle △P

90mm

140mm

90mm

140mm

TECO
1Hp motor

Yokogawa
EJA 110A

Frequency transformer

Test section
5Point
T-Type TC

Power supply

INSTEK
GPR-16H50D

Power meter

Yokogawa
WT-210

Yokogawa
MX100

PC

Recorder

風洞系統圖

Test section set up

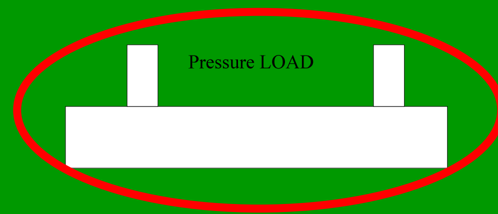

Long Win
LW-9052 Press
Load Apparatus
Press force range:
0 — 100 kgf

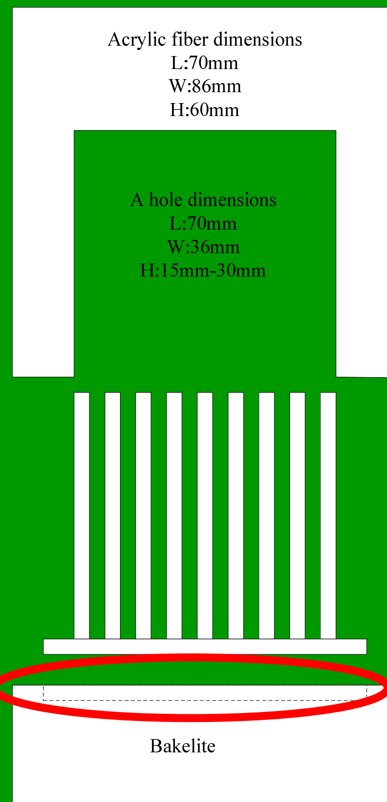

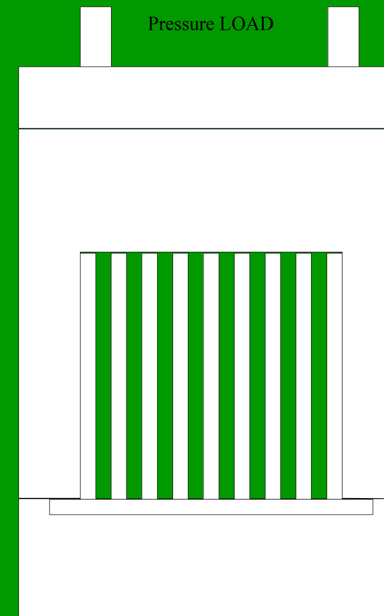

Tj and Tb

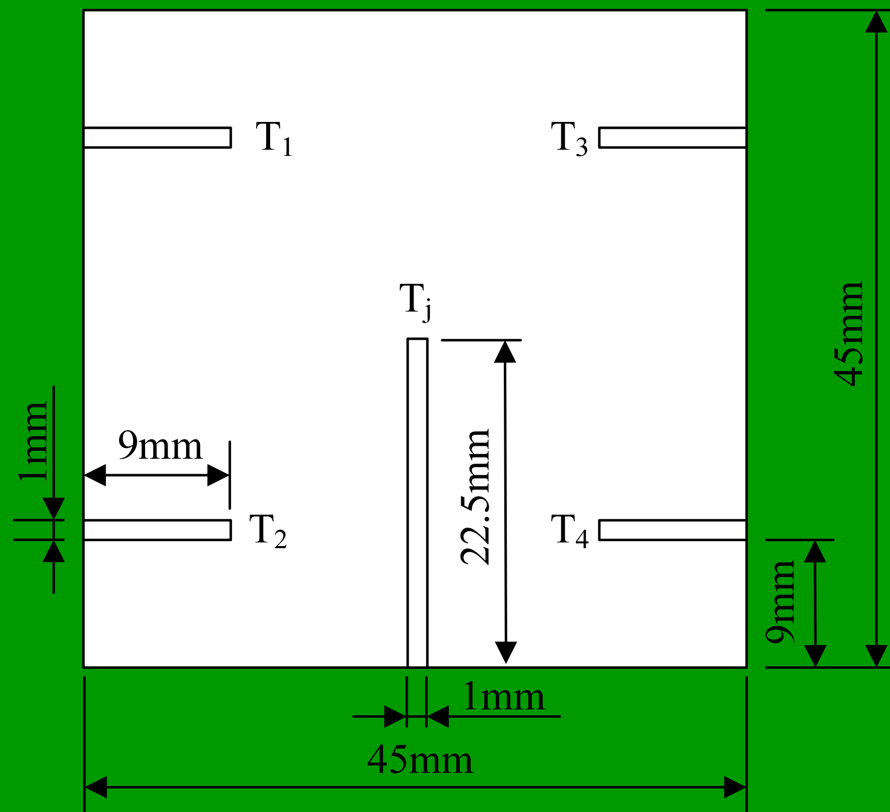

$$T_{base} = \frac{(T_1 + T_2 + T_3 + T_4 + T_j)}{5}$$

Plate Fin

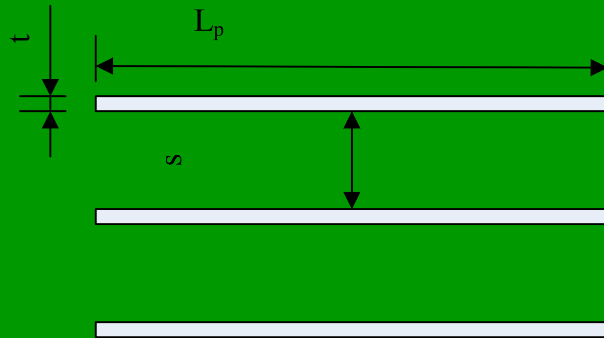

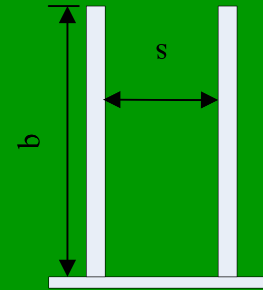

b=10mm
t=0.2mm
s=1.2mm

- ***Hartnett and Kostic[1989]***
  - *s/b=1.2/10 fully developed laminar flow solution*

$$Nu_H \cong 6.59$$

- Pr =0.712(300k)

$$f = \frac{24\left(1 - 1.3553\alpha + 1.9467\alpha^2 - 1.7012\alpha^3 + 0.9564\alpha^4 - 0.2537\alpha^5\right)}{\mathrm{Re}}$$

$$j = Nu\,\mathrm{Pr}^{-1/3} / \mathrm{Re}$$

Offset Fin

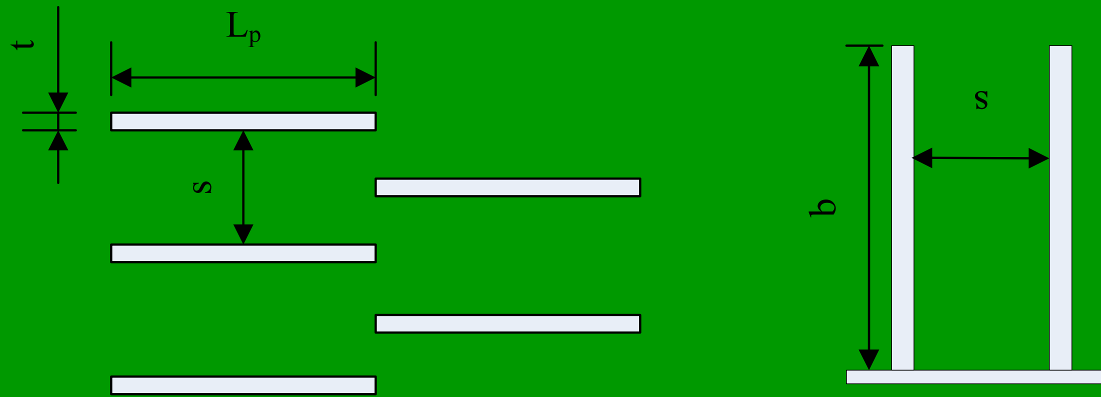

b=10mm
t=0.2mm
s=1.2mm
Lp=12.5mm

- ***Joshi and Webb[1987] for laminar flow***

$$f = 9.624\,\mathrm{Re}_{Dh}^{-0.742}\left(\frac{s}{b}\right)^{-0.186}\left(\frac{t}{Lp}\right)^{0.305}\left(\frac{t}{s}\right)^{-0.266}$$

$$j = 0.652\,\mathrm{Re}_{Dh}^{-0.54}\left(\frac{s}{b}\right)^{-0.154}\left(\frac{t}{L_p}\right)^{0.15}\left(\frac{t}{s}\right)^{-0.068}$$

Louvered Fin

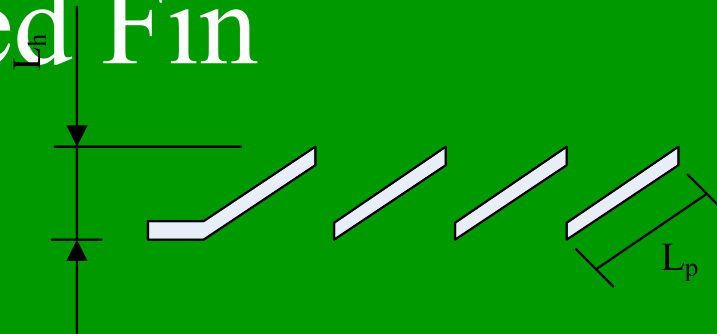

- ***Davenport[1983]***
  - ***H: Fin Pin height***
  - ***L_L: Louver length***
  - ***L_L: 6mm H: 10mm L_P:1mm L_h: 0.5mm***

$$j = 0.249\,\mathrm{Re}_L^{-0.42} L_h^{0.33} H^{0.26} \left(\frac{L_L}{H}\right)^{1.1} \qquad (300 < \mathrm{Re}_{Dh} < 4000)$$

$$f = 5.47\,\mathrm{Re}_L^{-0.72} L_h^{0.37} L_P^{0.2} H^{0.23} \left(\frac{L_L}{H}\right)^{0.89} \qquad (70 < \mathrm{Re}_{Dh} < 1000)$$

$$f = 0.494\,\mathrm{Re}_L^{-0.39} H^{0.46} \left(\frac{L_h}{L_P}\right)^{0.33} \left(\frac{L_L}{H}\right)^{1.1} \qquad (1000 < \mathrm{Re}_{Dh} < 4000)$$

Geometry

Heat Exchanger Geometry
All Dimensions are in (mm)

	Sample no.	Number of fin	Pitch	Length of fin	width of fin	Height of fin	Thickness of base	Thickness of fin	
plate fin	#1	10	2.77	45	45	20	2	1	
	#2	13	1.5	45	45	20	2	1.31	
	#3	15	1.4	45	45	20	2	1.03	
	#4	10	2.77	45	45	30	2	1	
	#5	13	1.52	45	45	30	2	1.28	
	#6	15	1.4	45	45	30	2	1.03	
pin fin	#7	64	2.7	45	45	15	2	2*2	In line
	#8	64	2.7	45	45	30	2	2*2	
	#9	100	1.66	45	45	15	2	2*2	
	#10	100	1.66	45	45	30	2	2*2	Staggered
pin fin	#11	32	7.4	45	45	15	2	2*2	
	#12	50	5.32	45	45	15	2	2*2	

Table 1. Detailed geometry of the test heat sink.

Fin height 20 mm, confined - h
Fin height 30 mm, confined - h
Fin height 20 mm, bypass - h
Fin height 30 mm, bypass - h
Fin height 20 mm, confined - ΔP
Fin height 30 mm, confined - ΔP
Fin height 20 mm, bypass - ΔP
Fin height 30 mm, bypass - ΔP

h (W/m²k)
80
60
40
20
0

ΔP (Pa)
50
40
30
20
10
0

0 1 2 3 4 5 6
V (m/s)

- Fin height 20 mm, pitch 2.77 mm - h
- Fin height 20 mm, pitch 1.9 mm - h
- Fin height 20 mm, pitch 1.4 mm - h
- Fin height 20 mm, pitch 2.77 mm - ΔP
- Fin height 20 mm, pitch 1.9 mm - ΔP
- Fin height 20 mm, pitch 1.4 mm - ΔP

h (W/m^2k)

ΔP (Pa)

V (m/s)

Cross flow VS. Impingement flow

Plate fin

Chart legend:
- Fin height 20 mm, cross flow - h
- Fin height 30 mm, cross flow - h
- Fin height 20 mm, impingement flow - h
- Fin height 30 mm, impingement flow - h
- Fin height 20 mm, cross flow - ΔP
- Fin height 30 mm, cross flow - ΔP
- Fin height 20 mm, impingement flow - ΔP
- Fin height 30 mm, impingement flow - ΔP

Left axis: h (W/m^{2}k), 0–200. Right axis: ΔP (Pa), 0–250. X-axis: V (m/s), 0–6.

Cross flow VS. Impingement flow

Inline pin fin

H 15 mm, cross flow - h
H 30 mm, cross flow - h
H 15 mm, impingement flow - h
H 30 mm, impingement flow - h
H 15 mm, cross flow - ΔP
H 30 mm, cross flow - ΔP
H 15 mm, impingement flow - ΔP
H 30 mm, impingement flow - ΔP

h (W/m²k)
250
200
150
100
50
0

ΔP (Pa)
200
160
120
80
40
0

0 1 2 3 4 5 6
V (m/s)

T ver

R (°C/W)

1

0.1

10^{-4} 10^{-3} 10^{-2} 10^{-1} 10^{0}

Pumping Power (kW)

P=2.77 mm, H=20 mm, cross flow
P=1.9 mm, H=20 mm, cross flow
P=1.4 mm, H=20 mm, cross flow
P=2.77 mm, H=30 mm, cross flow
P=1.9 mm, H=30 mm, cross flow
P=1.4 mm, H=30 mm, cross flow
P=2.77 mm, H=20 mm, impingement flow
P=1.9 mm, H=20 mm, impingement flow
P=1.4 mm, H=20 mm, impingement flow
P=2.77 mm, H=30 mm, impingement flow
P=1.9 mm, H=30 mm, impingement flow
P=1.4 mm, H=30 mm, impingement flow

模擬尺寸

Type 1

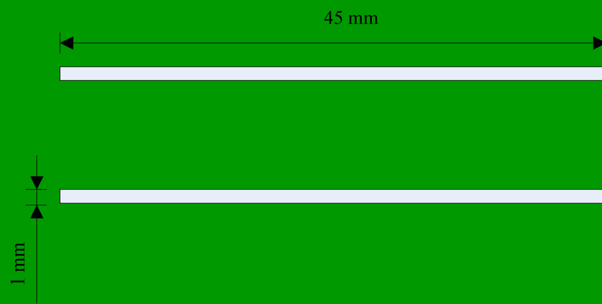

Type 3

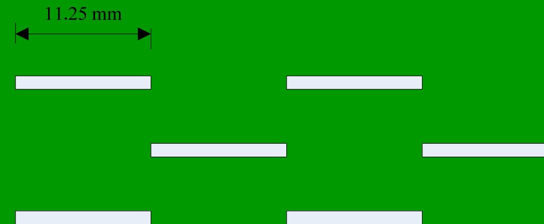

fin pitch, fin high, 及底板厚度皆相同

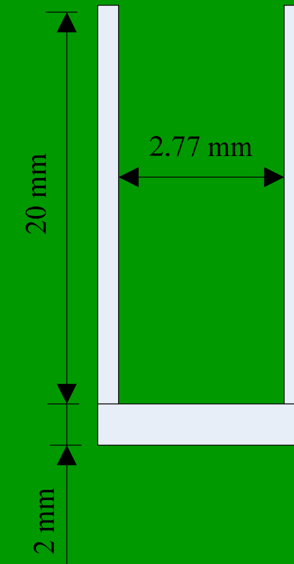

Type 2

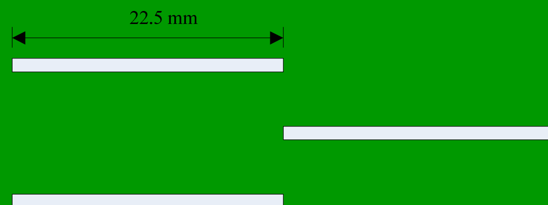

Type 4

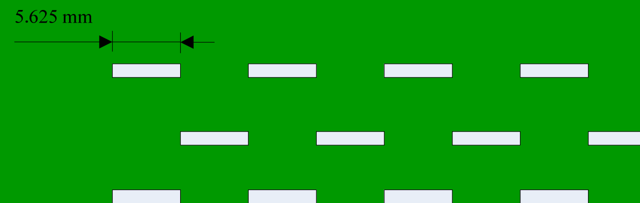

固體部分採用銅
流體則使用空氣

Fan/system interaction

Natural Convection

Outline

- Why Natural Convection?
- Thermal Resistance of LED
- Natural Convection Heat Transfer
- Augmentation by EHD
- Augmentation by Piezoelectric Fans
- Summary
- References

Why Natural Convection?

- Natural Convection is a noise-free and power-free thermal management method
- Under a junction temperature of 120 °C, white LEDs exhibit exceptional lifetime, exceeding 50000 hrs..

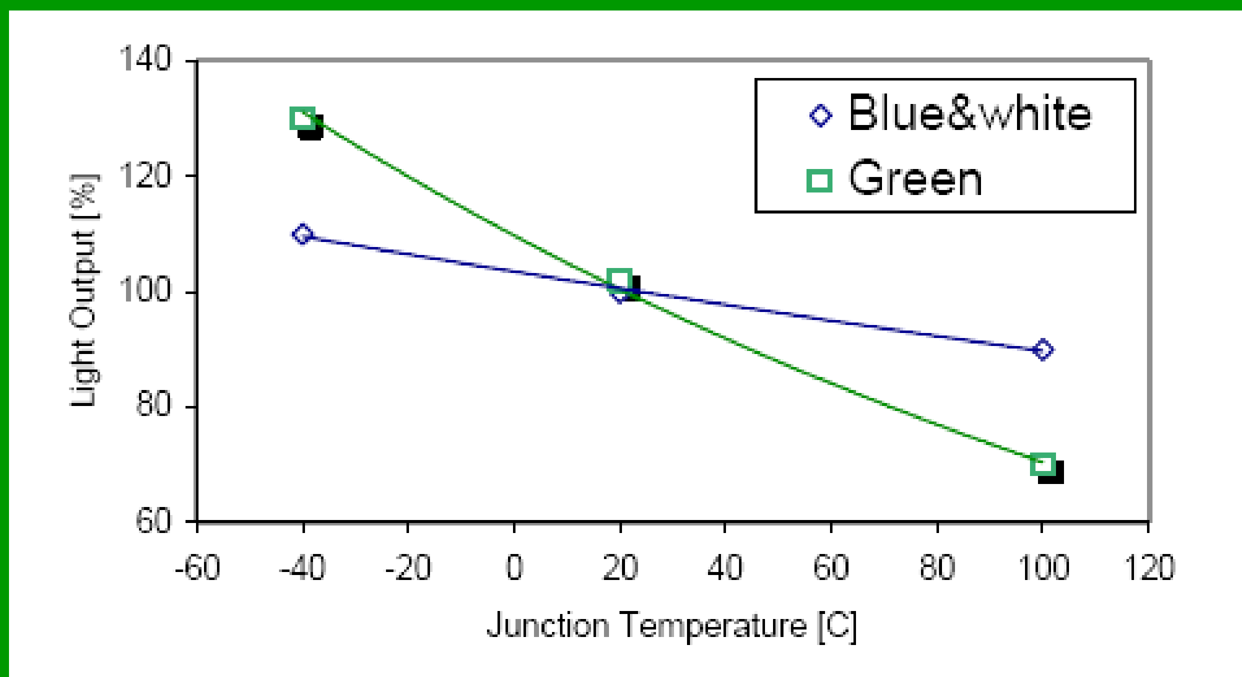

Fig. 1 Variation of the light output with the junction temperature [1].

Thermal Resistances of LED

$R_{silicone_3}$ $R_{phosphor}$ $R_{silicone_1}$ T_j R_{bump} $R_{sub\text{-}mount}$ R_{attach_1}

R_{lens} $R_{lead\ frame}$ $R_{silicone_2}$ R_{air} R_{cup}

$R_{plastic\ mold}$ R_{attach_2}

R_2 R_1

R_{ext_3} R_{solder_3} $R_{conductive\ pad}$

T_{board} R_{board}

$R_{adhesive}$ R_{cont}

R_{ext_2}

$T_{ambient}$ $T_{ambient}$ $T_{ambient}$

$R_{heat\ sink}$ R_{hs}

R_{ext_1} R_{conv}

$R_1 = R_{JBA}$

$R_2 = R_{JEA}$

Fig. 2 Typical resistance network for a LED illumination system [2].

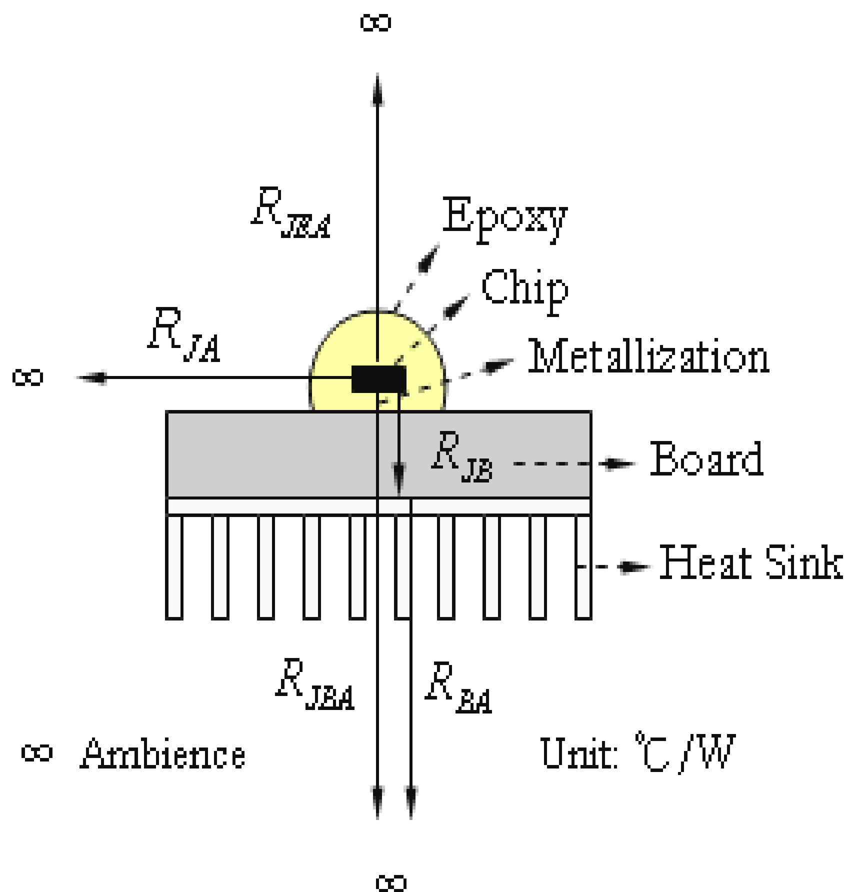

Fig. 3 A LED unit

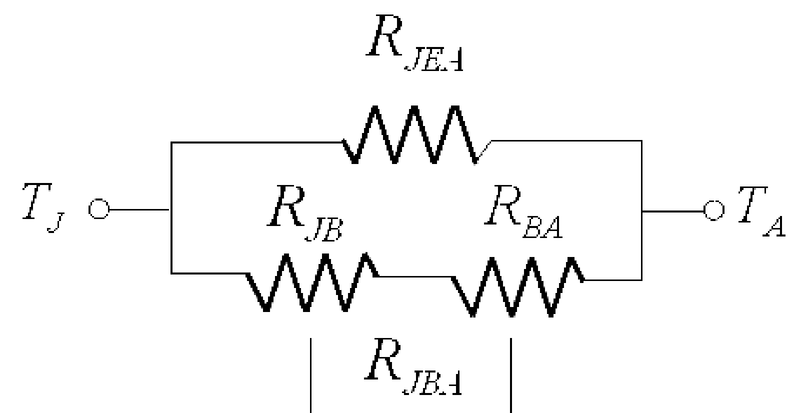

Fig. 4 Simplified resistance network.

$$\frac{1}{R_{JA}} = \frac{1}{R_{JEA}} + \frac{1}{R_{JBA}}$$

$$R_{JA} = R_{JBA} = R_{JB} + R_{BA}$$

J: junction
E: epoxy
B: board
A: ambience
cont: contact
hs: heat sink
conv: convection

R_{JB} and R_{BA} are of comparable magnitude

Our task : Minimize R_{BA}

$$R_{BA} = R_{cont} + R_{hs} + R_{conv}$$

工業技術研究院
能源與資源研究所
Industrial Technology Research Institute
Energy & Resources Laboratories

Heat Transfer Engineering, 26(2):50–53, 2005

The Effect of Plate Size on the Natural Convective Heat Transfer Intensity of Horizontal Surfaces

EWA RADZIEMSKA and WITOLD M. LEWANDOWSKI

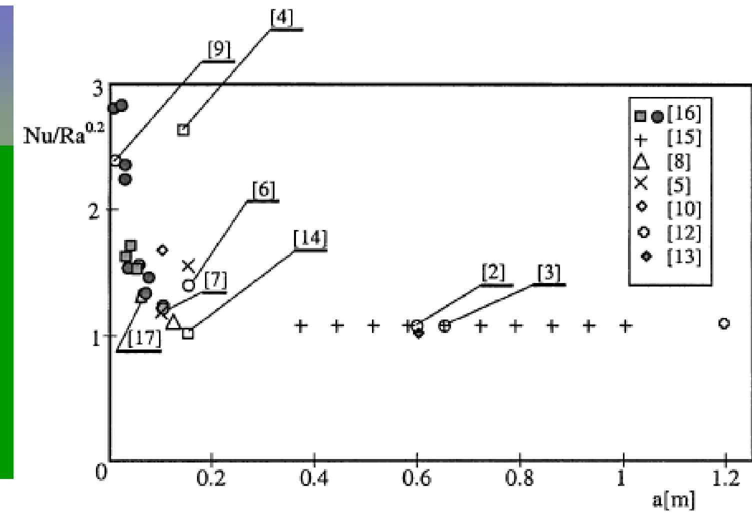

Table 1 Natural convection correlations for isothermal horizontal surfaces

Authors	Correlation	Converted correlations for Ra = 10^6 (for the purpose of comparison)	Width of the plate (a), m	Length of the plate (L), m	Fluid	Ra range
Al-Arabi and Sakr [3]	$Nu = 0.54(GrPr)^{0.25}$	$Nu = 1.077(GrPr)^{0.2}$	0.65	1.3	Air	$10^4 < Ra < 10^7$
Fishenden and Saunders [2]	$Nu = 0.54Ra^{0.25}$	$Nu = 1.077(GrPr)^{0.2}$	0.61	0.61	Air	$10^5 < Ra < 10^7$
Sharma and Adelman [4]	$Nu = 0.782Ra^{0.288}$	$Nu = 2.638Ra^{0.2}$	0.212	0.141	Water	$1.79 \times 10^5 < Ra < 10^9$
Reilly et al. [5]	$Nu = 0.591Ra^{0.25}$	$Nu = 1.179Ra^{0.2}$	0.2	0.098	—	—
Al-Arabi and El-Riedy [6]	$Nu = 0.17Ra^{0.36}$	$Nu = 1.55Ra^{0.2}$	0.302	0.149	—	—
Yousef et al. [7]	$Nu = 0.7Ra^{0.25}$	$Nu = 1.397Ra^{0.2}$	0.15	0.25–0.6	Air	$2 \times 10^5 < Ra < 10^9$
Lloyd and Moran [8]	$Nu = 0.622Ra^{0.25}$	$Nu = 1.2Ra^{0.2}$	0.1	0.1	Air	$3 \times 10^6 < Ra < 4 \times 10^7$
Yang et al. [9]	$Sh = 0.54Ra^{0.25}$	$Nu = 1.077Ra^{0.2}$	0.127	0.127	Electrolyte	$2.2 \times 10^4 < Ra < 8 \times 10^6$
Wilkes and Peterson [10]	$Nu = 0.125Ra^{0.25}$	$Nu = 2.245Ra^{0.2}$	0.025	0.025	Air	$10^4 < Ra < 10^7$
Griffith and Davis [12]	$h = 5.063(\Delta T)^{0.12}$	$Nu = 1.669Ra^{0.2}$	0.1	—	Air	—
Giesecke [13]	$h = 2.63(\Delta T)^{0.25}$	$Nu = 1.116Ra^{0.2}$	1.2	—	Air	—
Fujii and Imura [14]	$h = 3.158(\Delta T)^{0.25}$	$Nu = 1.015Ra^{0.2}$	0.6	—	Air	—
Michiejew [15]	$Nu = 0.16Ra^{1/3}$	$Nu = 1.01Ra^{0.2}$	0.15	0.3	Water	—
Radziemska	$Nu = 0.54(GrPr)^{0.25}$	$Nu = 1.077Ra^{0.2}$	0.25–1.0	—	—	$10^4 < Ra < 10^7$
and Lewandowski [16]	$Nu = 1.71Ra^{0.2}$	$Nu = 1.71Ra^{0.2}$	0.04	0.1	Water	$10^5 < Ra < 10^8$
	$Nu = 1.519Ra^{0.2}$	$Nu = 1.519Ra^{0.2}$	0.05	0.1	Water	$10^5 < Ra < 10^8$
	$Nu = 1.219Ra^{0.2}$	$Nu = 1.219Ra^{0.2}$	0.1	0.1	Water	$10^5 < Ra < 10^8$
	$Nu = 2.802Ra^{0.2}$	$Nu = 2.802Ra^{0.2}$	0.0048	0.1	Air	$10^4 < Ra < 10^7$
	$Nu = 2.393Ra^{0.2}$	$Nu = 2.393Ra^{0.2}$	0.0092	0.1	Air	$10^4 < Ra < 10^7$
	$Nu = 1.216Ra^{0.2}$	$Nu = 1.216Ra^{0.2}$	0.1	0.1	Air	$10^4 < Ra < 10^7$
	$Nu = 2.363Ra^{0.2}$	$Nu = 2.363Ra^{0.2}$	0.025	0.1	Air	$10^4 < Ra < 10^7$
	$Nu = 2.836Ra^{0.2}$	$Nu = 2.836Ra^{0.2}$	0.204	0.1	Air	$10^4 < Ra < 10^7$
	$Nu = 1.556Ra^{0.2}$	$Nu = 1.556Ra^{0.2}$	0.0531	0.1	Air	$10^4 < Ra < 10^7$
	$Nu = 1.463Ra^{0.2}$	$Nu = 1.463Ra^{0.2}$	0.0714	0.1	Air	$10^4 < Ra < 10^7$
	$Nu = 1.531Ra^{0.2}$	$Nu = 1.531Ra^{0.2}$	0.033	0.1	Air	$10^4 < Ra < 10^7$
	$Nu = 1.337Ra^{0.2}$	$Nu = 1.337Ra^{0.2}$	0.0659	0.1	Air	$10^4 < Ra < 10^7$
Lewandowski et al. [17]	$Nu = 1.228Ra^{0.2}$	$Nu = 1.228Ra^{0.2}$	0.07	0.1	Air	$10^5 < Ra < 10^8$

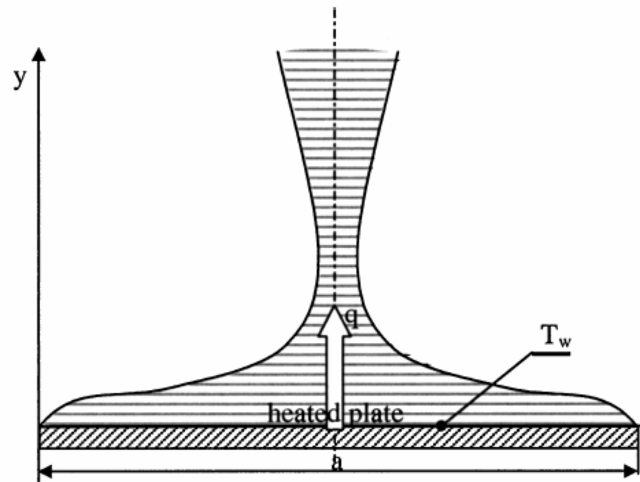

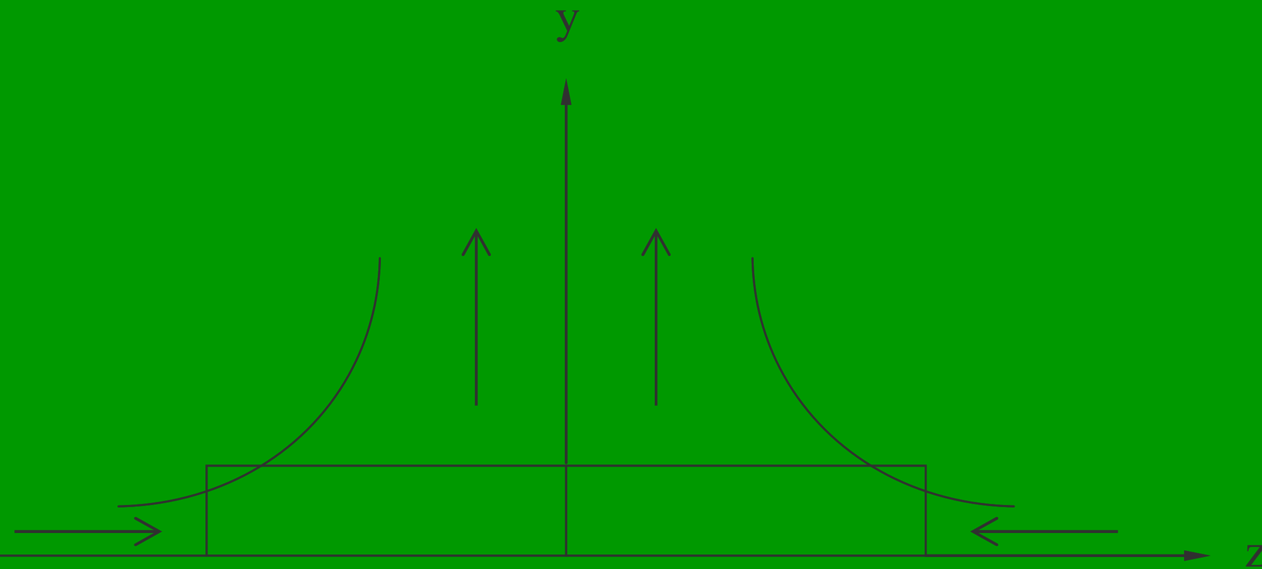

(a) Single chimney mode flow pattern.

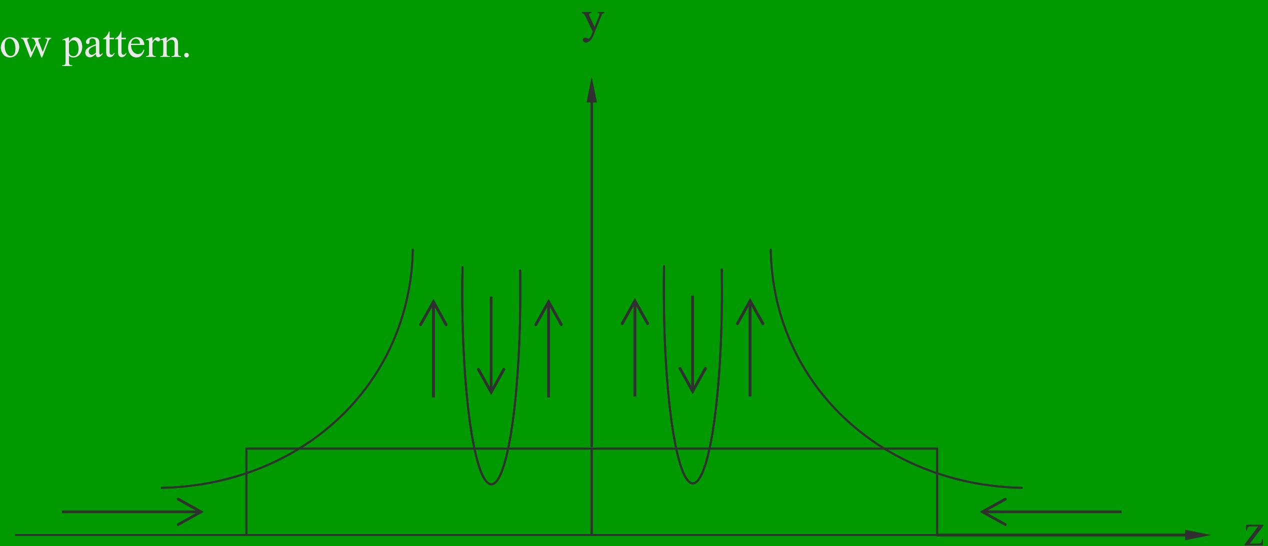

(b) Multiple chimney mode flow pattern.

Test Samples: Plate Fin

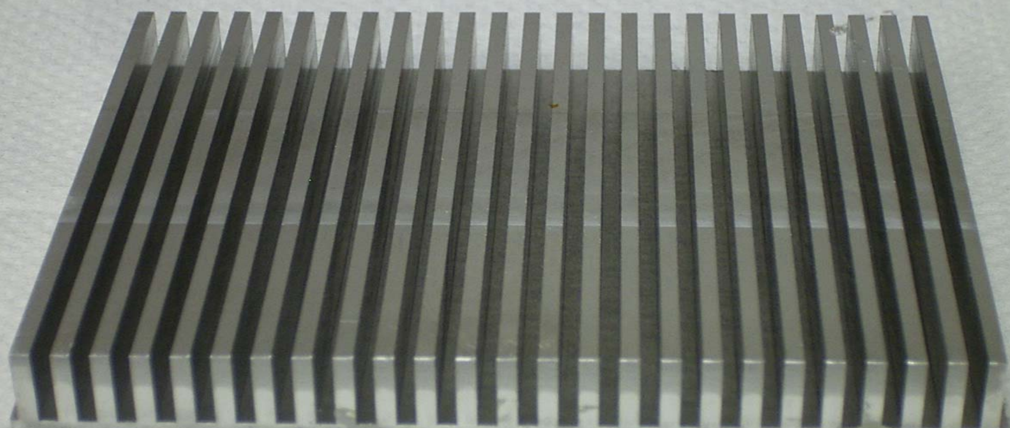

Test Samples: Pin Fin (Square)

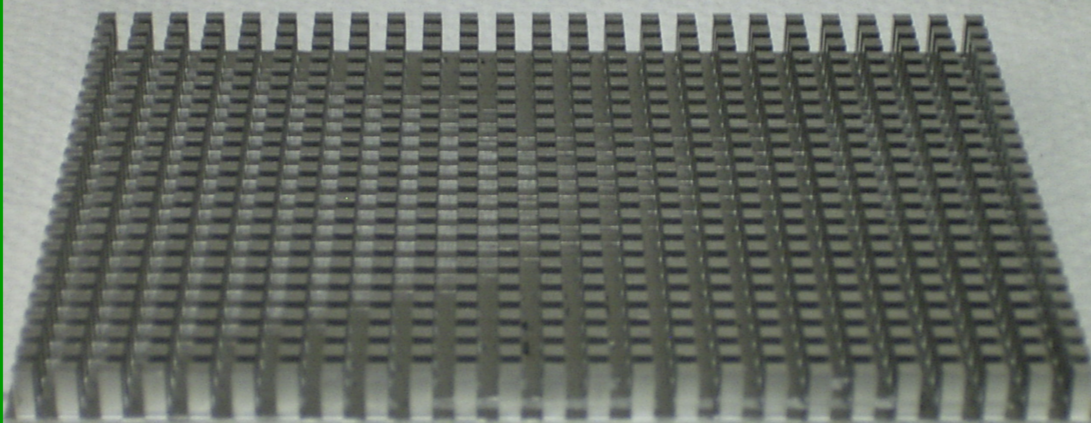

Experimental Investigation of Heat Sink Via Natural Convection

Environmental Chamber

Heat Sink

Heater

g

Insulation Box

Tilting Mechanism

$\Delta x = 3$ mm

20 30 30 20

17.5 30 30 17.5

The experimental setup.

Some Terminologies

Heat transfer coefficient

$$h = \frac{Q_{in}}{A_t(T_b - T_a)} = \frac{Q_t - Q_{loss}}{A_t(T_b - T_a)}$$

Rayleigh number

$$Ra = \frac{g\beta\left(T_b - T_a\right)L^3}{\nu\alpha}$$

Nusselt number

$$Nu = \frac{hL}{k}$$

Film temperature

$$T_f = \frac{T_b + T_a}{2}$$

a: ambience
b: base plate
f: film
t: total

Fig. 6 Performance comparison between pin fin and plate fin heat sinks.

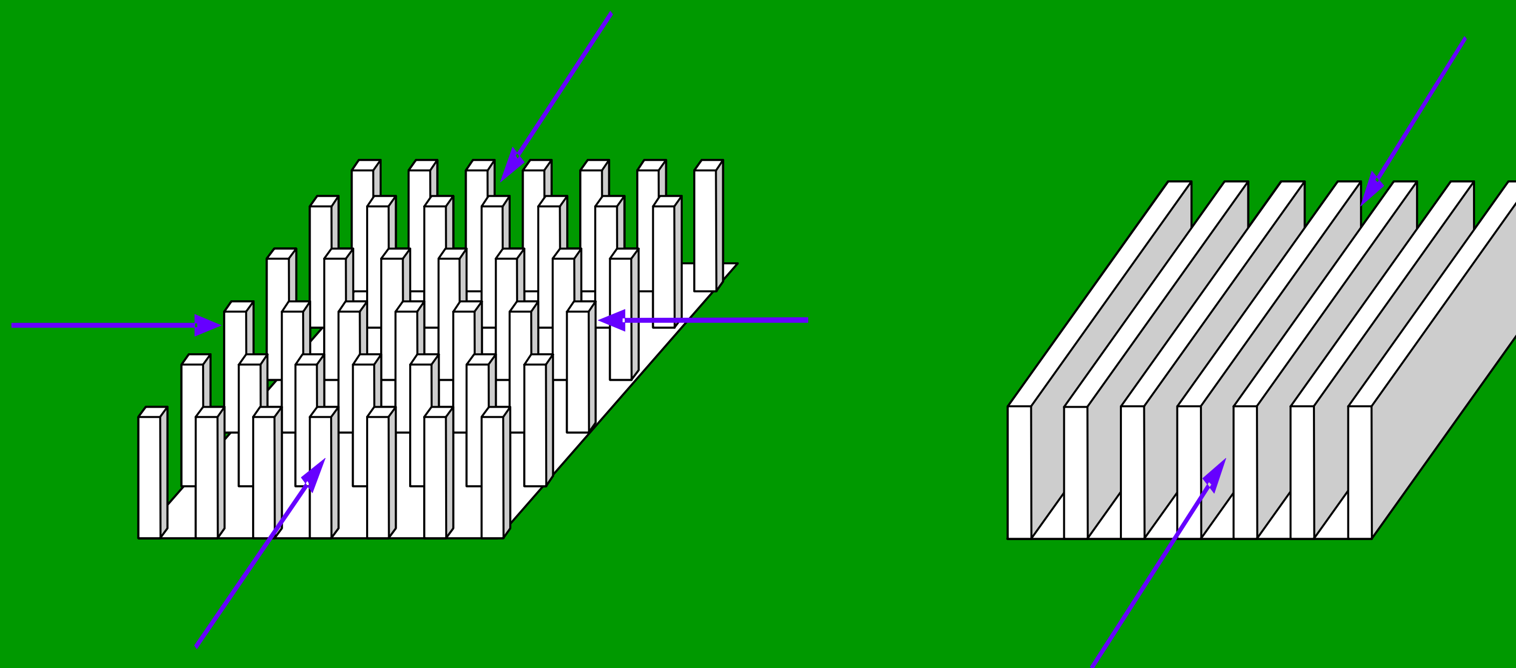

Schematic of induced main flow for pin fin and plate fin geometry.

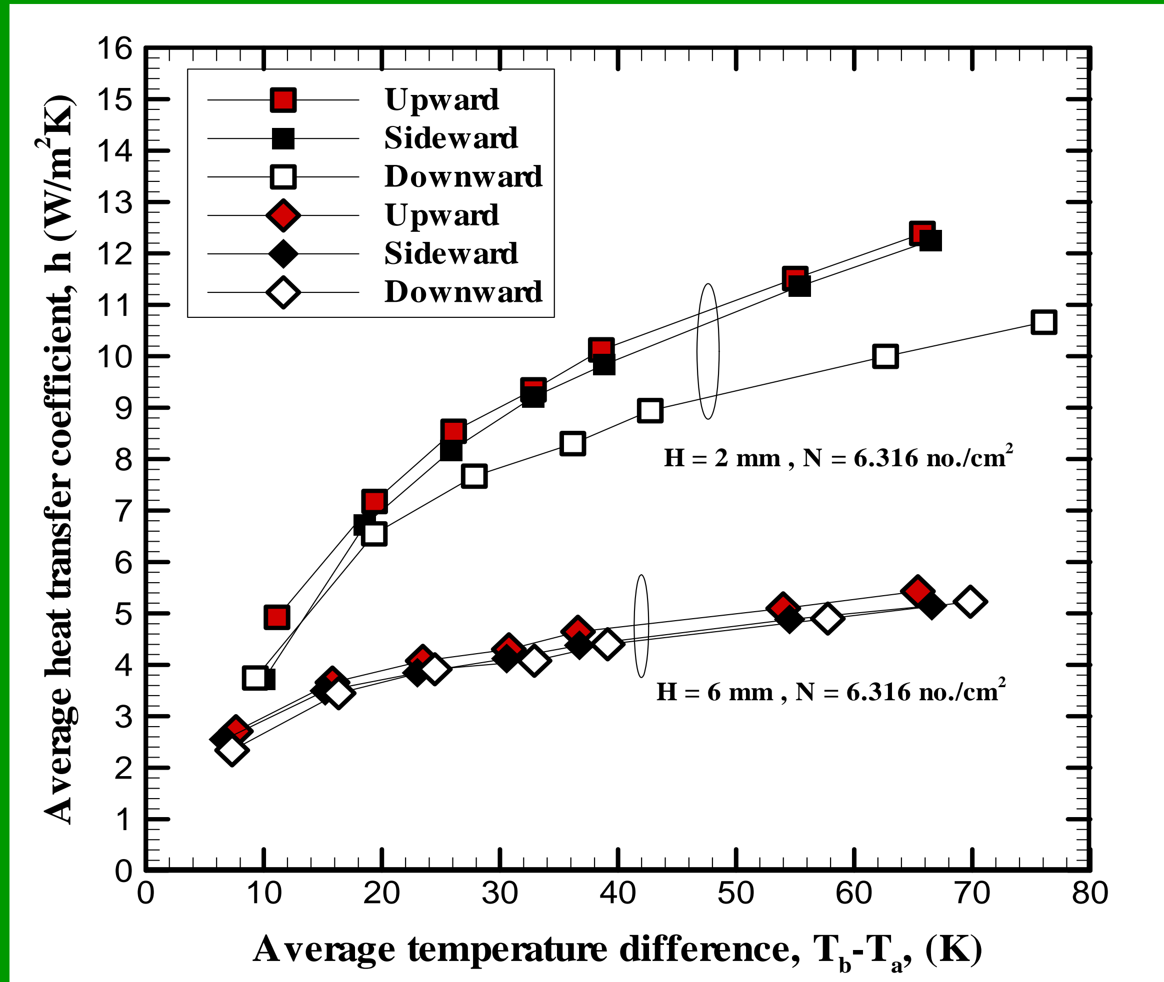

Performance comparison among the three orientations.

Dependence on the performance on the pin height.

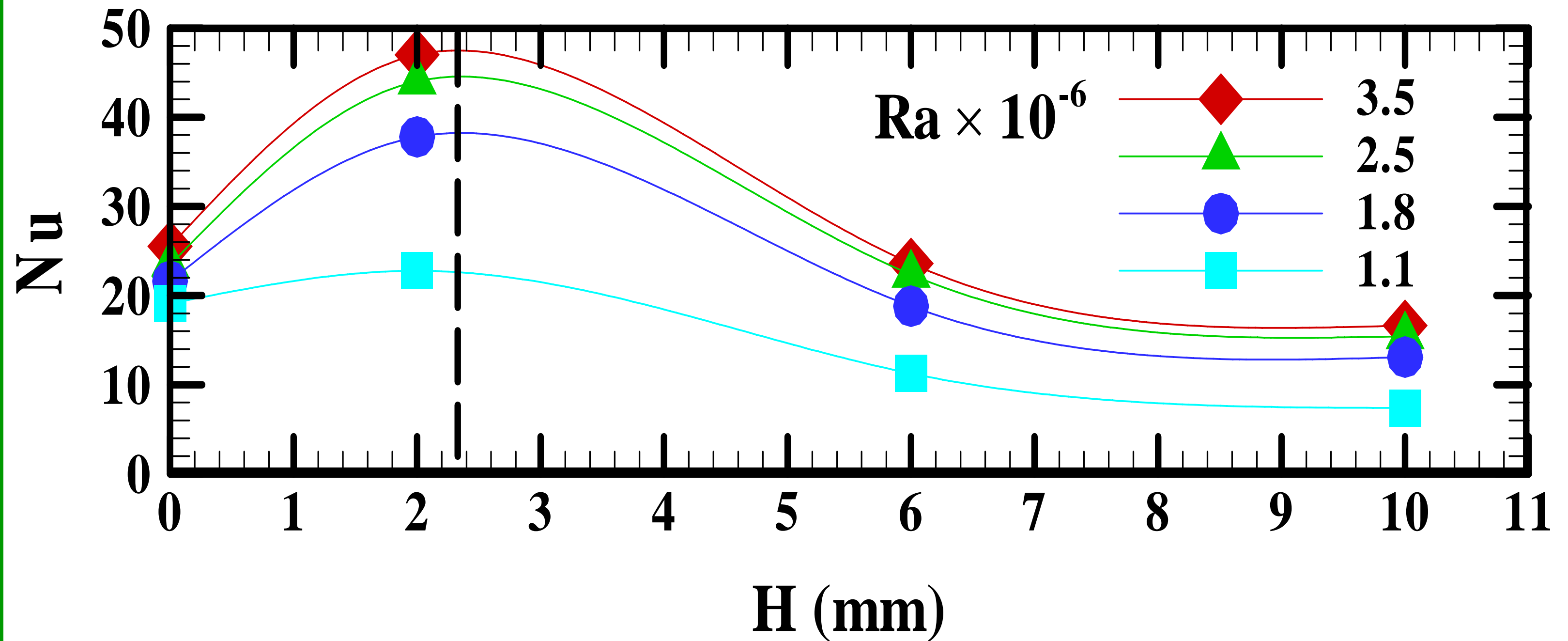

Dependence on the performance on the number density.

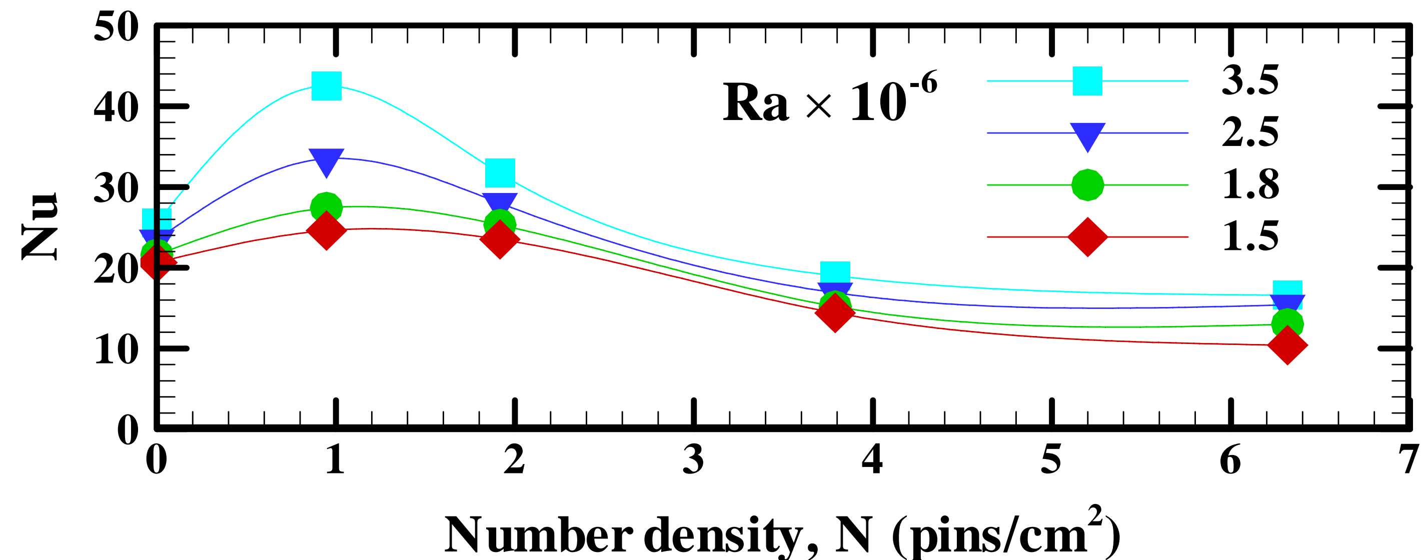

EHD Convection

EHD stands for Electro Hydro Dynamics which is the study of the flow of a fluid under the effect of an electric field.

When a Newtonian, impressible fluid is subject to the presence of electric field, the Navier-Stokes equation becomes:

$$\rho \frac{D\vec{V}}{Dt} = -\nabla p + \mu \nabla^2 \vec{V} + \rho \vec{g} + \vec{f}_e$$

EHD body force

The EHD body force consists of:

1. **Coulomb force,** resulting from the net free charges within the fluid
2. **Dielectrophoretic force**, resulting from the difference between permittivity of the fluid and gas phases.
3. **Electrostrictive force**, resulting from the non-uniformity of the electric field within the fluid.

$$\vec{f}_e = \rho_c \vec{E} - \frac{1}{2}\left|\vec{E}\right|^2 \nabla \varepsilon + \frac{1}{2}\nabla\left[\left|\vec{E}\right|^2 \rho \left(\frac{\partial \varepsilon}{\partial \rho}\right)_T\right]$$

Coulomb force

electrostrictive force

dielectrophoretic force

For a single-phase flow,

Neglect dielectrophoretic force: The permittivity gradient is negligible due to slight temperature difference.

Neglect electrostrictive force: electrostriction doesn't affect the flow field in the absence of a two-phase interface.

$$\vec{f}_e = \rho_c \vec{E} - \frac{1}{2}\left|\vec{E}\right|^2 \nabla \varepsilon + \frac{1}{2}\nabla\left[\left|\vec{E}\right|^2 \rho \left(\frac{\partial \varepsilon}{\partial \rho}\right)_T\right]$$

$$\Rightarrow \quad \vec{f}_e = \rho_c \vec{E}$$

Corona wind

A fluid motion driven by an electric field is termed a corona wind or an ionic wind.

Corona region (Ionization region)

Near the charged electrode, ionization occurs and creates positive ions and free electrons in a process known as the electron avalanche. The positive ions are attracted toward or repelled away from the curved electrode (depending on the polarity). The electrons thus migrate in the opposite direction.

Unipolar region

The energized electrons, accelerated by the electric field, inelastically collide with the neutral atoms, entraining the stagnant fluid from the ambience to the grounded surface.

Positive Corona

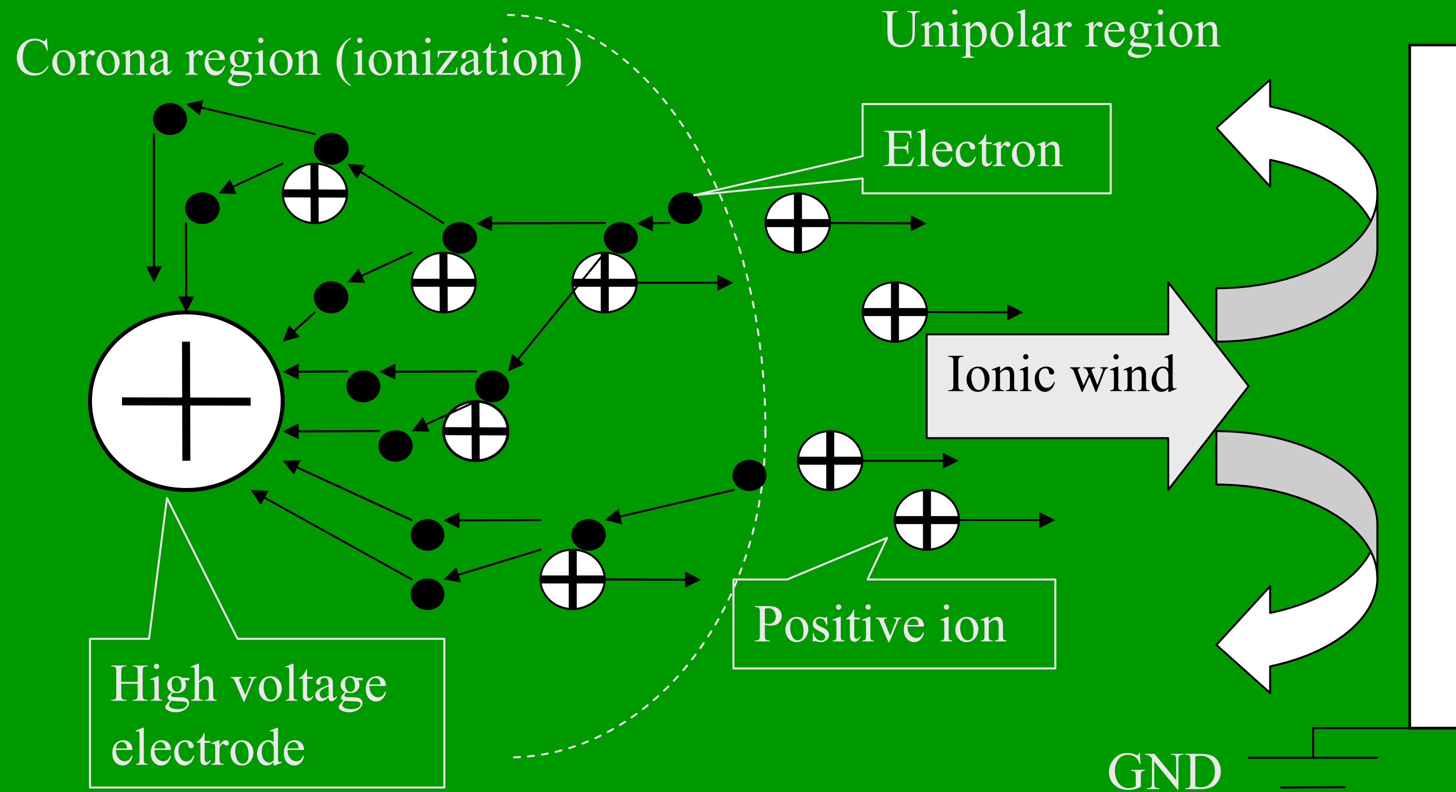

Positive corona generation and ionic wind.

Negative Corona

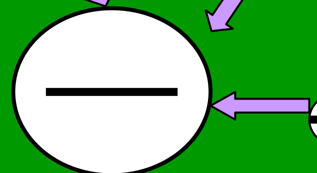
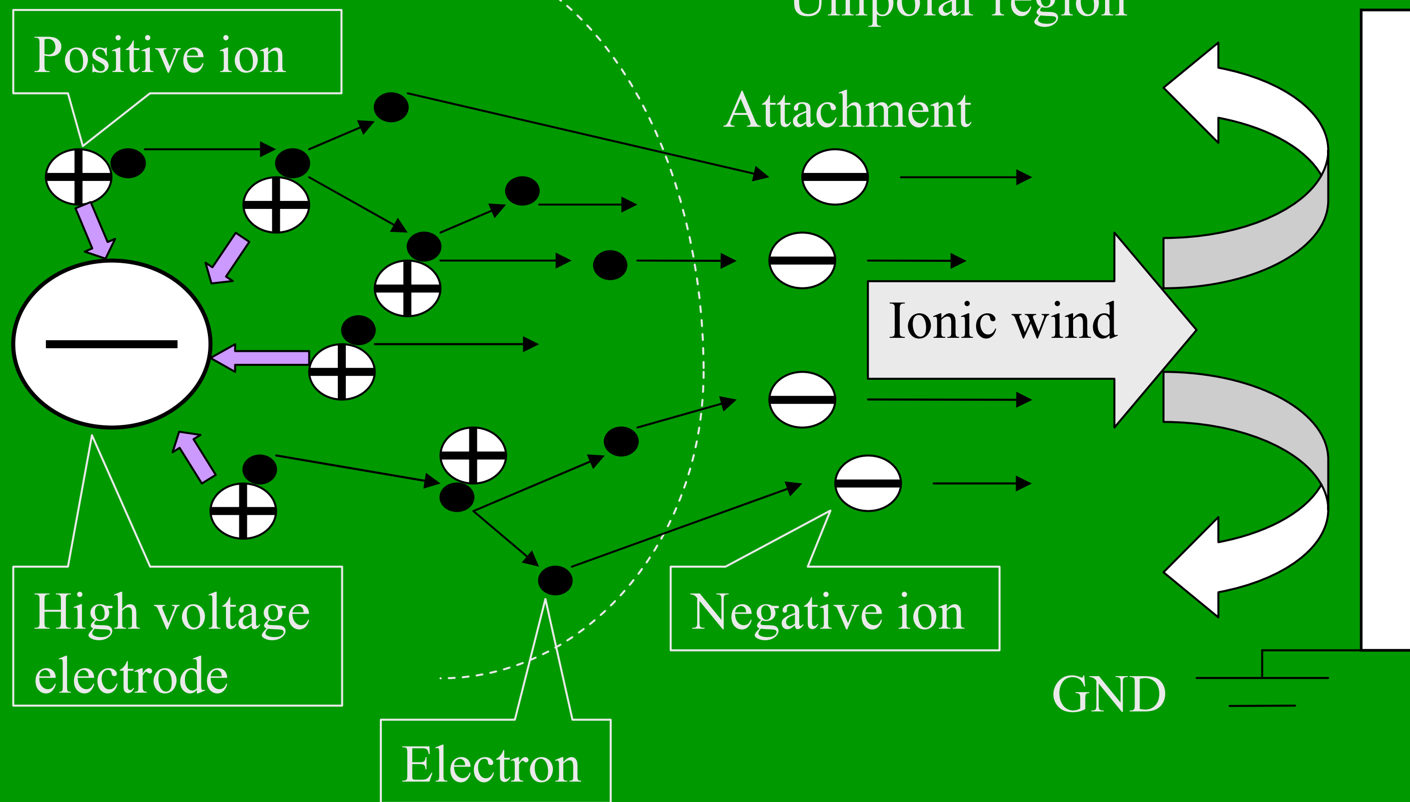

Negative corona generation and ionic wind.

Electrode geometry

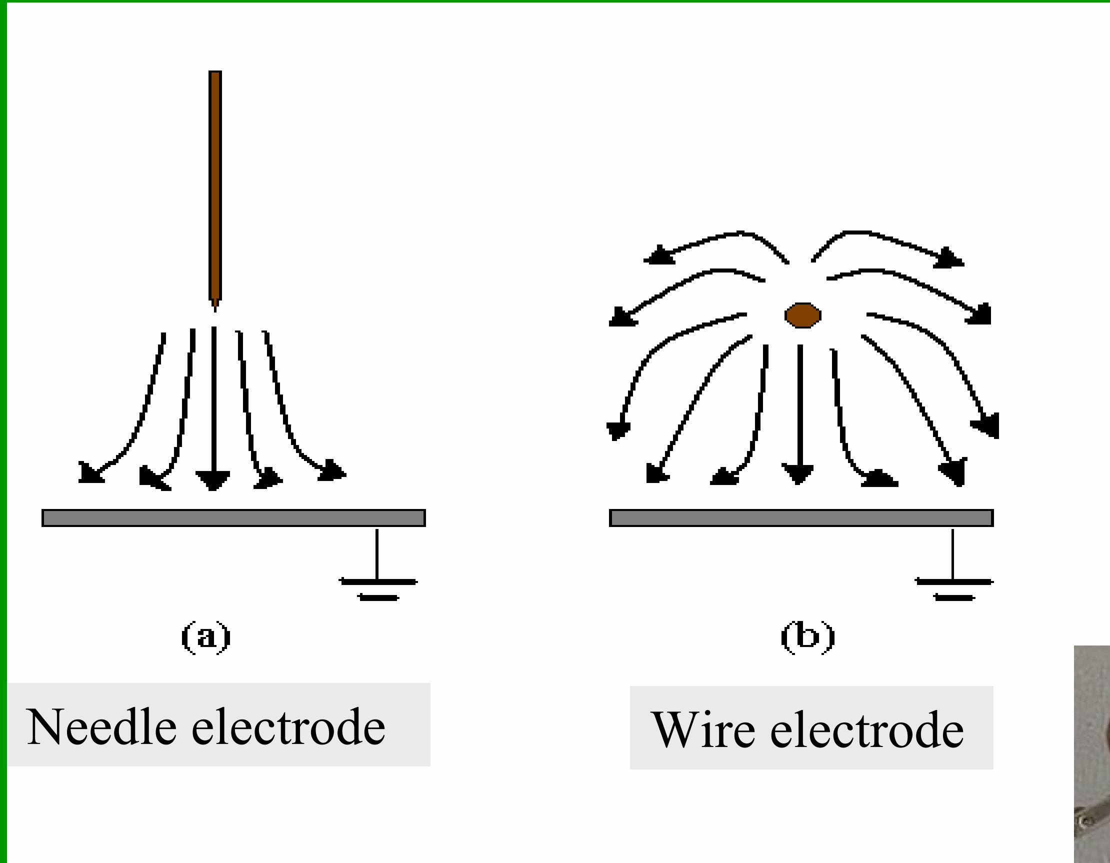

$$E_p = \frac{2V}{R \log_{10}\left(\frac{4x}{R}\right)}$$

Typical electrode types.

Electrode materials

Generally, metallic materials such as **copper, brass, Platinum**, **stainless steel**, and **tungsten steel** have been chosen as electrodes. The selected material should not react with the surrounded fluid.

In the present study, tungsten steel is utilized as the electrode material.

Onset voltage:

The voltage at which corona discharge phenomenon takes place.

Threshold voltage:

The voltage to which a chain-reaction of electron avalanche occurs and triggers rapid molecule collision, thus creating electroconvection.

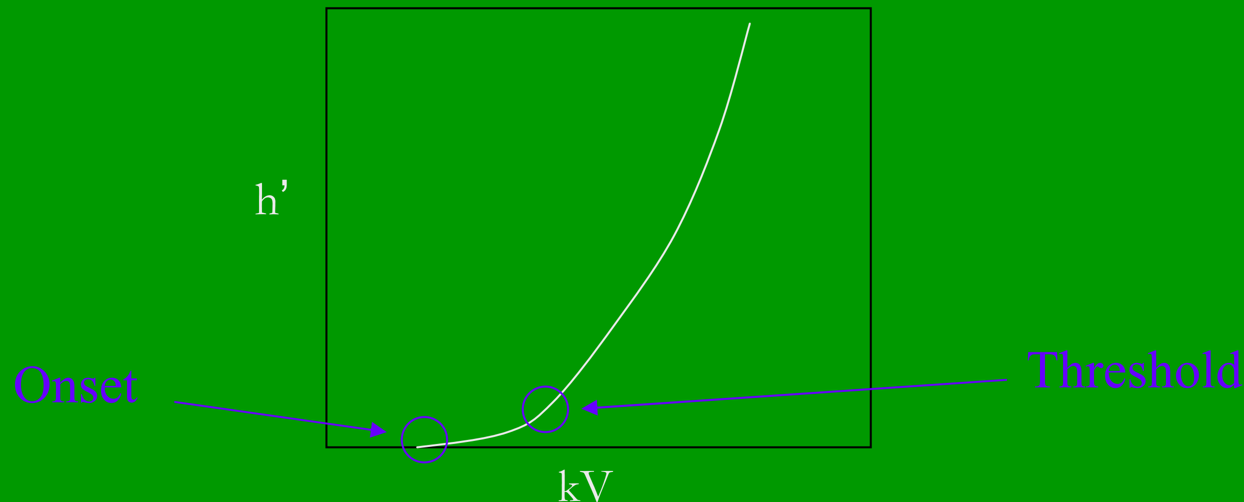

Design Criterion for Electrodes

1. low threshold voltage
2. high slope I-V curve
3. high spark-over voltage

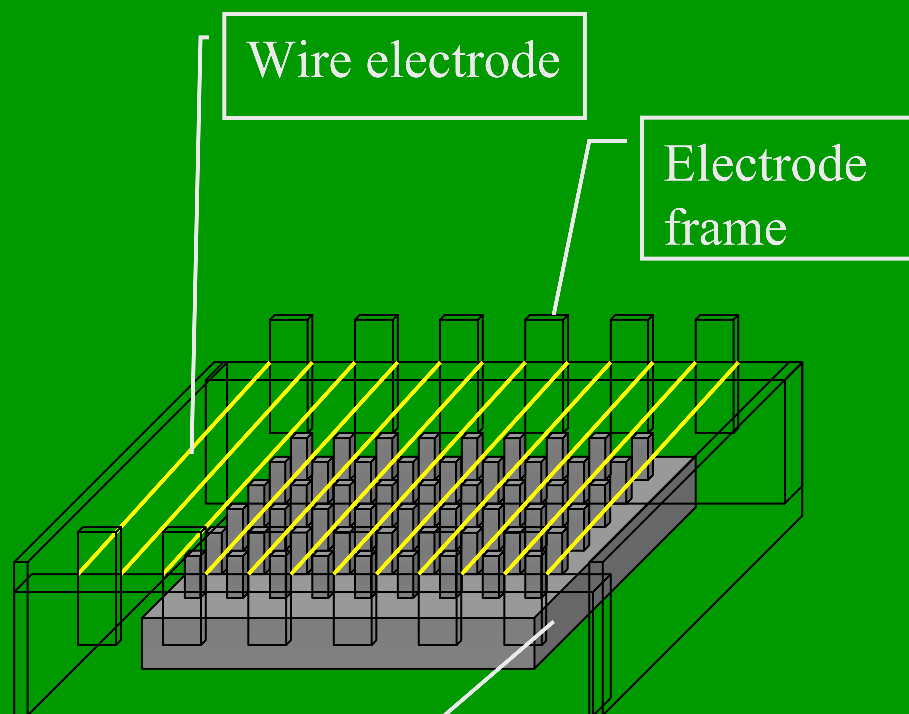

The electrode arrangement.

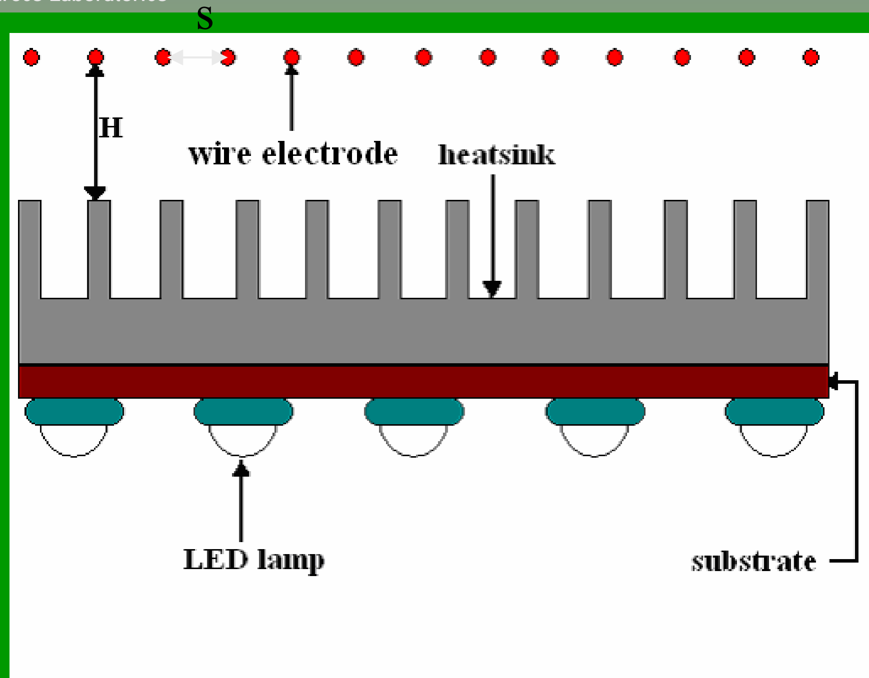

H: separation distance
S: electrode spacing

Fig. 16 Illustration of the electrode arrangement.

Enhancement ratio

$$E_R = \frac{Nu_{EHD}}{Nu_{natural}}$$

$$h' = \frac{h_{EHD}}{h_{natural}} = \frac{(T_b - T_a)_{natural}}{(T_b - T_a)_{EHD}}$$

Upward facing

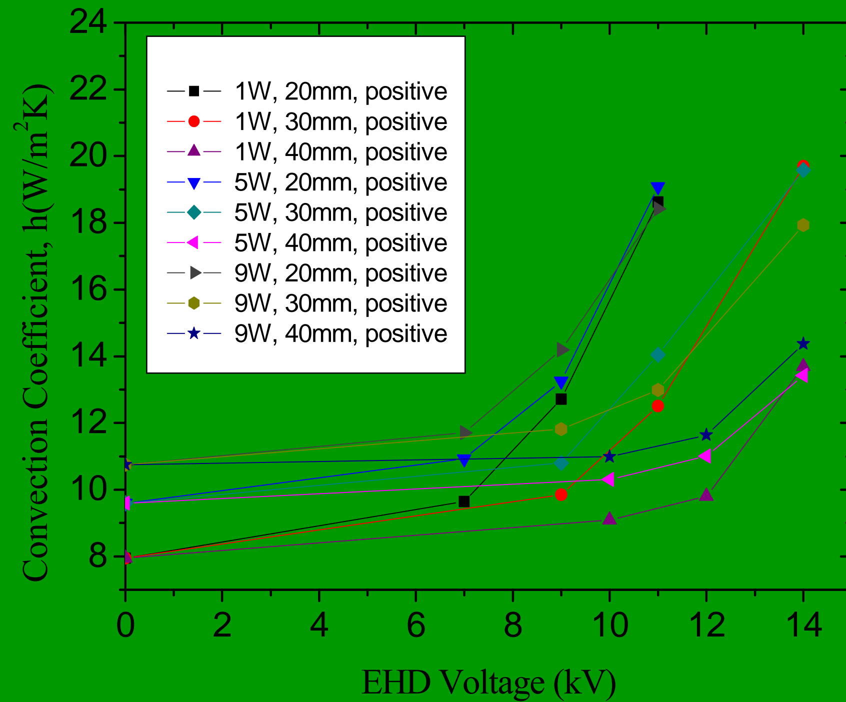

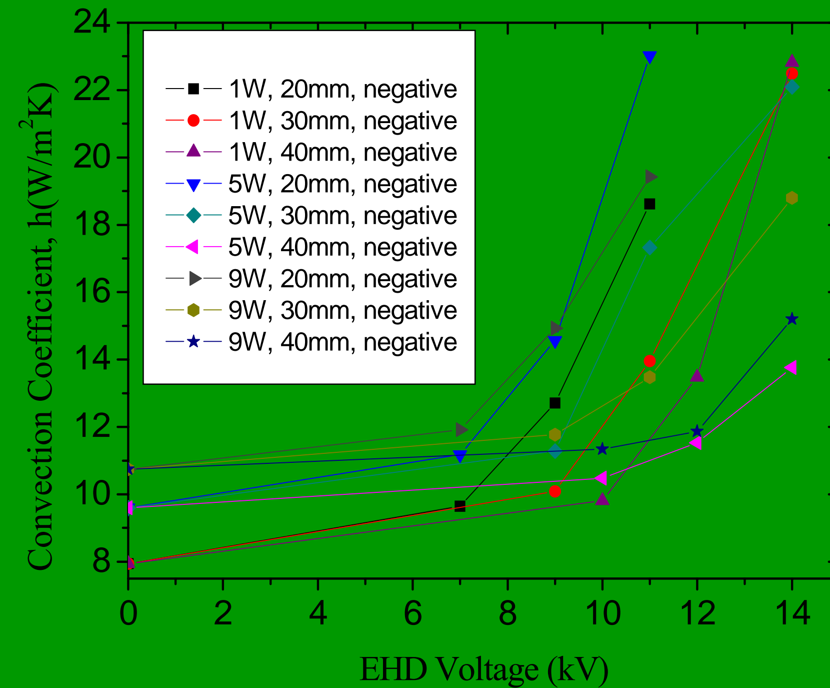

Supplied voltage versus heat transfer enhancement, 20 mm electrode spacing, positive polarity and negative polarity.

Gradual increase of heat flux

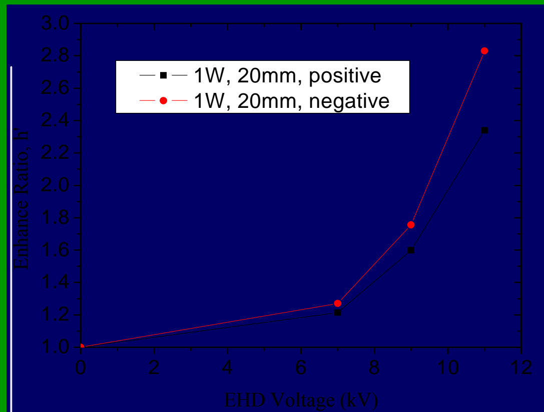

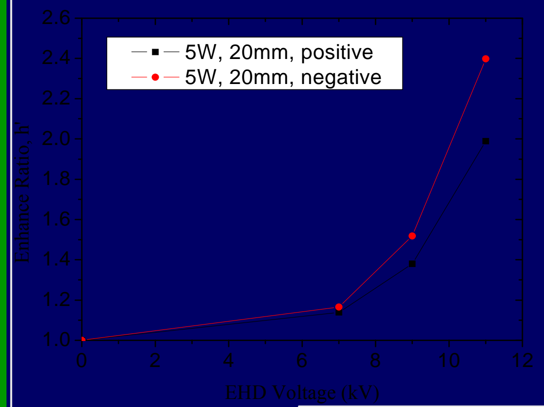

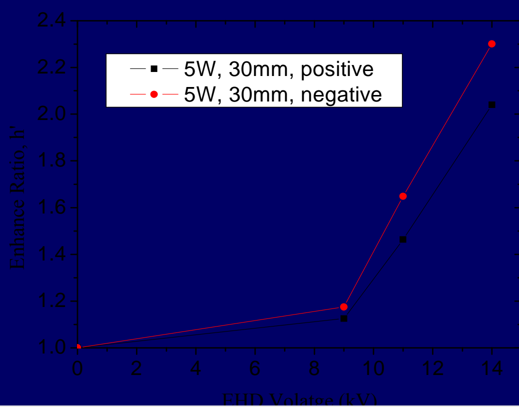

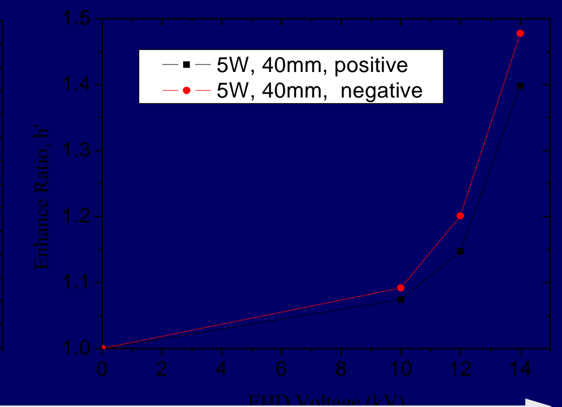

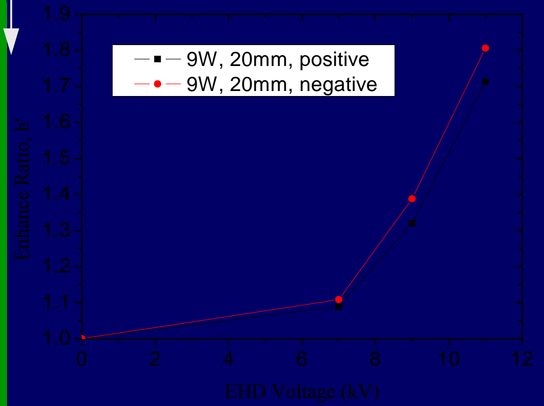

Gradual increase of electrode spacing

Effect of electrode polarity on the heat transfer enhancement.

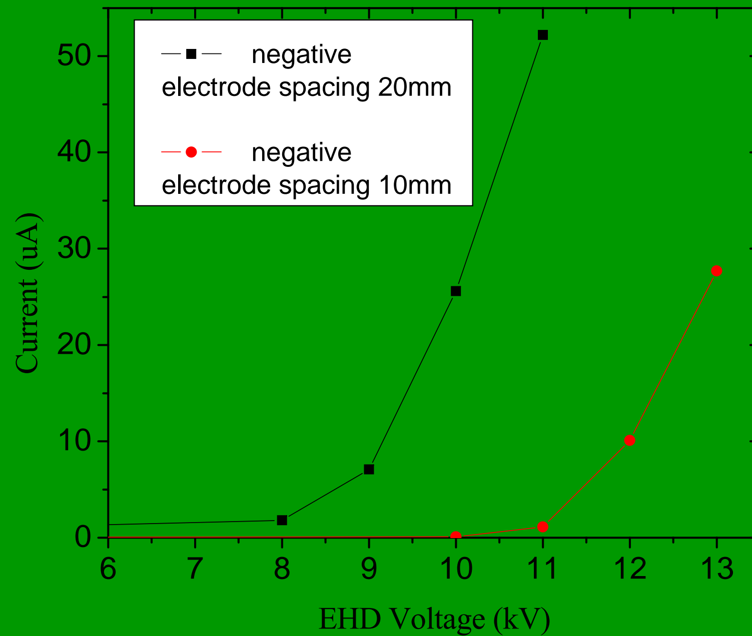

Effect of electrode spacing (S) on the current density.

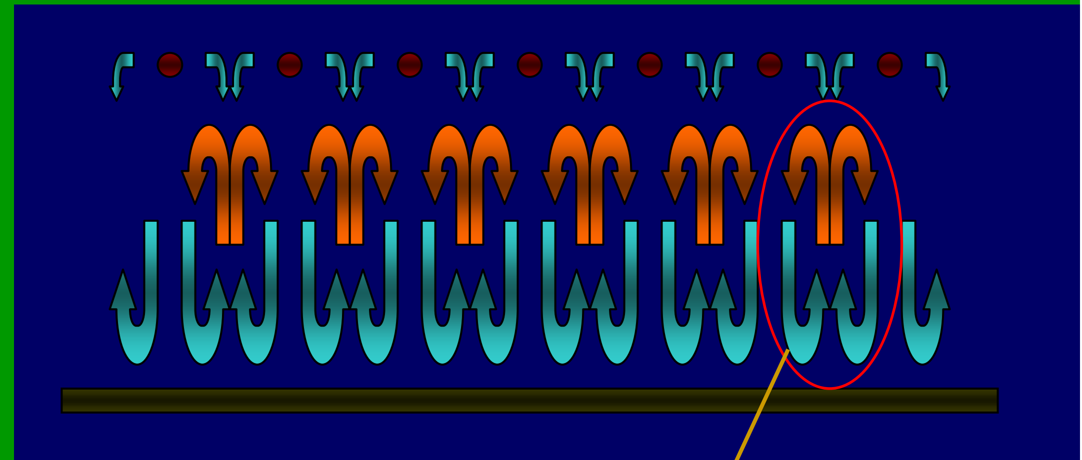

Flow pattern between each individual electrode.

Concurrent presence of corona wind and buoyancy plume.

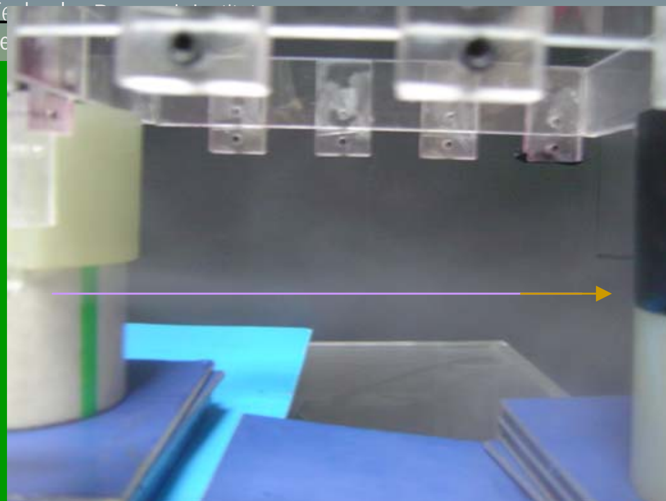

(a)

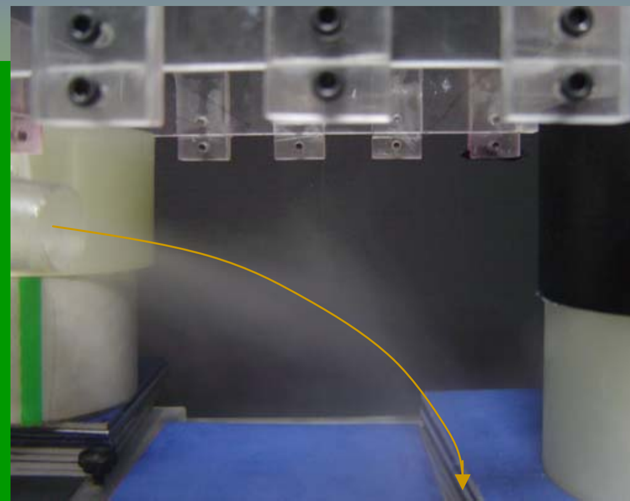

(b)

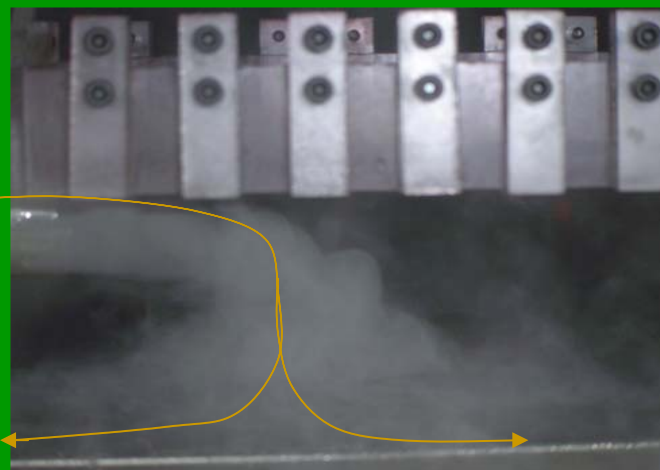

(c)

Flow visualization, (a) 0 kV, (b) +5 kV, (c) +10 kV.

Piezoelectric Fans

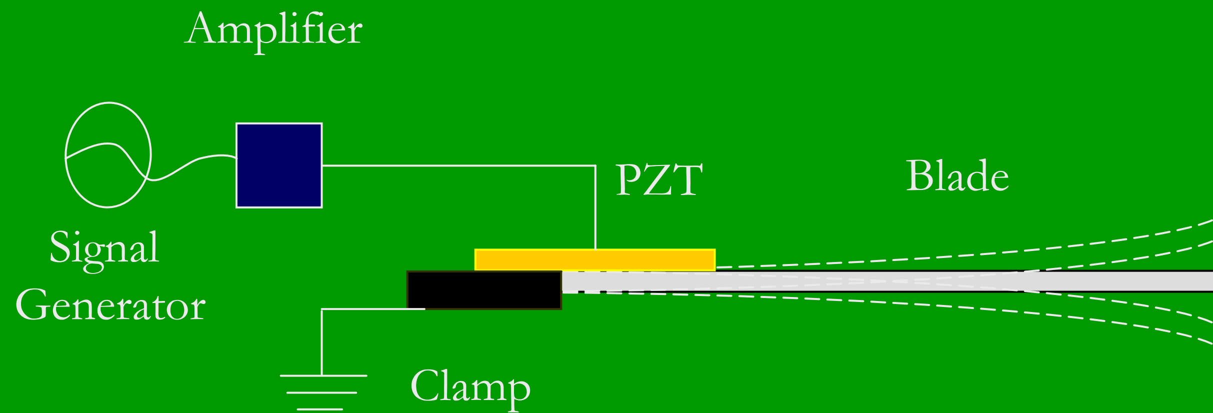

Schematic of a piezoelectric fan.

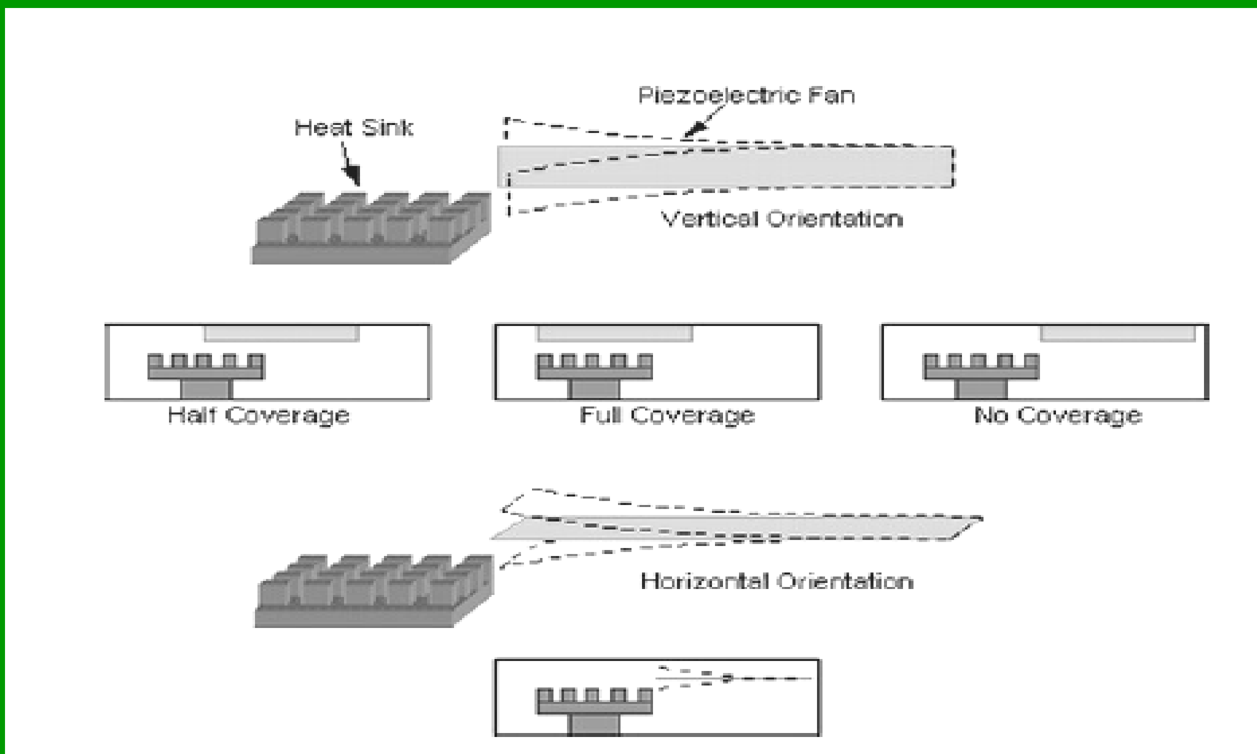

Different arrangements of the piezoelectric fans [4].

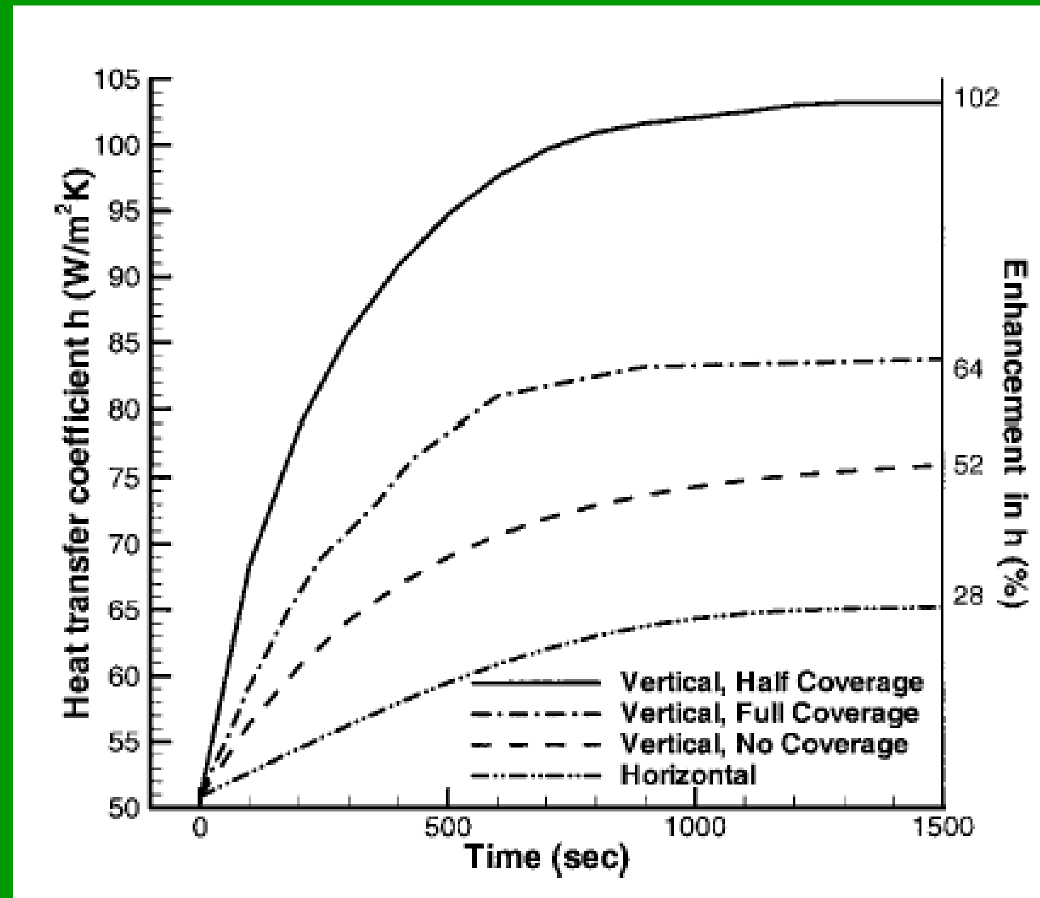

Enhancement in heat transfer coefficient for the four different fan positions in the enclosure. The area is based on the heat source.

Summary

- **To minimize the overall thermal resistance of LEDs, one shall both reduce** R_{JEA} **and** R_{JBA} **, if possible.**
- **Minimize chip level thermal resistance,** R_{JB}
- **Minimize package level thermal resistance,** R_{BA}

1. Reduce contact resistance, R_{cont}, (reduce surface roughness, use better conductivity grease)

2. Reduce heat sink resistance, R_{hs}, (avoid spreading resistance)

3. Reduce convective resistance, R_{conv} **,** (enhance heat transfer coefficient (h), enhance convective surface area (A).)

Natural Convection

- Generally, for both pin fin and plate fin heat sinks, the upward facing orientation yields the highest heat transfer coefficients, followed by the sideward facing and the downward facing orientation.
- With the same fin height of 10 mm and fin spacing of 2mm, the heat transfer coefficient of pin fins are greater than those of plate fins by 0% ~ 23% due to the more open ends for inducing air flow.
- The orientation effect on the pin fin heat sinks becomes less pronounced as the pin height or as the number density is gradually increased. This interesting result is attributed to the choking phenomenon occurring inside the heat sinks.

EHD Convection

- The electric field intensity is increased with the supplied voltage, and so does the heat transfer coefficient.
- Design criteria shall be taken to avoid flow field interference of the corona wind generated from the individual electrode.
- The negative polarity slightly outperforms the positive one by 6% due to its higher current density and mobility between the electrodes and the grounded surface.
- EHD has been proven as a feasible cooling technique in the present study by showing a threefold heat transfer enhancement at the expense of small power consumption.

Ongoing Project associated with Electronic Cooling

1. Enhanced Natural Convection – Via EHD.
   Influence of bypass flow on the heat sink performance.
   Change of spreading resistance with/without the presence of vapor chamber
   High performance heat sink subject to pumping power concerns.
   Two-phase flow/heat transfer/flow visualization within vapor chamber subject to with/without sintered structure.
   Micro-scale fluid flow visualization within sintered structure.
   High flux cooling via spraying means & micro air-conditioning techniques.

Micro- and Nano- Thermofluids Characterization & Applications

What is Nano-fluid ?

Thermofluids mixed with Nanopowder (1~100 nm), such as Cu, CuO, Al_2O_3, usually with concentration less than 5%

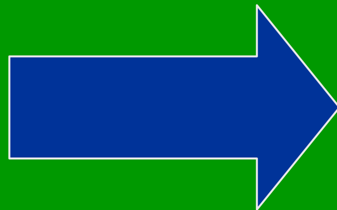

Fluid

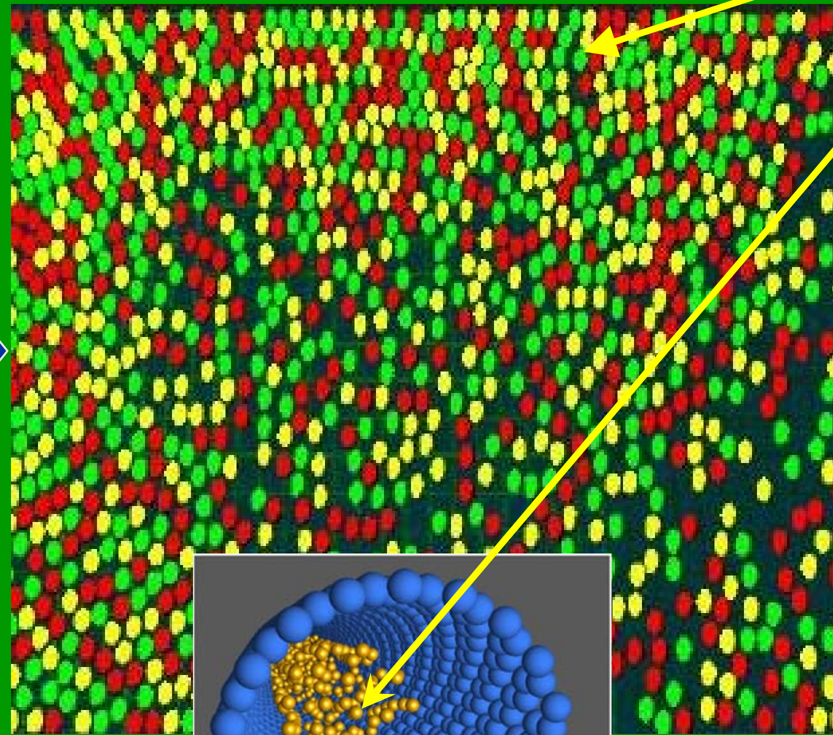

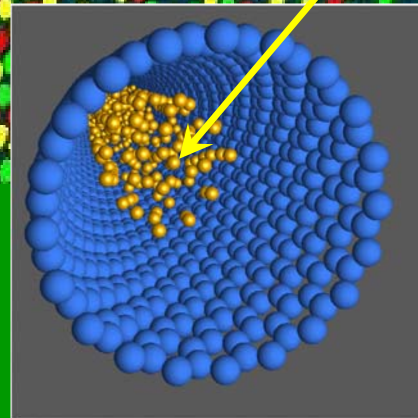

Characteristics

(1) Effective Area ↑
(2) Thermal conductivity↑
(3) Increase Dispersion
(4) Increase Mixing
(5) Increase turbulent intensity

工業技術研究院
能源與資源研究所
Industrial Technology Research Institute
Energy & Resources Laboratories

No additional friction

Increase heat transfer coefficient (10~40% or even higher)

Accompany with ER/MR fluid with better controlled ability

YES

YES

YES

Benefits of Nano-fluid

NO

NO

NO

Clog

Sedimentation

Erosion

Nanofluid can significantly increase thermal conductivity

The rmal conductivity ratio (k/k_o)

1.5
1.4
1.3
1.2
1.1
1

0 0.01 0.02 0.03 0.04 0.05 0.06

Volume fraction

Ethylene glycol + Al_2O_3
Ethylene glycol +CuO
Ethylene glycol + Cu (2 manths old)
Ethylene glycol + Cu (fresh)
Ethylene glycol + Cu + Acld

Preliminary study were done by US Argonne Nat. Lab., Energy Technology Div.

Physical properties of the nanopowder and relevant long term characteristics were underway byArgonne Nat. Lab., Material Science Lab.

Ref: Applied Physics Letters, 78, p. 718, 2001

Possible Mechanisms of Heat Transfer Augmentation by Nano-fluid

Fact: Based on the existing theory, the predicted *k* value is only **1/10 of the experimental value**

Likely mechanism

(**Ref: Int. J. of Heat Mass Transfer, 45, pp. 855, 2002**)

(1) Brownian motion enhancement

(2) Liquid layering at liquid/particle interface

(3)Ballistic phonon transport

(4)Nanoparticle cluster

(5)Other possible mechanism needs to be explored in the future

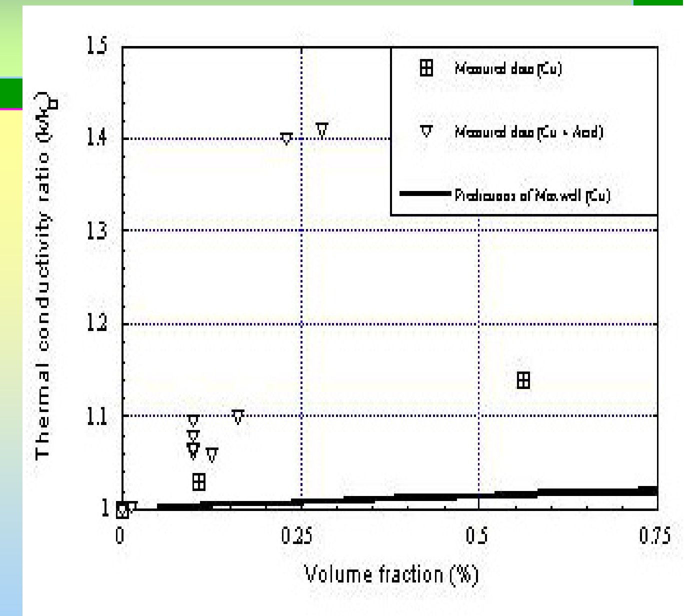

Parameters that should be accounted for the nano-fluid

- Solid fraction
- Size (critical size)
- Shape
- Activator/Dispersant

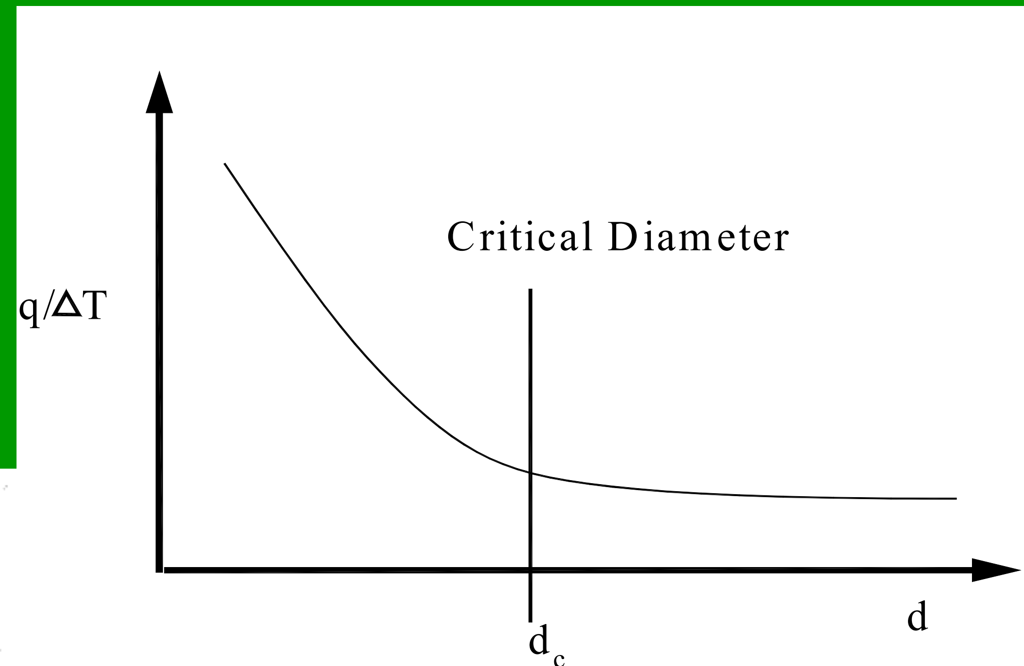

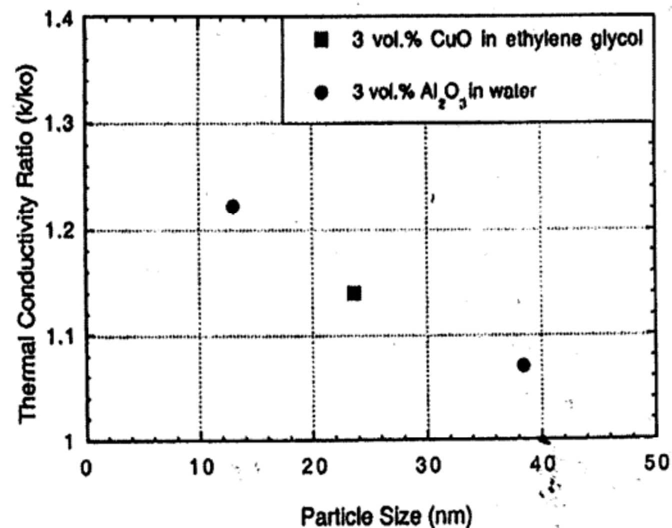

Figure 7. Thermal conductivity ratio of oxide nanofluids as a function of particle size at a fixed concentration (courtesy of S. Choi).

Preparation of effective nano-fluid

One-step method **Two-step method**

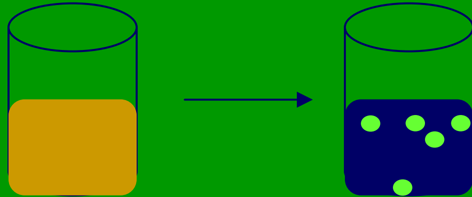

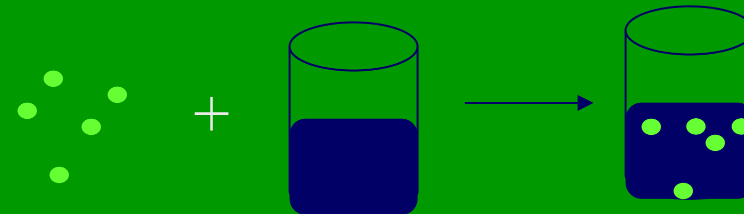

- Change the pH value of the suspensions
- Use surface activators and/or dispersant
- Ultrasonic vibration

Common activators/dispersants:

Thiols (硫醇), oleic acid (油酸), laurate salt

Current Efforts in ERL for nano-scale thermofluids system

Properties measurements , c_p, k, μ
Transient hot-wire - k

Integrated with ER/MR fluids

Statistic dynamic Analysis

MD simulation

Testing/Optimization of the shape/size of nano-powder

System analyzing Of nanofluids

Micro Channels

DSMC simulation

one-step method

Two-step nanofluid

Dispersion Technique

Enhancements of k values using Multi-wall CNT & CuO particle

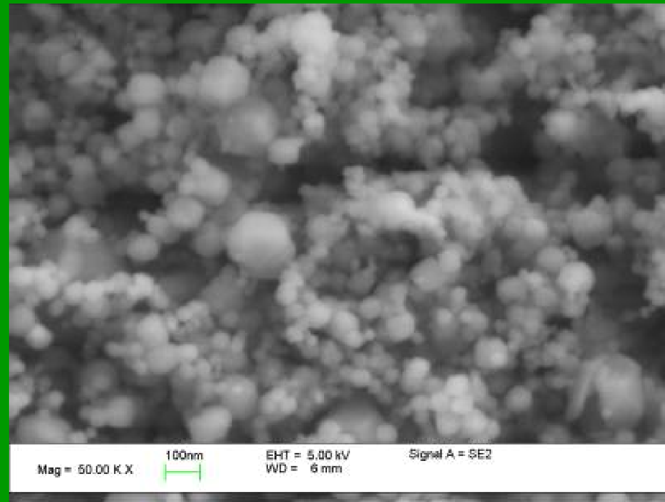

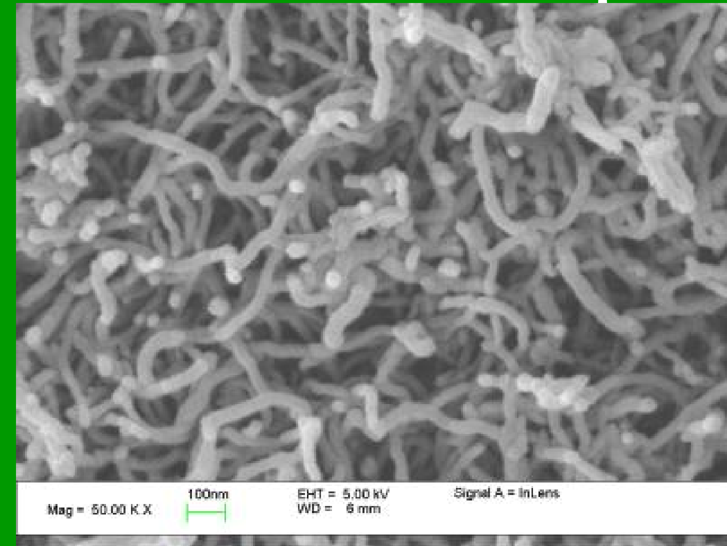

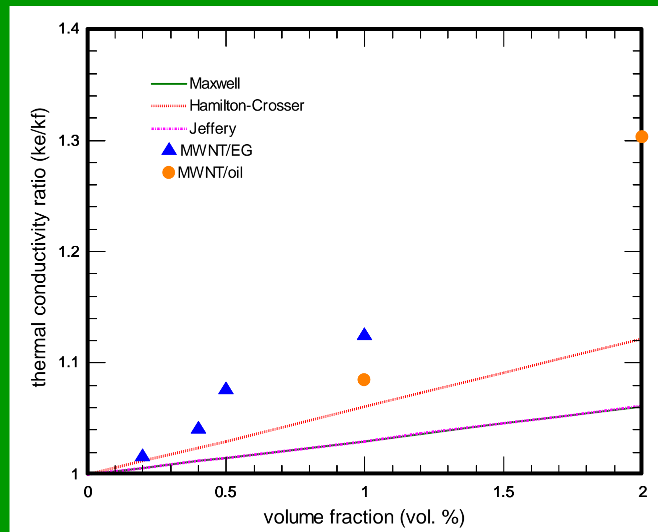

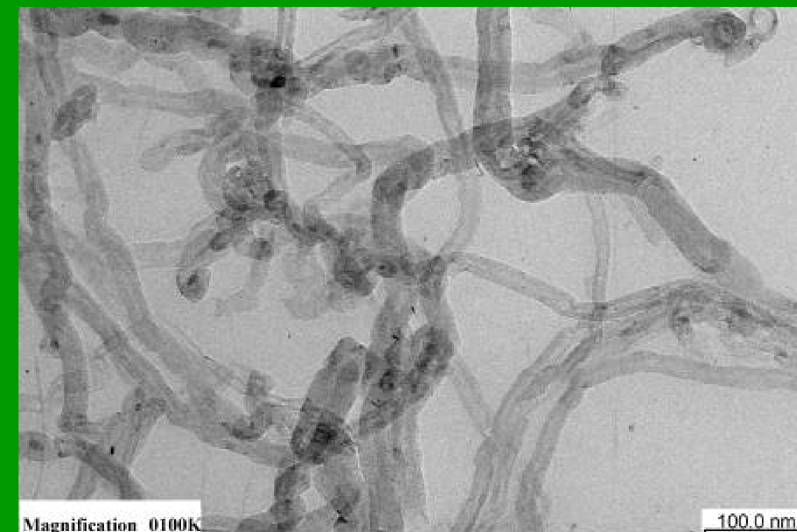

Int. Comm. Heat Mass Transfer, Vol. 32, pp. 1202-1210

Nanofluids via chemical reduction method

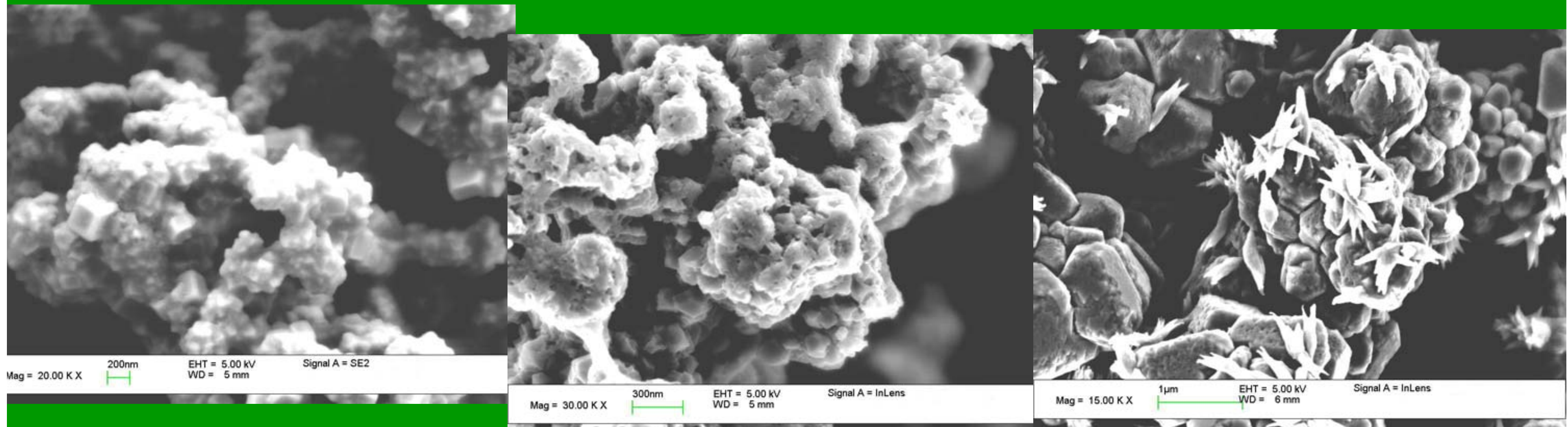

2(a) 2(b) 2(c)

Typical SEM micrographs of Cu nanoparticles for
(a) specimen No. 4, (b) specimen No. 5, and (c) specimen No. 9.

Int. J. Heat Mass Transfer, under review

工業技術研究院
能源與資源研究所
Industrial Technology Research Institute
Energy & Resources Laboratories

Chemical Reduction Method

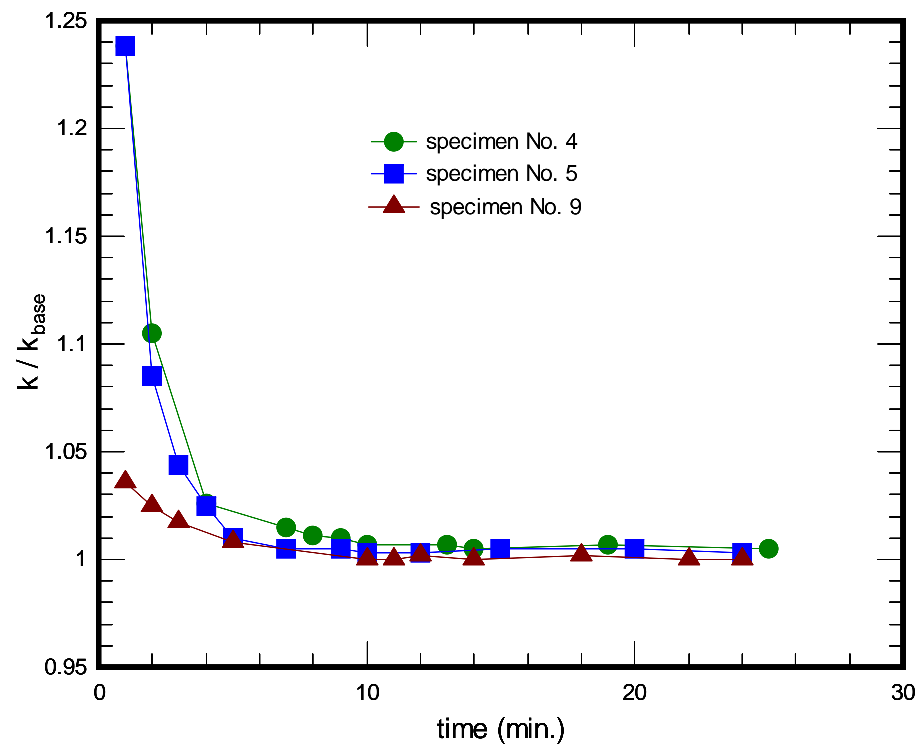

The normalized thermal conductivity data for the Cu-water nanofluids as a function of the measured time.

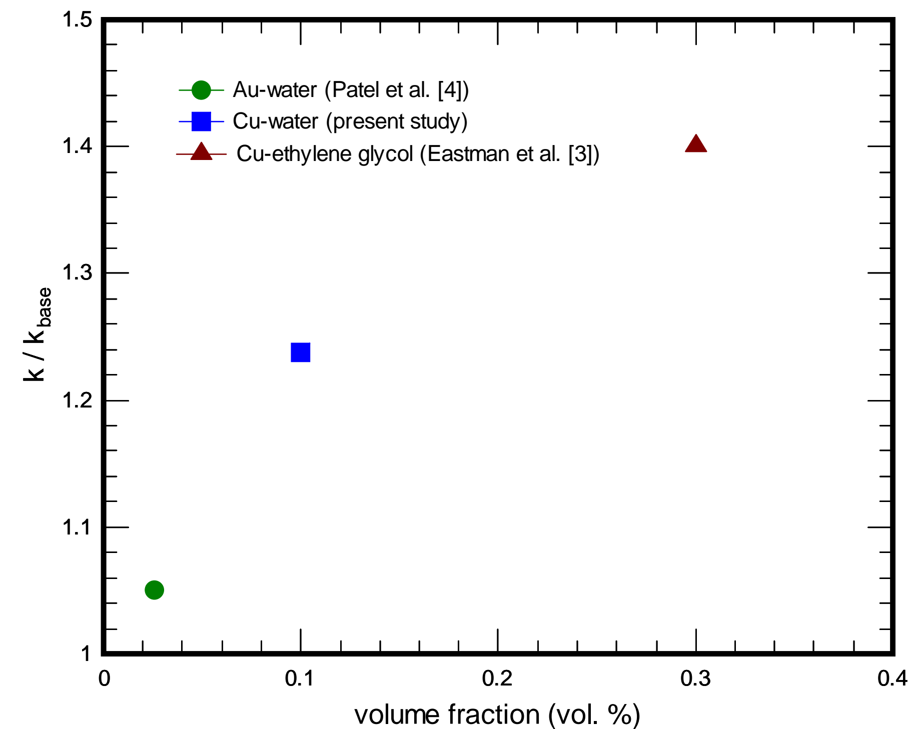

The thermal conductivity as a function of volume fraction for the Au and Cu water base nanofluids.

Integrated with ER/MR Fluids

→Improve the controlled ability of thermofluids system

- MR (Magnetorheology) – ER (Electrorheology), with controlled electrical or magnetic field into the Rheology fluids (with micro-sized/nano-sized suspensions)
- Within milliseconds, the suspensions will then be polarized to generate a chain-like structure that simulate a solid-like structure. Locally, this solid-like structure functions like a damping device or valve.
- It is likely that ER/MR fluid may be integrated with nanofluid to increase the controlled ability of the thermofluids system. But….

Nanofluid for Control - ER/MR

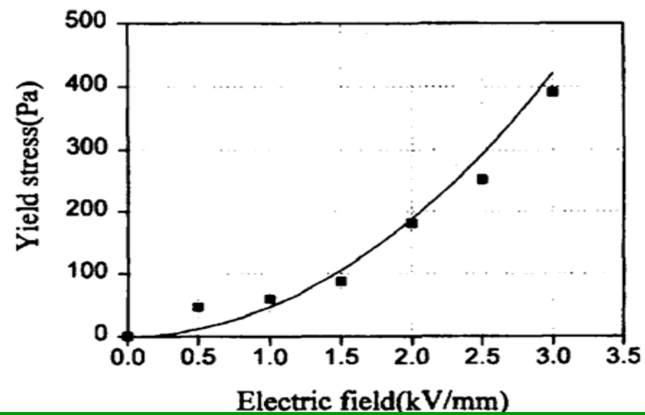

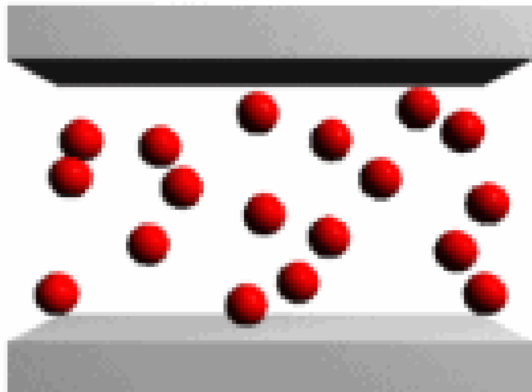

Nanofluid for Control - ER/MR

(a) Without magnetic field

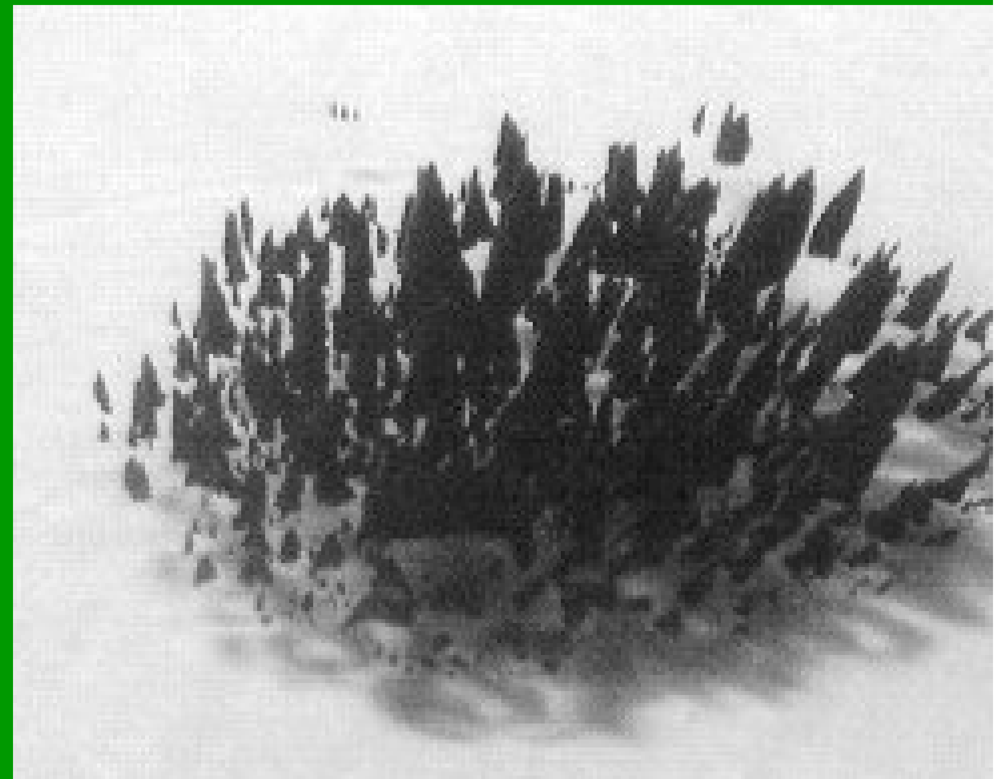

(b) With Magnetic Fluid

工業技術研究院
能源與資源研究所
Industrial Technology Research Institute
Energy & Resources Laboratories

Development of Micro Nozzle/Diffuser Pump

Working Principles of Nozzle/Diffuser micro-pump

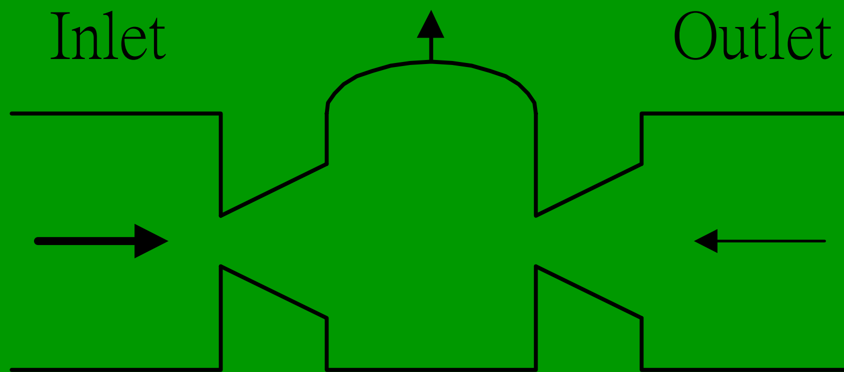

from diffuser > from nozzle

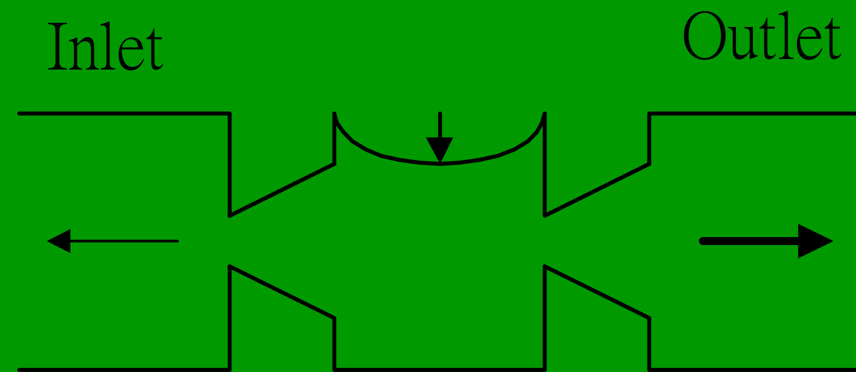

from nozzle < from diffuser

J. of Micromechanics and Microengineering, Vol. 14, pp. 26-31, 2004

J. of Micromechanics and Microengineering, Vol. 14, pp. 26-31, 2004

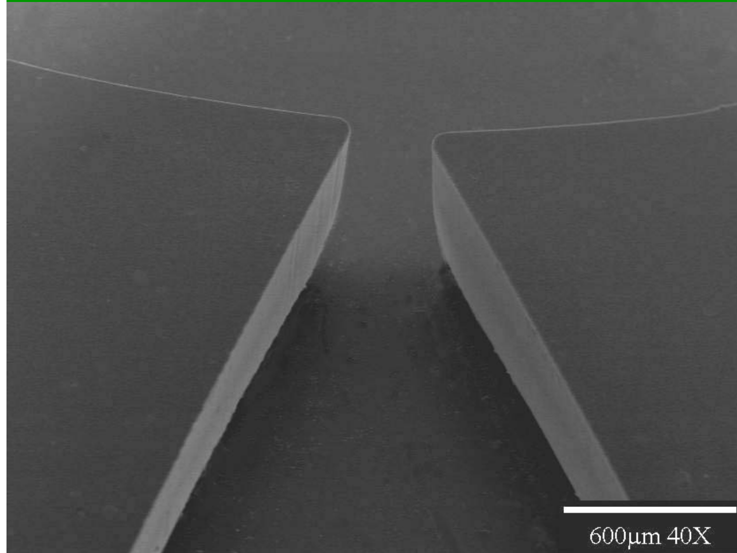

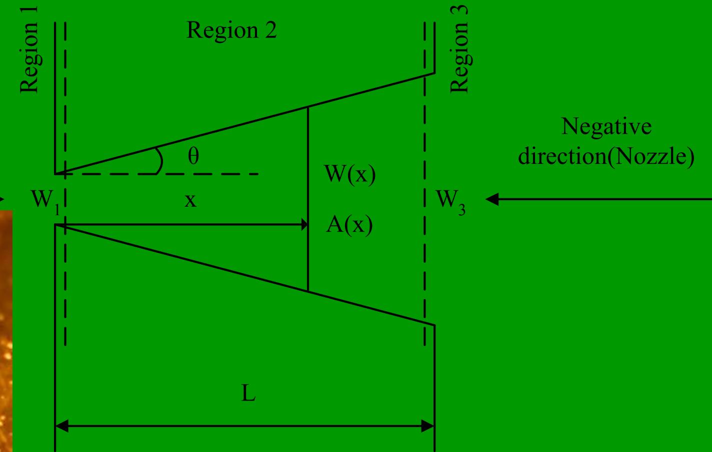

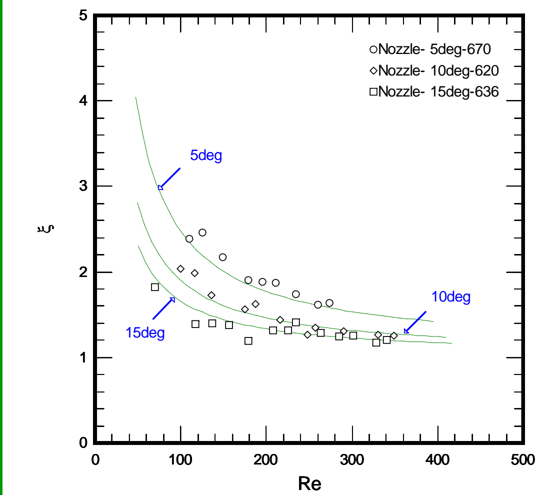

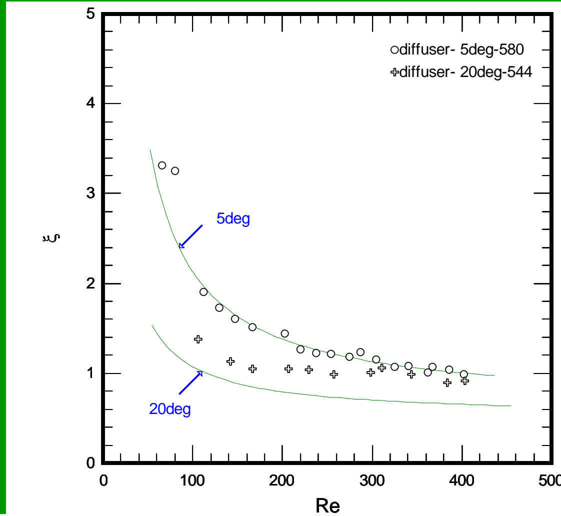

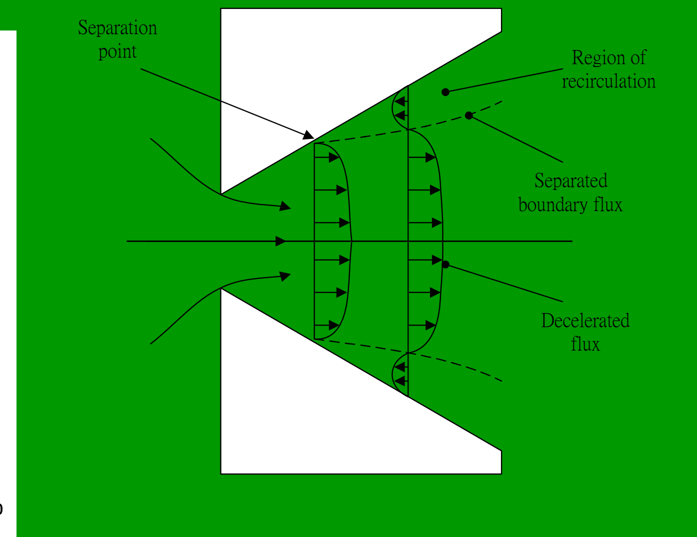

工業技術研究院
能源與資源研究所
Industrial Technology Research Institute
Energy & Resources Laboratories

Performance of Micro Nozzle/Diffuser

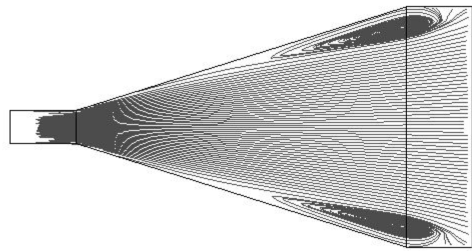

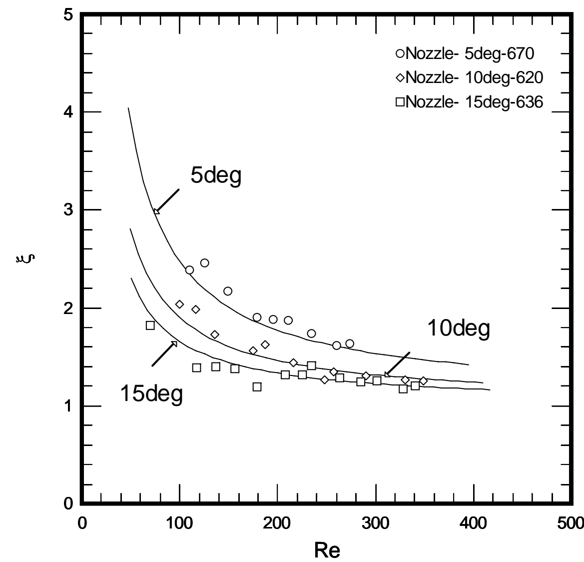

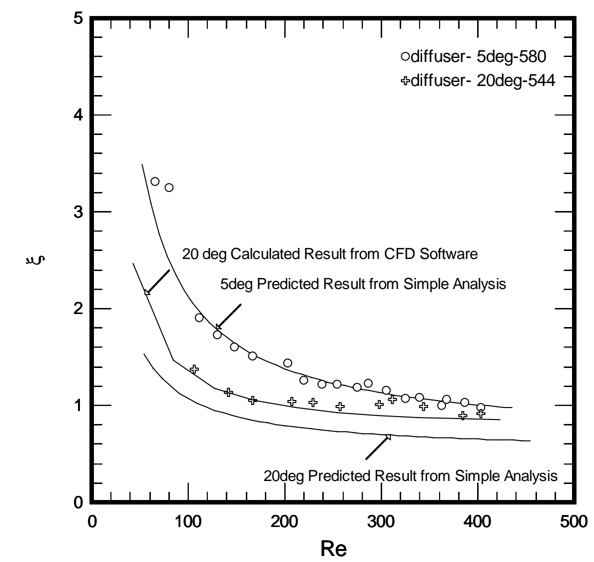

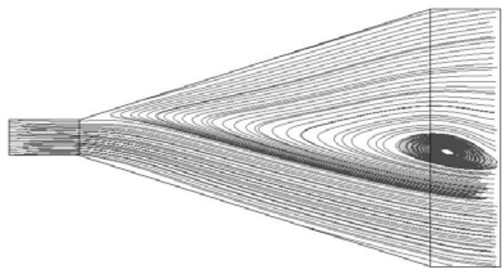

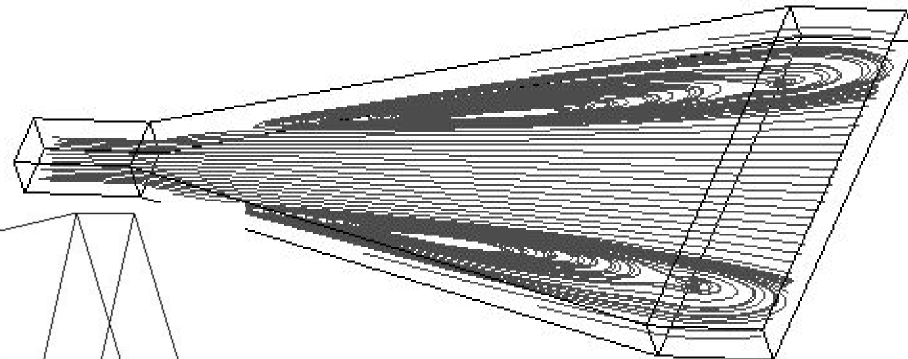

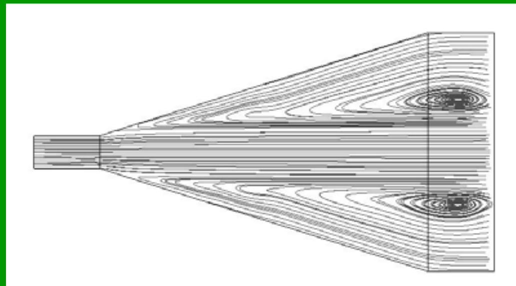

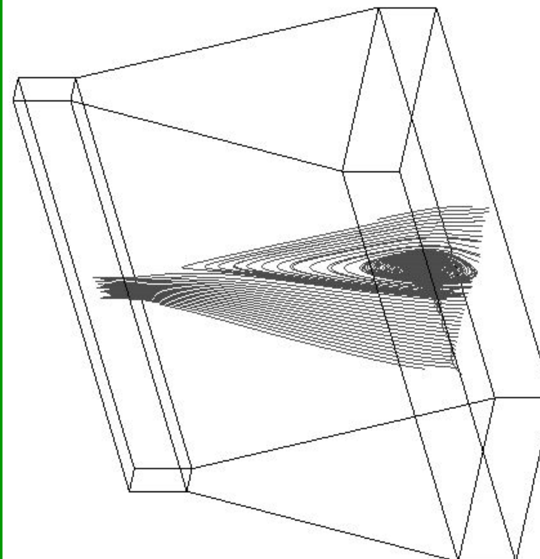

J. of Micromechanics and Microengineering, Vol. 14, pp. 26-31, 2004.
J. of mechanical Engng. Science, Paper in review
Software: CFDRC

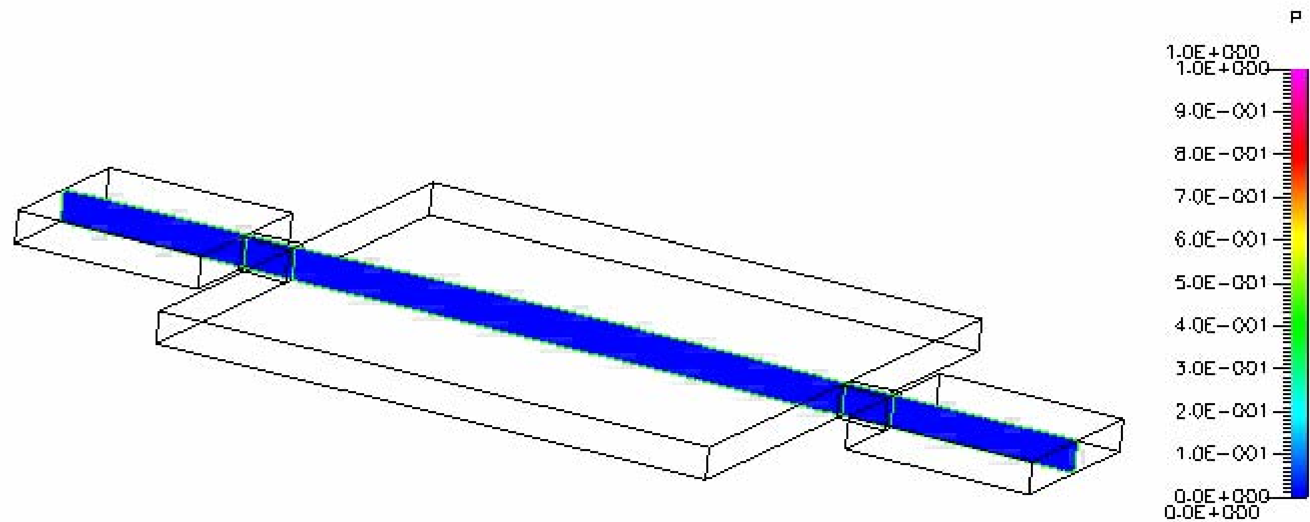

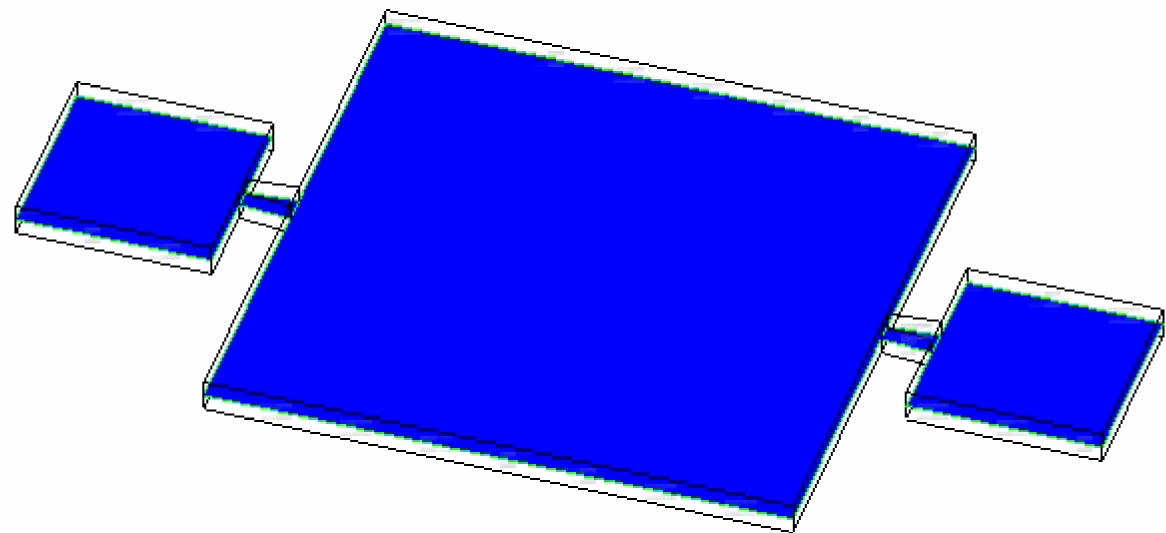

Paper in Review

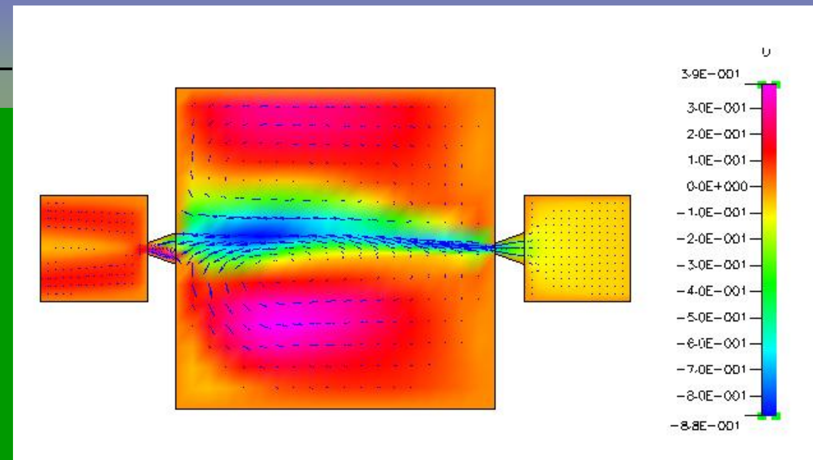

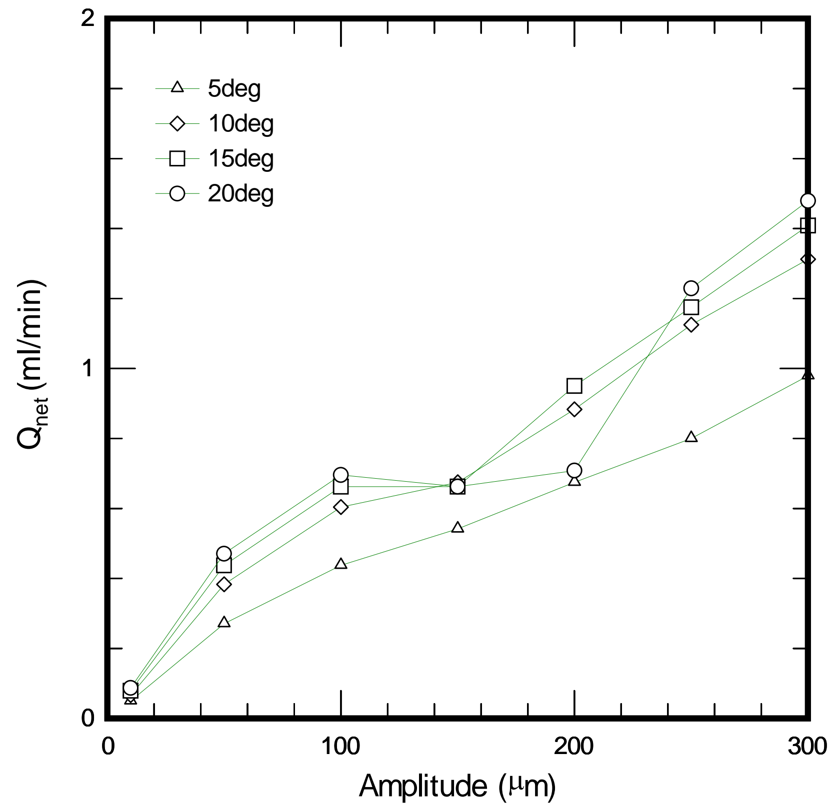

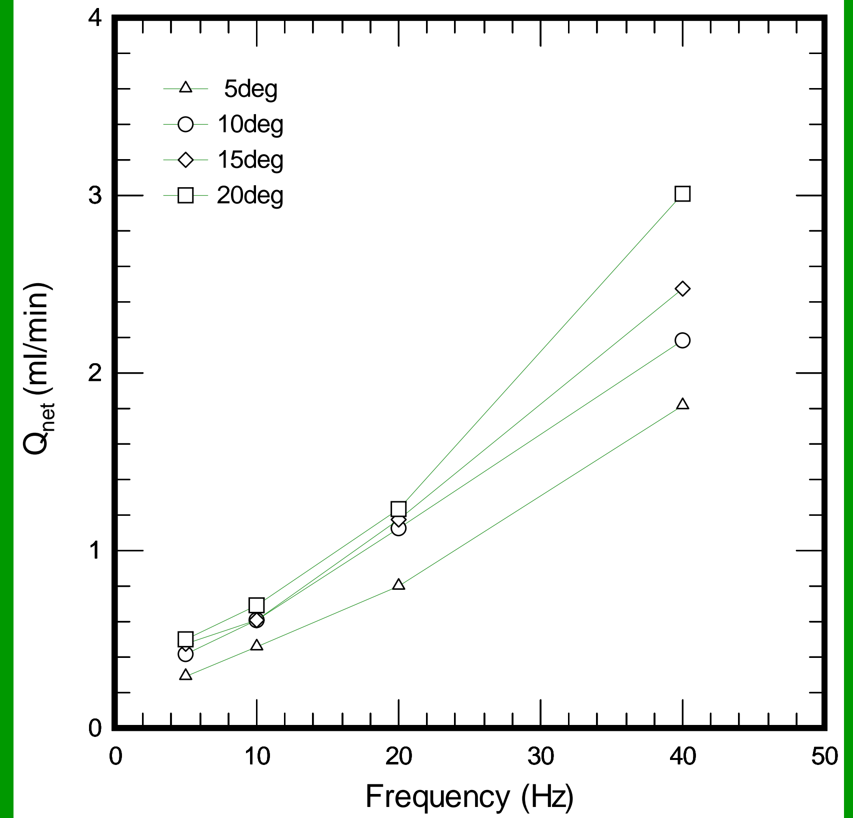

Paper in review

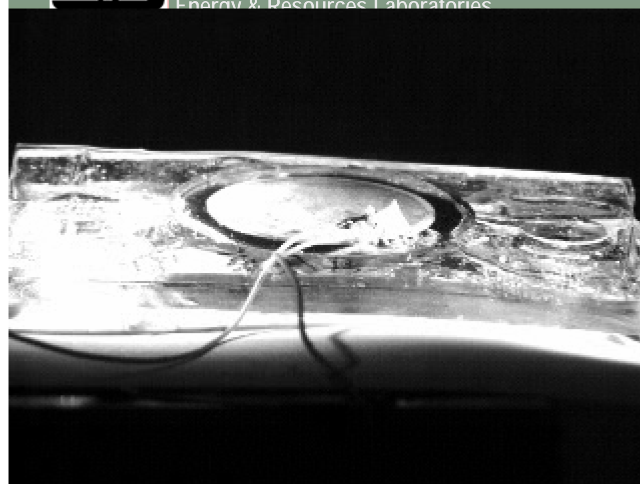

PDMS **PMMA** **PZT membrane**

2 Hz **20 Hz** **100 Hz**

Paper in Review

組裝完成之微幫浦

初始條件跟邊界條件

- 2D及3D擴散器
  - u_{inlet} = 常數
  - p_{outlet} = 1 大氣壓
- 3D微幫浦
  - p_{inlet} = 1 大氣壓
  - p_{outlet} = 1 大氣壓
  - 腔體上壁設定爲移動邊界

微幫浦的邊界條件設定圖

動態格點變化

擴散管/噴嘴原理分析

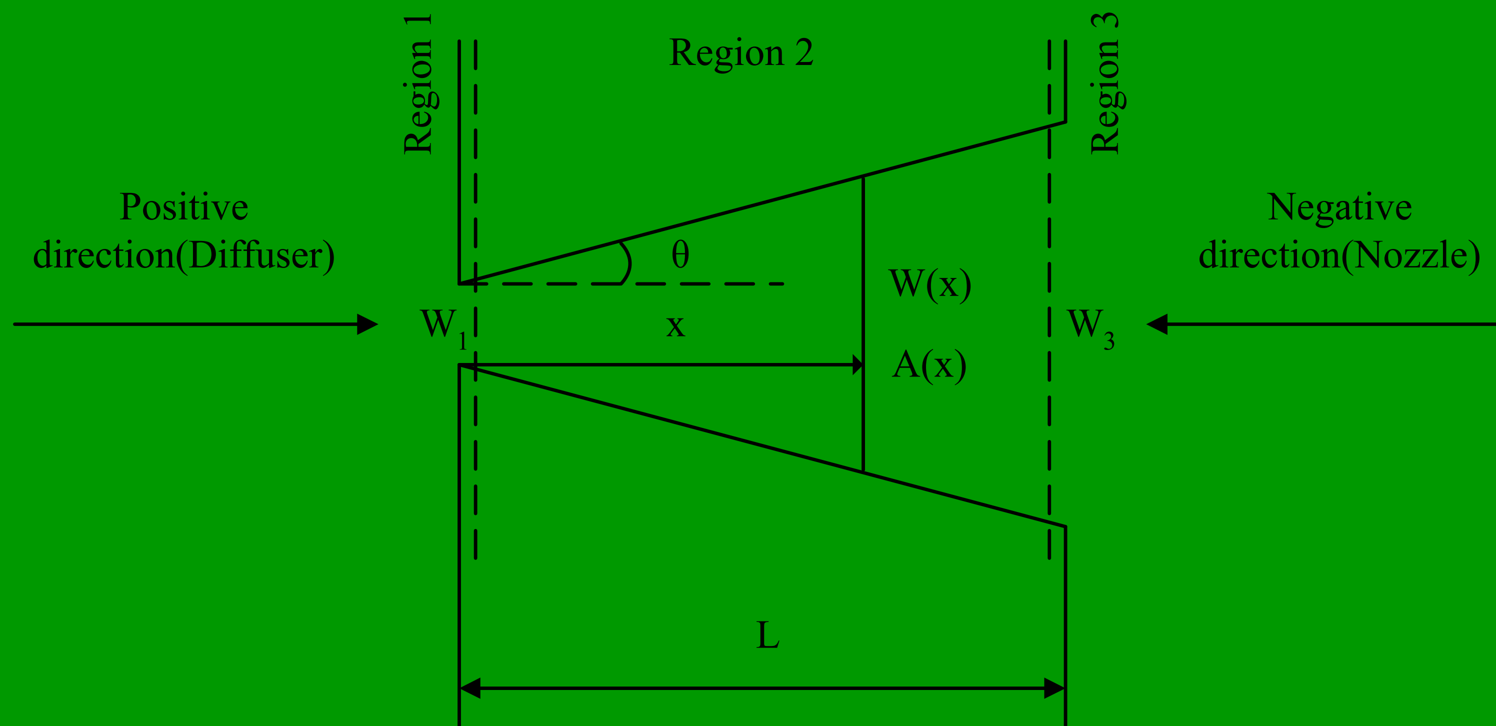

結果與討論 - Nozzles & Diffusers

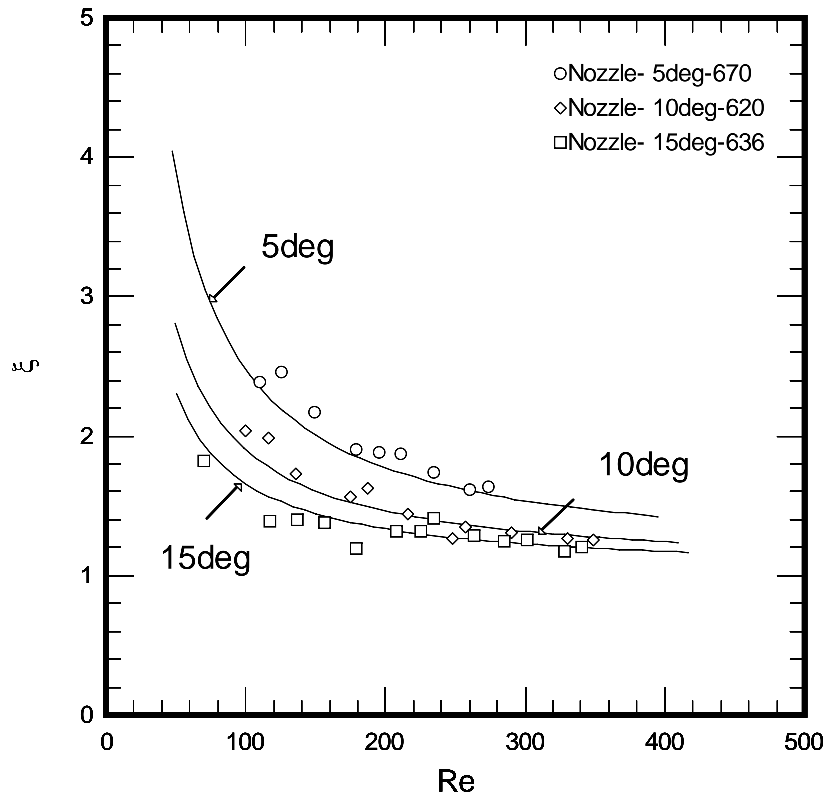

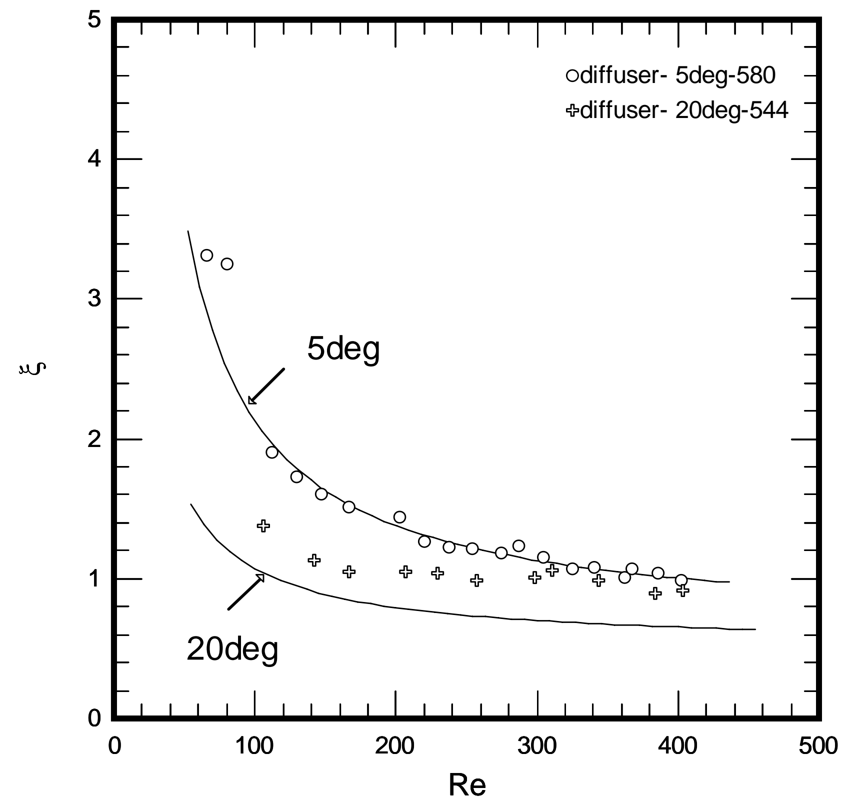

結果與討論

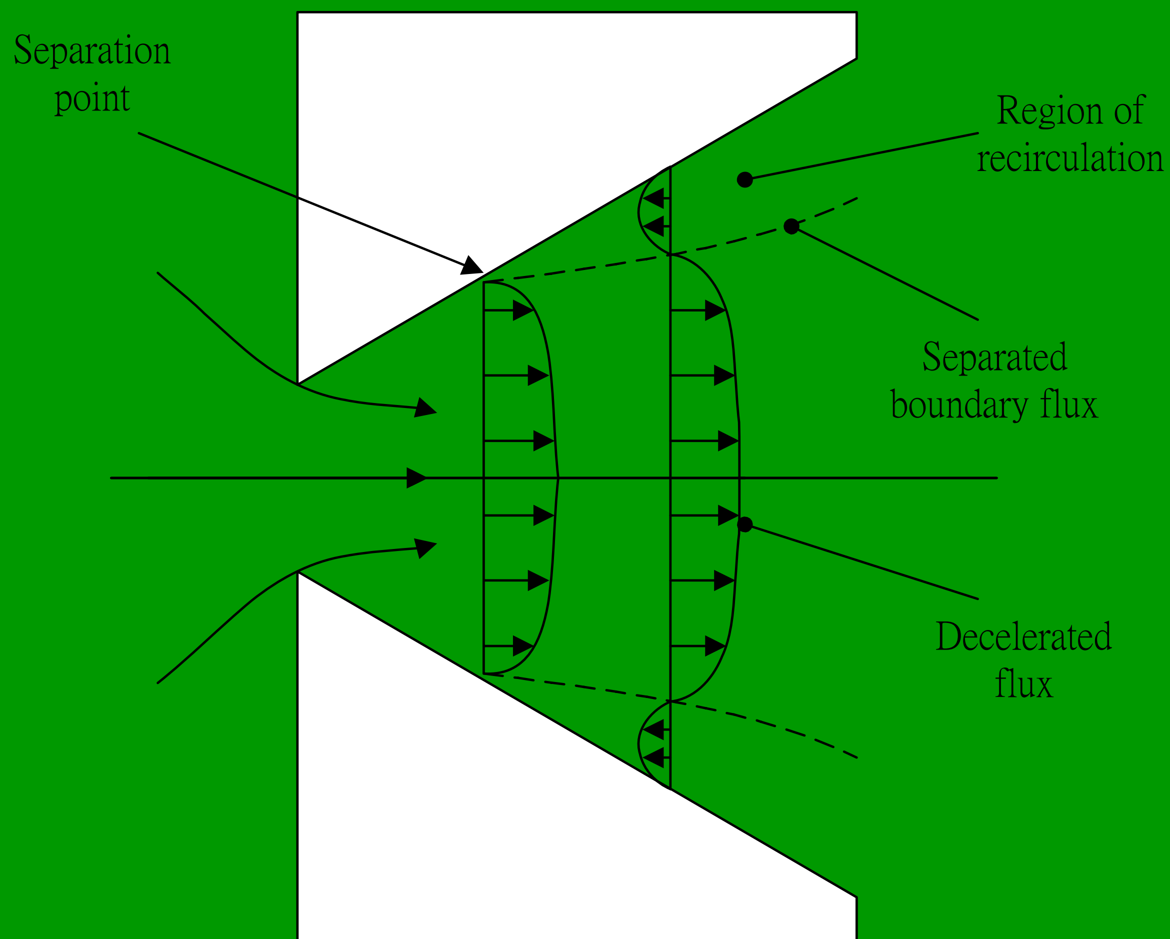

回流的形成原因探討

- 流體在邊界層內流動包含3種力
  - 慣性力（inertia force）
  - 黏滯力（viscous force）
  - 壓力（pressure force）
- 壓力梯度對邊界層內速度的變化影響
  - $dp/dx<0$
  - $dp/dx=0$
  - $dp/dx>0$

回流的形成原因探討

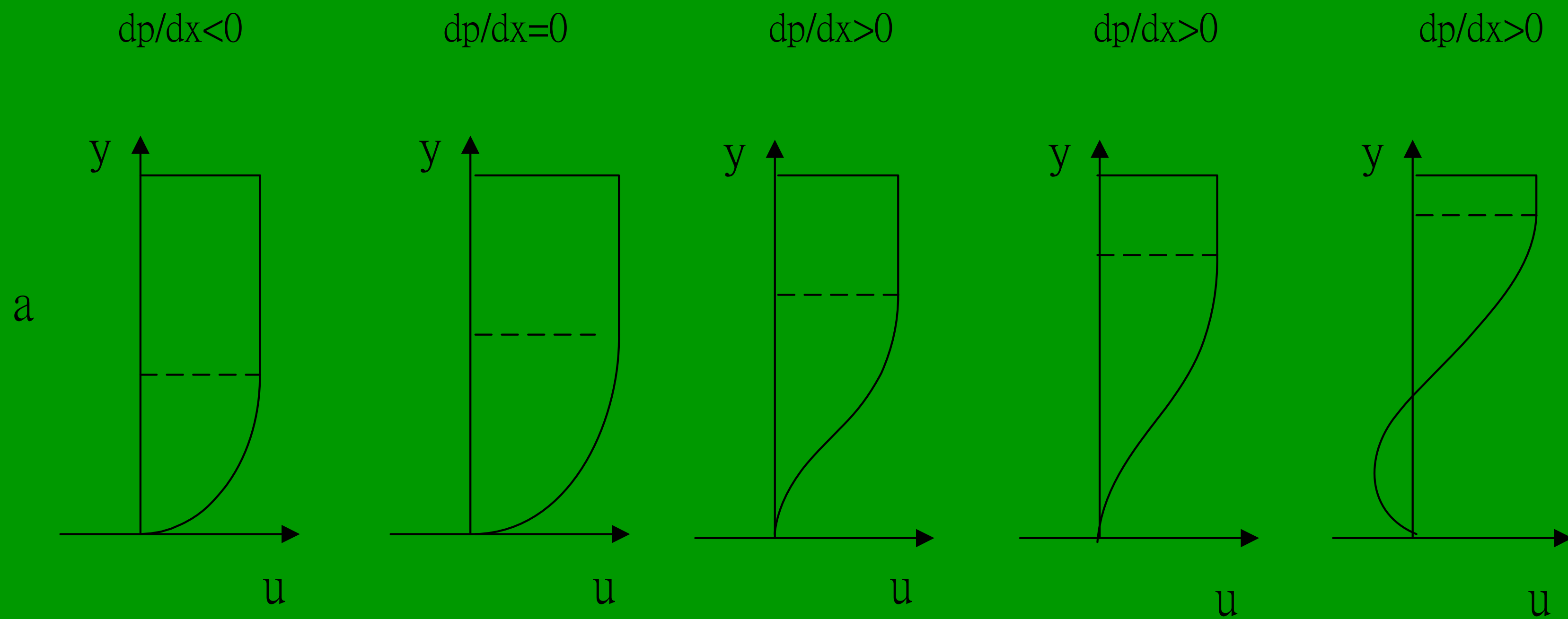

(a)速度分布圖(b)速度梯度分布圖

擴散器之2D數值模擬

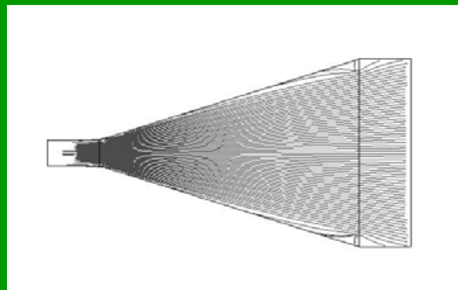

(a) u_{inlet} = 0.102 m/s

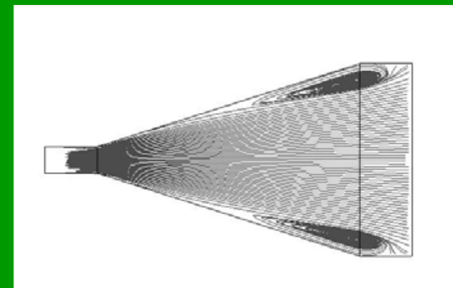

(b) u_{inlet} = 0.111 m/s

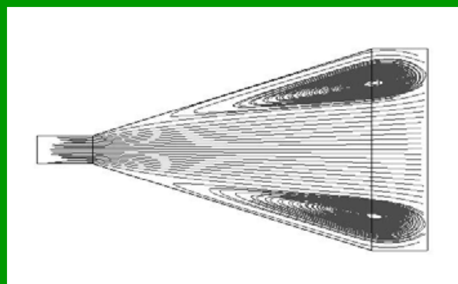

(c) u_{inlet} = 0.148 m/s

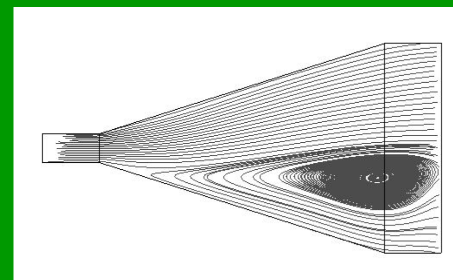

(d) u_{inlet} = 0.167 m/s

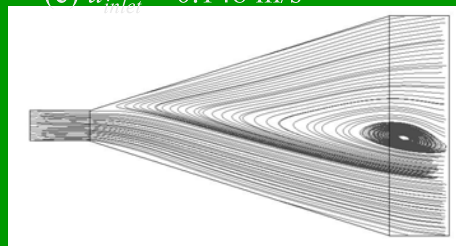

(e) u_{inlet} = 0.556 m/s

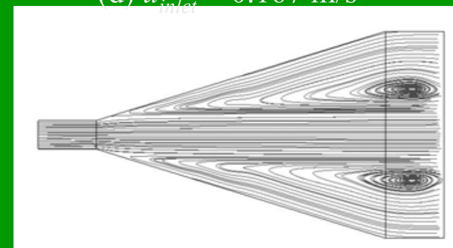

(f) u_{inlet} = 9.26 m/s

擴散器之2D數值模擬

1 ml/min

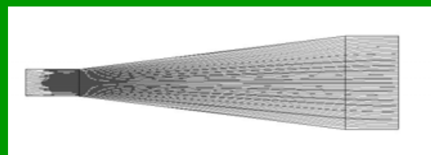
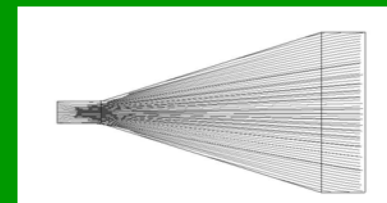

2 ml/min

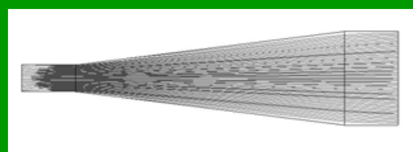
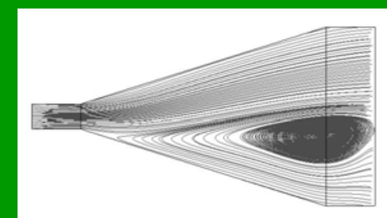

4 ml/min

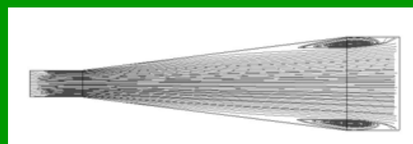
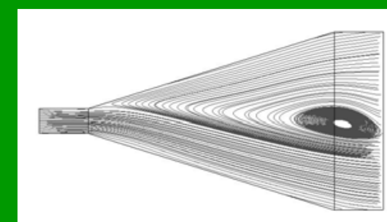

10 ml/min

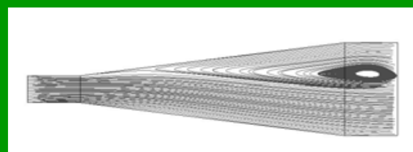
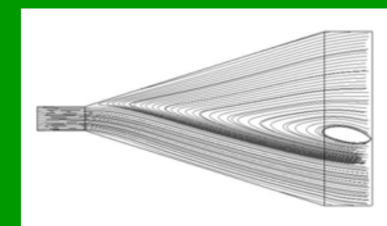

擴散器之2D數值模擬

流速對回流影響之3D模擬

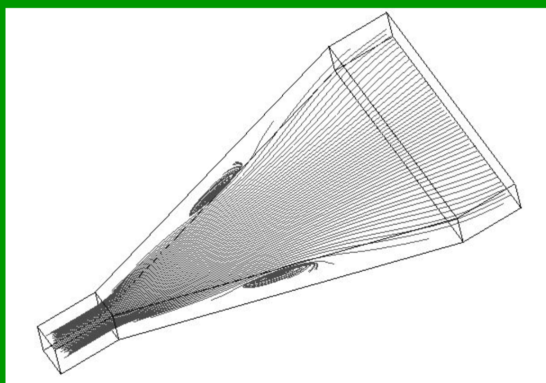

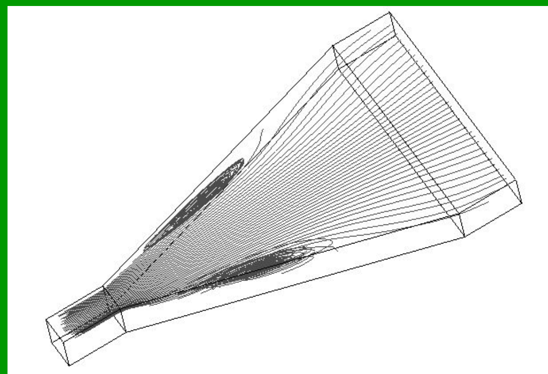

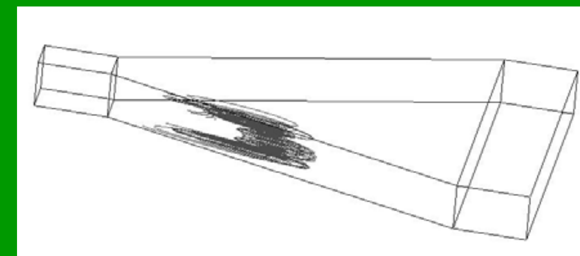

管厚400μm流速0.27778m/s（a）管中央（b）距上管壁100μm（c）回流區流線分布圖

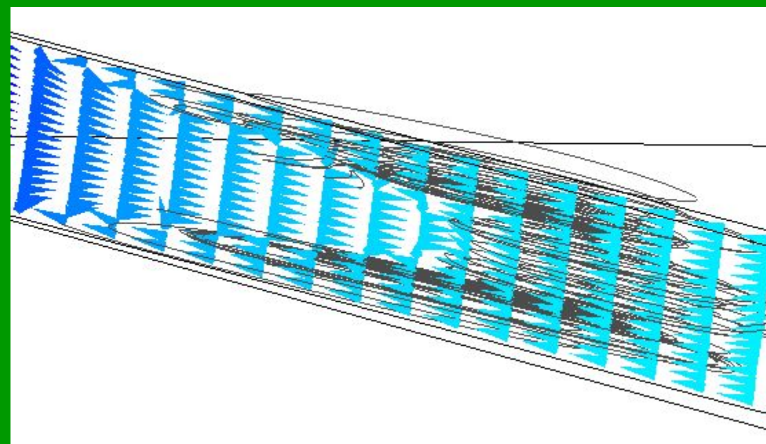

流速對回流影響之3D模擬

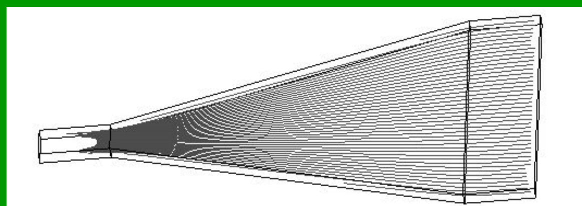

H = 100 μm u_{inlet} = 0.167 m/s

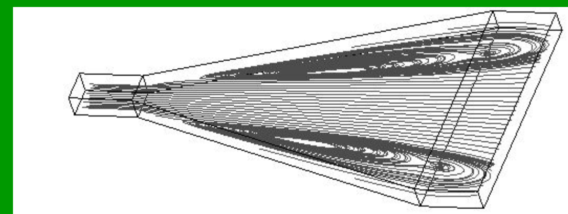

H = 200 μm u_{inlet} = 0.167 m/s

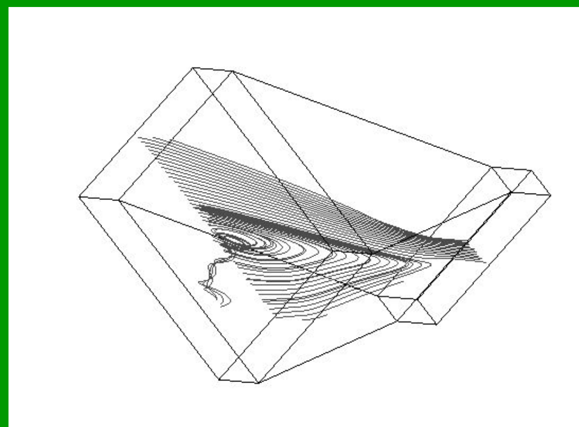

H = 1600 μm u_{inlet} = 0.167 m/s

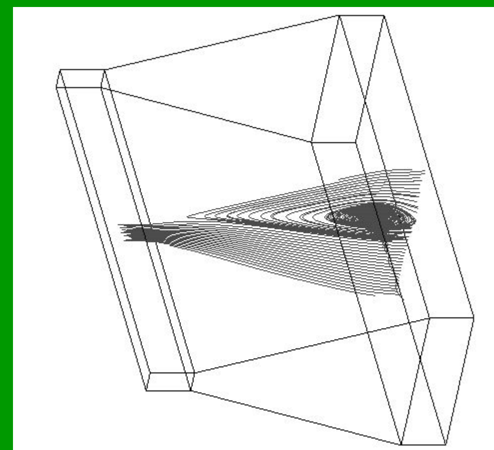

H = 6000 μm u_{inlet} = 0.167 m/s

結果與討論

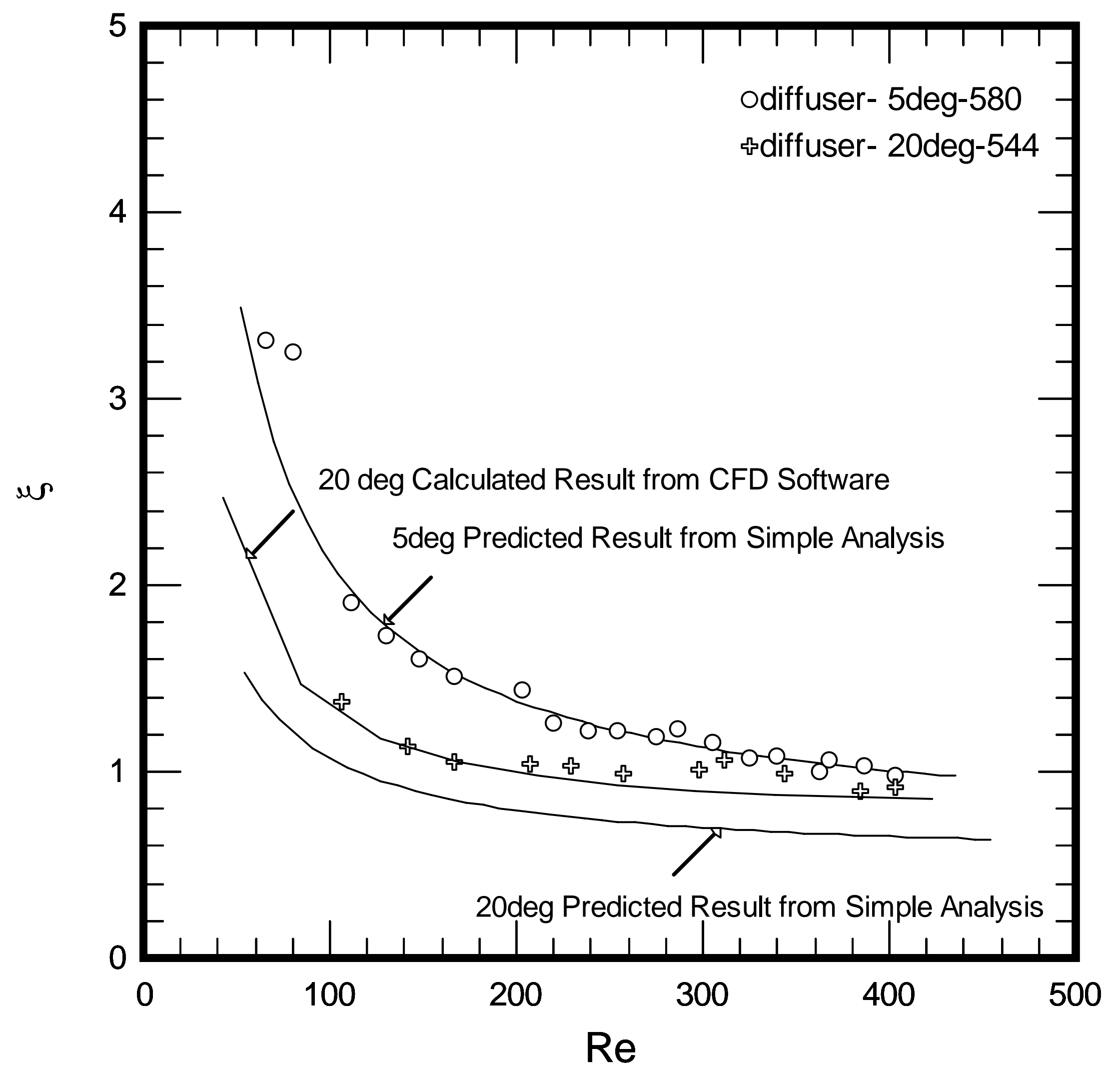

結果與討論

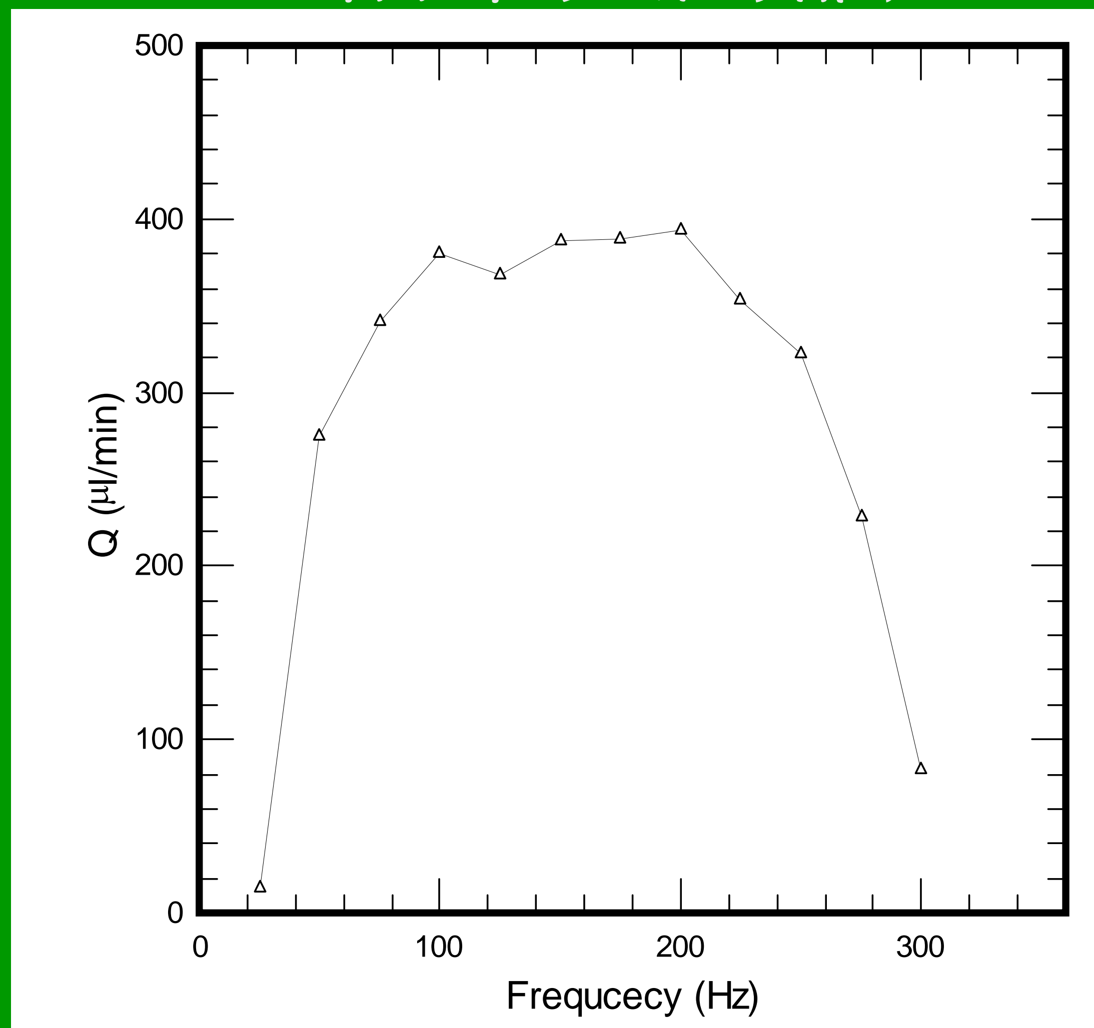

擴散器/噴嘴元件10度之微幫浦頻率與流量之關係圖

結果與討論

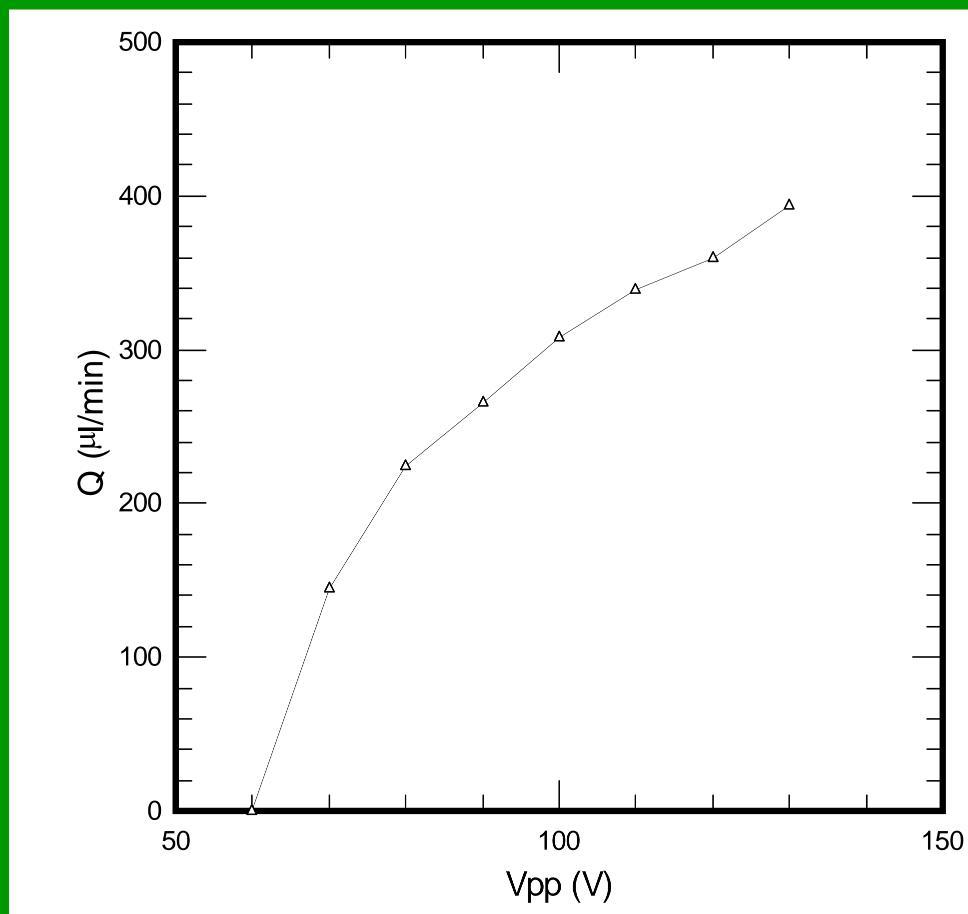

擴散器/噴嘴元件10度之微幫浦電壓與流量之關係圖

微幫浦截面定義

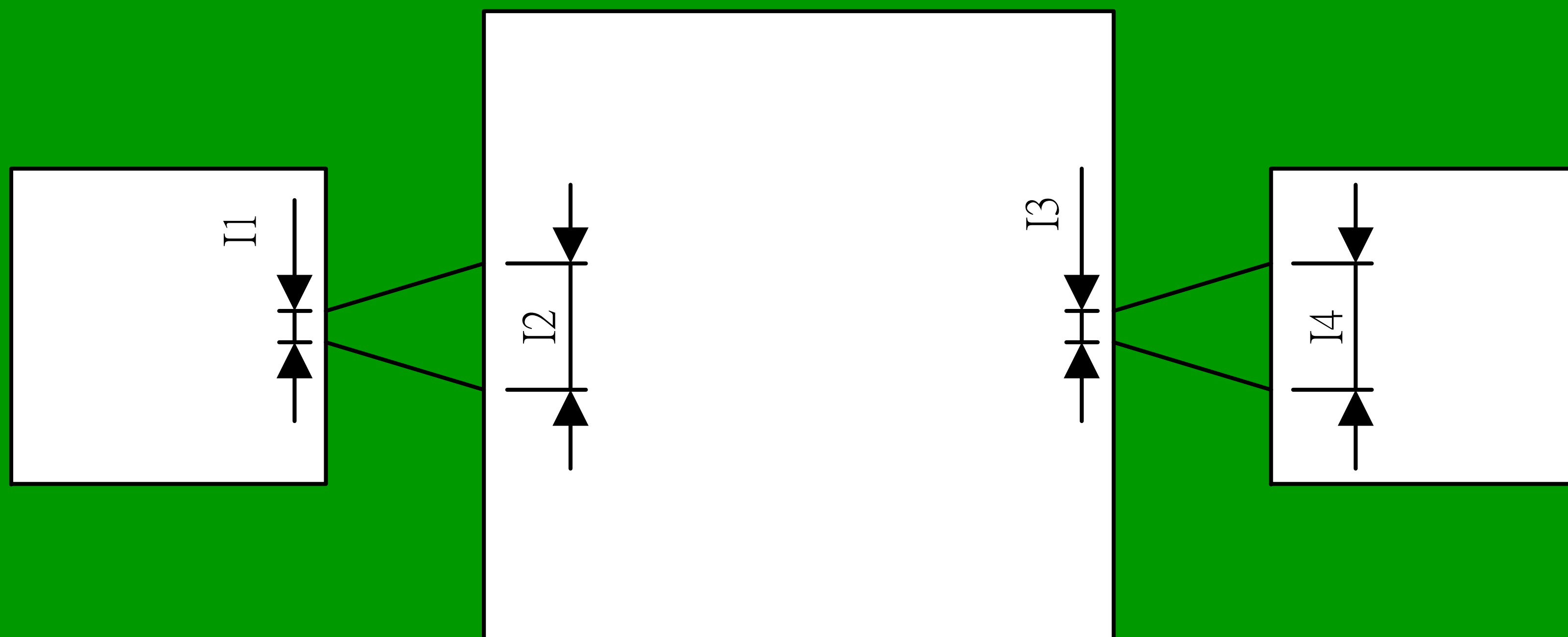

幫浦循環

stage 1

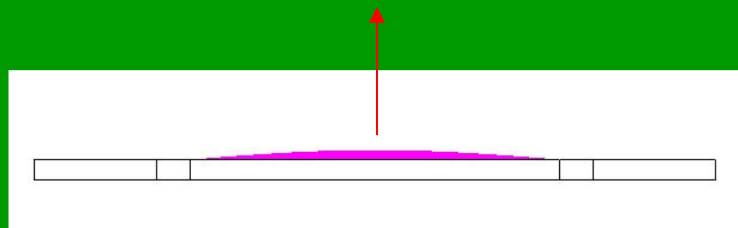

stage 2

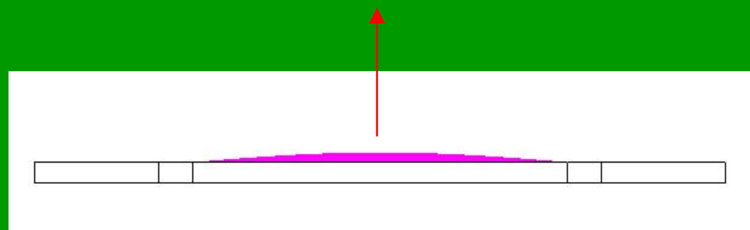

stage 3

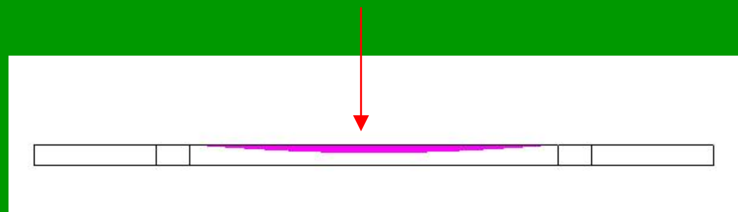

stage 4

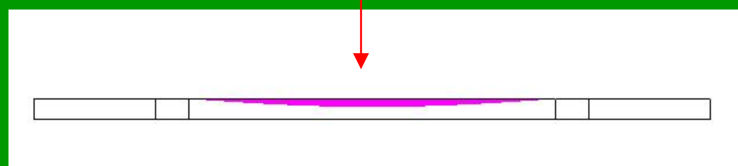

結果與討論

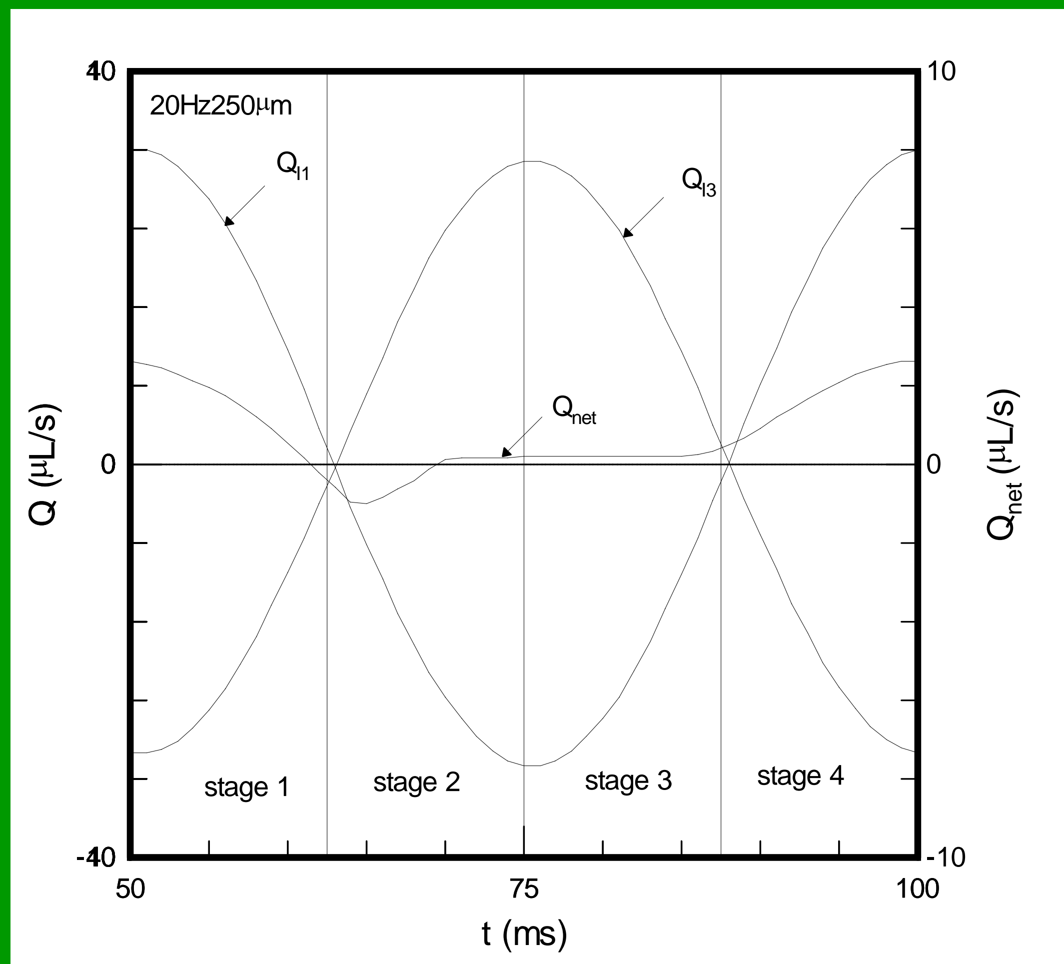

結果與討論

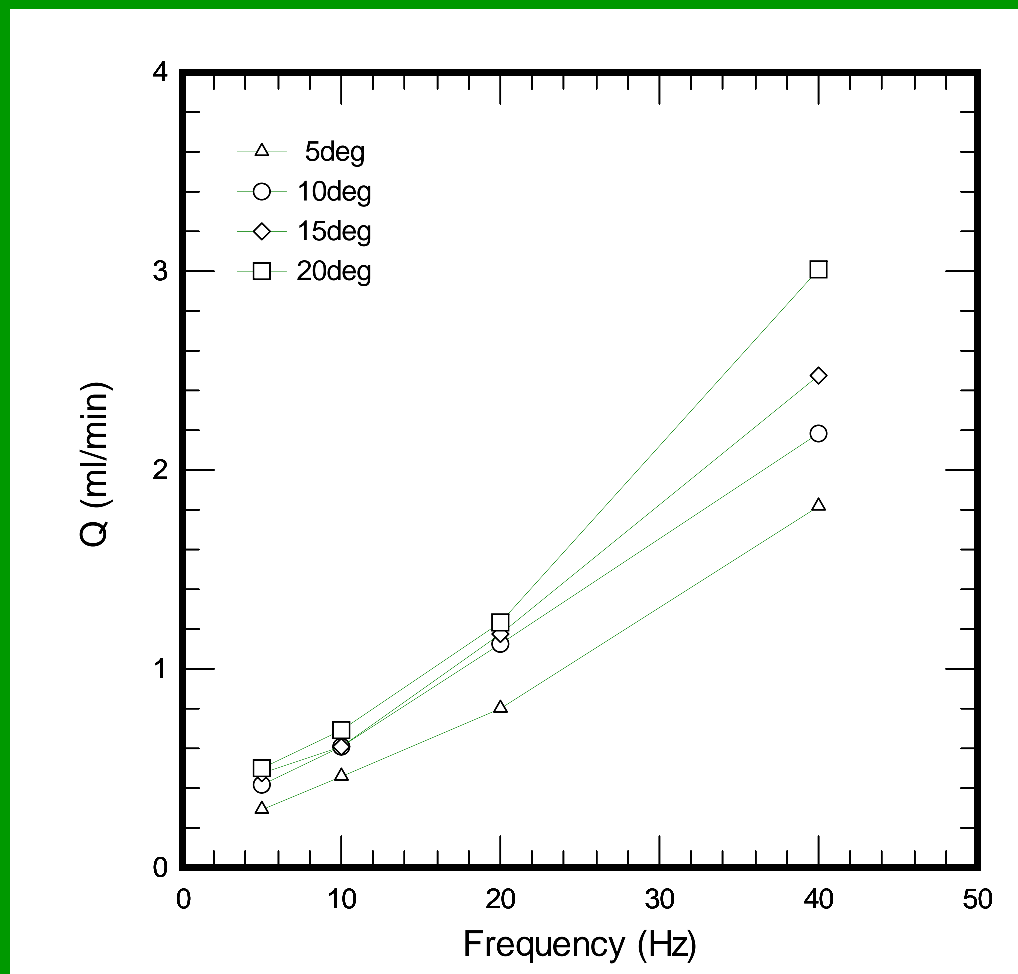

不同角度擴散器之微幫浦在不同頻率下之流量圖

結果與討論

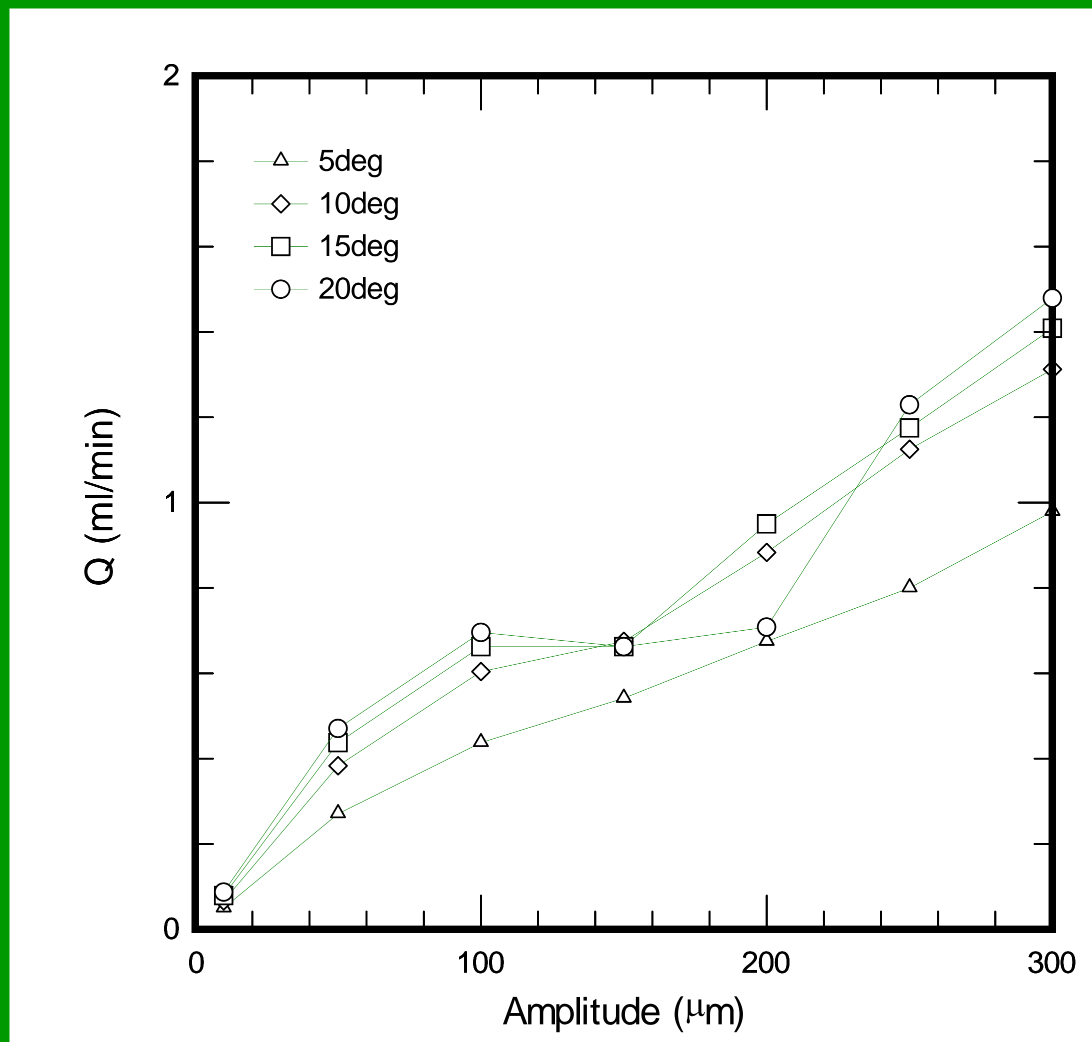

不同角度擴散器之微幫浦在不同振幅下之流量圖

結果與討論

擴散器20deg之微幫浦在20Hz振幅200μm在50ms時之速度向量分佈圖

結果與討論

U
3.9E-001
3.0E-001
2.0E-001
1.0E-001
0.0E+000
-1.0E-001
-2.0E-001
-3.0E-001
-4.0E-001
-5.0E-001
-6.0E-001
-7.0E-001
-8.0E-001
-8.8E-001

擴散器20deg之微幫浦在20Hz振幅200 μm在62ms時之速度向量分佈圖

結果與討論

擴散器20deg之微幫浦在20Hz振幅300μm在62ms時之速度向量分佈圖

結果與討論

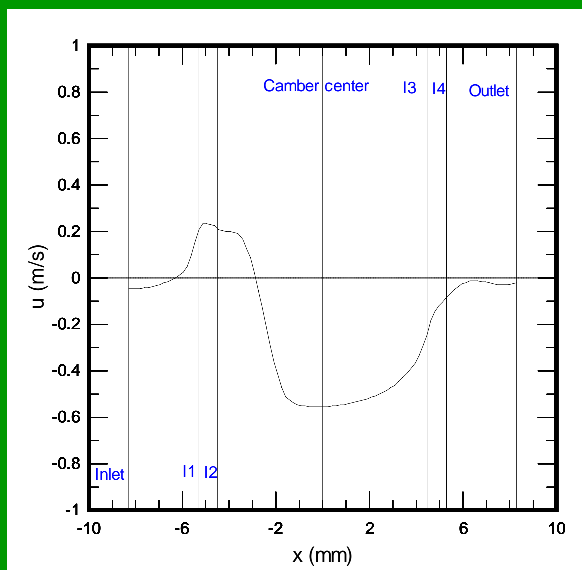

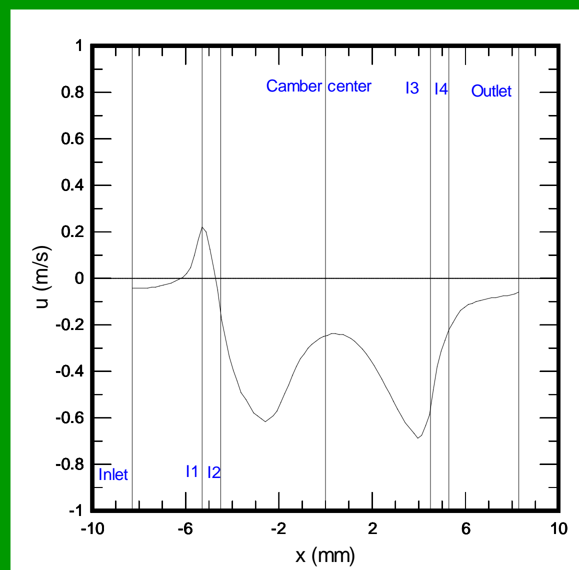

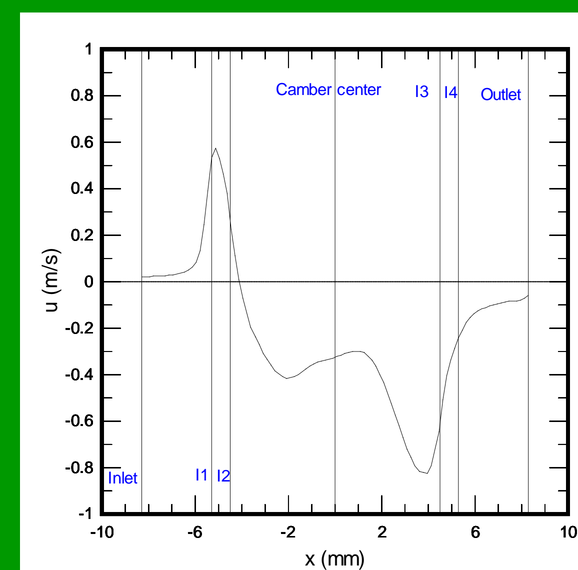

(a) (b) (c)

擴散器20deg之微幫浦在20Hz振幅(a)100μm (b)200μm(c)300μm在62ms時之x軸距離與速度關係圖

串聯式微幫浦

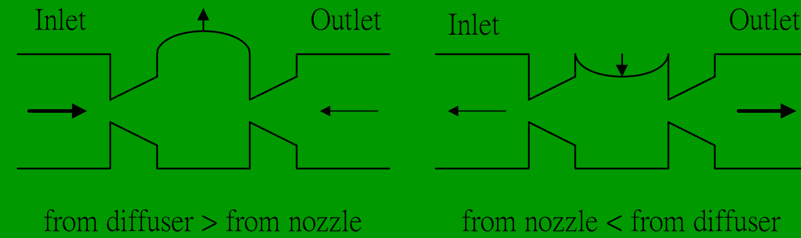

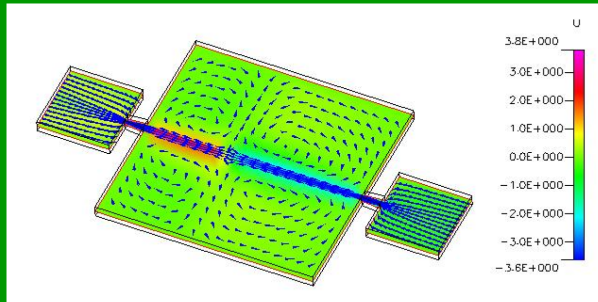

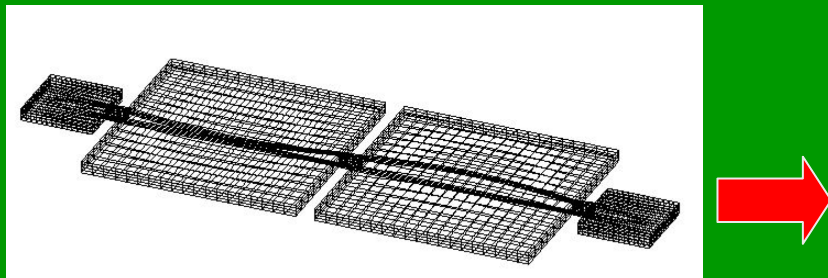

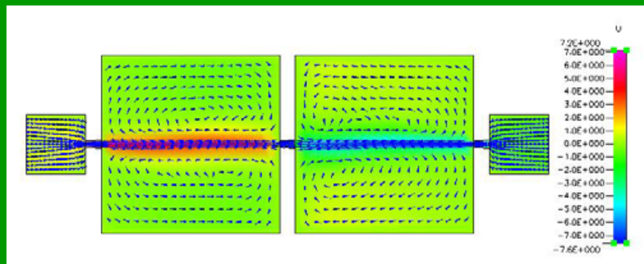

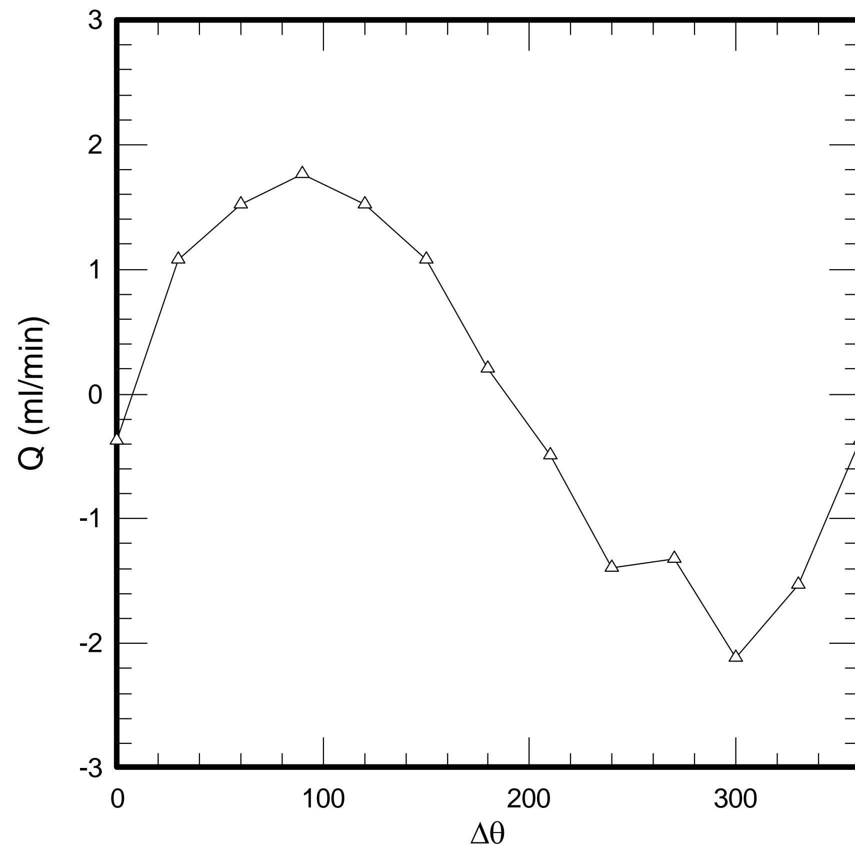

工業技術研究院
能源與資源研究所
Industrial Technology Research Institute
Energy & Resources Laboratories

相位差90°在10Hz振幅爲250 μ m時之速度分佈圖

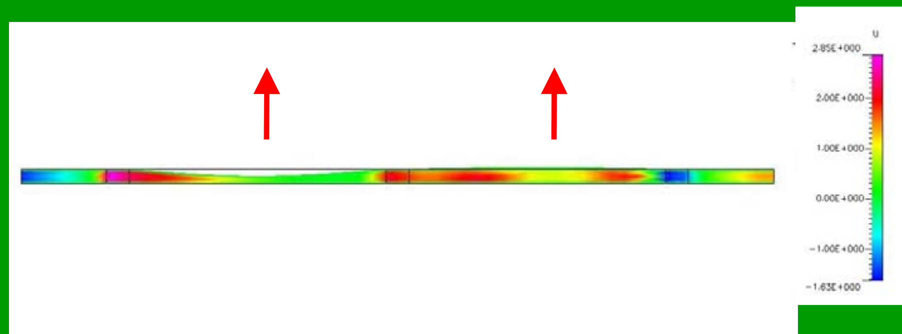

6 μ s

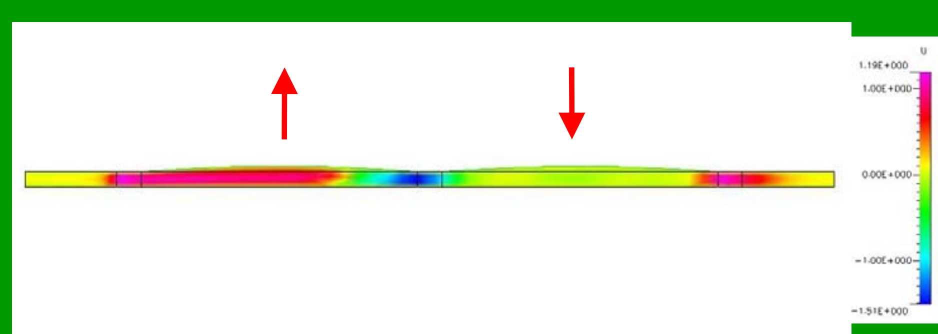

40 μ s

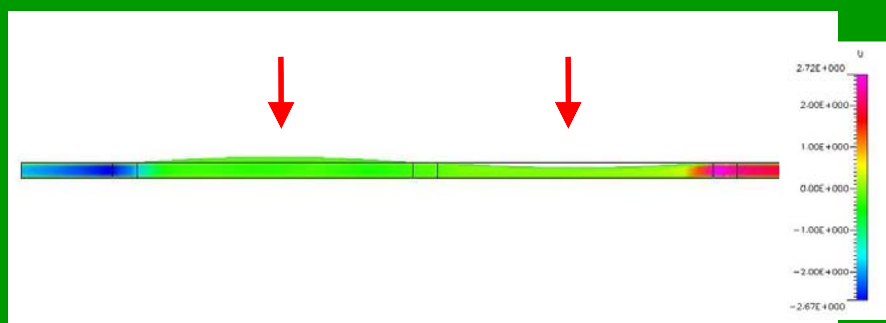

64 μ s

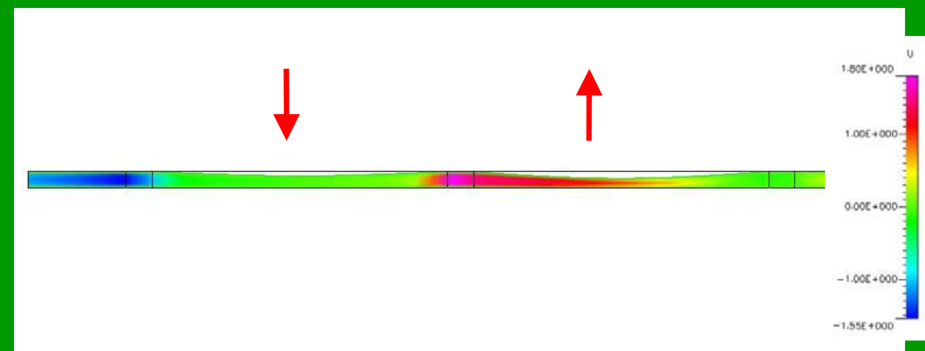

86 μ s

相位差90°在40 μs時之速度分佈圖

由最低點往上移動過平行軸

由最高點往下移動

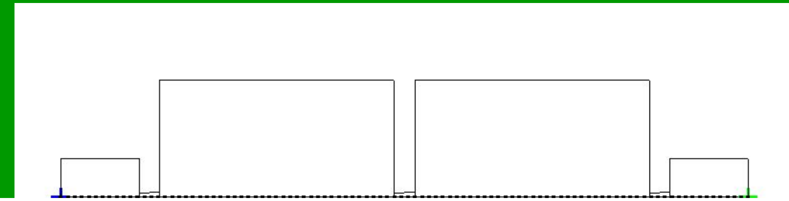

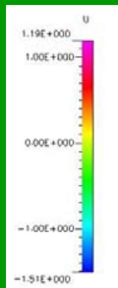

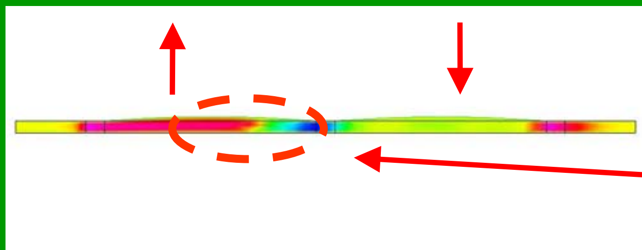

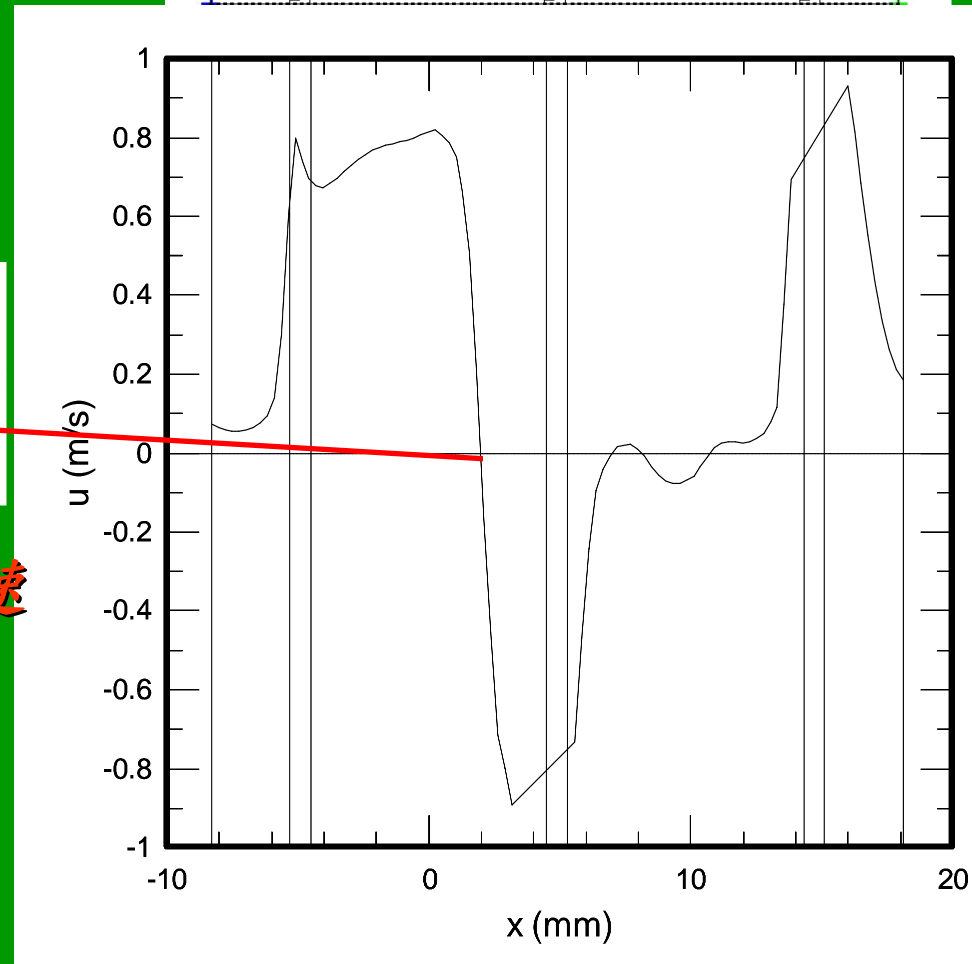

前方腔體工作流體正快速的流入左側腔體形成類似主動式閥門的效果

相位差90º在86 μs時之壓力分佈圖

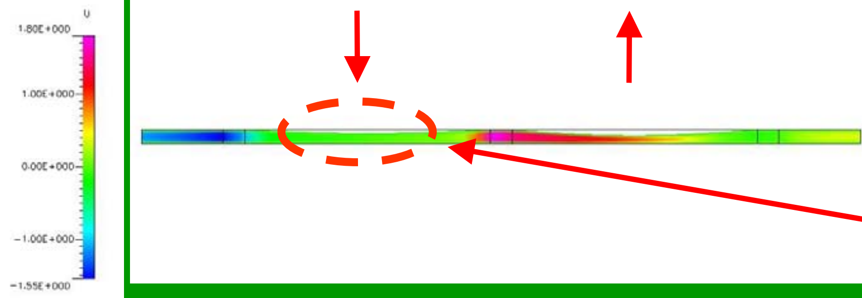

前方腔體薄膜快速往下擠壓
使腔體內部壓力快速上升

後方腔體薄膜快速往上移動
使腔體內部壓力快速下降

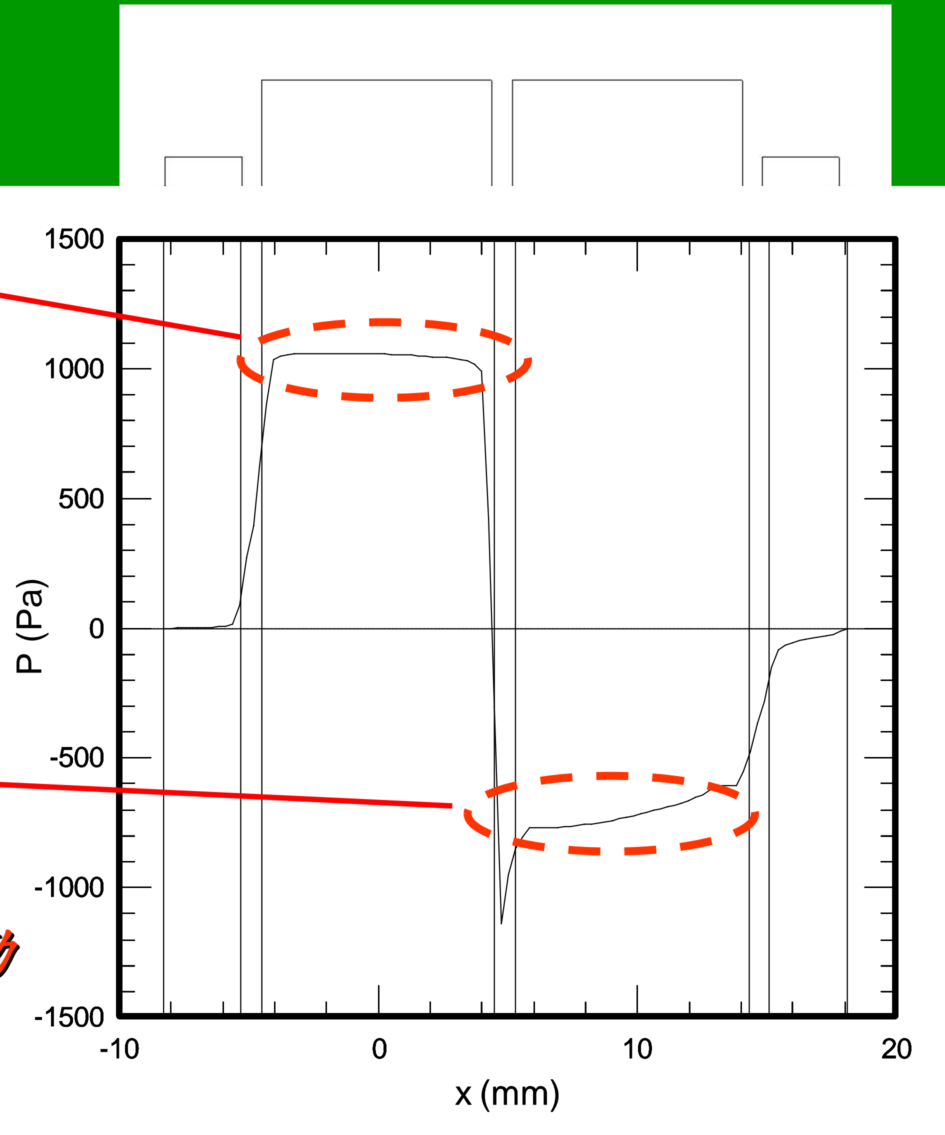

相位差270°在10Hz振幅爲250 μ m時之速度分佈圖

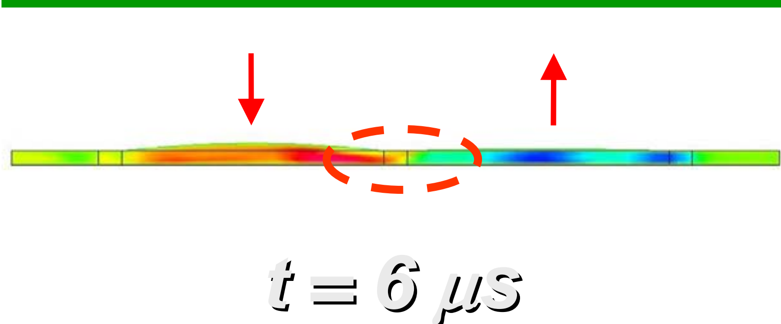

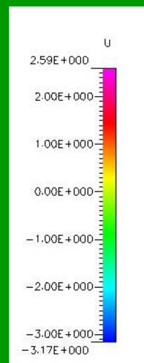

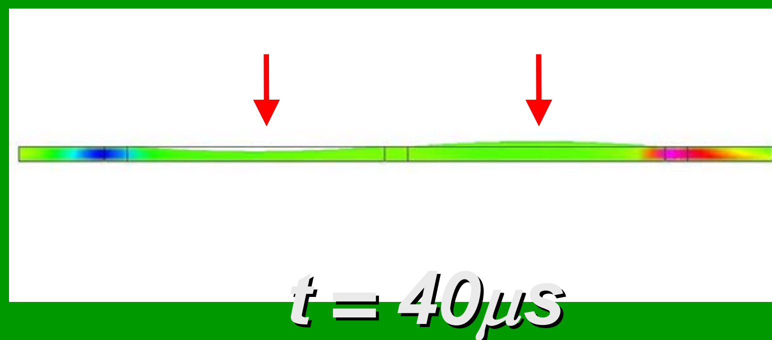

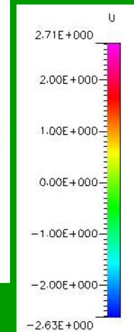

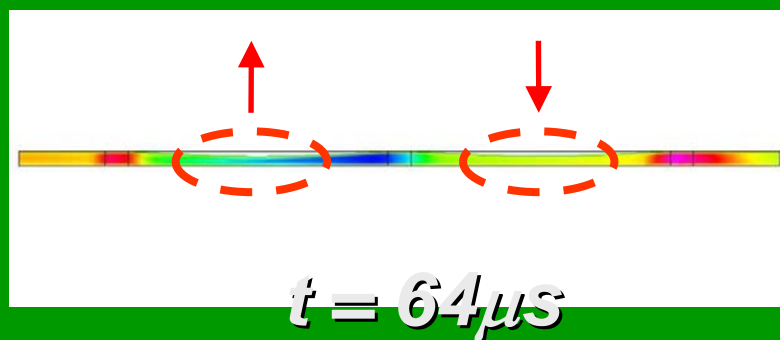

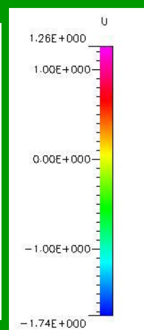

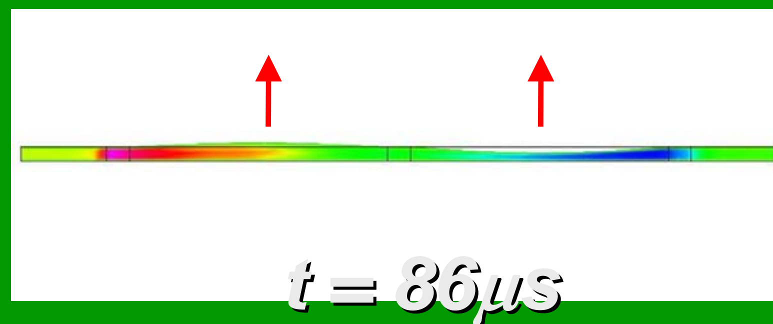

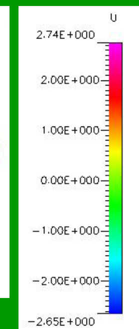

結論

- 噴嘴及擴散器之壓降主要包含入口段及出口段因管徑變化所產生之次要損失及漸擴/漸縮段之摩擦損失。
- 擴散器/噴嘴系統之壓降損失係數隨雷諾數增加而減少，壓降損失係數比隨雷諾數增加而增加。
- 擴散器/噴嘴系統之壓降損失係數隨角度增加而減少，壓降損失係數比隨角度增加而增加。
- 長度對噴嘴及擴散器之壓降損失係數及壓降損失係數比影響相對較小。

工業技術研究院
能源與資源研究所
Industrial Technology Research Institute
Energy & Resources Laboratories

Bubble Ink Jet Simulation

Grid constructions

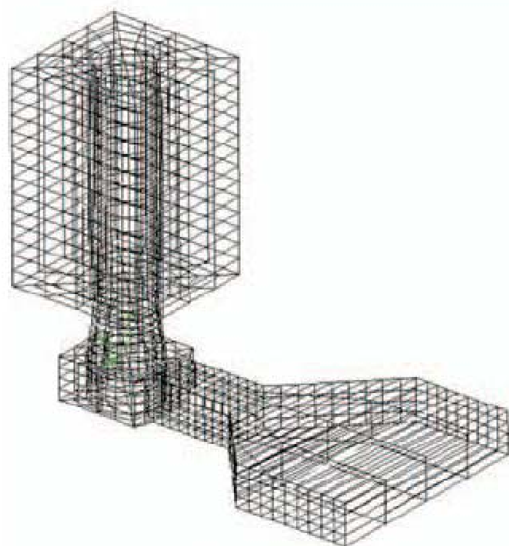
(a) Model A

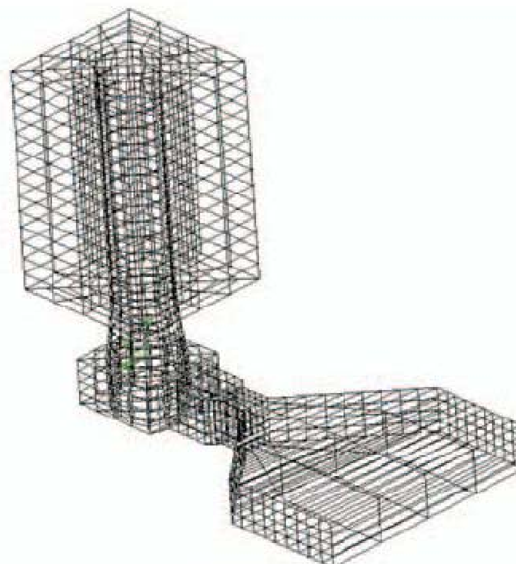
(b) Model B

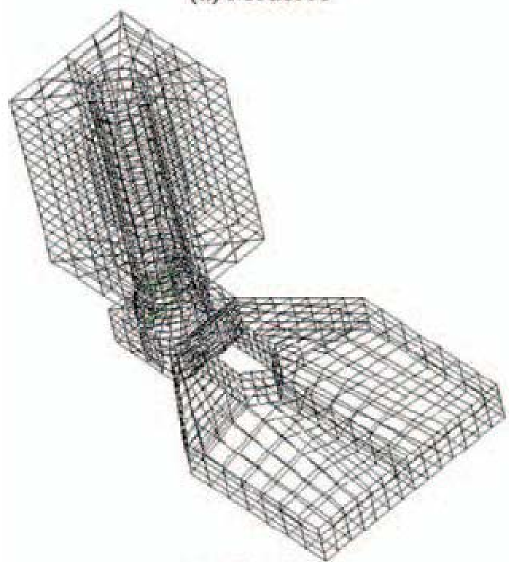
(c) Model C

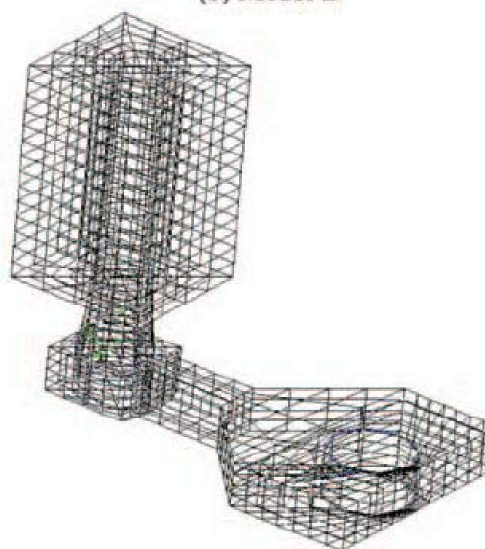
(d) Model D

工業技術研究院
能源與資源研究所
Industrial Technology Research Institute
Energy & Resources Laboratories

Grid constructions

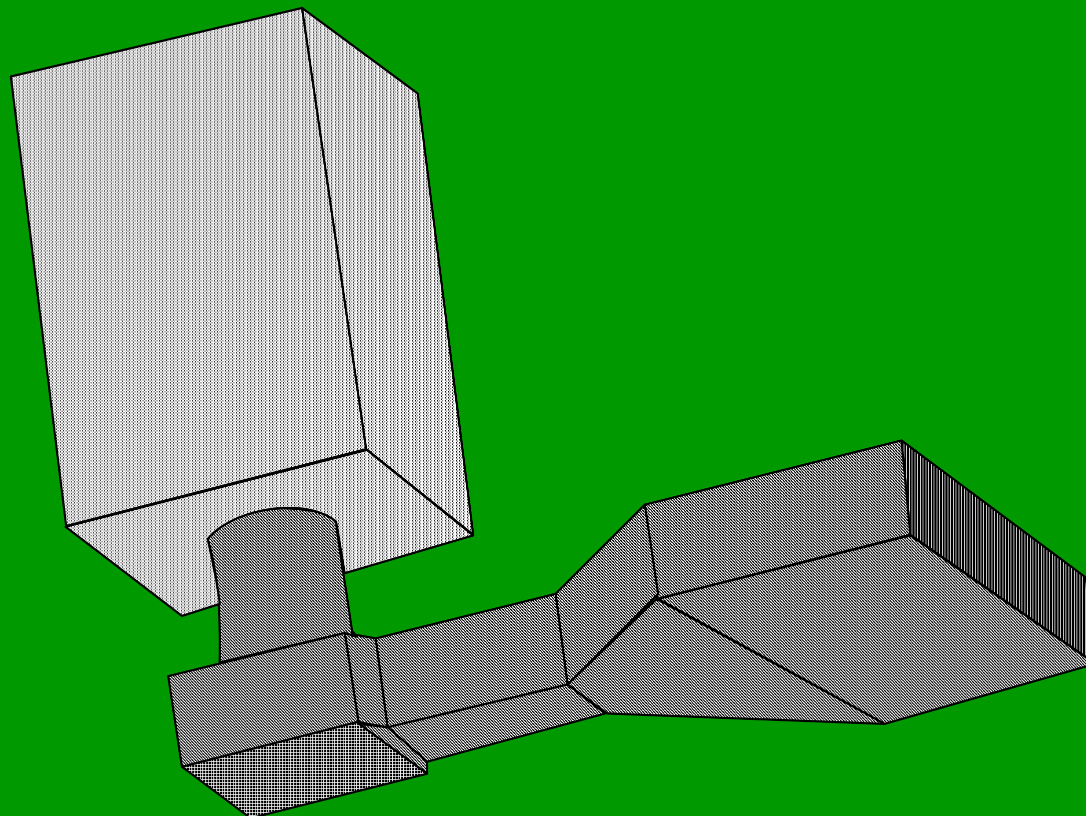

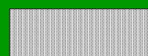

BC : Outlet

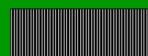

BC : Inlet

BC : Wall

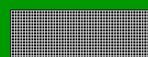

BC : Wall
Grid Deformation

Relation of the bubble growth rate

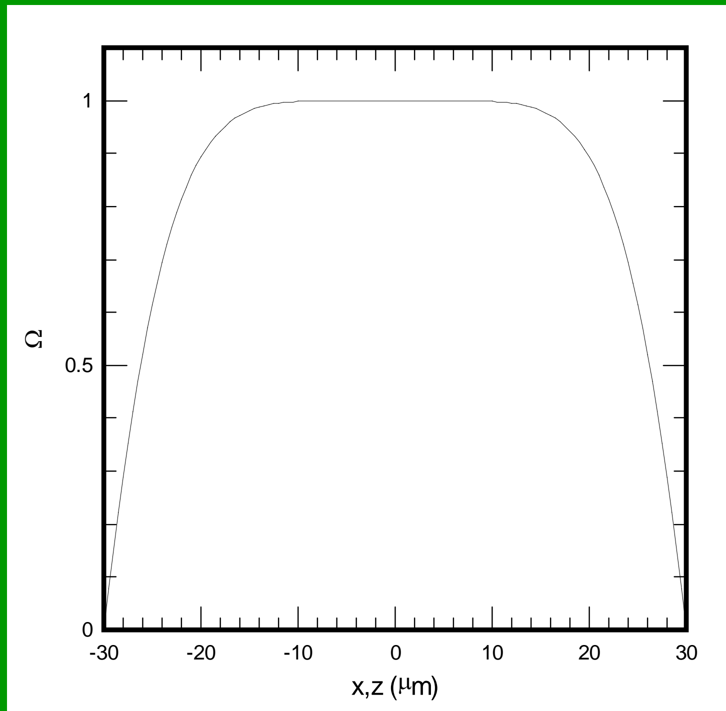

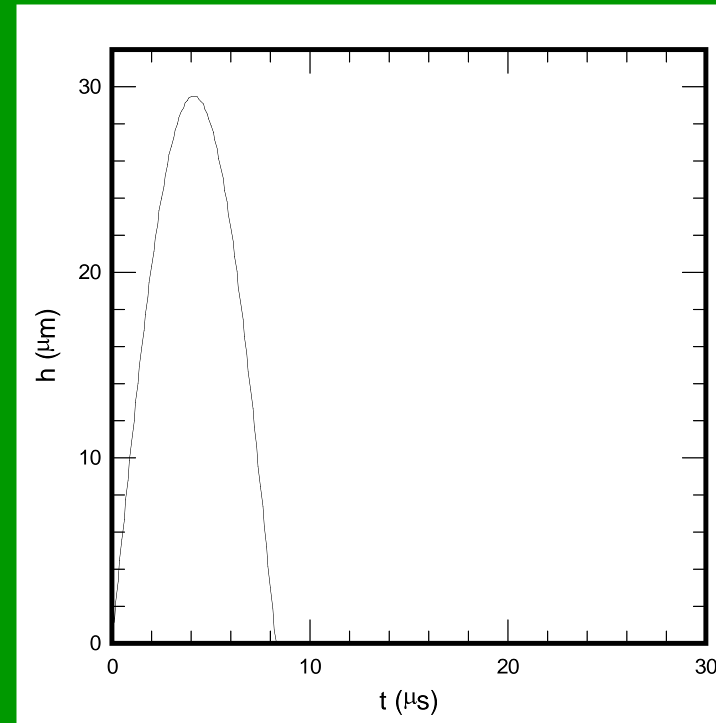

$$\Omega_x = \cos\left(1\times10^{15}\times x^3\times\pi/15\right)$$

$$\Omega_z = \cos\left(1\times10^{15}\times z^3\times\pi/15\right)$$

$$h_{\max} = 29.5\times10^{-6}\times\sin\left(0.38\times10^{6}\times t\right)$$

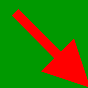

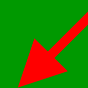

$$h(x,z,t) = step\left(82\times10^{-7}-t\right)\Omega_x\Omega_z h_{\max}$$

The stages of liquid refilling

w (m/s)

t (μs)

0
1
2
3
4

W

Density distribution and the refilling velocity

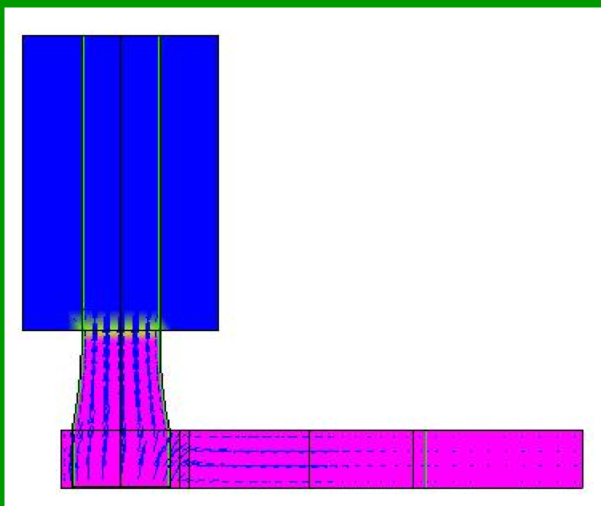
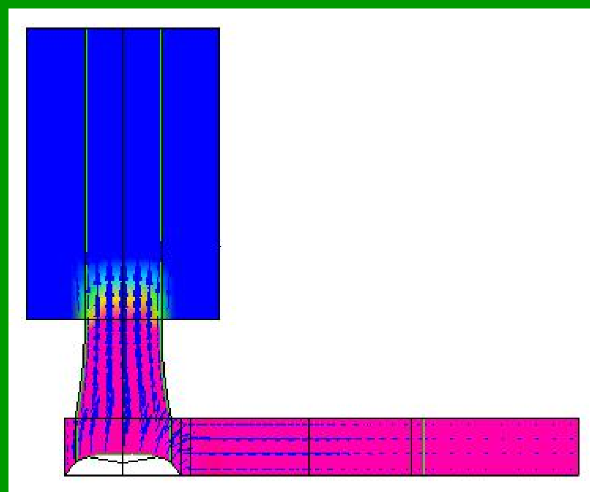
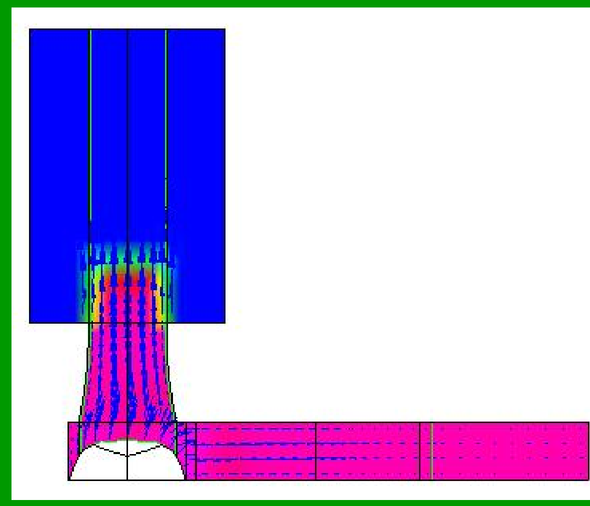

0.1 μs

1 μs

2 μs

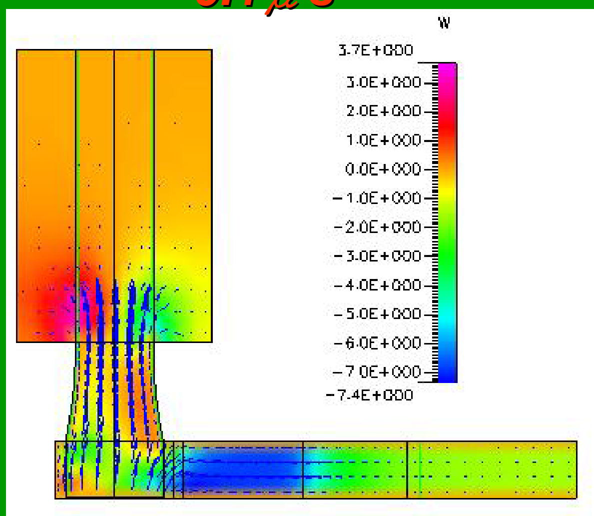

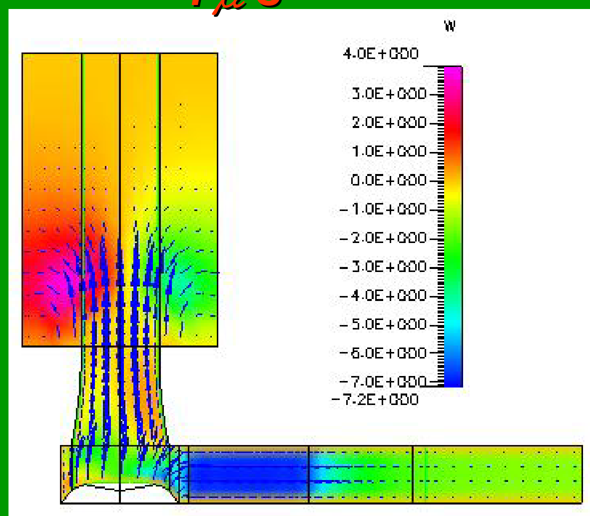

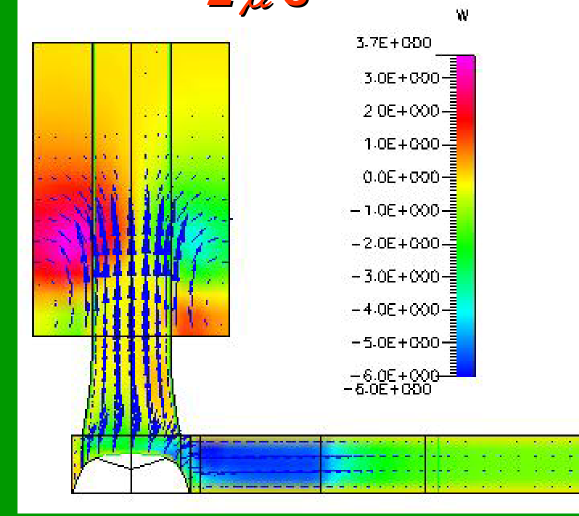

Density distribution and the refilling velocity

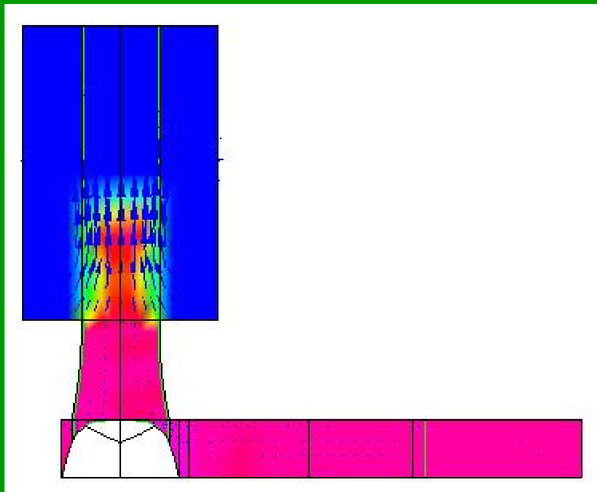

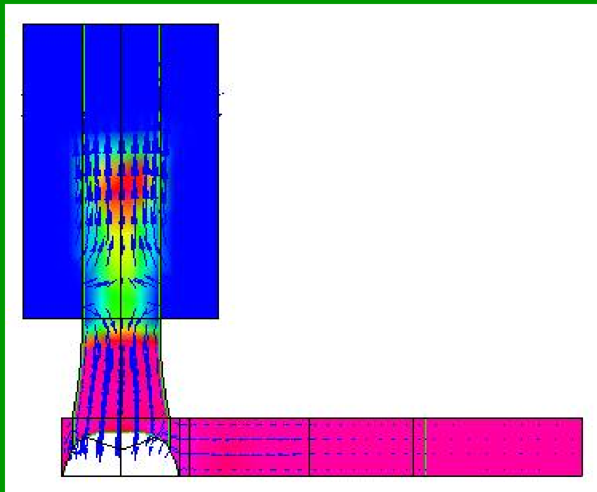

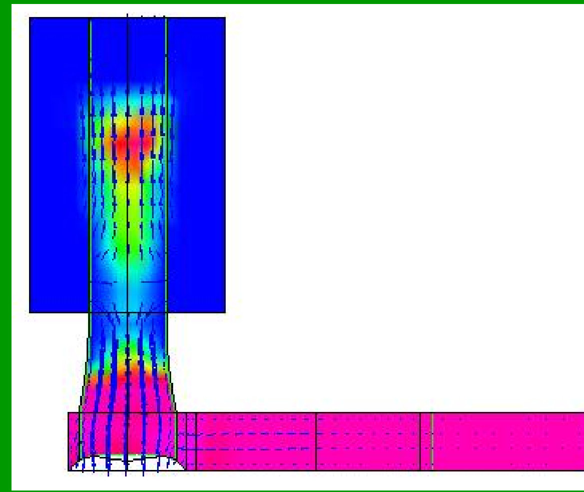

4.1 μs

6 μs

7.5 μs

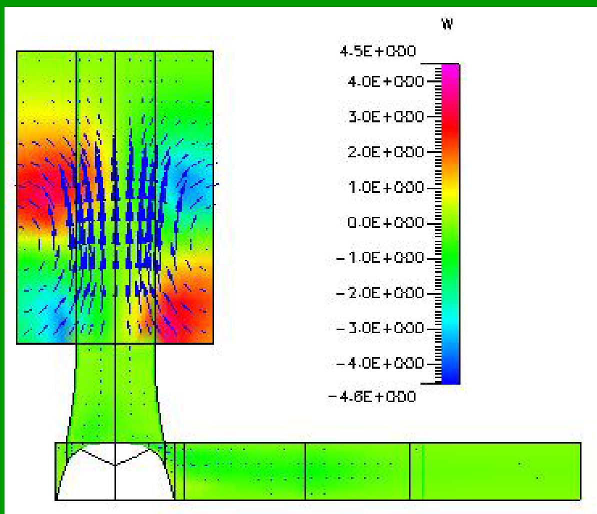

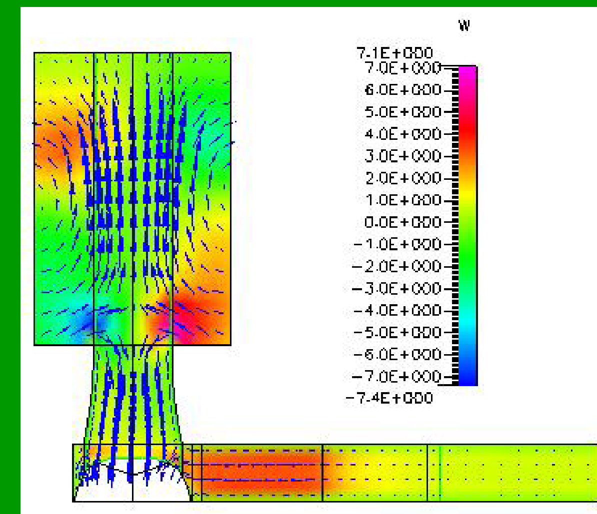

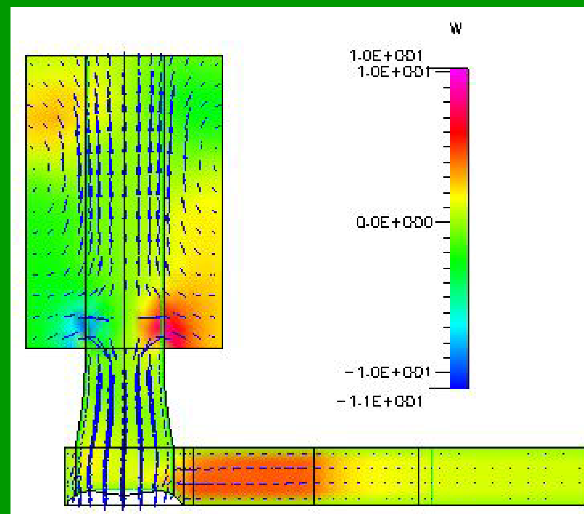

Density distribution and the refilling velocity

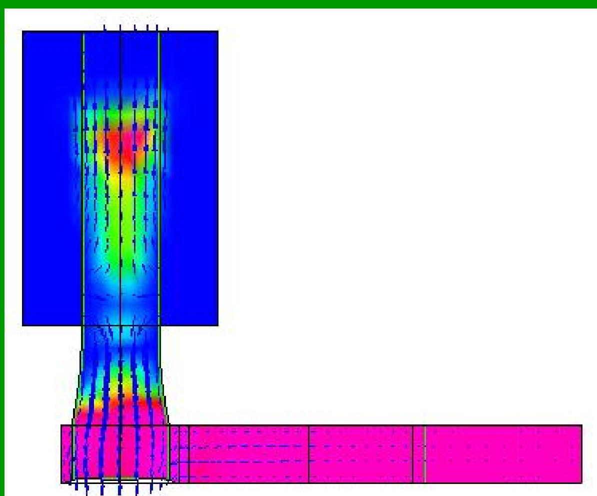

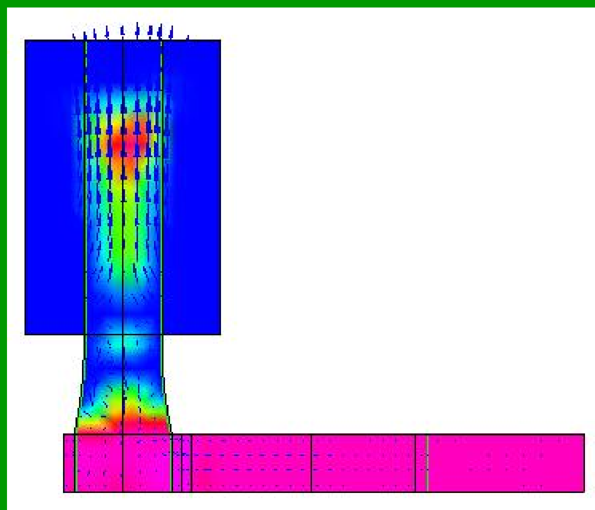

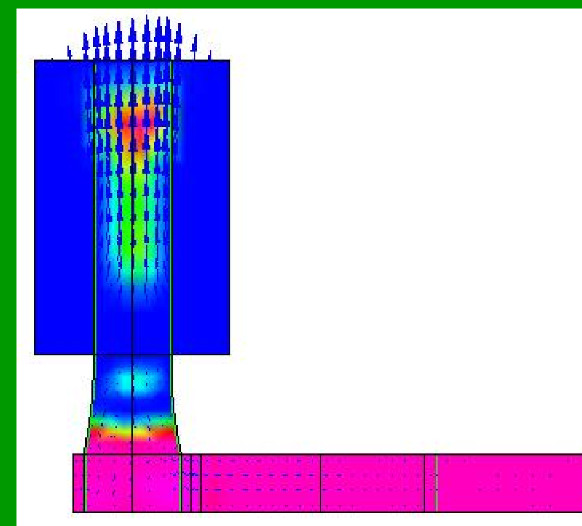

8 μs

8.4 μs

10 μs

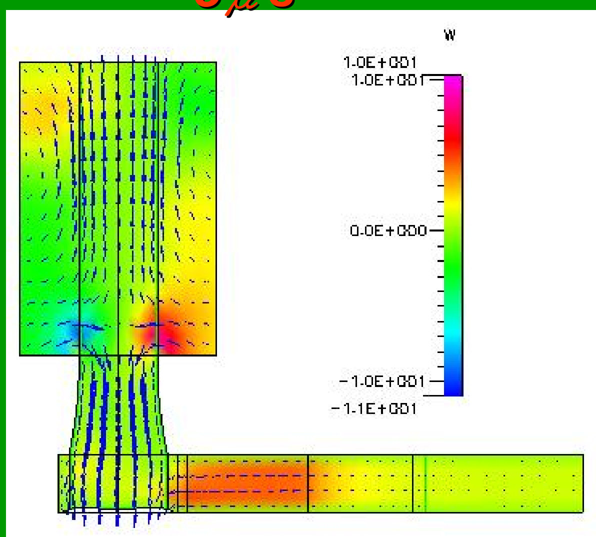

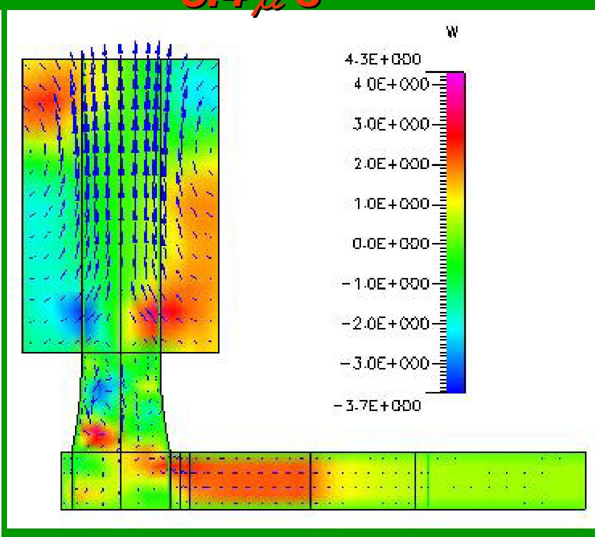

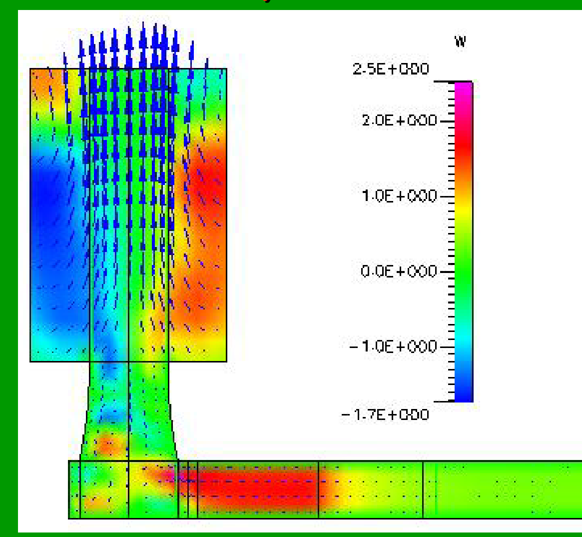

Refilling velocity vs. time for Models

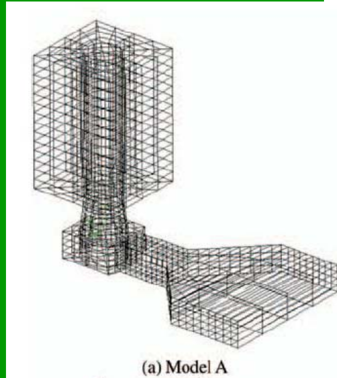
(a) Model A

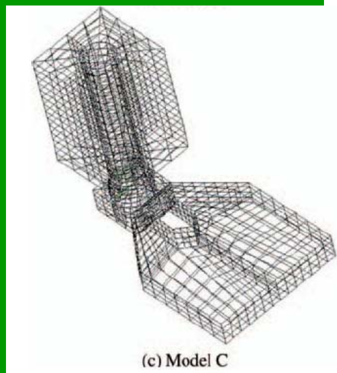
(c) Model C

Model A
Model D
Model B
Model C
w (m/s)
t (μs)
W

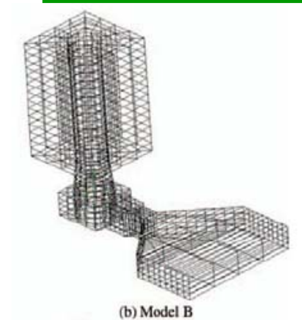
(b) Model B

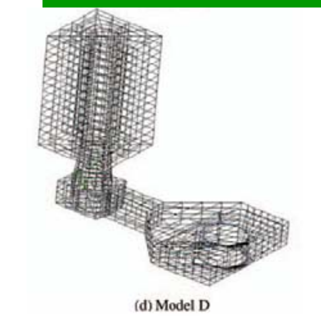
(d) Model D

工業技術研究院
能源與資源研究所
Industrial Technology Research Institute
Energy & Resources Laboratories

Density variation vs. time for Models

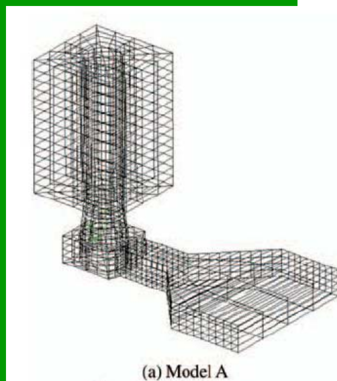
(a) Model A

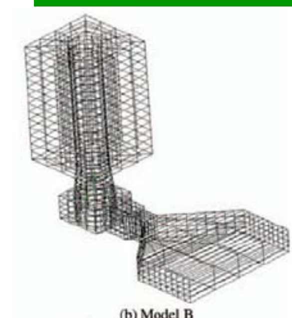
(b) Model B

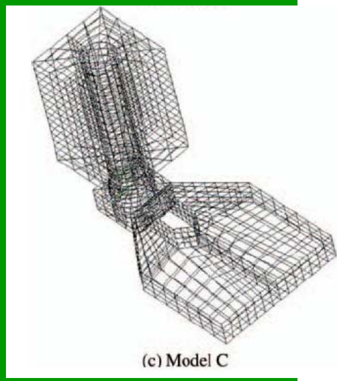
(c) Model C

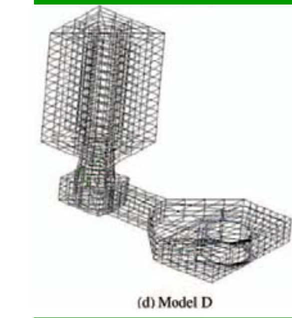
(d) Model D

Model A
Model D
Model B
Model C
Density

ρ (kg/m^3)

0
100
200
300
400
500
600
700
800
900
1000
1100
1200

0
100
200
300

t (μs)

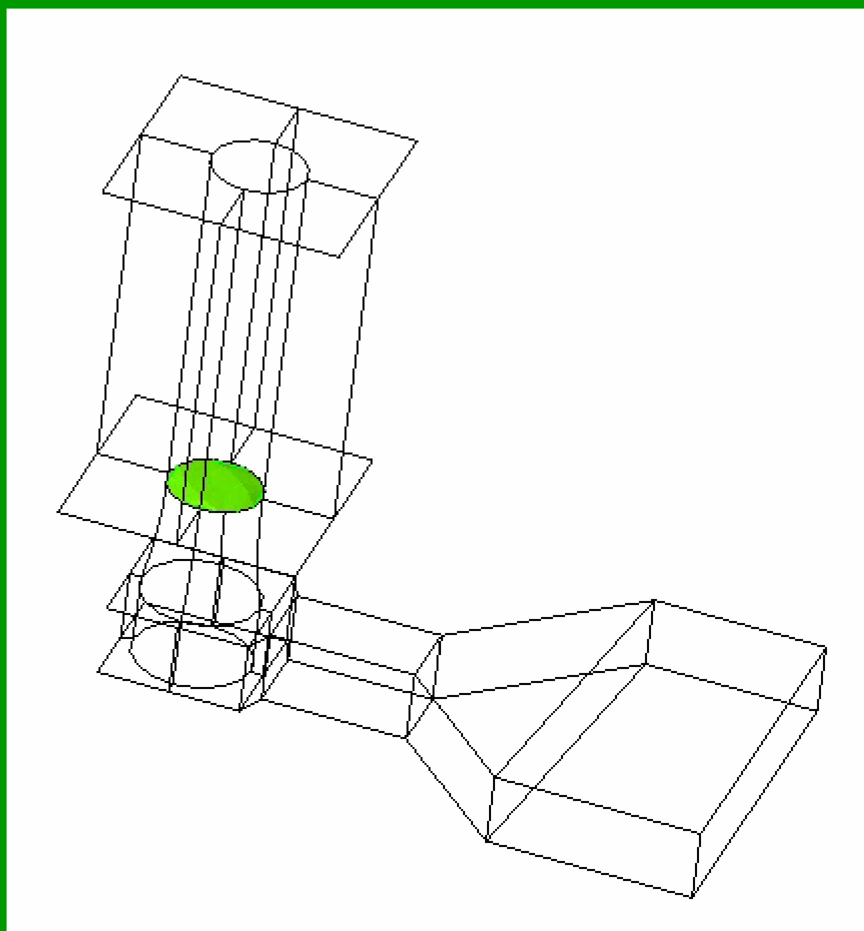

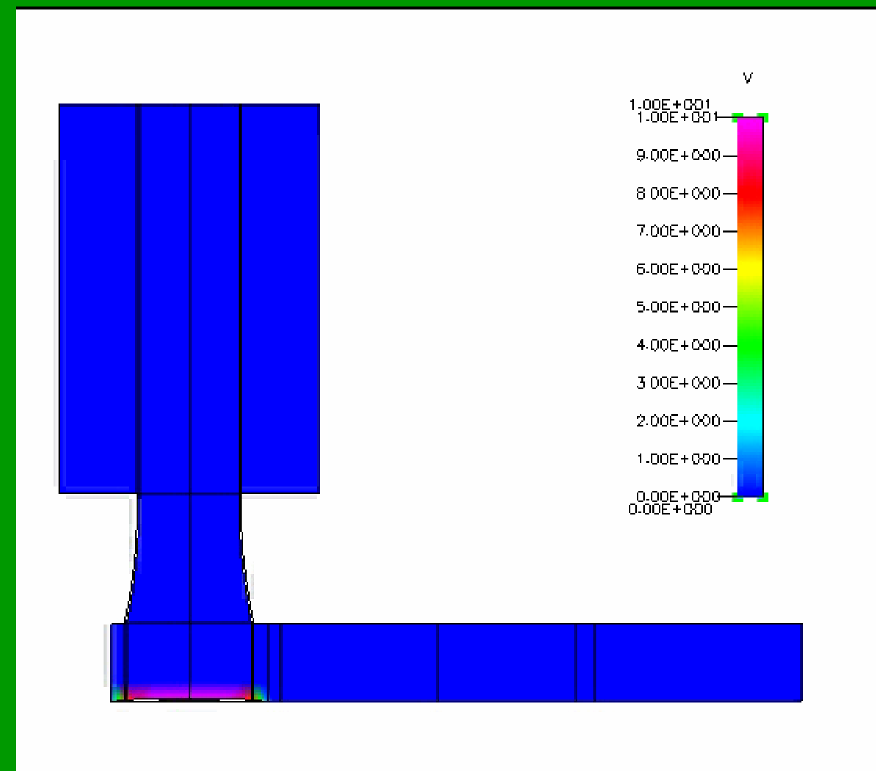

V
1.00E+001
9.00E+000
8.00E+000
7.00E+000
6.00E+000
5.00E+000
4.00E+000
3.00E+000
2.00E+000
1.00E+000
0.00E+000

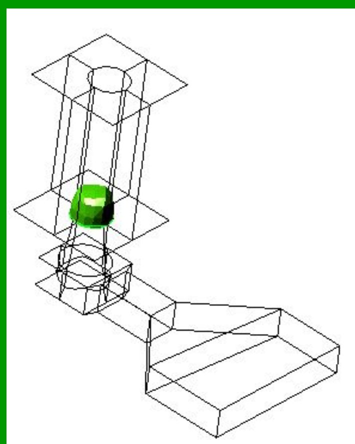

1.8 μs

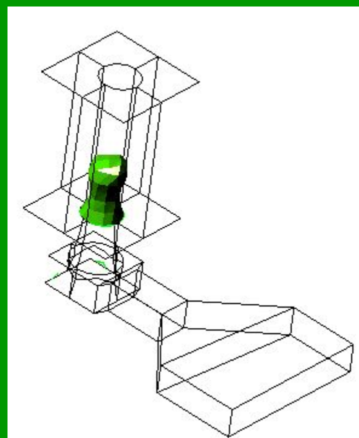

4.2 μs

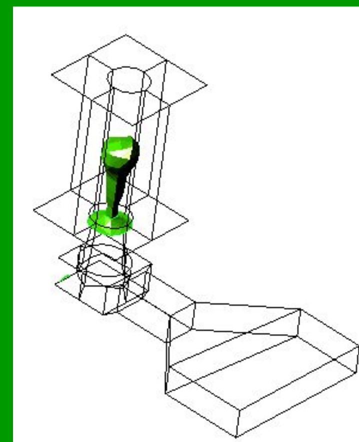

6.0 μs

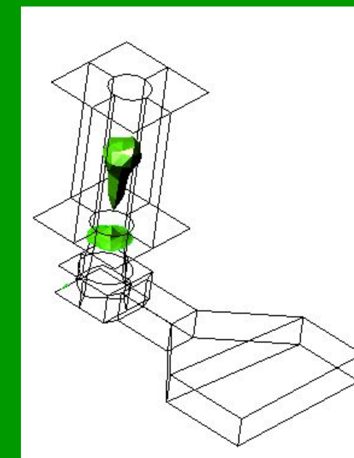

6.6 μs

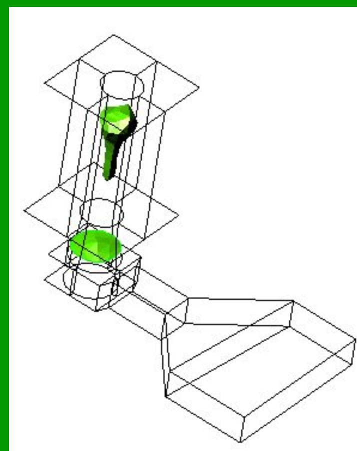

9.0 μs

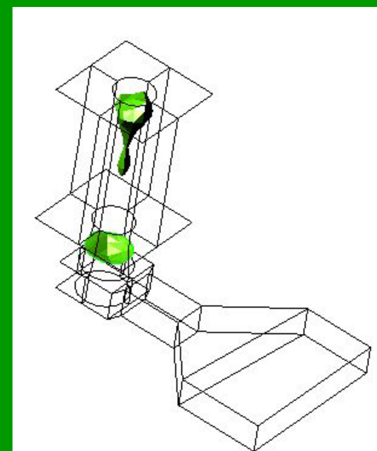

10.8 μs

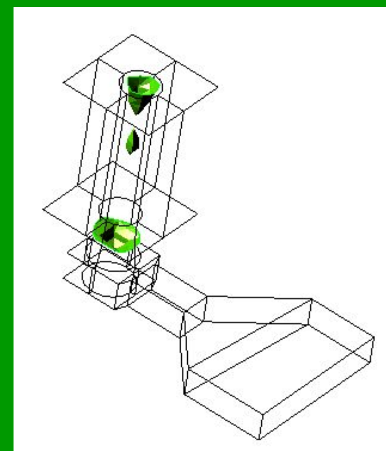

12.6 μs

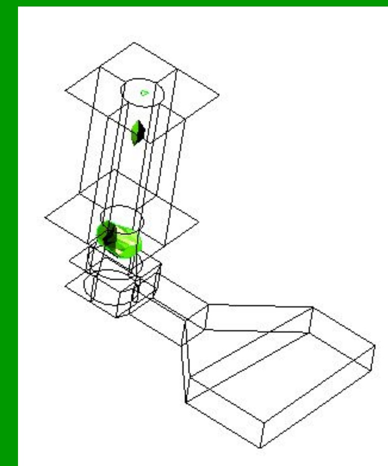

15 μs

Density variation at the interface vs. time

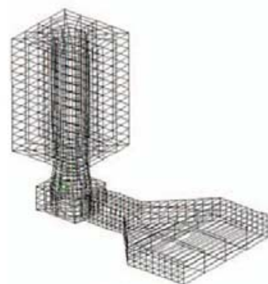

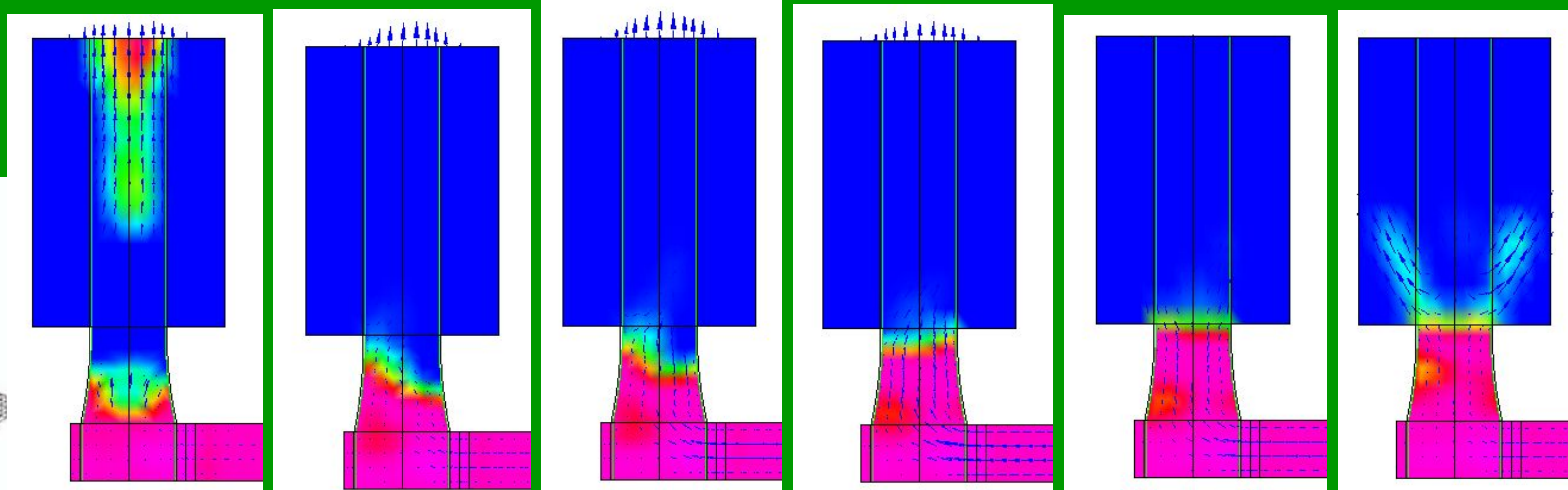

12 μs   24 μs   36 μs   48 μs   63 μs   105 μs

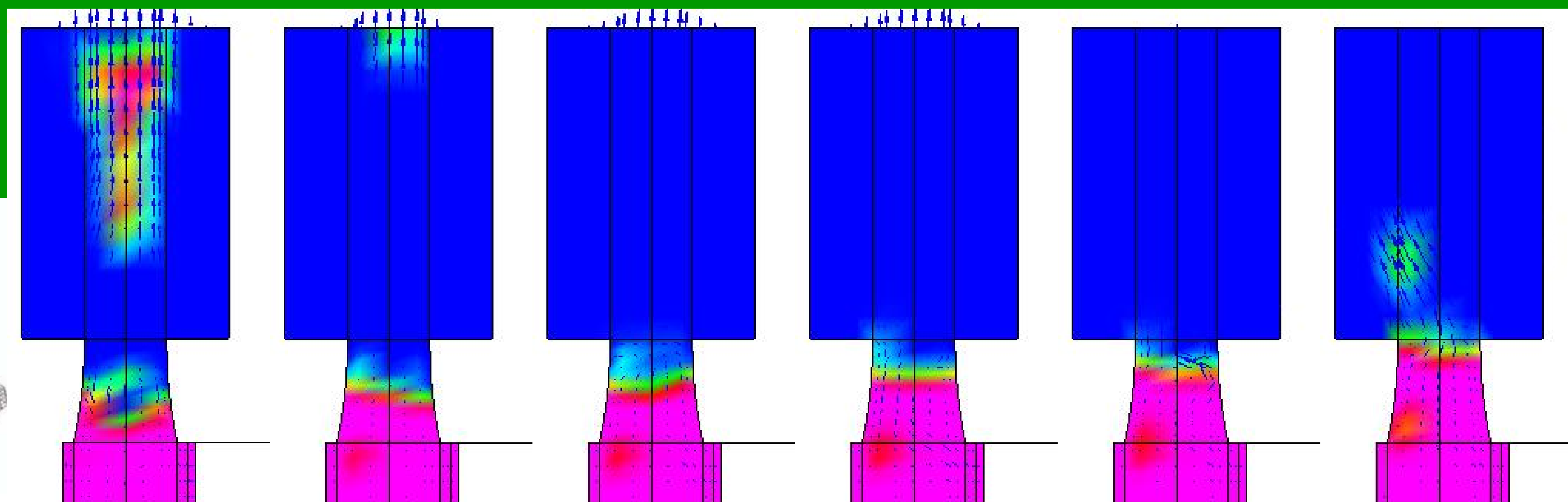

可進行分析之參數

- 不同幾何形狀之流道設計
- 不同黏滯力流體
- 不同流體表面張力
- 衛星液滴及殘存液滴之形成
- 充填速度之探討
- 重力影響
- 不同墨水匣夾擺設角度
- 不同氣泡形成時間
- 墨水匣內部背壓

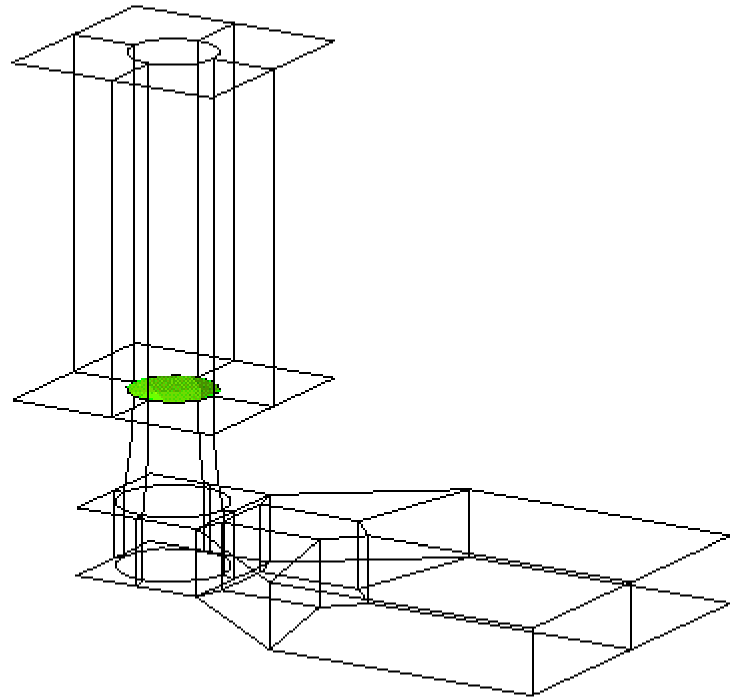

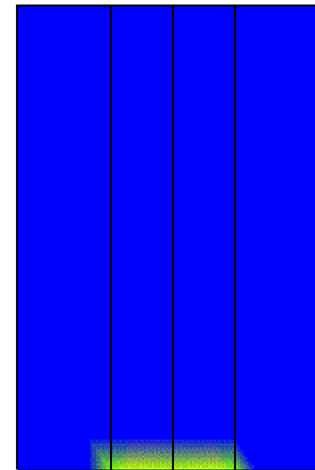

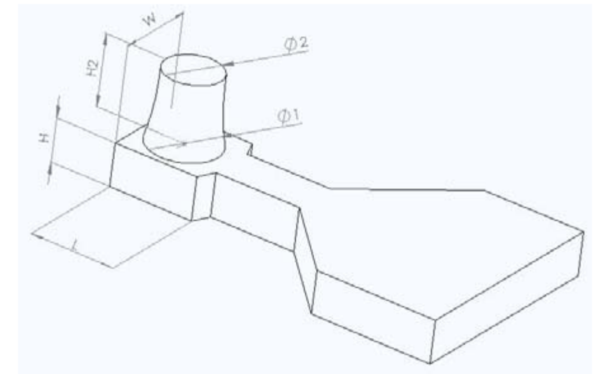

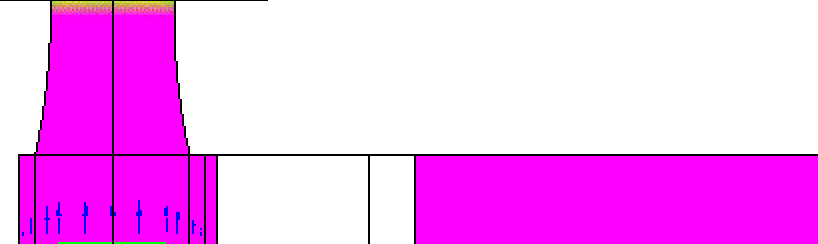

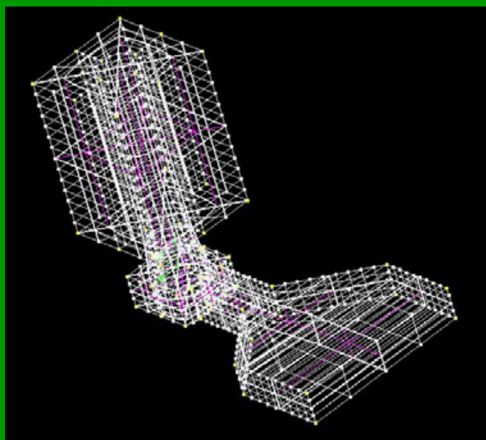

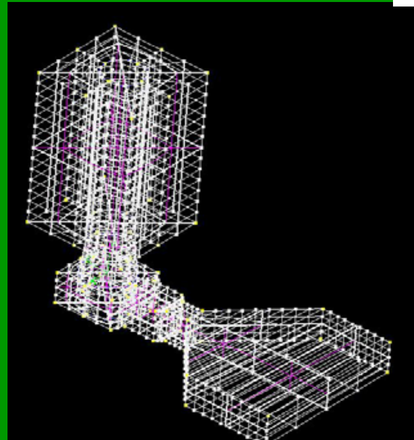

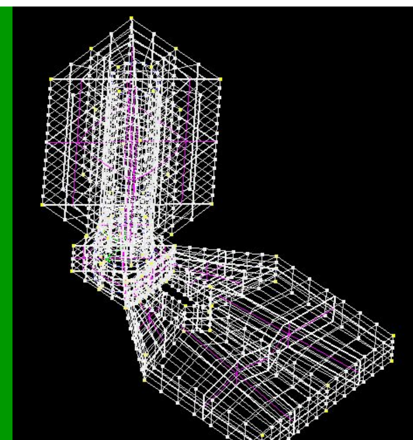

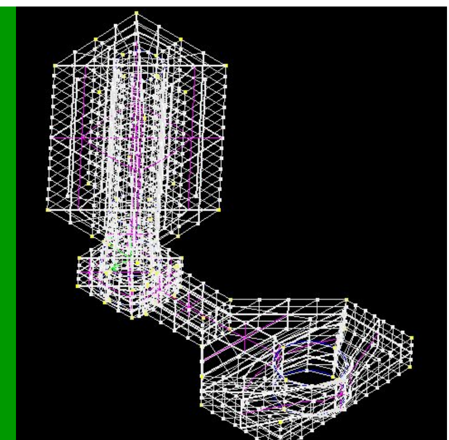

J. Of Mechanical Engineering Science, 2004, Vol. 215, No. 9, pp. 1111-1121.

Micro-/Nano- Fluidic Energy Conversion

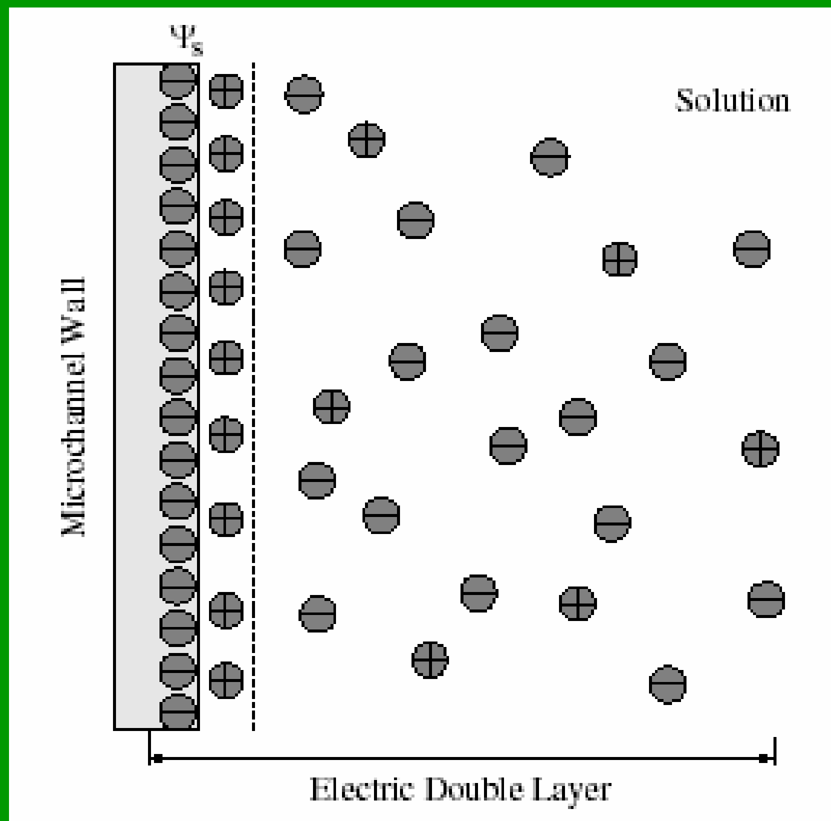

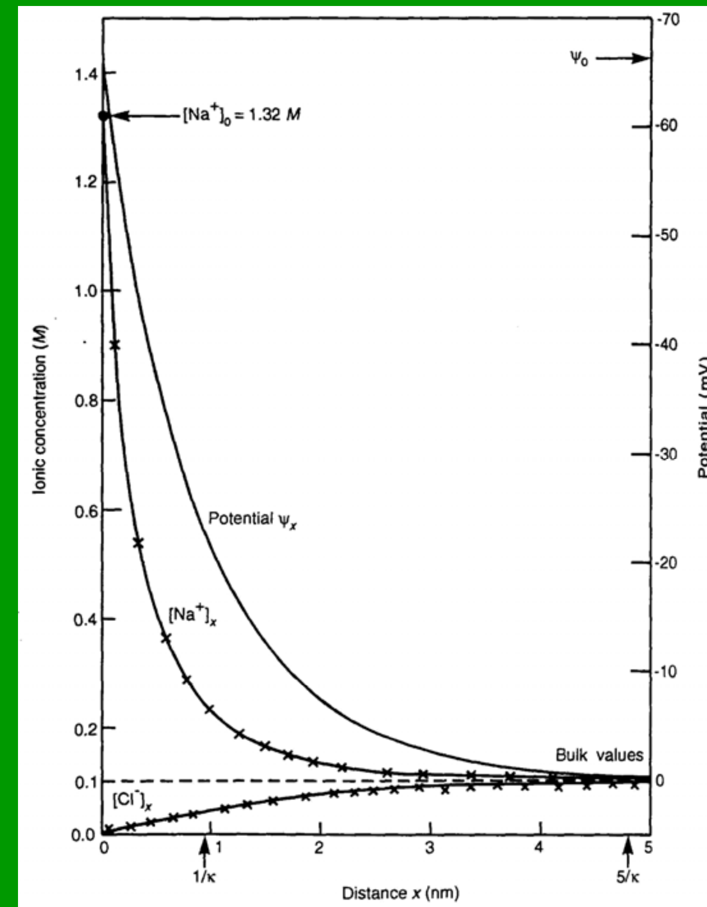

電動能微幫浦理論簡介

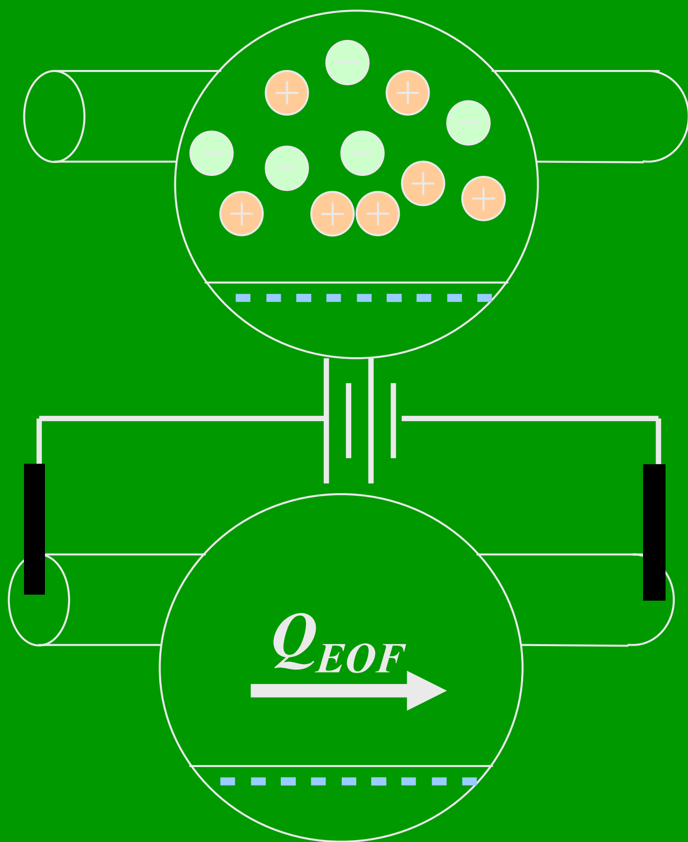

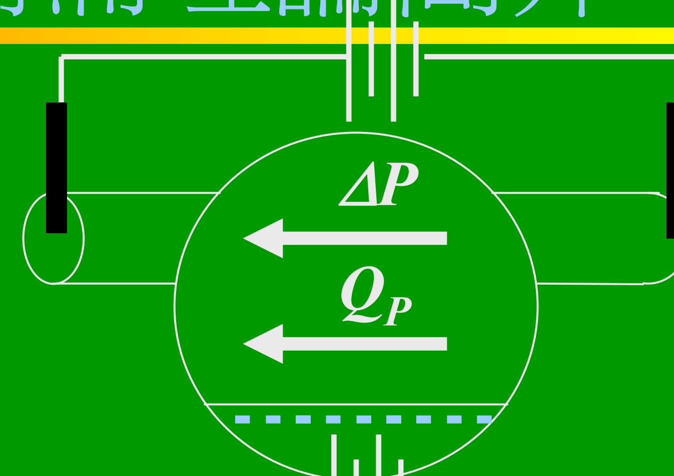

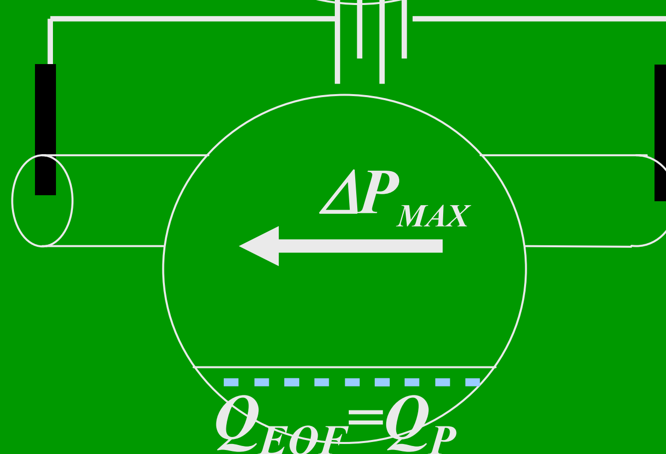

Output Energy: ΔP*Q

Input Energy: Δϕ*I

Efficiency:

$$\chi_{EK\ \mathrm{Pump}} = \frac{Q\Delta P}{I\Delta\phi}$$

應用奈米管之優點

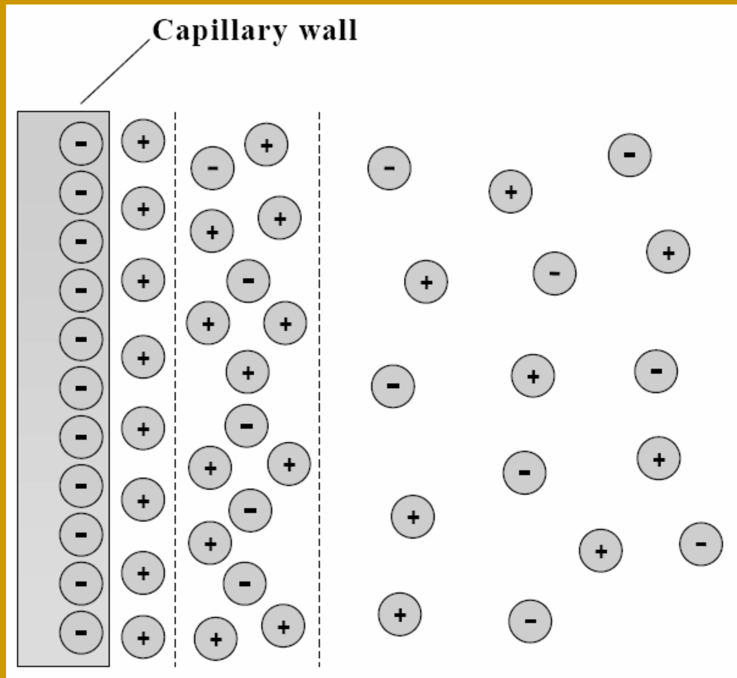

Diffusion Layer

Debye Length $\lambda_D \propto \sqrt{n}^{-1}$

微尺度:

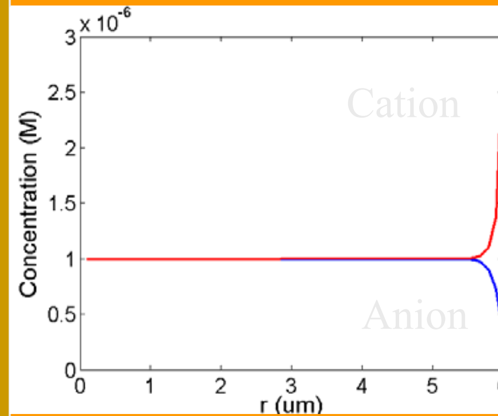

奈米尺度:

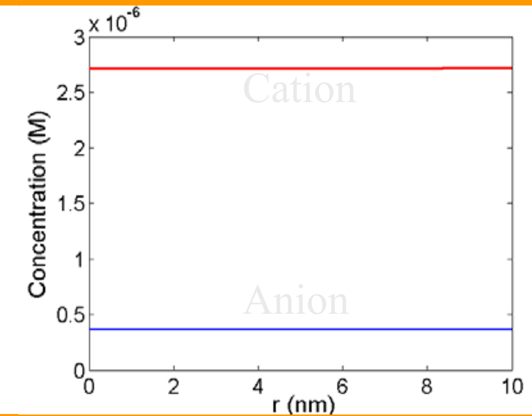

應用奈米管之優點:

- ***Unipolar Solution*** → ***高效率***
- ***$\Delta P \propto 1/r^2$*** → ***高靜壓***

微幫浦性能比較：靜壓

Maximum back pressure at zero flowrate, kPa

1000
100
10
1
0.1

Ahn and Allen (1995)
Dewa et al. (1997)
Esashi et al. (1989)
Stehr et al. (1996)
Koch et al. (1998)
Kamper et al. (1998)
Li et al. (2000)
Zengerle et al. (1995)
Böhm et al. (1999)
Wego and Pagel (2001)
Olsson et al. (1997)
Bardell et al. (1997)
Schabmueller et al. (2000)
Grosjean and Tai (1999)
Richter et al. (1991)
Zeng et al. (2002)
Chen et al. (2000)
Tsai and Lin (2001)
Geng et al. (2001)
Yun et al. (2001)

Rotary
Piezoelectric
Electrostatic
Electromagnetic
Thermopneumatic
Valveless
Peristaltic
EHD (Injection)
Electroosmotic
Bubble
Electrowetting

資料來源: Appl Mech Rev vol 57, no 3, pp. 191-221, May 2004

微幫浦性能比較：流量

Maximum flow rate/cross-section area at zero back pressure, μl/min.mm

10000
1000
100
10
1
0.1

Ahn and Allen (1995)
Dewa et al. (1997)
Esashi et al. (1989)
Stehr et al. (1996)
Koch et al. (1998)
Kamper et al. (1998)
Li et al. (2000)
Zengerle et al. (1995)
Böhm et al. (1999)
Wego and Pagel (2001)
Xu et al. (2001)
Olsson et al. (1997)
Bardell et al. (1997)
Schabmueller et al. (2000)
Grosjean and Tai (1999)
Richter et al. (1991)
Fuhr et al. (1992)
Zeng et al. (2002)
Chen et al. (2000)
Lemoff and Lee (2000)
Tsai and Lin (2001)
Geng et al. (2001)
Black and White (1999)
Yun et al. (2001)

Rotary
Piezoelectric
Electrostatic
Electromagnetic
Thermopneumatic
Shape Memory Alloy
Valveless
Peristaltic
EHD (Injection)
EHD (Induction)
Electroosmotic
MHD
Bubble
Flexural Plate Waves
Electrowetting

資料來源: Appl Mech Rev vol 57, no 3, pp. 191-221, May 2004

電動能微幫浦之產品及優點

The Cooligy Electrokinetic Pump
a silent, reliable cooling solution

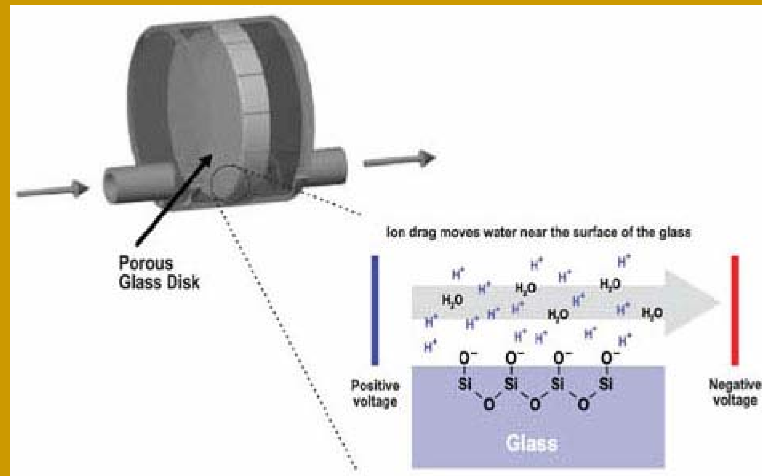

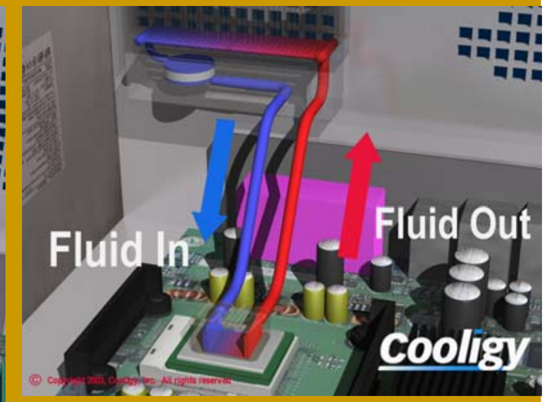

資料來源: www.coolige.com

電動能微幫浦之優點:

- 不需要動件
- 結構簡單
- 可靠度高
- 可產生大靜壓與不錯之流量

Micro EK – Pump: Technology Roadma

Group	Results	Year
Theoretical Predition:		
J.F. Osterle, Carnegie Institute of Technology	0.39%	1964
Morrison and Osterle	0.90%	1965
Sandiago et al., Standford University	1.30%	2002
J.Y. Min et al., Korea Advanced Institute of Science and Technology,	15%	2004
Experiments:		
P.K. Dasgupta and S. Liu, Texas Tech University	0.4-0.8 %	1994
Paul et al.	10 atm at 1.5 kV	1998
Santiago et al., Stanford University	20 atm at 2 kV	2000
Sandiago et al., Standford University	0.33 atm at 1 kV	2002
D.S. Reichmuth et al., Sandia National Lab	5.60%	2003

Micro-/Nano Cantilever-Sensor

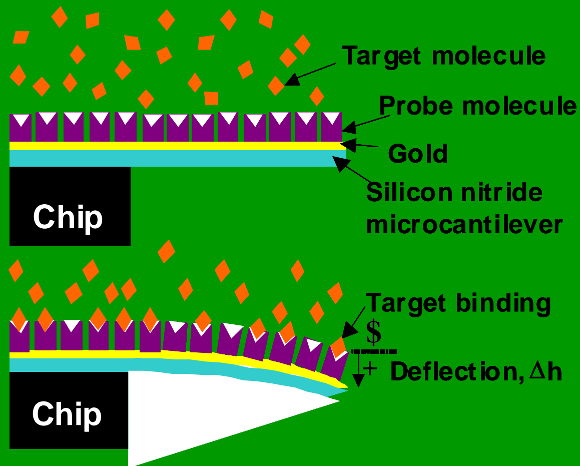

(M. Hagan et. al., J. Phys. Chem. B, Vol. 106, 2002)

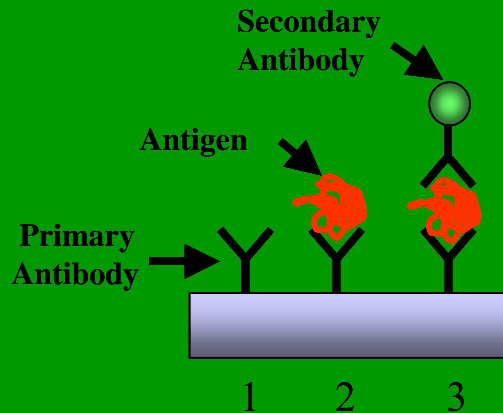

Enzyme-Linked Immunosorbent Assay (ELISA)

- MEMS/NEMS
  - Designs
  - Fabrications
  - Packaging
  - Test/Inspection
- Signal Detection
  - Static Model
  - Dynamic Model
- Signal Process
  - Readout Systems
  - Patterns recognition
  - Circuitry Design
- Sensor Application
  - Coating reagents (for physical, chemical and biological applications)

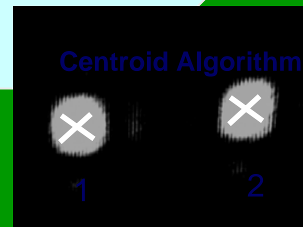

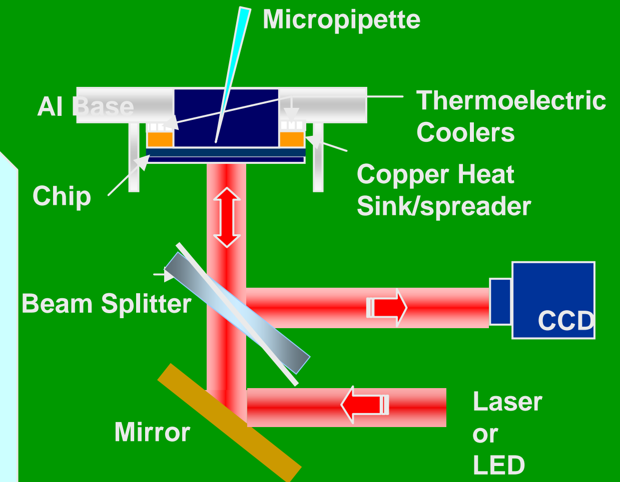

Side view

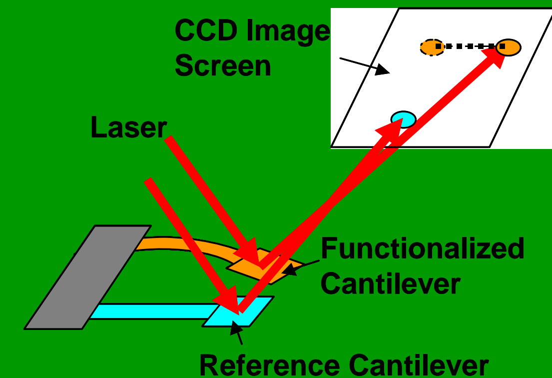

(Min Yue, Nanoengineering Laboratory, UC Berkeley, 2003)

Summary

- Intensive works associated with macro-scale air-conditioning had been done for the past ten years in ERL/ITRI, considerable work are still in progress.
- Intensive work are related to electronic cooling, Micro and Nanoscale fluid flow behaviors.
- I personally welcome those professors/students who wish to team up with us in the research area.

Thank you for your attention